Scientia Africana, Vol. 21 (No. 1), April, 2022. Pp 1-18 *https://dx.doi.org/10.4314/sa.v21i1.1*
© Faculty of Science, University of Port Harcourt, Printed in Nigeria *ISSN 1118 – 1931*

PALEOENVIRONMENTAL AND PALEODEPOSITIONAL ARCHITECTURE OF *SAMO* FIELD IN NIGER-DELTA BASIN OF NIGERIA USING SEISMIC AND WELL LOG DATA

[1]Ikhane, P.R., [1]Bayewu, O.O., [2]Coker, J.O., [1]Oyebolu, O.O. and [1]Adewoye, S.A.
[1]*Department of Earth Sciences, Olabisi Onabanjo University, Ago-Iwoye.*
E-Mail: Ikhane.phillips@oouagoiwoye.edu.ng
[2]Department of Physics, Olabisi Onabanjo University, Ago-Iwoye.
E-mail: coker.joseph@oouagoiwoye.edu.ng
Corresponding Author: coker.joseph@oouagoiwoye.edu.ng

Received: 22-11-2021
Accepted: 02-02-2022

ABSTRACT

The use of Seismic data and well log data within the context of sequence stratigraphy is a valuable tool for the recognition of ancient cycles and sequences because they reflect information on the different processes that deposit sediments in different palaeoenvironment. An integrated geophysical well log data and seismic data from our wells within the SAMO field have been utilized to delineate the upper Miocene-Pliocene depositional environment parts of the Niger-Delta Basin. Identification of the different lithologies and depositional environment present in the penetrated borehole was achieved using gamma ray log. This enables the establishment of different rock units in the well from the gamma ray log values and signatures. Three succession signatures which include; the bell, cylindrical and the funnel being more prominent were identified from the log motifs in the different sand bodies attenuated in the wells from the field. The mapped sequences generated Low stand System Tracts (LST) progradational, Trangressive System Tracts (TST) retrogradational and High stand System Tract (HST) aggradational packages. All these reflect the depositional systems that dominated the different phases as a result of base level changes. Furthermore, values quantified from the logs revealed that porosity and permeability are more prominent in places where sand bodies accumulated in the slope channel setting indicative of slope-fills and turbidity fans. This deep-sea channels and switch complex fault system suggest good hydrocarbon bearing potential associated with the distal Niger-Delta province. Also a good quality reservoir was inferred from the sands of both LST and HST while the shale of the TST could serve as a good reservoir.

Keywords: Hydrocarbon, Paleoenvironments, Procreation; Reservoir; Sequence.

INTRODUCTION

The technological advancement in borehole geophysics and seismic data acquisition has enabled the delineation of structural and stratigraphic configuration of the subsurface with high degree of precision and reliability.

Seismic data is very good in depicting the geometry and configuration of fields because they provide a continuous lateral view of the subsurface as well as the acoustic impedance of the related formation velocities and densities while well data though limited in defining the lateral variation of the subsurface as a result of anisotropy effect of the subsurface but gives the actual ground truth of hole bore. Integrating the two data sets give a robust interpretation of the field

under review. The use of seismic data and well logs within a sequence stratigraphic context is rapidly emerging as a valuable tool for the recognition of ancient cycles and sequences in the Niger Delta. The application of seismic and well log data sets is not a new concept, as both have been combined in the study and understanding paleoenvironments. Sediments and sedimentary processes that deposit sediments contain information reflected in well logs and this is responsible for the characteristic log motif displayed in different paleoenvironment. Therefore, interpretation of sedimentary facies can be derived through the use of well or borehole logs (Weber, 1971).

Thus, by combining seismic data along with well logs, the degree of confidence in mapping complex structural and stratigraphic areas would be greatly improved (Barde *et al*., 2000. 2002; Adejobi and Olayinka, 1997), because as lateral facies change, vertical lithologic transitions will easily be detected.

Location and Geologic Settings of the Study Area

The Niger Delta is an oil province of Nigeria situated in the Gulf of Guinea on the west coast of Central Africa. Niger Delta area lies within latitudes 4° and 6° N and longitudes 3° and 9° E in the Southern geo-political region of Nigeria. The geology of the southwestern Cameroon delineates the onshore portion of the Niger Delta in which the northern boundary is the Benin flank--an east-northeast trending hinge line south of the West Africa basement massif and the northeastern boundary defined by the Cretaceous rocks on the Abakaliki High and further in the east-south-east by the Calabar flank a hinge line bordering the adjacent Precambrian. The offshore margin is defined by the Cameroon volcanic line to the east and bounded at the eastern portion by the Dahomey basin which is a West African transform-fault passive margin to the west.

The Niger Delta is ranked among the major hydrocarbon provinces in the world; Nigeria has been rated as the sixth largest oil producer and the twelfth giant hydrocarbon province (Okosun *et al.*, 2012). The basin has spectacularly maintained a thick sedimentary apron and salient petroleum geological features favorable for petroleum accumulation from the onshore through the continental shelf and to the deep-water terrains. Theonshore and continental shelf of Niger Delta are being examined for more than six decades now. Its hydrocarbon potential is been harnessed as prospectivity is shifted deep offshore. The deep-sea channel sands are the main exploration target in this (deep offshore) section of the Niger Delta (Whiteman, 1982).

The *SAMO* field (Figure 1) is located around the eastern part of the Niger Delta Basin (Figure 2). The Niger Delta province is believed to possess a sediment that is about 12 km thick at the middle part of the area, which covers an extent of about 75,000 km^2 (Reijers *et al*., 1997). Due to the unbroken progradation throughout the Tertiary, three depositional lithofacies are readily identified despite local facies variation. The three formation are locally designated from bottom to top as Akata Formation, Agbada Formation and Benin Formation (Figure3).

Scientia Africana, Vol. 21 (No. 1), April, 2022. Pp 1-18 https://dx.doi.org/10.4314/sa.v21i1.1
© Faculty of Science, University of Port Harcourt, Printed in Nigeria *ISSN 1118 – 1931*

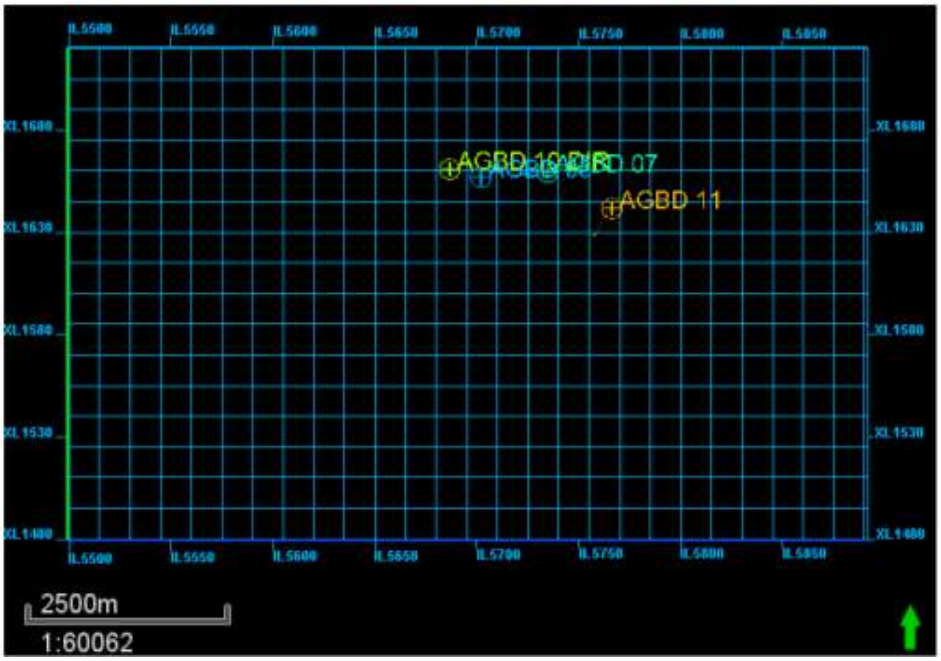

Fig 1: A base map showing the spatial relationship of the wells in the field

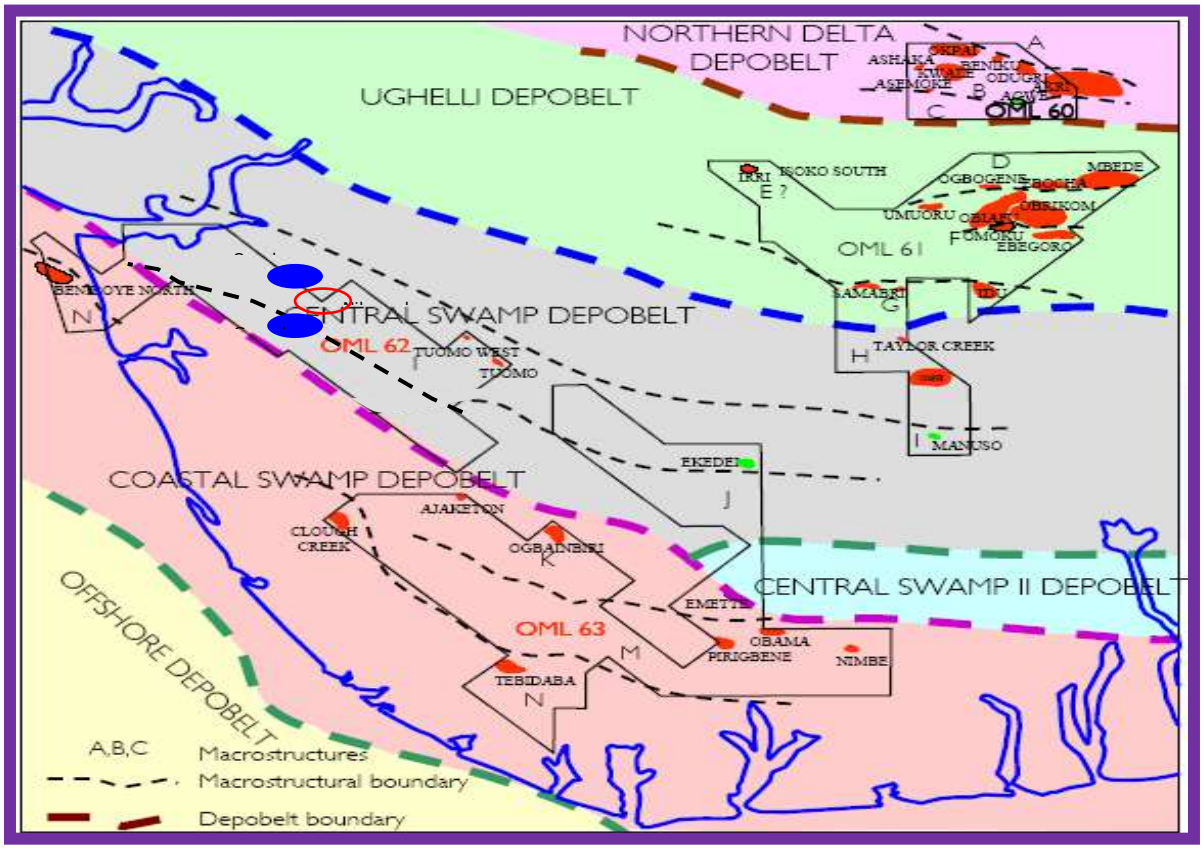

Figure 2: Map of Niger Delta showing the main depobelts in the basin (Modified from Stacher, 1995)

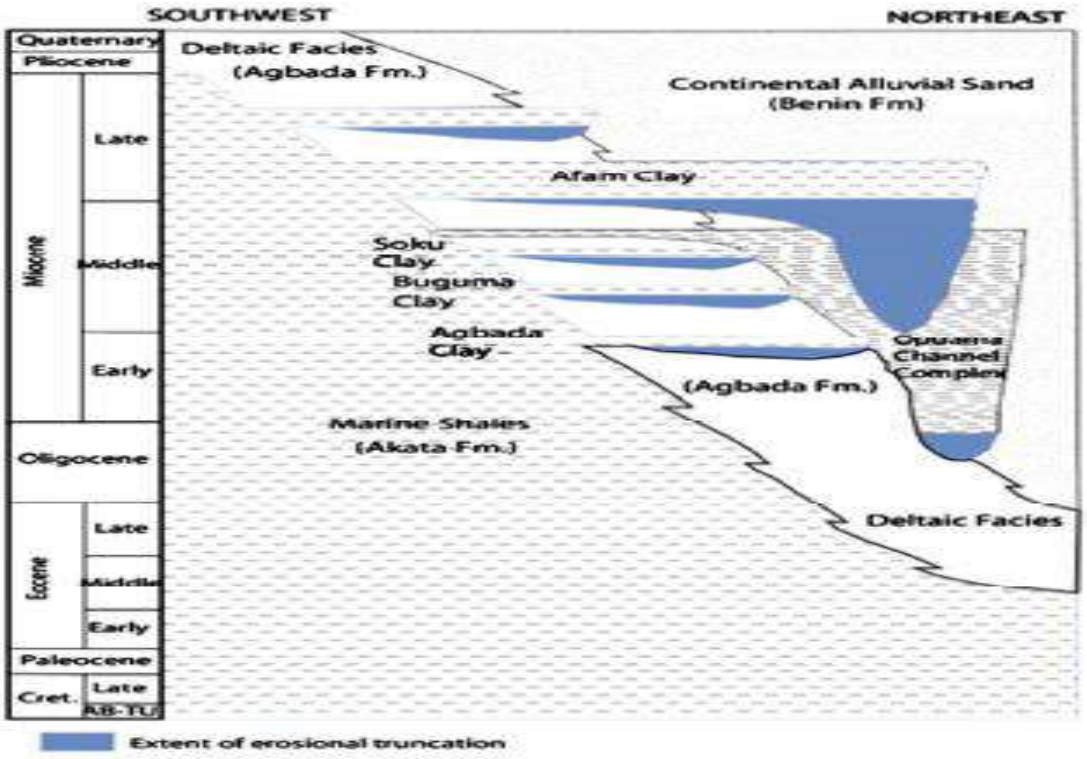

Figure 3.Stratigraphic column showing formations of the Niger Delta (Shannon and Naylor, 1989 and Doust and Omatsola, 1990).

The Akata Formation being the basal lithological unit in the basin is a marine pro-delta megafacies with an approximate thickness of 6000 meters. It comprises mainly of shales with occasional turbidite sandstones and siltstones the crops out in the outer delta area. Paleontological evidence mainly of planktonic foraminifera depicts an age range of Paleocene to Holocene for the marine shale and it is overpressured. It is the principal source rock in the geology of the Niger Delta. Deep sea fan sands were deposited within the upper Akata Formation by turbidity currents during development of the Delta (Burke, 1972).

The Agbada Formation stratigrapically underlies the Benin Formation and consists mainly of sandstones, siltstones and sands. The sandstones and sands are coarse to very fine grained, slightly unconsolidated with calcareous matrix in places. Lignite streak are common and they are poorly sorted except where they grade into shale. The formation consists of numerous offlap rhythms generating a paralic sequence of barrier sands, point bar sands, distributary channel sands and sand beds laid down as tidal channel fills, river mouth bars, natural leeves and shallow marine sand bars. It constitutes the main hydrocarbon reservoir in the basin.

The Benin Formation is a continental with Late Eocene to Recent deposit of alluvial and upper coastal plain sands. It marks the upper most unit of the delta complex and consists mainly of 2000 m thick fresh water-bearing massive continental sands and gravels which are deposited in the upper deltaic plain environment.

Scientia Africana, Vol. 21 (No. 1), April, 2022. Pp 1-18 *https://dx.doi.org/10.4314/sa.v21i1.1*
© Faculty of Science, University of Port Harcourt, Printed in Nigeria *ISSN 1118 – 1931*

MATERIALS AND METHODS

Research materials for this study were made available from wells drilled at *SAMO* field by Shell Petroleum Development Company (SPDC) in the Niger Delta. The materials include 3D Pre-Stack Seismic Data and Well log data suites from four wells which contain Gamma Ray (GR) Logs, Spontaneous Potential (SP) Logs, Porosity Logs and Resistivity Logs. The four wells were named as AGBD 10, AGBD 05, AGBD 07 and AGBD 11 (Figure 4). The Interpretation and well log correlation were done using PETREL, OPENDTECT and SURFER 13 software.

Well logs for the 4 wells were imported and used for the lithologic identification, and environment of deposition. The key logs used for lithologic discrimination were gamma ray, resistivity, compensated neutron porosity and bulk density logs. Available data sets were quality checked to determine data consistency.

The methods used for the study involve data gathering and loading of seismic volumes, well data, geologic information and QC seismic, seismic volume attribute analysis, well log interpretation and correlation, seismic data interpretation (faults and horizon interpretation), interpreting environment of deposition, well to seismic ties and acoustic analysis, petrophysical evaluation and well correlation and horizon interpretation.

Volume seismic attributes analysis provides new images that enhance the physical and geometric descriptions of the subsurface thereby giving a better and improved understanding of the subsurface. The definition of the structural and stratigraphic arrangement of the seismic interpretation is aided by geometric attributes, while physical attributes can be used as direct hydrocarbon or lithologic indicators. This was carried out on the seismic data using OPENDTECT 4.6.

Well log analysis is aclarification of well logs, whose features are deduced to develop the vertical stratigraphic sections (Homewood *et al.*, 1992) and its various stratigraphic markers. The gamma ray log provided aids the correlation of Sand-Sand and Shale-Shale across the wells. This generates a platform on which the logs, seismic data, core images and grid data were displayed and it evidently enables the completion and simulation of observations. The geological fault interpretation was done on a fine grid of every 10 inline and cross line of the seismic data. Petrophysical parameters calculated include volume of shale, porosity, permeability, water saturation. These parameters helped in understanding the rock properties of different facies interpreted from each depositional environment.

Well log correlation reveals the potential reservoirs and is subsequently mapped as horizons on the seismic volume. In all, six (6) sand units (Figure 4) were identified but the ones with appreciable thickness were eventually considered. This was carried out after the gamma log interpretation and after delineating sands on log. Peaks of seismic were interpreted as the troughs.

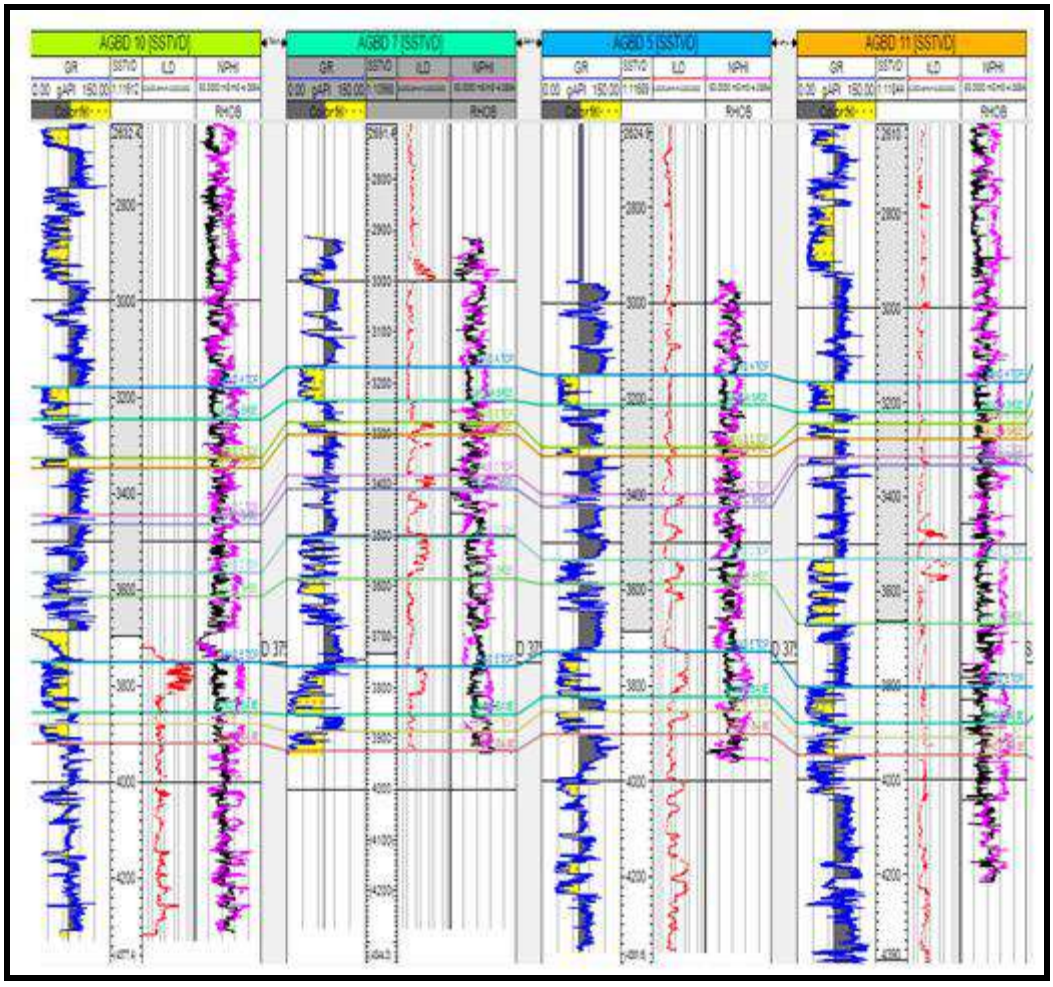

Figure 4: **Correlation across Well AGBD 10, AGBD 05, AGBD 07 and AGBD 11**

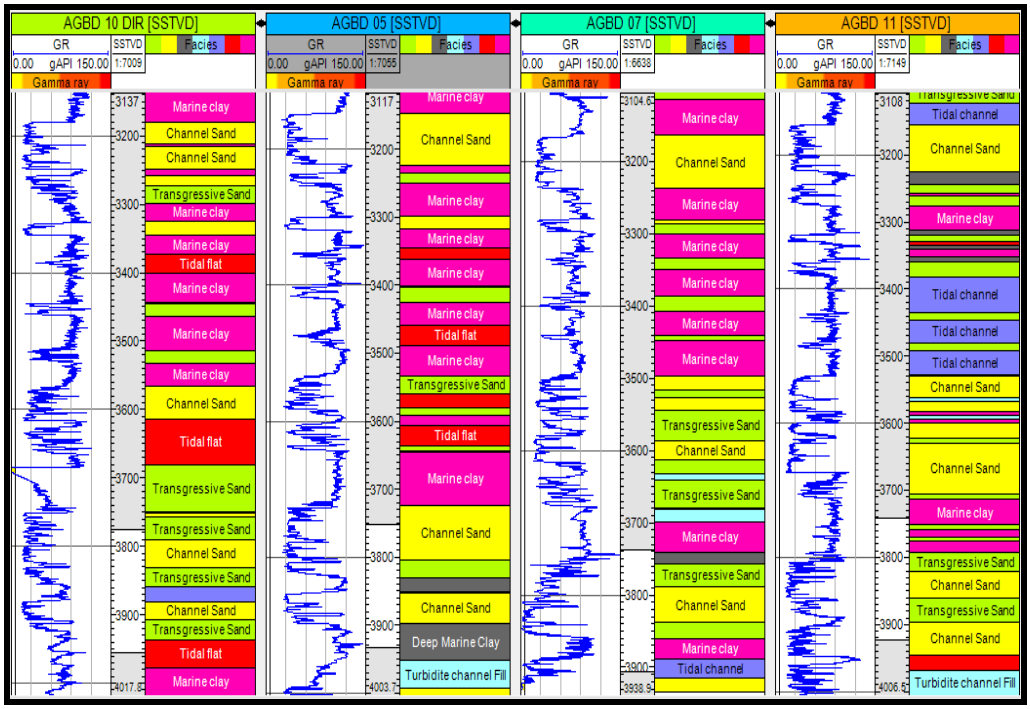

Figure 5: Lithofacies and depositional environment signatures in well logs

Scientia Africana, Vol. 21 (No. 1), April, 2022. Pp 1-18 *https://dx.doi.org/10.4314/sa.v21i1.1*
© Faculty of Science, University of Port Harcourt, Printed in Nigeria *ISSN 1118 – 1931*

The log motifs are applied in the classification of lithofacies and depositional environment (Figures 7 and 8). It is also the key parameter for determination of gross reservoir thickness. At the deeper sections where GR log values poorly differentiate the reservoirs from the non-reservoirs, we integrated it with sonic, density and resistivity logs, and the raw porosity log for better lithology definition.

Gamma Ray log values and signatures (Figure 5) following the Rider (1996) model and seismic data helped in determining lithofacies and depositional environments of the different rock units in the wells considered in the field.

Bell shaped log patterns observed on gamma ray logs is a typical feature of fluvial channel deposits and indicate fining upward trends or an upward increase in gamma ray log value. The funnel shaped motif observed is indicative of decrease shale content and coarsening upward sequence resulting from rapid sedimentation (deltaic progradation). The consistent trend of the gamma ray values with sharp top and base delineated is typical of cylindrical shaped log motif and is indicative of a consistent lithology. The serrated log responses at some interval are a clear indication of intercalation of thin shale sequence in a sandstone body.

The key surfaces delineated after recognition of facies stacking patterns and parasequences enhanced by the consistent display of log trends includes; Sequence Boundary (SB), Maximum Flooding Surfaces (MFS), and the transgressive or flooding surfaces. Key flooding surfaces were picked on the basis of density, neutron and resistivity log responses from wells.

Maximum Flooding Surface (MFS) was recognised on the logs and seismic data as: the boundary between retrogradationalparasequence sets and progradationalparasequence sets; units with maximum shale peaks and well-developed shales clearly seen on the GR, Resistivity and Neutron logs. Maximum Flooding Surfaces were also correlated across the wells as shown in Figure 6.

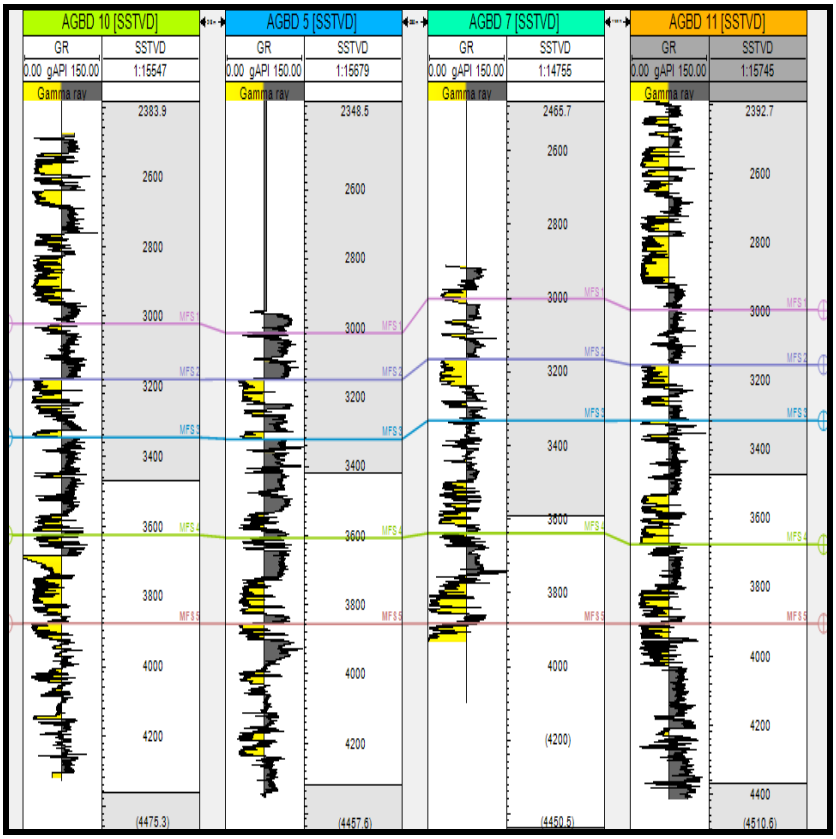

Figure 6: MFS correlation of the wells in the study area

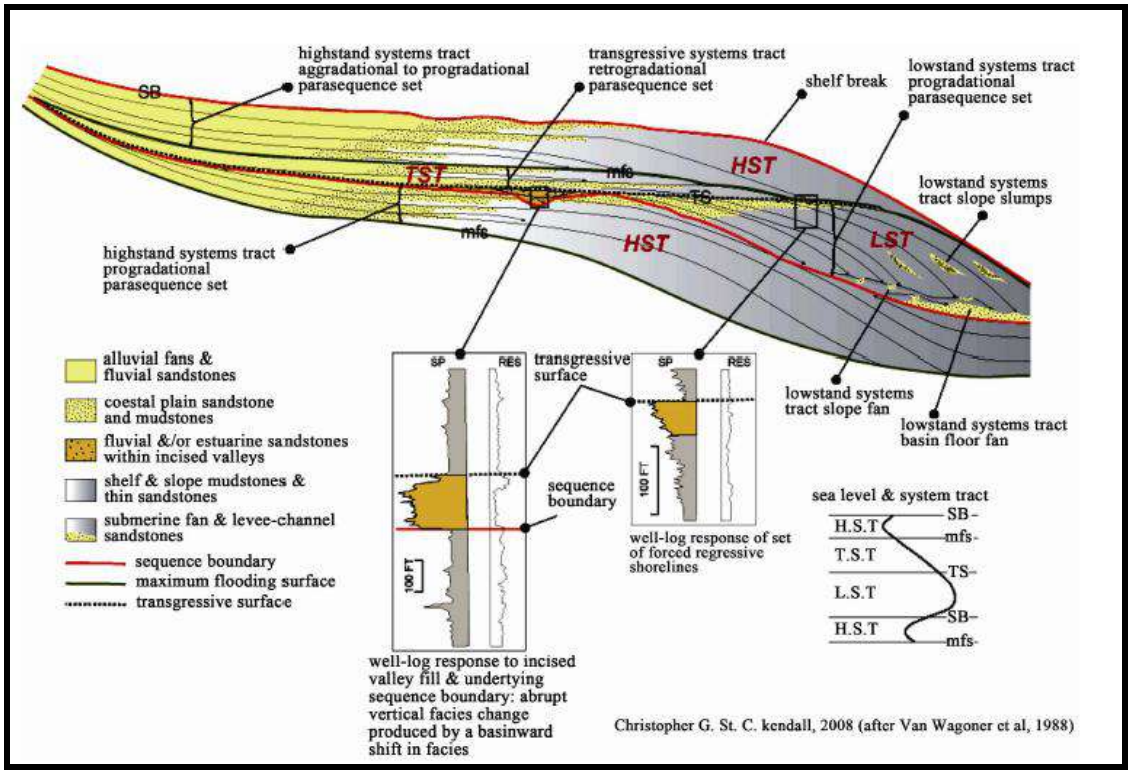

Figure 7.Sequence stratigraphic model showing key stratigraphic surfaces and various systems tracts (Van Wagoner *et al.*, 1988).

Scientia Africana, Vol. 21 (No. 1), April, 2022. Pp 1-18 *https://dx.doi.org/10.4314/sa.v21i1.1*
© Faculty of Science, University of Port Harcourt, Printed in Nigeria *ISSN 1118 – 1931*

The Maximum Flooding Surface tops the Transgressive System Tracts (TST). It represents the most landward transgression of the shoreline.

Sequence Boundaries (SBs) were acknowledged in regions of lesser Gamma Ray, high Resistivity, SP and sonic logs responses within the surface section. Sequence boundaries were recognized by the most basinwardchange in facies within a coarsening upward sequence (Emery and Myers, 1996) i.e. recognized by sand-rich facies, within a coarsening upward sequence. These are usually located between two maximum flooding surfaces and are recognized by an erosional surface between a lowstand and a highstand system tract. Sequence Boundary (SB) was used to define the base of a progradational stacking pattern in the section.

Systems Tracts (Lowstand Systems Tract, Transgressive Systems Tract, and Highstand Systems Tract) were recognized and mapped with the aid of the depositional sequence model (Figure 7).

Figure 8 shows gamma ray log responses for depicting different environments of deposition.

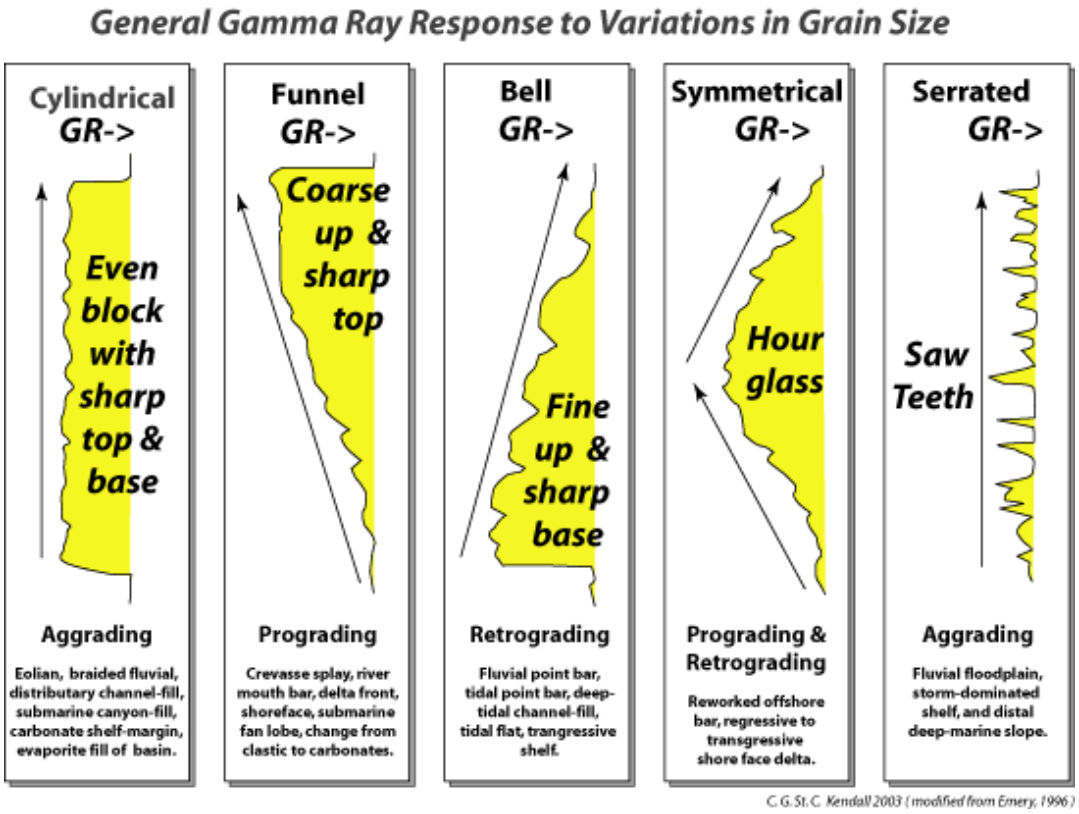

Figure 8. Well log response character for different environments from gamma ray pattern (Rider, 1996),

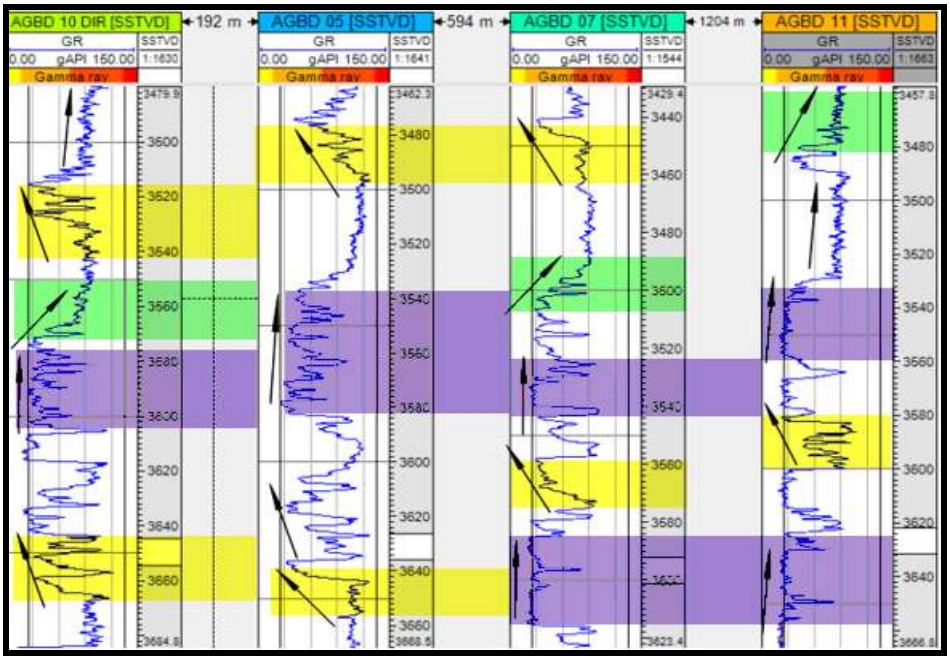

Figure 9. Representative parasequence stacking patterns in the four wells,

RESULTS AND DISCUSSION

Lithostratigraphy

The lithology of the field is dominated by alternating shale and sand and the dominant sequence is coarsening upward trend and block shaped. Lithologic description is solely based on gamma ray, resistivity and other log motifs.

Bell-Shaped Successions

The bell-shaped interval delineated from the gamma ray logs in the wells, where they occur have thicknesses less than 15 m. They occur in the portion of the sands of AGBD 10 and in other wells. It is observed that some gamma ray log responses in the sand at some interval display bell motif above a thin funnel motif. This gives rise to the serrated nature of the log response characteristic of tidal channel to deep tidal channel and fluvial or deltaic channel succession.

Cylindrical-Shaped Successions

The *SAMO* field reservoir units also display a cylindrical shaped sand succession (Figure 10). This shape characterized by the gamma ray logs of the sand bodies of AGBD 10, AGBD 5, AGBD 7 and AGBD 11. The upper and lower boundaries of sand successions are sharp and bounded by marine clay.

Funnel-Shaped Successions

The funnel shaped succession is more pronounced in this field than the bell shaped type. They also occur as serrated. They characterize the sands of the sand bodies of AGBD 10, AGBD 5, AGBD 7 and AGBD 11. The gamma ray log trend of AGBD 10 (Figure.10), which occurs between depths of 3250 and 3300 m, is serrated and funnel-shaped with a thickness of about 6 m. The style is typicallydeduced to specify deposition of cleaning upward sediment or arise in the sand constituent of the turbidite bodies, as related to a deep marine situation.

Scientia Africana, Vol. 21 (No. 1), April, 2022. Pp 1-18 *https://dx.doi.org/10.4314/sa.v21i1.1*
© Faculty of Science, University of Port Harcourt, Printed in Nigeria *ISSN 1118 – 1931*

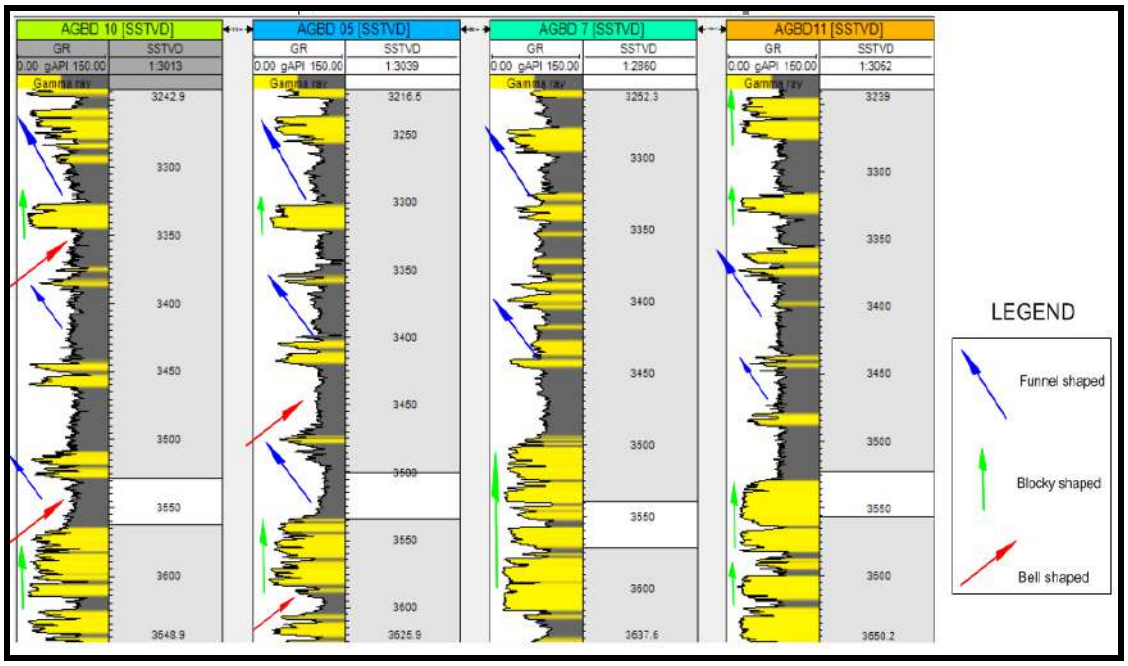

Figure 10: Shaly-sandtone facies defined by predominant funnel-shaped Gamma Ray Logs

Lithofacies and Depositional Environments

The stratigraphic column as observed in the gamma ray log in the study area is divided into three (3) lithofacies, namely; coarse grained basal sandstones facies; shaly sandstone facies and shale facies.

The coarse grained basal sandstone facies comprise of amalgamated and isolated sharp-based fining upward sand bodies identified by block to bell-shaped gamma ray log motif with little or no parting on the Neutron-Density Logs (Figure 4). The sand units are locally separated by thin bands of shale/mudstone. These faciesare interpreted as fluvial channel deposits based on these characteristics (Figure 11). These channel deposits signify deposition in a coastal plain setting landward of the tidal zone. The Shaly-Sandstone Facies is characterized by the predominance of fine-medium grained sandstones and mudstone/shale interbeds generating a log response interval of serrated funnel shaped and serrated bell to blocky shaped pattern (Figure 12). These intervals also display high values on the neutron density and porosity log motifs.

The shale facies is predominantly composed of shale units with thin siltstone intercalations displaying a retrogradationalparasequence pattern (Figure 9). The channel sand from the gamma ray log is integrated with the seismic and shown as an attribute (Figure 13).

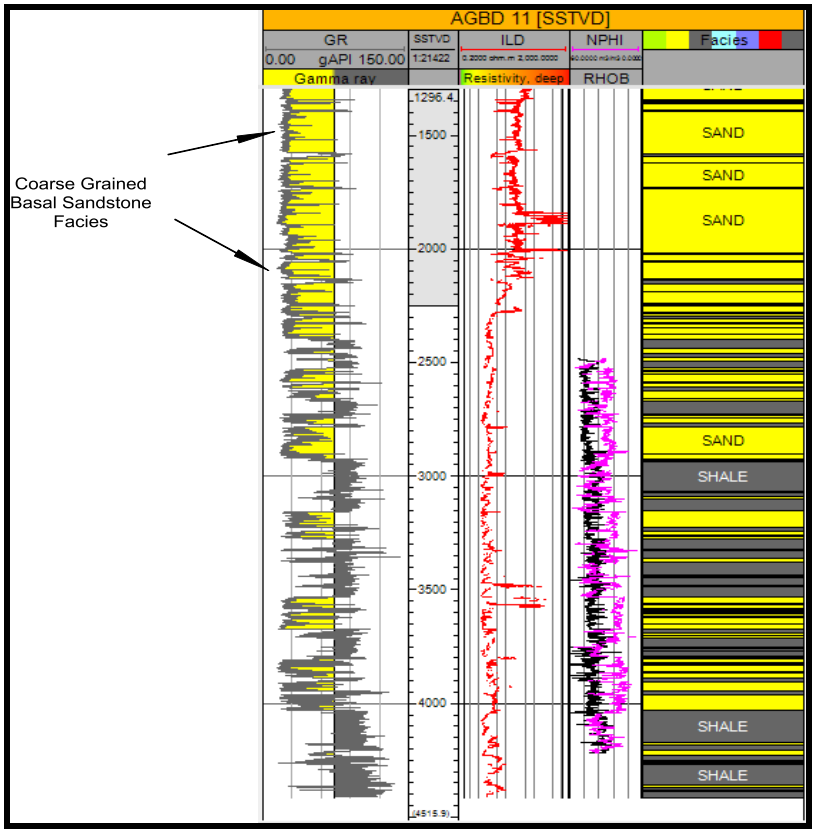

Figure 11.Coarse grained basal sandstone facies on AGBD 11.

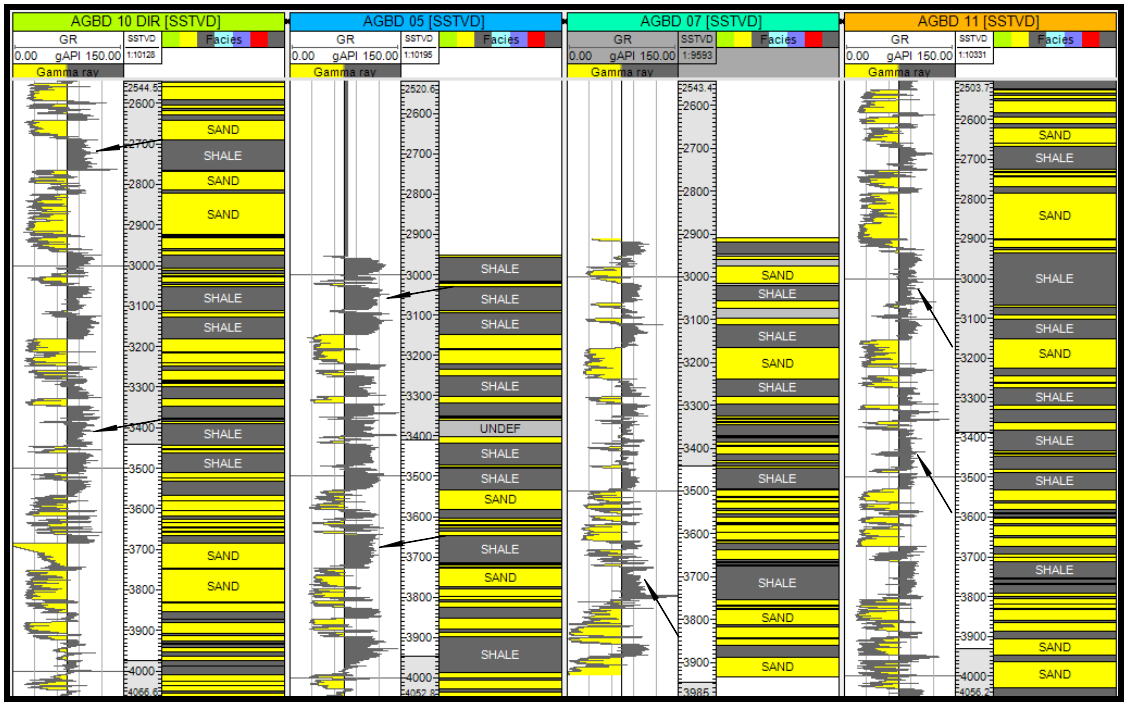

Figure 12.Shale facies and intercalations of sandstone and shale in the wells.

Scientia Africana, Vol. 21 (No. 1), April, 2022. Pp 1-18 *https://dx.doi.org/10.4314/sa.v21i1.1*
© Faculty of Science, University of Port Harcourt, Printed in Nigeria *ISSN 1118 – 1931*

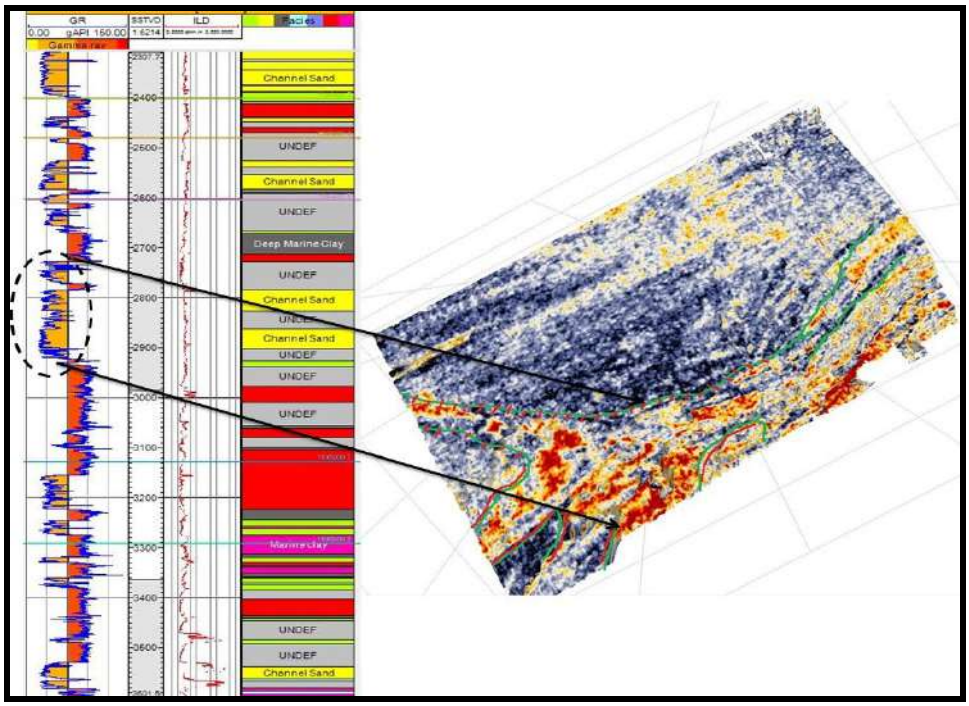

Figure 13: Evidence of channeled sand fills (blocky shaped succession) from the gamma log and seismic slice.

From the stated analyses above, the palaoenvironment of deposition (Figure 14) was inferred as;

i. Marine environment: facies in of the AGBD 05 and AGBD 11 are of marine and deep marine environment.

ii. Transitional environment: the transitional environment is revealed as tidal flats and deltas

- Tidal Flats**:** mud covered flats that are alternately exposed and inundated.
- Deltas: formed at the mouth of a river, delta consist of cross bedded sands that fine outward and upward.

iii. Channeled environment: the channeled sands in the AGBD 05, AGBD 10, AGBD 11 and AGBD 07 were revealed to be of channeled environment. They also have Hydrocarbon potentials when integrated with resistivity logs from the well.

Depositional Sequence Tract architecture and sequence stratigraphy of the study well

Transgressive Systems Tract (TST) his system tract develops as a result of an increase in the rate of sea-level rise which has an overall deepening upward bathymetric signature (Posamentier *et al.*, 1988). It is a period of increasing rate of relative sea level that is characterized by an overall fining upward sequence.The TST is composed of retrogradationalparasequence sets. The TST in the wells at an interval of 3000m - 3150m is defined based on its fining upward sequence. The lower section of this interval is predominantly shale, the mid-section shows sandstone and shale intercalation, while a predominance of shale caps the top section of the interval.

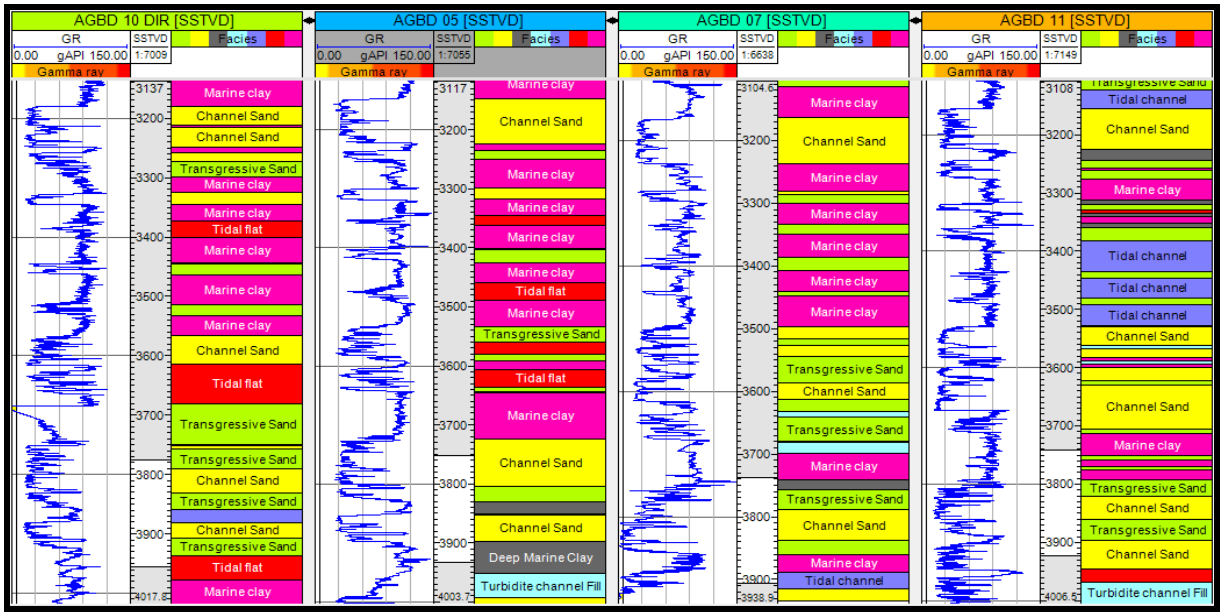

Figure 14: Deposition of facies in their environment in the study well.

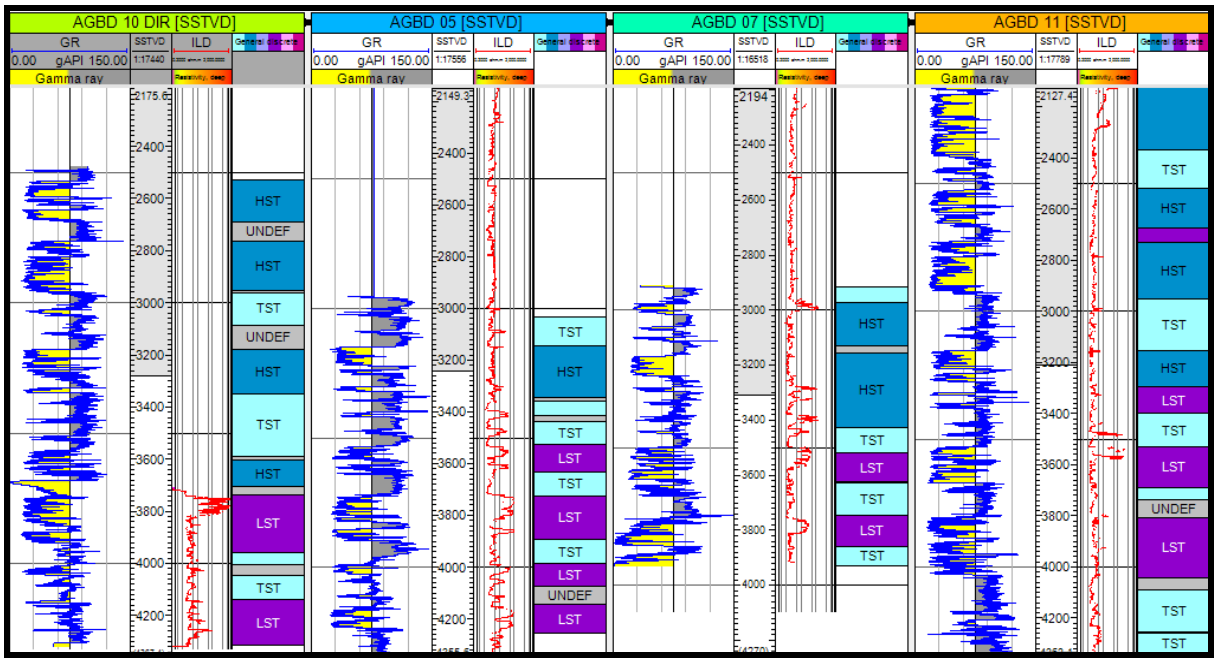

Figure 15: Transgressive system tract of the wells.

Highstand Systems Tract (HST)

During this stage, the sea-level rise decreases and they are characterized by initially aggradational deep sea shale that grade into intervals of shallowing upwards (Boggs, 1995). This system tract is first defined at an interval of 2950m - 3030m. This progradational sequence is characterized by shale, silt and sand lithofacies, with gradual decrease in the percentage occurrence of shale. This suggest an overall coarsening (shallowing upward) sequence.

Scientia Africana, Vol. 21 (No. 1), April, 2022. Pp 1-18 *https://dx.doi.org/10.4314/sa.v21i1.1*
© Faculty of Science, University of Port Harcourt, Printed in Nigeria *ISSN 1118 – 1931*

Lowstand Systems Tract (LST) The LST is a period defined by very low rate of relative sea level rise or standstill and comprising progradational to aggradationalparasequence sets. The LST in well 11 is defined at an interval of 3350m - 3600m (Figure 15). This interval shows interbedding of shale and sandstone at the lower section, and siltstone, shale and sandstone interbedded at the top, though the siltstone and shale beds thin upwards while the sandstone becomes relatively thick.

Maximum Flooding Surface (MFS)

These are the periods between maximum relative sea level rise and maximum relative sea level characterized by abundant and diverse fauna. The maximum flooding surface tops the transgressive system tract and depicts the shift from retrogradational stacking in the transgressive system tract to aggradational or progradational stacking in the initialhighstand system tract.

The marine sand of TST and the thick massive sand of LST could form excellent hydrocarbon reservoir given the right conditions from the studied well. These sands are well sorted with high resistivities and low gamma ray logs values (Figure 14). S. However, the shale units delineated from the TST and HST may be suggested to form the top and bottom seal for the hydrocarbon in the *SAMO* field reservoir sands.

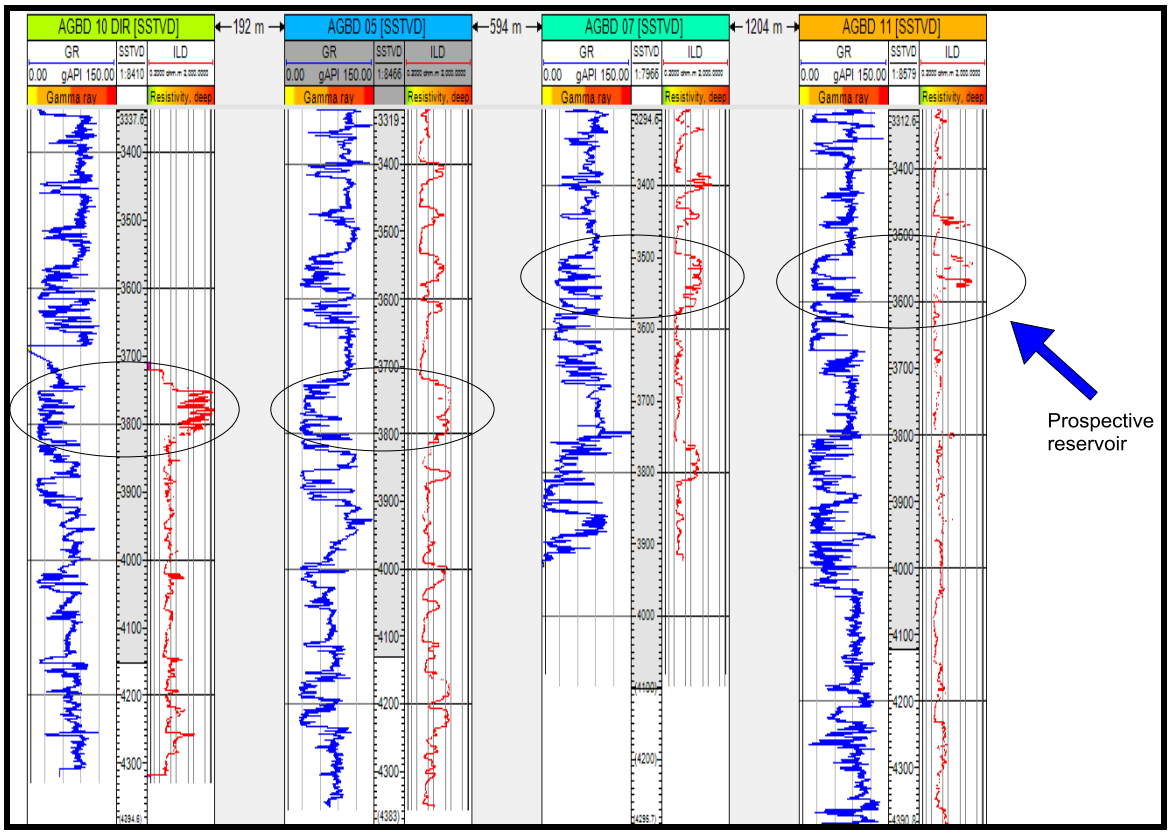

Fig 16.Reservoir potential of the wells.

CONCLUSION

Well log and seismic data of *SAMO* field located within the central swamp depobelt, Niger Delta basin were utilized to study the sequence stratigraphy and to interpret its depositional facies. The combination of the gamma ray log responses with seismic data interpretation helped in generating a series of log facies. The log facies were used to describe the depositional environment of the four wells. Log facies were recognized in the study area. The facies here included the Coarse Grained Basal Sandstone, Shaly-Sandstone Facies and Shale Facies. The facies represents palaeo-depositional environments of basin plain, crevasse splay, slope channel and transgressive marine shelf.

The predominant lithologies observed in the wells from the logs are sand, silt and clay. Bulk of the sand bodies is those of the slope channel-fills and turbidite fans. The interpreted lithologies were interpreted from different log shape motifs from the available Gamma-ray/Resistivity logs. Hence we had the bell shaped of the gamma ray log, with sharp base and top indicating fining upward sequence of decreasing sand size and increasing shaley contents. Also the blocky (boxcar or cylindrical) intervals of approximately low gamma ray log values typical of channel deposits/ barrier island in the four wells. The funnel shaped log pattern whose lithology is interpreted to indicate a sudden coarsening (sandy) upward trend (progradational delta). Also a symmetrical log shaped signifying regressive and trangressive phase of the field. The palaeo-reconstruction indicates that the reservoir sedimentary setting is predominantly channel environment and comprises fluvial sand deposits.

The depositional sequences underwent major significant flooding episodes. Derived variations in relative sea water level delineated third order depositional systems that were made up of Lowstand Systems Tract (LST) at the base of the section, Transgressive Systems Tract (TST) which is at the middle of the section and the Highstand Systems Tract (HST) which marked the top of each section.

In terms of hydrocarbon implication, the sand units of the LST and HST formed the channel and shoreface sands of the delta. The high resistivity log values within the sand area showed that they are good hydrocarbon reservoirs potential. The shales from the TST which majority of the MFS were identified form a good seal to the reservoir layers. The reservoir sands of the LST and that of HST and the shale layers of the TST can together provide good stratigraphic traps for hydrocarbon and therefore should also be a point of consideration during hydrocarbon exploration.

REFERENCES

Adegoke, A.K. (2012): Sequence Stratigraphy of some late Miocene Sediments, Coastal Swamp Depobelts, and Western Offshore Niger Delta. International Journal of Science and Technology, 2 (No.1): 1-3

Adejobi, A.R., Olayinka, A.I. (1997): Stratigraphy and hydrocarbon potential of the Opuama channel complex area, western Niger delta. Nigeria. Association of petroleum Exploration (NAPE) Bull., 12:1-10.

Scientia Africana, Vol. 21 (No. 1), April, 2022. Pp 1-18 *https://dx.doi.org/10.4314/sa.v21i1.1*
© Faculty of Science, University of Port Harcourt, Printed in Nigeria *ISSN 1118 – 1931*

Allen, J.R.L. (1965): Late Quatenary Niger Delta and adjacent areas: sedimentary environments and lithofacies. AAPG Bull., l (49): 547-600.

Barde, J.P., Chambertain, P., Gralla, P., Harwijanto, J., Marsky, J. and Schroeter, T. (2000). Explaining a complex hydrocarbon system in the Permo- Triassic of the pre-Caspian basin by integration of independent models.Abstracts, 62nd European Association of Geoscientists and Engineers Conference and Technical Exhibition, 2 (21), 4.

Barde, J.P., Gralla, P., Harwijanto, J. and Marsky, J. (2002): Exploration at the eastern edge of the pre-scapian basin impact of data integration on upper Permian and Triasicprospectivity. American Association Petroleum Geology. Bulletin, 86: 399-415.

Boggs. S. (1995): Principles of Sedimentology and Stratigraphy," 2nd Edition, Prentice Hall, Englewood Cliffs.725p

Burke, K.C. (1972):Longshore drift submarine canyons and submarine fans in the development of the Niger Delta. *AAPG Bulletin 56*:1975-1983

Emery, D. &Myers, K.J. (EDS). (1996): Sequence Stratigraphy. Oxford, Blackwell Science.

Fayose, E.A. and Ola, P.S. (1990): Radiolarian occurrences in the Ameke type section, eastern Nigeria. J. Mining and Geol., 26:132-138.

Okosun, E.A., Chukwu, J.N., Ajayi, E.G., and Olatunji, O.A., (2012).Biostratigraphy, Depositional Environment and Sequence Stratigraphy of Akata Field (Akata 2, 4, 6 and 7 Wells), Eastern Niger Delta, Nigeria. International Journal of Scientific & Engineering Research 3 (7): 1 - 27

Omatsola, E. (1982): Geology of Niger Delta, Shell International Mij. The Hague; Netherlands, 103-112.

Posamentier, H. W. and Allen, G. P. (1999): Siliciclastic sequence stratigraphy: concepts and applications. SEPM Concepts in Sedimentology and Paleontology No. 7: 210.

Posamentier, H. W. and James, D. P. (1993): An overview of Sequence Stratigraphy – uses and abuses, sequence stratigraphy and facies association. *In* H. W. Posamentier, C. P. Summerhayes, B. U. Haq and G. P. Allen, Eds.), *Sequence Stratigraphy and facies association.International Association of Sedimentologist Special Publication* 18 :3-18. Oxford: Wiley. Blackwell

Posamentier, H. W., Jervey, M. T. and Vail P. R. (1988): Eustatic controls on clastic deposition I – conceptual framework. *In Sea Level Changes–An Integrated Approach* (C. K. Wilgus, B. S. Hastings, C. G. St. C. Kendall, H. W. Posamentier, C. A. Ross and J. C. Van Wagoner, Eds.), 110–124. SEPM Special Publication 42.

Reijers, T.J.A., Petters, S.W. and Nwajide, C.S. (1997): The Niger Delta Basin. In Selley, R.C. (eds.). African Basins-Sedimentary Basin of the World 3: Amsterdam. *Elsevier Science*pp. 151-172.Riders, M., (1996). Geological interpretation of well logs (2nd Edition): Whittles Publishing, 280 pp.

Short, K.C. and Stauble, A.J. (1967): Outline of Geology of Niger Delta: American Association of Petroleum Geologists Bulletin, 51:761-799.

Stacher, P. (1995): Present understanding of the Niger delta hydrocarbon habitat, in Oti, M. N. and Postma, G., eds., Geology of deltas: Rotterdam, A.A. Balkema, 257-267.

Tuttle, M. L. W., Charpentier, R. R. and Brownfield, M. E. (1999): "The Niger Delta Petroleum System: Niger Delta Province, Nigeria, Cameroon, and Equatorial Guinea, Africa," USGS Open-File Report 99-50-H

Vail, P. R., Mitchum, R. M. JR. and Thompson, S., III (1977): Seismic stratigraphy and global changes of sea level, part four: global cycles of relative changes of sea level. *American Association of Petroleum Geologists Memoir* 26: 83–98.

Vail, P. R., Audemard, F., Bowman, S. A., Eisner, P. N. and Perez-Cruz, C. (1991): The stratigraphic signatures of tectonics, eustasy and sedimentology– an overview. *In Cycles and Events in Stratigraphy*. (G. Einsele, W. Ricken and A. Seilacher, Eds.), 617–659. Berlin, Springer-Verlag

Van Wagoner, J.C., Posamentier, H.W., Mitchum, R.M.JR., Vail, P.R., Sarg, J.F., Loutit, T.S. and Hardenbol, J. (1988):An Overview of Sequence Stratigraphy and Definitions, Sea level changes, an integrated approach, in: C. K. Wilgus, B. S. Hastings, H.M. Posamentier, J.C. Van Wagoner, C.A. Ross, and C. G. Kendall, (eds.)Society of Economic Paleontologist and Mineralogist Special Publications, 42: 39 – 45

Weber, K.J. (1971): Sedimentological aspects of oil fields in the Niger Delta. Geologic En Mijnbouw, 50: 559-576.

Weber, K.J. and Daukoru, E.M. (1975): Petroleum geological aspects of the Niger Delta. *9th World Petroleum Congress Proceedings*, 209-221.

Whiteman, A.J. (1982): Nigeria: Its Petroleum Geology, Resources and Potential. Graham and Trotman, London, 394pp.

Scientia Africana, Vol. 21 (No. 1), April, 2022. Pp 19-26 *https://dx.doi.org/10.4314/sa.v21i1.2*
© Faculty of Science, University of Port Harcourt, Printed in Nigeria *ISSN 1118 – 1931*

BIOMONITORING AND BIOMARKER RESPONSE OF FISH SMOKERS TO POLY AROMATIC HYDROCARBONS IN RIVERS STATE, NIGERIA

Agu, G. E. and Oriakpono, O. E.
[1]Department of Animal and Environmental Biology, Faculty of Science,
University of Port Harcourt, P.M.B. 5323, Port Harcourt, Rivers State, Nigeria.
[2]Department, University, East-West Road, P.M.B 5323, Nigeria.
*****Corresponding author's Email: ezinne_agu@uniport.edu.ng
obemeata.oriakpono@uniport.edu.ng

Received: 22-11-2021
Accepted: 12-02-2022

ABSTRACT

A study was carried out on 40 volunteer fish smokers, 10 from each Station. Station 1 (Alakahia market), Station 2 (Choba Market), Station 3 (Choba main market) and Station 4 (Rumosi Market) all in Obio/akpor Local government of Rivers state, Nigeria. The study was carried out for a period of 12 weeks, to evaluate the health status of exposed individuals to poly aromatic hydrocarbons gotten from smokes, using haematological parameters and urine analysis. The cyanohaemoglobin method was used to determine haemoglobin (Hb), packed cell volume (PCV) was determined by micro haematocrit method, Red blood cell (RBC) was determined with the improved Neubauerhaemaocytometer, WBC was determined with the improved Neubauer counter, Neutrophils, lymphocytes and Eosinophils were determined on blood film stained with mayGrunwald-Giemsa stain while Gas Chromatography was used for urine samples.PCV from station 1, 2, 3 and 4 had a mean value of 38.33, 38, 33.33 and 35.00 respectively with significant difference (P<0.05) occurring in station 3 when compared to the other stations and within stations 2, 3 and 4. Hb had a mean value of 12.8, 12.67, 11.13 and 11.67 in stations 1, 2, 3 and 4 respectively also with significant difference (P<0.05) occurring in station 3 when compared to the other stations and within stations 2,3 and 4. WBC had a mean value of 4.77, 6.23, 5.93and 4.83 in stations 1, 2, 3 and 4 with no significant difference (P>0.05), the RBC had a mean value of 4.40, 4.33, 3.60 and 3.90 in stations 1, 2, 3 and 4, Neutrophil had a mean value of 36.67, 46.0, 41.0 and 41.0 in stations 1, 2, 3 and 4. Stations 1, 2, 3 and 4 had a mean value of 58.33, 47.67, 57.67 and 57.33 for lymphocytes and 5.0, 9.33, 1.33 and 1.67 for Eosinophil. It was recorded that the different stations had no statistically significantly difference (P>0.05) for RBC, Neutrophil, Lymphocyte and Eosinophil. The urine analysis revealed that station 1 had a total PAH of 0.1726, station 2 had a total of 0.058 while station 3 and 4 had a total of 0.088 respectively. The results reveal that the smokers have PAHs in their body with increases risk of Kidney disease, Anaemia, Bronchitis and other lung diseases.

INTRODUCTION

In most urban cities of Nigeria today, people are exposed to dangerous chemicals and other toxic compounds without any form of protection. This is caused due to occupational exposure or activities, occupations such as fish smoking is one of such occupations and these smokers are not usually properly educated, so they are ignorant of the long term effects of incomplete combustion of carbonaceous materials on their health (Suchanova*et al*., 2008). About 100 different chemicals are formed during the incomplete combustion of coal, oil, gas and garbage or other

organic substances such as tobacco or charbroiled meat (ATSDR, 1995). These compounds are known to be carcinogenic (Suchanova*et al*., 2008). Human exposure to PAHs occurs in three main ways; Inhalation, dermal contact and consumption of contaminated food or diet (Farhadian*et al*., 2011). Regarding to the generation of smoke, it has been showed that poplar wood generated the highest number and concentration of total and carcinogenic PAHs, while oak, cherry tree, beech samples were similarly less effective. Hard wood instead of soft wood have been recommended considering the amount of PAHs produced (Guillen *et al*.,2000). Smoking of food especially fish is one of the most ancient technologies which has been used for years (Simko,2002), the highest concentration of PAHs in smoked products such as smoked fish is obtained immediately after the smoking is done. The concentration decreases due to decomposition, trigged by light and interactions with other compounds also present in the environment (Simko, 1991). The actual levels of PAHs in smoked foods depends on several variables in the smoking process, including types of smoke generator, combustion temperature and the degree of smoking (Gracia-Falcon and Simal-Gandara, 2005). Wood smoke exposure causes a decrease in lung function and an increase in the severity of existing lung diseases, it has also been reported that wood smoke aggravates asthma, emphysema, pneumonia and bronchitis with long term exposure leading to arteriosclerosis, throat, lung and lymph system cancer (American Lung Association, 1991). Exposure of preschool children living in homes heated with wood burning, stoves or in houses with open fireplaces yielded the following effects; decreased pulmonary lung function in young asthmatics (Koenig *et al*., 1993), increased incidence of acute bronchitis and frequency of wheezing and coughing and also increased incidence duration and possible severity of acute respiratory infections (Collins *et al*., 1990; Kammen*et al*., 1998). PAHs are considered environmentally significant because of their potential toxicity to the higher organisms and resistance to microbial attack (Kanaly and Harayama, 2000). Some PAH are highly carcinogenic, genotoxic and cytotoxic (Boldrin*et al*., 1993), PAHs and their derivatives have been recognized as the major culprit causing human lung cancer, anaemia, asthma, splenomegaly, bladder cancer and breast cancer etc, (Okana*et al*., 2005; Booker and White, 2005; Hazra*et al*., 2004; Miller *et al*., 2005). Some major compounds found in PAHs include Benzo(a)pyreneand Anthracene.Anthracene exhibit toxicity to fish, algae and show bioaccumulation in the food chain (Sutherland, 1992) while benzo(a)pyrene short term exposure can result in skin rash or eye irritation with redness and/or a burning sensation while long term exposure can lead to loss of colour, thinning of the skin, wart and bronchitis (EPA, 2004). Considering the health risk of smoking fish not just to the consumers of the smoked fish but also to the smokers themselves, this study is aimed at evaluating the health effects incurred by fish smokers using biomarkers in blood and urine analysis.

Scientia Africana, Vol. 21 (No. 1), April, 2022. Pp 19-26 *https://dx.doi.org/10.4314/sa.v21i1.2*
© Faculty of Science, University of Port Harcourt, Printed in Nigeria *ISSN 1118 – 1931*

MATERIALS AND METHODS

Sample Collection: Samples were collected from 40 exposed subjects, 10 from each station. These exposed subjects are individuals that use fire wood to smoke fish and the study location was based on accessibility to the markets and availability of volunteers. Station 1 (Alakahia market), Station 2 (Choba Market), Station 3 (Choba main market) and Station 4 (Rumosi Market) all in Obio/akpor local government of Rivers state, Nigeria. A total of 5ml of venous blood was collected from 40 volunteers using sterilized syringes; urine samples were also collected for analysis. The samples were transported on ice to the laboratory and were processed within 2 h after collection.

Biochemical Analysis: The cyanohaemoglobin method was used to determine haemoglobin (Hb) by using diagnostic kits from Sigma diagnostics USA, and packed cell volume (PCV) was determined by micro haematocrit method. Red blood cell (RBC), and thrombocyte count were determined with the improved Neubauerhaemaocytometer according to Dacie and Lewis (1991). WBC was determined with the improved Neubauer counter, while differential counts as Neutrophils, lymphocytes and Eosinophils were determined on blood film stained with mayGrunwald-Giemsa stain (Miale, 1982). The urine was collected in an amber vials with a cap and a Teflon septum. Samples were preserved at pH<2.0 with sodium bisulphate, 10ml of the sample were removed and discharged through the septum with glass syringe. 3ml of n-pentane were then injected through the septum with a 5ml syringe. The sample was extracted for 2mins in a Vortex apparatus. The vials were then opened and 1.5ml of the organic extract were placed into the vials and used for the GC analysis.

Method of Data Analysis: Data were analyzed using Tukey test at a level of 5% probability, using Assitat Software Version 7.7 en (2017).

RESULTS

The effects of PAH from Fish smoking on the haematological parameters of the fish smokers are shown in Table 1, for PCV station 1, 2, 3 and 4 had a mean value of 38.33, 38, 33.33 and 35.00 respectively with significant difference ($P<0.05$) occurring in station 3 when compared to the other stations and within stations 2,3 and 4. Hb had a mean value of 12.8, 12.67, 11.13 and 11.67 in stations 1, 2, 3 and 4 respectively also with significant difference ($P<0.05$) occurring in station 3 when compared to the other stations and within stations 2,3 and 4. WBC had a mean value of 4.77, 6.23, 5.93and 4.83 in stations 1, 2, 3 and 4 with no significant difference ($P>0.05$), the RBC had a mean value of 4.40, 4.33, 3.60 and 3.90 in stations 1, 2, 3 and 4, Neutrophil had a mean value of 36.67, 46.0, 41.0 and 41.0 in stations 1, 2, 3 and 4. Stations 1, 2, 3 and 4 had a mean value of 58.33, 47.67, 57.67 and 57.33 for lymphocytes and 5.0, 9.33, 1.33 and 1.67 for Eosinophil. It was recorded that the different stations had no statistically significantly difference ($P>0.05$) for RBC, Neutrophil, Lymphocyte and Eosinophil. The urine analysis revealed that station 1 had a total PAH of 0.1726, station 2 had a total of 0.058 while station 3 and 4 had a total of 0.088 respectively.

Table 1. Effects of PAH from Fish smoking on the haematological parameters of the fish smokers

Stations	PCV (%)	Hb (g/dl)	WBC (mm^3)	RBC (10^12/ L)	L (%)	N (%)	E (%)
1	38.33±0.58 [a]	12.80±0.17 [a]	4.77±1.70[a]	4.40±0.53[a]	58.33±9.24 [a]	36.67±14.50 [a]	5.00±5.29[a]
2	38.00±2.00[ab]	12.67±0.65[ab]	6.23±1.86[a]	4.33±0.76[a]	47.67±4.73 [a]	46.00±1.73 [a]	9.33±5.01[a]
3	33.33±2.89 [b]	11.13±0.98[b]	5.93±1.16[a]	3.60±0.46[a]	57.67±7.23[a]	41.00±6.93 [a]	1.33±0.58[a]
4	35.00±1.00[ab]	11.67±0.35[ab]	4.83±0.92[a]	3.90±0.17[a]	57.33±0.58[a]	41.00±2.65[a]	1.67±2.36[a]

Key: PCV= Pack cell volume, Hb= Haemoglobin, WBC= White blood cell, RBC= Red blood cell, N= Neutrophil, L= Lymphocyte,E= Eosinophil,

[a-b] Different letters in the same column indicate significance difference ($p<0.05$) within the stations

Reference range (Timzing et al., 2014)
RBCs × 10^12/ L: Male: 4.5-5.5; Female: 4.0 -5.0
HB: 13-18g/dl
PCV%: Male 40-54; Female 36-46
WBC: 4-11,000cells/mm^3
Neutrophil (%): 40-75
Eosinophil (%): 1-6
Lymphocytes (%): 20-45

Table 2. Urine Analysis of Fish Smokers

PAH (mg/µL)	Station 1	Station 2	Station 3	Station 4
Acenaphthene	0.018±0.030	-	0.004±0.0031	0.004±0.0031
Acenaphthylene	0.021±0.017	0.005±0.005	0.015±0.024	0.015±0.024
Anthracene	0.025±0.017	0.003±0.004	0.003±0.004	0.003±0.004
Benzo(a)pyrene	0.001±0.0008	0.005±0.003	0.009±0.010	0.009±0.010
Benzo(b)flouranzthene	-	-	0.001±0.0006	0.001±0.0006
1,12-Benzoperylene	0.001±0.002	0.002±0.002	0.006±0.007	0.006±0.007
Chrysene	0.059±0.007	0.003±0.001	0.003±0.0008	0.003±0.0008
1,2,5,6Dibenzanthracene	0.0003±0.0005	-	0.007±0.008	0.007±0.0008
Fluoranthene	0.004±0.003	0.001±0.0007	0.004±0.003	0.004±0.003
Fluorene	0.0003±0.0005	0.003±0.002	0.017±0.022	0.017±0.022
Indeno(1,2,3)pyrene	0.005±0.0006	0.002±0.003	0.004±0.004	0.004±0.004
Naphthalene	0.003±0.005	0.001±0.002	0.004±0.003	0.004±0.003
Phenanthrene	-	0.001±0.002	0.007±0.003	0.007±0.003
Pyrene	0.035±0.044	0.032±0.042	0.004±0.005	0.004±0.005
Total PAHs	0.1726	0.058	0.088	0.088

DISCUSSION

The results from the haematological analysis carried out will be compared to the data of Timzing*et al*., (2014) who compiled a comprehensive haematological reference range for normal Nigerian adults, considering the fact that haematological parameters are influenced by various factors like ethnicity and religion (Subhashree, 2012). The PCV of all the stations were generally lower than the normal value of PCV (0.41 or 41%) for healthy Nigerian adults according to Obi *et al*. (1984), and among the stations, it was

Scientia Africana, Vol. 21 (No. 1), April, 2022. Pp 19-26 https://dx.doi.org/10.4314/sa.v21i1.2
© Faculty of Science, University of Port Harcourt, Printed in Nigeria *ISSN 1118 – 1931*

station 3 that had the least value indicating that the smokers in that station are at a greater risk. Low PCV has been linked to anaemia and Booker and White (2005) also reported similar results due to exposure to benzo(a)pyrene which is a major component of PAHs. Pack cell volume measures the amount or percentage of blood that is composed of red blood cells (Charles, 2017), and also any factor that raise or increase the amount of other blood constituent have been reported to decrease PCV (Sedesse, 2011). One of the factors identified is an abnormal increase in white blood cells due to infection and diseases (Sedesse, 2011). Damages to the kidney can also lead to lower value of PCV considering that the kidney also plays a pivotal role in regulating the PCV (Dunn *et al.*, 2007). PAHs contains some compounds like benzo(b)fluoranthene which have been linked to kidney damage, these damages done to the kidney (leading to kidney diseases) also affects the red blood cell negatively by reducing the amount of red blood cell in circulation and this might be why the red blood cell analyzed was also low, the kidney is known to play a vital role in red blood cell production via erythropoietin hormone secreted by the peritubulary capillary lining cells of the kidney (Adamson, 1996; NIDDK, 2014; AKF, 2018). When compared with the station, it was found that station 3 was the most adversely affected Hb, the liver plays a very important role in protein synthesis and any pathological changes on the liver will likely affect the Hb synthesis (Mehrnaz*et al.*, 2018). The results on PCV, HB and RBC is in agreement with Mehrnaz*et al.*, (2018). The WBC also increased in the stations when compared to the reference range of 4.4 – 4.8, this increase in WBC is an indicator of diseases, infection or inflammations in the body (Mayo Clinic, 2018b), the levels of lymphocyte also increased in all the stations with station 1 having the highest value, the values form the different stations were also higher than the reference range of 39.9 – 42.1 according to Timzing*et al.*, (2014). Abnormally high lymphocyte have also been linked to inflammations and infections (Mayo Clinic, 2018a) and considering that wood smokes have been linked to bronchitis which is an inflammation of the bronchiole and respiratory infections (American Lung Association, 1991; Kammen*et al.*,1998) on can rightly expect such haematological changes. The neutrophil levels was also lower in the in all the stations compared to the reference range of 49.1 – 52.3, but station 1 was the least, This decrease in neutrophil leads to Neutropenia which weakens the immune system and increases a patients susceptibility to diseases. This decrease in the neutrophil level recorded in the stations has been linked to the presence of benzene (Qu, *et al.*, 2004), the results on HB, WBC, Neutrophil, and Lymphocytes also agree with Awodele*et al.*, (2015). The Eosinophil level was higher only in stations 1 and 2 when compared to the reference range of 1.32 – 1.91 with stations 3 and 4 being within the normal range, this abnormally high mean value is known be caused by infections (Mayo Clinic, 2018c). When we look at the haematological results generally, we can see that the fish smokers from the different stations all had a negative result showing that the smoking process has negative effect on them. The urine analysis done confirmed the presence of these PAHs in their body but it doesn't

truly ascertain the amount but only indicates the amount excreted. This means that more of the PAHs might still be in circulation in the blood and exerting its negative effect in the liver, kidney and other vulnerable organs. Station 1 had the highest amount of PAHs with a value of 0.1726 while station 2 had the least with 0.058.

CONCLUSION

Smoking of Fish exposes the smokers to PAHs and other toxic pollutants from the smokes and increases the risk of Anaemia and lung disease such as bronchitis as revealed by the haematological results. Therefore, it's important that a more environmentally healthy alternative of fish processing be considered, also proper sensitization of the market women should be carried out by the environmental health agencies and also the government on the health risks attached to fish smoking so as to discourage its practice.

REFERENCES

Adamson, J.W. (1996). Regulation of red blood cell production. *The American Journal ofMedicine.* 101(2A): 4S-6S.

Agency for Toxic Substances and Disease Registry (1995). Toxicology profile for Polycyclic aromatic hydrocarbon. Atlanta, G A: US departmentof Health and Human Services, Public Health Service

American kidney fund (AKF) (2018). Anaemia symptoms, causes and treatment. Retrieved on April 17, 2018 from.http://www.kidneyfund.org/anemia/

American Lung Association. (1991). Public Breif: Magnitude of Lung Disease

Awodele, O., Akindele,A., Adebowale, G. O. and Adeyemi, O. O. (2015). Polycyclic Aromatic Hydrocarbons, haematological and oxidative stress levels in commercial photocopier operators in lagos, Nigeria.*Ghana Medical Journal*. 49(1): 37-43.

Boldrin,B., Teihm,A.and Fritzsche, C. (1993). Degradation of Phenanthrene, Flourine, flouranthene and Pyrene by a mycobacterium *sp*., *Applied EnvironmentalMicrobiology*. 59(6), pp 1927 – 1930.

Booker, C. D. and White, K. L (2005).Benzo(a)pyrene induced anamia and splenomegaly in NZB/WF-1 mice. *Food chemistry and Toxicology*, 43(9): 1423 – 1431.

Charles P. D. (2017). Hematocrit Blood Test. Retrieved on April 20, 2018 from https://www.emedicinehealth.com/hematocrit_blood_test/article_em.htm?_e_pi_=7%2CPAGE_ID10%2C8209444870

Collins, D. A., Martins, K. S. and Sithole, S. D. (1990). Indoor wood smoke pollution causing low respiratory disease in children.*Trop. Doctor*. 20:151-155.

Dacie, J. V., and Lewis, S. N. (1991). *Practical Haematology*, 5th ed. Churchill Livingstone ,Edinburgh, 390pp.

Dunn, A.,Lo, V. and Donnelly, S. (2007). The role of the kidney in blood volume regulation: the kidney as a regulator of the hematocrit. *Am J Med Sci*.; 334(1):65-71.

Environmental Protection Agency US (2004). Drinking Water Standards and Health Advisories, Edition, on-line version.

Scientia Africana, Vol. 21 (No. 1), April, 2022. Pp 19-26 *https://dx.doi.org/10.4314/sa.v21i1.2*
© Faculty of Science, University of Port Harcourt, Printed in Nigeria *ISSN 1118 – 1931*

Farhadian,A., Jinap,S., Hanifah, H. N. and Zaidul, I. S. (2011). Effects of meat preheating and wrapping on the levels ofPAHs in charcoal grilled meat. *Food Chem.* Pp.141 – 146

Gracia-Falcon, M. S. and Simal-Gandara, J. (2005). Polycyclic aromatic hydrocarbons in smoke from different woods and their transfer during traditional smoking into chorizo sausages with collagen and tripe casing.*Food Addit. Contam*., 22: 1-8.

Guillen,M. D., Sopelana,P.andPartearroyo,M.A. (2000). PAHs in liquid smoke flavourings obtained from different types of wood, effects of storage in polyethylene flask on their concentrations. *J. Agric. Food Chem*., 48: 5083-5087.

Hazra, A., Grossman,H. B., Zhu,Y. Luo, S., Spitz,M. R. and Wux (2004). Benzo(a)pyrenediol epoxide induced p21 aberrations associated with genetic predisposition to bladder cancer, Genes chromosomes cancer, 41(4): 330-338.

Kammen, D.M., Wahhaj,G.andYiadom, M. Y.(1998). Acute respiratory infections (ARI) and Indoor air pollution. EHP Activity No. 263-cc, U.S.EPA.

Kanaly,R. A. and Harayama, S. (2000). Biodegradation of HMW-PAHs by bacteria. *JournalofBacteriology*. 182: 2059_2067.

Koenig, J. Q. *et al*., (1993). Pulmonary functionchanges in children association with fine particulate matter. *Environm.Res.* 63: 26-38.

Mayo clinic (2018a). Lymphocytosis: causes. Retrieved on May 4, 2018 from https://www.mayoclinic.org/symptoms/lymphocytosis/basics/causes/sym-20050660

Mayo clinic (2018b). High white blood cell count: causes. Retrieved on May 4, 2018 from https://www.mayoclinic.org/symptoms/high-white-blood-cell-count/basics/causes/sym-20050611

Mayo Clinic (2018c). Eosinophilia. Retrieved on May 3, 2018 from https://www.mayoclinic.org/symptoms/eosinophilia/basics/causes/sym-20050752

Mehrnaz,S., Negin, S., Mohammad, T. R. and Abdolali,M. and Gholamreza, H.(2018). Effects of Phenanthrene on some haematological indices yellow fin seabream (Acanthopagruslatus). *Iranian Journal of Toxicology*, !@(1): 47 – 52.

Miale, J. B. (1982). *Laboratory Medicine Haematology*, 6th Ed. The C. V. Mosby Co., London, pp. 883.

Miller, M. E., Holoway,A.C. and Foster, W. G. (2005). Benzo(a)pyrene increases invasion in MDA-MB-231 breast cancercellsvia increases Cox-2 expression and prostaglandin E2 (PGE 2) output, Clinical Experimental Metastasis, 22(2): 149-156.

National Institute of Diabetes and Digestive and Kidney Diseases (NIDDK) (2014). Anemia in Chronic Kidney Disease. Retrieved on April 17, 2018 from https://www.niddk.nih.gov/health-information/kidney-disease/chronic-kidney-disease-ckd/anemia?_e_pi_=7%2CPAGE_ID10%2C2007845028

Obi, G. O. (1984). Normal values for haemoglobin packed cell volume, and erythrocyte sedimentation rate in

healthy Nigerian adults.*Afr J Med Med Sci.* 1984 Mar-Jun;13(1-2):1-6.

Qu, Q., Shore, R. and Li, G. (**2004).**Hematological changes among Chinese workers with a broad range of benzene exposures. ***Am J Ind Med***; 42:275-85.

Sedesse, P. (2011). Causes of Low Hematocrit Blood Test Results. Retrieved on April 17, 2018 from http://www.explain-health.com/Causes-low-hematocrit-blood-test-anemia.html

Simko, P.(1991). Changes in benzo(a)pyrenecontentsin smoked fish during storage. *FoodChem.*, 40: 293-300

Simko,P. (2002). Determination of PAHs in smoked meat products and smoke flavouring food addictives. B:Analytical Technologies in the biomedical and life science, *J.Chromatogra.,* 770: 3-18.

Subhashree, A.R., Parameaswari, P. J., Shanthi, B.,Revathy, C. and Parijatham, B. O. (2012). The Reference Intervals for the Haematological Parameters in Healthy Adult Population of Chennai, Southern India. *J ClinDiagn Res*. 2012 Dec; 6(10): 1675–1680.

Suchanova, M., Jana Haj,L.,Tomaniova, M., Kocourek, V. and Babika,L. (2008). PAHsin smokescheese.*J.Sci.Food Agric.*, 88(8): 1307 – 1317.

Sutherland,J. B. (1992). Detoxification of PAHsny fungi. *Journal of Industrial microbiology*, 9: 53-62.

Timzing, M., Osawe, S. and Monday T.(2014). Comprehensive Reference Ranges for Hematology and Clinical Chemistry Laboratory Parameters Derived from Normal Nigerian Adults. PLoS One. 2014; 9(5): e93919. doi: 10.1371/journal.pone.0093919.

Scientia Africana, Vol. 21 (No. 1), April, 2022. Pp 27-36 *https://dx.doi.org/10.4314/sa.v21i1.3*
© Faculty of Science, University of Port Harcourt, Printed in Nigeria *ISSN 1118 – 1931*

A REVISED MATHEMATICAL SOLUTION TO THE PENNE BIOHEAT EQUATION FOR DEEP ROOTED TISSUES USING THE VARIABLE SEPARATION METHOD

[1]Akpolile, A.F. [1]Mokobia, C.E. [2]Ikubor, J.E. [3]Ugbede, F.O. and [1] Agbajor, G.K.
[1] Department of Physics, Delta State University, P.M.B 1, Abraka.
[2] Department of Radiology, Delta State University Teaching Hospital, Oghara.
[3] Department of Physics with Electronics, Evangel University, Akaeze, Ebonyi State, Nigeria.
Corresponding author email: anita.franklin@yahoo.com

Received: 10-02-2022
Accepted: 24-03-2022

ABSTRACT

The temperature distribution of tissues under the skin surface was obtained using Penne's bio-heat equation and the separation of variables technique. The resulting solution indicated a slight temperature difference between the recorded skin temperature and the temperature of the tissue of interest (TOI), which is a direct indication of the TOI's temperature. According to the graphical analysis, temperature is proportionally related to time and tissue distance from the skin surface. As a result, the given analytic solution may be utilized to easily analyze deep-rooted tissues while accounting for thermal properties.

Keywords: Tissues, temperature, heat transfer, bio-heat.

INTRODUCTION

The spatial distribution of temperature and heat transmission in tissues is critical in thermoregulation and many physiological processes in living creatures since there is a link between disease and temperature. The disease condition causes an elevation in temperature as a result of enhanced vascularity, hormonal activity, and metabolic activity. Researchers have created many bio-heat transfer models to estimate the temperature distribution in biological live tissues and achieve precise responses (Kabiri and Talaee, 2021). These models are aimed at improving temperature regulation during hypothermia and hyperthermia, predicting temperature distributions in core organs where direct temperature measurement is intrusive, and determining changes in organ temperature as a result of changes in bodily activities. Because of its simplicity, Penne's bio-heat equation is one of the most well-known models for studying heat exchange in tissues. Heat transport is aided by thermal conduction, convection, blood perfusion, and metabolic heat production in tissue (Ciesielski and Mochnacki, 2012). When the temperature of the blood differs from the temperature of the tissue through which it flows, convective heat transmission occurs, affecting the temperatures of both the blood and the tissue. Many physiological processes rely on perfusion-based heat transport interactions, such as thermoregulation and inflammation. Several factors influence the blood/tissue thermal interaction, including perfusion rate and vascular anatomy, which vary substantially between tissues, organs, and diseases. Furthermore, using the traditional Fourier's rule of heat conduction, the Pennes bioheat equation may be used to

define the energy conservation equation for biological heat transfer (Lillicrap et al., 2017). In fact, key bioheat transfer results have been published in recent decades such as Pennes bioheat transfer equation (Pennes, 1948) and further microstructure bioheat transfer models (Weinbaum et al.,1984; Chen and Holmes, 1980). Modeling heat-related processes such as bioheat transfer and heat-induced stress aid in the development of biological and biomedical technologies such as thermotherapy, hyperthermia cancer treatment, thermal diagnostics, cryogenic surgery, and other uses (Hassain and Mohammadi, 2013). Quantitative and exact measurements of bioheat transfer are essential to completely know and anticipate the biological system's heat transfer mechanism. The intricacy of the accurate thermal analysis process of living tissues is due to its heterogeneity and anisotropy, as well as conduction, convection, and radiation heat flow, cell metabolism, and blood perfusion, among other factors. Because of its heterogeneity and anisotropy, as well as conduction, convection, and radiation heat flow, cell metabolism, and blood perfusion, among other aspects, the precise thermal analysis procedure of living tissues is complicated. As a result, building precise thermal models is highly challenging, and the majority of the suggested bio-heat equations are extremely complex, albeit not impossible to solve analytically. The analytical solutions to these equations are important in bio-heat transfer research because they reflect the equations' genuine physical properties and can be used to evaluate numerical results and establish the correctness of the in-vitro model analysis. In the existing literature, several methods for deriving analytical solutions to these equations have been provided (Al-Humedia and Al- Saadawi, 2021; Damor et al., 2015;Grysa and Marciag,2019;Sakar et al.,2015;Zhou and Chen,2009; Zhou and Chen,2007;Tsu-Ching et al.,2007;Gutierrez,2007;Romero et al.,2009;Damor et al.,2013; Roca Oriaa et al.,2019). The general heat equation for conduction with extra elements for heat sources is the linear bio-heat transfer equation for tissue (Lakhssassi et al.,2010). The primary goal of this study is to develop an analytical solution for the temperatures of tissues deep beneath the skin utilizing the well-known bio-heat equation while taking into account the thermal properties of the tissues such as density, conductivity, and thermal diffusivity.

Mathematical Conceptualization

Penne's bio-heat equation is given by (Akpolile et al., 2021);

$$\rho c \frac{\partial T}{\partial t} = \nabla(k\nabla T) + Q + w_b c_b (T_b - T) \quad (1)$$

where ρ, c and *k* are the density (kg/m^3), the specific heat (J/kg.K) and the thermal conductivity (W/m.K) of the tissue respectively. w_b is the mass flow rate of blood per unit volume of tissue (kg/(s.m^3)), C_b is the specific heat of the blood ; Q is the metabolic heat produced per unit volume from the tissue (W/m^3); T_b denotes the temperature of the arterial blood (K); T represents the tissue temperature,∂T/∂t denotes the rate of temperature rise.

Scientia Africana, Vol. 21 (No. 1), April, 2022. Pp 27-36 https://dx.doi.org/10.4314/sa.v21i1.3
© Faculty of Science, University of Port Harcourt, Printed in Nigeria *ISSN 1118 – 1931*

The boundary conditions is described as follows;

$$\left.\begin{array}{ll} \text{(i)} & T(x,t)|_{t=0} = f(x) \text{ , where } f(x) \text{ is a characteristics of distance.} \\ \text{(ii)} & T(x,t)|_{x=0.001} = T_b + Q_0 \\ \text{(iii)} & \theta(x,t)|_{x=0.001} = 0 \\ \text{(iv)} & \theta(x,t)|_{t=0} = f(x) \end{array}\right\} \quad (2)$$

For a small volume of human tissue, assuming a one-dimensional situation, the equation 1 above can be expressed as;;

$$\rho c \frac{\partial T}{\partial t} = k \frac{\partial^2 T}{\partial x^2} + Q + w_b c_b (T_b - T) \quad (3)$$

For easy computation, the following variables are defined as (Akpolile et al., 2021);

(i) $Q = B_b Q_o$ (4)

(ii) $B_b = w_b C_b$ (5)

(iii) $T - T_b - Q_o = \emptyset$ (6)

(iv) Q_o is a constant (7)

The equation 3 can be rewritten as;

$$\rho c \frac{\partial T}{\partial t} = k \frac{\partial^2 T}{\partial x^2} + B_b Q_o + B_b (T_b - T) \quad (8)$$

$$\rho c \frac{\partial T}{\partial t} = k \frac{\partial^2 T}{\partial x^2} + B_b Q_o + B_b T_b - B_b T \quad (9)$$

$$\rho c \frac{\partial T}{\partial t} = k \frac{\partial^2 T}{\partial x^2} - B_b T + B_b Q_o + B_b T_b \quad (10)$$

$$\rho c \frac{\partial T}{\partial t} = k \frac{\partial^2 T}{\partial x^2} - B_b (T - T_b - Q_o) \quad (11)$$

Using equation 6;

$$\rho c \frac{\partial \emptyset}{\partial t} = k \frac{\partial^2 \emptyset}{\partial x^2} - B_b \emptyset \quad (12)$$

$$\rho c \frac{\partial \emptyset}{\partial t} - k \frac{\partial^2 \emptyset}{\partial x^2} = -B_b \emptyset \quad (13)$$

Using method of separation of variables;

$$\emptyset(x,t) = X(x)\,T(t) \quad (14)$$

Differentiating equation 14 with respect to x and t gives equations (15 – 17);

$$\emptyset_t = X(x)T'(t) \quad (15)$$

$$\emptyset_x = X'(x)\,T(t) \quad (16)$$

$$\emptyset_{xx} = X''(x)\,T(t) \quad (17)$$

The homogenous part of equation 13 is

$$\rho c \frac{\partial \emptyset}{\partial t} - k \frac{\partial^2 \emptyset}{\partial x^2} = 0 \quad (18)$$

Substituting equations (15 – 17) into 18; it will yield,

$$\rho c(X(x)T'(t)) - k(X''(x)\,T(t)) = 0 \quad (19)$$

$$\rho c(X(x)T'(t)) = k(X''(x)\,T(t)) \quad (20)$$

From equation 20, collect like terms;

$$\frac{\rho c\,(T'(t))}{T(t)} = \frac{k(X''(x))}{X(x)} \quad (21)$$

Assume that equation 21 is equivalent to a constant, which we will call $-\lambda$.

$$\frac{\rho c\,(T'(t))}{T(t)} = \frac{k(X''(x))}{X(x)} = -\lambda \quad (22)$$

The equation 22 implies that:

$$\frac{\rho c\,(T'(t))}{T(t)} = -\lambda \quad (23)$$

$$\frac{k(X''(x))}{X(x)} = -\lambda \quad (24)$$

Rearranging equation 23, we obtain:

$$\frac{T'(t)}{T(t)} = \frac{-\lambda}{\rho c} \quad (25)$$

By integrating equation25, we obtain:

$$\int \frac{T'(t)}{T(t)} = \int \frac{-\lambda}{\rho c}\partial t \quad (26)$$

$$\ln T(t) = \frac{-\lambda}{\rho c}t + C \quad (27)$$

where C is the integration constant. Taking the natural logarithm of both sides of equation 27 will give;

$$T(t) = e^{\frac{-\lambda}{\rho c}t+C} = e^{\frac{-\lambda}{\rho c}t}.\,e^{C}$$

$$T(t) = A_0\, e^{\frac{-\lambda}{\rho c}t} \quad (28)$$

where A_0 is a constant. Considering equation 24;

$$\frac{X''(x)}{X(x)} = \frac{-\lambda}{k} \quad (29)$$

$$X''(x) = \frac{-\lambda}{k}X(x) \quad (30)$$

$$X''(x) + \frac{\lambda}{k}X(x) = 0 \quad (31)$$

Let X = r; then equation 31 will be

$$r^2 + \frac{\lambda}{k}r = 0 \quad (32)$$

$$r\left(r + \frac{\lambda}{k}\right) = 0 \quad (33)$$

$$r_1 = 0 \text{ or } r_2 = -\frac{\lambda}{k} \quad (34)$$

Substituting the roots of the equation, we have;

$$X = ae^{r_1 x} + be^{r_2 x} = ae^{0.x} + be^{-\frac{\lambda}{k}x}$$

$$X = a + be^{-\frac{\lambda}{k}x} \quad (35)$$

where a and b are arbitrary constants.

Scientia Africana, Vol. 21 (No. 1), April, 2022. Pp 27-36 https://dx.doi.org/10.4314/sa.v21i1.3
© Faculty of Science, University of Port Harcourt, Printed in Nigeria *ISSN 1118 – 1931*

$$\emptyset(x,t) = \left(a + be^{-\frac{\lambda}{k}x}\right) A_0\, e^{\frac{-\lambda}{\rho c}t} \quad (36)$$

The equation 36 is the homogenous solution. Then the particular solution for $\emptyset(x,t)$ is;

$$\emptyset(x,t) = -P_0 B_b e^{-\frac{\lambda}{k}x} \quad (37)$$

where P_0 is a constant. The general solution for $\emptyset(x,t)$ is;

$$\emptyset(x,t) = \left(a + be^{-\frac{\lambda}{k}x}\right) A_0\, e^{\frac{-\lambda}{\rho c}t} - P_0 B_b e^{-\frac{\lambda}{k}x} \quad (38)$$

From equation 6, we have;

$$T = \emptyset + T_b + Q_o \quad (39)$$

Applying equation 4, we have;

$$T(x,t) = \emptyset(x,t) + T_b + \frac{Q}{B_b}$$

$$T(x,t) = \left(a + be^{-\frac{\lambda}{k}x}\right) A_0\, e^{\frac{-\lambda}{\rho c}t} - P_0 B_b e^{-\frac{\lambda}{k}x} + T_b + \frac{Q}{B_b}$$

Applying equation 5, we have;

$$T(x,t) = \left(a + be^{-\frac{\lambda}{k}x}\right) A_0\, e^{\frac{-\lambda}{\rho c}t} - P_0 w_b c_b e^{-\frac{\lambda}{k}x} + T_b + \frac{Q}{w_b c_b} \quad (40)$$

where a, b, P_0 and A_0 are arbitrary constants which can bo obtained by applying the boundary conditions.

Applying equation 2 (iii) to equation 40, we have;

$$\left(a + be^{-\frac{0.001\lambda}{k}}\right) A_0\, e^{\frac{-\lambda}{\rho c}t} = 0 \quad (41)$$

$$\Rightarrow A_0\, e^{\frac{-\lambda}{\rho c}t} \neq 0$$

$$a + be^{-\frac{0.001\lambda}{k}} = 0$$

$$a = -be^{-\frac{0.001\lambda}{k}} \quad (42)$$

Applying equation 2 (iv) to equation 50, we have;

$$\left(a + be^{-\frac{\lambda}{k}x}\right) A_0\, e^{\frac{-\lambda}{\rho c}.0} = f(x) \quad (43)$$

$$\left(a + be^{-\frac{\lambda}{k}x}\right) A_0 = f(x)$$

$$\Rightarrow A_0 = f(x) \quad (44)$$

$$a + be^{-\frac{\lambda}{k}x} = f(x) \quad (45)$$

Substituting equation 42 into 45, it becomes;

$$-be^{-\frac{0.001\lambda}{k}} + be^{-\frac{\lambda}{k}x} = f(x)$$

$$be^{-\frac{\lambda}{k}x} - be^{-\frac{0.001\lambda}{k}} = f(x)$$

$$b\left(e^{-\frac{\lambda}{k}x} - e^{-\frac{0.001\lambda}{k}}\right) = f(x) \quad (46)$$

Taking the Log of both sides of equation 46;

$$\log b\left(e^{-\frac{\lambda}{k}x} - e^{-\frac{0.001\lambda}{k}}\right) = \log f(x)$$

$$\mathrm{b}\log e^{-\frac{\lambda}{k}x} - \mathrm{b}\log e^{-\frac{0.001\lambda}{k}} = \log f(x)$$

$$\mathrm{Fb}.-\frac{\lambda}{k}x\log e + \mathrm{b}.\frac{0.001\lambda}{k}\log e = \log f(x)$$

$$\mathrm{b}\left(-\frac{\lambda}{k}x + \frac{0.001\lambda}{k}\right) = \log f(x)$$

$$\frac{\lambda \mathrm{b}}{k}(-x + 0.001) = \log f(x)$$

$$\lambda \mathrm{b}(0.001 - x) = k\log f(x)$$

$$\mathrm{b} = \frac{k\log f(x)}{\lambda(0.001-x)} \qquad (47)$$

substituting equation 47 into equation 42

$$a = -\frac{k\log f(x)}{\lambda(0.001-x)}e^{-\frac{0.001\lambda}{k}} \qquad (48)$$

Applying equation 2(ii) to equation 44; we have:

$$T(x,t)|_{x=0.001} = T_b + Q_0 = \left(a + be^{-0.001\frac{\lambda}{k}}\right)A_0\, e^{\frac{-\lambda}{\rho c}t} - P_0 w_b c_b e^{-0.001\frac{\lambda}{k}} + T_b + \frac{Q}{w_b c_b} \qquad (49)$$

Applying equation 5 to equation 49

$$T_b + \frac{Q}{w_b c_b} = A_0\, e^{\frac{-\lambda}{\rho c}t}\left(a + be^{-0.001\frac{\lambda}{k}}\right) - P_0 w_b c_b e^{-0.001\frac{\lambda}{k}} + T_b + \frac{Q}{w_b c_b} \qquad (50)$$

$$A_0\, e^{\frac{-\lambda}{\rho c}t}\left(a + be^{-0.001\frac{\lambda}{k}}\right) - P_0 w_b c_b e^{-0.001\frac{\lambda}{k}} = 0 \qquad (51)$$

$$A_0\, e^{\frac{-\lambda}{\rho c}t}\left(a + be^{-0.001\frac{\lambda}{k}}\right) - P_0 w_b c_b e^{-0.001\frac{\lambda}{k}} \qquad (52)$$

$$\Rightarrow A_0\, e^{\frac{-\lambda}{\rho c}t} = -P_0 w_b c_b e^{-0.001\frac{\lambda}{k}} (53)$$

$$a + be^{-0.001\frac{\lambda}{k}} = -P_0 w_b c_b e^{-0.001\frac{\lambda}{k}} \qquad (54)$$

Considering equation 53;

$$P_0 = \frac{-A_0\, e^{\frac{-\lambda}{\rho c}t}}{w_b c_b e^{-0.001\frac{\lambda}{k}}} \qquad (55)$$

$$P_0 = \frac{-f(x)\, e^{\frac{-\lambda}{\rho c}t}}{w_b c_b e^{-0.001\frac{\lambda}{k}}} \qquad (56)$$

Substituting equations 56, 52, 51, 48 into 44;

$$T(x,t) = f(x)\, e^{\frac{-\lambda}{\rho c}t}\left(\left(-\frac{k\log f(x)}{\lambda(0.001-x)}e^{-\frac{0.001\lambda}{k}}\right) + \frac{k\log f(x)}{\lambda(0.001-x)}e^{--\frac{\lambda}{k}x}\right) - \left(\frac{f(x)\, e^{\frac{-\lambda}{\rho c}t}}{w_b c_b e^{-0.001\frac{\lambda}{k}}}w_b c_b e^{-\frac{\lambda}{k}x}\right) + T_b + \frac{Q}{w_b c_b}$$

$$T(x,t) = f(x)\, e^{\frac{-\lambda}{\rho c}t}.\frac{k\log f(x)}{\lambda(0.001-x)}\left(\left(-e^{-\frac{0.001\lambda}{k}}\right) + e^{--\frac{\lambda}{k}x}\right) - \left(\frac{f(x)\, e^{-\lambda\left(\frac{t}{\rho c}+\frac{x}{k}\right)}}{e^{-0.001\frac{\lambda}{k}}}\right) + T_b + \frac{Q}{w_b c_b}$$

Scientia Africana, Vol. 21 (No. 1), April, 2022. Pp 27-36 https://dx.doi.org/10.4314/sa.v21i1.3
© Faculty of Science, University of Port Harcourt, Printed in Nigeria *ISSN 1118 – 1931*

$$T(x,t) = \frac{f(x)k\log f(x)}{\lambda(0.001-x)}\, e^{\frac{-\lambda}{\rho c}t}\left(\left(-e^{-\frac{0.001\lambda}{k}}\right)+e^{--\frac{\lambda}{k}x}\right)-\left(\frac{f(x)\,e^{-\lambda\left(\frac{t}{\rho c}+\frac{x}{k}\right)}}{e^{-0.001\frac{\lambda}{k}}}\right)+T_b+\frac{Q}{w_b c_b} \quad (57)$$

where $f(x)$ is the source term, T is the tissue temperature is (^{o}K), k is the thermal conductivity (m^2/s), λ is the tissue thickness (m), x is the tissue's distance from the skin's surface (m), and t is time (s). The equation (57) was used to model the temperature values for deep-seated human tissues applying the maple V18.0 software. The obtained values are presented in Table 1.

Table 1: Thermal parameters of tissues

TISSUE	k(W/m.K)	ρ_t(kg/m^3)	C_t(J/kg/^{o}K)	λ(m)	x(m)	Q(W/m^2)	C_b(J/kg/^{o}K)	w_bx10^{-3} (s^{-1})
LIVER	0.520	1060	3600	0.12	0.02	700	3770	15
KIDNEY	0.556	1060	3830	0.03	0.07	900	3770	61

Source: (Kabiri and Talaee,2021)

RESULTS AND DISCUSSION

The temperature of deep-seated tissues could be determined using the defined analytical solution of Penne's bio-heat equation in equation 57. Thermal parameters from known works of literature were used in the computations, as stated in Table 1 above. The fluctuation of temperature (T) with time (t) and distance (x) is illustrated in Figures 1, 2, 3, and 4. They are all linear graphs, indicating that temperature is proportional to time. In the graphs below (1 and 3), an intercept at 311.2503 and 311.74037 on the T axis, respectively, was observed, and also, T increases in a constant proportion to t, but the temperature, T, is the same at all points in Figures 2 and 4 below. Also, from figures 2 and 4, a slight variation was observed for the temperature, suggesting that different tissues have different temperature values which could be attributed to the properties of the tissue under investigation. From the equation under study and the diagrams obtained, it is observed that tissue temperature is dependent on the metabolic heat produced in the tissue, tissue thickness, and distance of the tissue from the skin surface, suggesting that the skin temperature measured using the 19 thermometer placed under the armpit cannot be assumed to be the exact temperature value of the tissue under study, especially in cases of illnesses like cancer. The temperature profile appears to coincide with data from previous works of literature (Damor et al.,2013; Liu and Cheng. 2008), indicating that the same model was used under different situations.

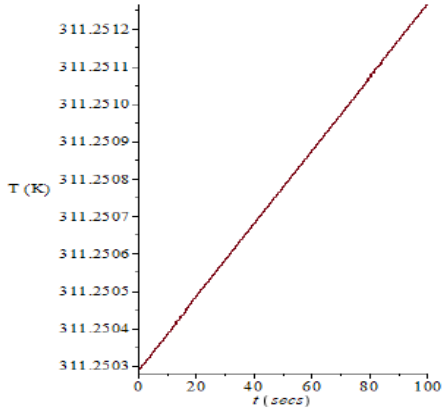

Figure 1: A plot of temperature (T) against time (*t*) for liver tissue

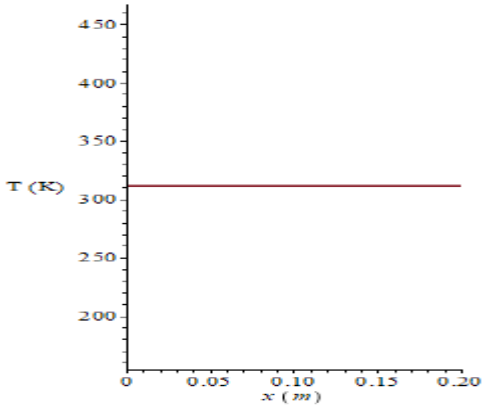

Figure 2: A plot of temperature (T) against distance (*x*) for liver tissue

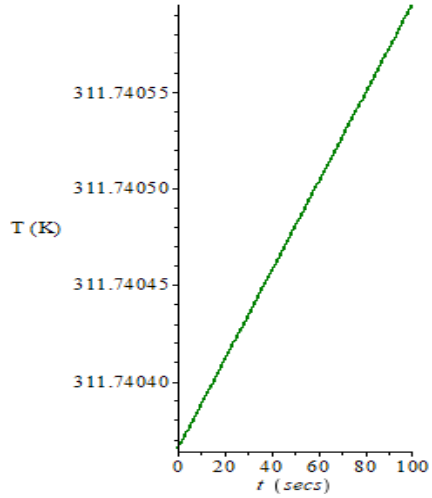

Figure 3: A plot of temperature (T) against time (*t*) for kidney tissue

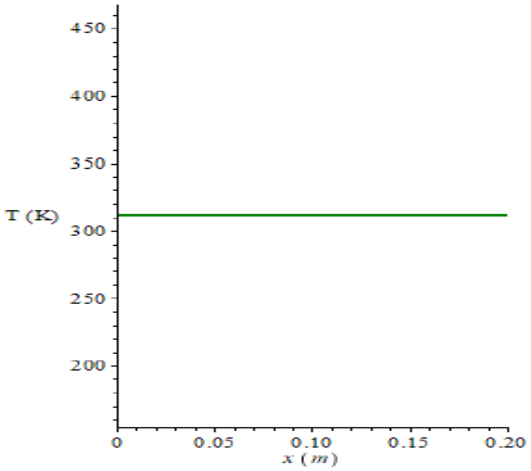

Figure 4: A plot of temperature (T) against distance (*x*) for kidney tissue

CONCLUSION

The goal of this research is to use the approach of separable variables to solve Penne's bio-heat transfer equation analytically and to apply the above solution in estimating the temperature of deep-seated tissues in the body. Tissue thickness was successfully integrated into the bio-heat transfer model in this work, providing a solution that indicated that the temperature distribution had a proportionate increase in time and distance from the skin. The estimated temperature value for the tissue under examination was found to be slightly different from skin temperature in the theoretical analysis, especially in cases of the disease. The results obtained agreed with other investigations in comparable areas for medical applications such as thermographic imaging of lesions. There has been no mathematical derivation relating to this subject.

REFERENCES

Akpolile, A.F., Mokobia, C.E. and Ikubor, J.E. (2021). Analytical Approach to the Penne's Bioheat Equation for the Evaluation of Temperature for Deep

Scientia Africana, Vol. 21 (No. 1), April, 2022. Pp 27-36 *https://dx.doi.org/10.4314/sa.v21i1.3*
© Faculty of Science, University of Port Harcourt, Printed in Nigeria *ISSN 1118 – 1931*

Seated Tissues. Advances in Mathematics: Scientific Journal , 10(7), pp 2957–2976; ISSN: 1857-8365 (printed); 1857-8438 (electronic) https://doi.org/10.37418/amsj.10.7.4

Al-Humedia, H.O. and Al-Saadawi, F.A. (2021). The numerical solution of bioheat equation based on shifted Legendre polynomial. International Journal of Nonlinear Analysis and Application, 12(2), pp 1061-1070.

Chen, M.M. and Holmes, K.R. (1980). Microvascular Contributions in Tissue Heat Transfer. Annals of New York Academy of Science, 335, pp 137-150.

Ciesielski, M. and Mochnacki, B. (2012). Numerical Analysis of Interrelations between Skin Surface Temperature and Burn Wound Shape. Scientific Research of the Institute of Mathematics and Computer Science, 1(11), pp 15-22.

Damor, R.S., Kumar, S. and Shukla, A.K (2015). Parametric study of fractional bio-heat equation in skin tissue with sinusoidal heat flux. Fractional Differential Calculus, 5(1), pp 43-53.

Damor, R.S., Kumar, S. and Shukla, A.K 2013). Numerical Solution of Fractional Bioheat Equation with Constant and Sinusoidal Heat Flux Condition on Skin Tissue. American Journal of Mathematical Analysis, 1(2), pp 20-24.

Grysa, K. and Maciag, A. (2019). Mathematical model of identification of the skin surface temperature caused by the temperature of tissue inflammation. Institute of electrical electronics engineers, Doi:10.1109/DJ.2019.8813329.

Gutierrez, G. (2007). Study of the Bioheat Equation with a Spherical Heat Source for Local Magnetic Hyperthermia. XVI Congress on Numerical Methods and their Applications, Cordoba, Argentina.

Hossain, S. and Mohammadi, F. (2013). One-dimensional Steady-state Analysis of Bioheat Transfer Equation: Tumour Parameters Assessment for Medical Diagnosis Application.In:Proceedings 6th international multi-conference on engineering and technological innovation (IMETI 2013), pp 26-30.

Kabiri, A. and Talaee, M.R. (2021). Analysis of hyperbolic Pennes bioheat equation in perfused homogeneous biological tissue subject to the instantaneous moving heat source. SN Applied Science,3: 398, https://doi.org/10.1007/s42452-021-04379-w

Lakhssassi, A., Kengne, E. and Semmaoui, H. (2010). Modified Pennes' equation modeling bio-heat transfer in living tissues: analytical and numerical analysis. Natural Science, 2(12), pp 1375-1385.

Lillicrap,T., Tahtalı, M., Neely, A., Wang, X., Bivard, A. and Lueck, C.(2017). A model based on the Pennes bioheat transfer equation is valid in normal brain tissue but not brain tissue suffering focal ischaemia. Australasian Physics and Engineering Science in Medicine, 40, pp 841–850.

Liu, K. and Cheng, P.(2008). 'Finite propagation of heat transfer in a multilayer tissue'. Journal of thermo-physics and heat transfer, 22, pp 775 – 782.

Pennes, H.H. (1948). Analysis of tissue and arterial temperatures in the resting human forearm. Journal of Applied Physiology, 1, pp 93-122.

Roca Oriaa, E.J., Bergues Cabrales, L.E and Bory Reyesc, J.(2019). Analytical solution of the bioheat equation for thermal response induced by any electrode array in anisotropic tissues with arbitrary shapes containing multiple-tumor nodules. Revista Mexicana de F´ısica, 65, pp 284–290.

Romero, R., Jimenez-Lozano, J.N., Shen, M. and Gonzalez, F.J.(2009). Analytical Solution of the Pennes Equation for Burn-Depth Determination from Infrared Thermographs. Mathematical Medicine and Biology, 27, pp 21-38, doi: 10.1093/imammb/dqp010, Advance Access publications.

Sakar, D., Haji-Sheikh, A. and Jain, A. (2015). Temperature distribution in multi-layer skin tissue in presence of a tumor. International Journal of Heat and Mass Transfer, 91, pp 602-610.

Tzu-Ching, S., Ping, Y., Win-Li, L. and Hong-Sen, K.(2007). Analytical Analysis of the Pennes' Bioheat Transfer Equation with Sinusoidal Heat Flux Condition on Skin Surface. IPEM, Medical Engineering & Physics, 29(9), pp 946-953.

Weinbaum, S., Jiji, L.M. and Lemons, D.E.(1984). Theory and experiment for the effect of vascular microstructure on surface tissue heat transfer. Part I. Anatomical foundation and model conceptualization. Journal of Biomechanical Engeering-T. ASME, 106, pp 321-330.

Zhou, M. and Chen, Q.(2007). Study of the surface temperature distribution of the tissue affected by the point heat source. Institute of Electrical and Electronics Engineering.

Zhou, M. and Chen, Q. (2009.). Estimation of Temperature Distribution in Biological Tissue by Analytic Solutions to Pennes' Equation. 2nd International Conference on Biomedical Engineering and Informatics (BMEI), Institute of Electrical and Electronics Engineering, Nanjing, China.

Scientia Africana, Vol. 21 (No. 1), April, 2022. Pp 37-52 *https://dx.doi.org/10.4314/sa.v21i1.4*
© Faculty of Science, University of Port Harcourt, Printed in Nigeria *ISSN 1118 – 1931*

HYDROGEOPHYSICAL EXPLORATION OF GROUNDWATER POTENTIAL IN SOUTHWESTERN BASEMENT TERRAIN OF PART OF AGO-IWOYE, SOUTH WESTERN NIGERIA.

[1]Bayewu, O. O., [2]Oloruntola, M. O., [1]Mosuro, G. O., [1]Odugbesan, O. O., [1]Bakare, K. O., [1]Olukayode, O. O., [3]Adenuga, O. A., and [1]Oyebolu, O. O.
[1]Department of Earth Sciences, Olabisi Onabanjo University, Ago Iwoye, Nigeria.
[2]Department of Geosciences, University of Lagos, Lagos, Nigeria.
[3]Department of Physics, Olabisi Onabanjo University, Ago Iwoye, Nigeria.
*Corresponding email: odugbesanoluwadamilare@gmail.com

Received: 11-08-2021
Accepted: 03-01-2022

ABSTRACT

Electrical resistivity survey of Ago-Iwoye southwestern Nigeria was done with the aim of delineating potential zones for groundwater exploitation. The rock types present are mainly gneissic rocks; granite gneiss, banded gneiss, biotite gneiss and porphyroblastic gneiss.Forty five (45) Vertical Electrical Soundings (VES) of schlumberger array were carried out using maximum electrode spacing (AB/2) of 100m. The results obtained were interpreted using partial curve matching which serves as model input for the computer iteration using WINRESIST software to determine the resistivity, thickness and depth of each layer in the sub-surface.The identified curve types are H, KH, HKH, A, K and QH types while the H type curve is predominant. The three prominent geo-electric layers were inferred, these are the topsoil, weathered layer (sand/clay/clayey sand) and fresh/fractured bedrock with resistivity values of 33.4Ωm - 2266.3Ωm, 8.3Ωm - 1106.3Ωm and 68.4Ωm - 21729.6Ωm respectively. The isopach reveals overburden thickness range of 2m – 52m, bedrock resistivity ranges from 1000Ωm - 19000Ωm and reflection coefficient range from 0.62 -0.92.The study area is predominantly of low yield but areas in the northeastern and western part of the study area have high aquiferous groundwater potential areas are only noticeable in the northeastern and western part of the study area.

Keywords: Geoelectric layers, Groundwater, Electrical Resistivity, Isopach, Reflection coefficient, overburden thickness

INTRODUCTION

The study area, Ago-Iwoye town belongs to the tropical climatic environment indicating a considerable amount of annual precipitation thereby providing the people with a considerable amount of surface water occurrences but this type of water is undependable throughout the year because of the high population demand for water in their different activities. Hence, there is need to depend more on water held in saturated zone of the subsurface under the hydrostatic pressure condition known as the groundwater usually occurring below the water table (Haque *et al*., 2021; Ariyo *et al*., 2021).

An essential factor capable of influencing groundwater occurrence is the geological setting of the exploration area because of the differences in the hosting media (aquifer). Geologically, earth regions are considered to be made up of either soft rocks (sedimentary environment) or hard rocks (crystalline environment).

Exploration and exploitation works have been able to successfully delineate and differentiate between groundwater occurrences in both geological terrains. The aquiferous region in the sedimentary environment includes gravel, sandstone, conglomerates, and fractured limestone while that of the basement include the search for thick overburden layers and fractured rock of the subsurface.

Exploring for groundwater in basement region (as in this study) requires the adoption of either an active or passive method of geophysical exploration considering the amount this method has successfully recorded as they are most reliable and accurate in mapping subsurface layers, structural investigations and rock variation (Carruthers, 1985; Emenike, 2001) capable of serving as the aquifer in this region.

Geophysical exploration method includes electrical resistivity, gravity, seismic, magnetic, remote sensing, and electromagnetic and so on. The electrical resistivity method which measures the changes in the apparent resistivity of the subsurface appears to be the most promising method with great success and low cost for locating productive well. Vertical Electrical Sounding (VES) technique is adopted and this method can provide information on the vertical variation in the resistivity of the ground with depth and the Constant Separation Traversing (CST) provides a means of determining lateral interval variation in the resistivity of the ground Bayewu *et al*., 2018, Olayinka and Mbachi, 1992; Olorunniwo and Olorunfemi, 1987). In view of this, the exploration strength of the Vertical Electrical Sounding (VES) technique necessitates its adoption in the delineation of the groundwater potential zone in the study area which is Ago-Iwoye, Southwestern Nigeria.

Location and Geological setting

Ago-Iwoye in South-western Nigeria is located between latitude 6˚55ˈ00" to 6˚57ˈ00"North and longitude 3˚54ˈ00" to 3˚55ˈ00"East (Figure 1). The accessibility of the area is best described in terms of transportation network, which consists of minor roads linking major roads with foot paths across the study area. The geomorphological setting of the study area reveal moderate low hills forming ridges and undulated plain dotted with small isolated hills or hills rock are noticed generally within Ago-Iwoye. Drainage pattern is predominantly dendritic with presence of River Ome as the major river channel and vegetation falling under the tropical rain forest belt of Nigeria (Adeyemi and Salami, 2004). Ago-Iwoye is recognized to belong to the Monsoon climatic environment characterized by both wet and dry season. The wet season is experienced in late March or early April to late September or early November while the dry season occurs from early November/ late November to early March. The average precipitation range is 250-450mm attaining an average rainfall of 750-1000mm at a temperature of 27°C during the wet season. This area is geologically within the Precambrian Basement Complex terrain of Southwestern Nigeria with presence of Granite, Granite gneiss, Banded gneiss and Pegmatite rocks (Figure 2).

Scientia Africana, Vol. 21 (No. 1), April, 2022. Pp 37-52 *https://dx.doi.org/10.4314/sa.v21i1.4*
© Faculty of Science, University of Port Harcourt, Printed in Nigeria *ISSN 1118 – 1931*

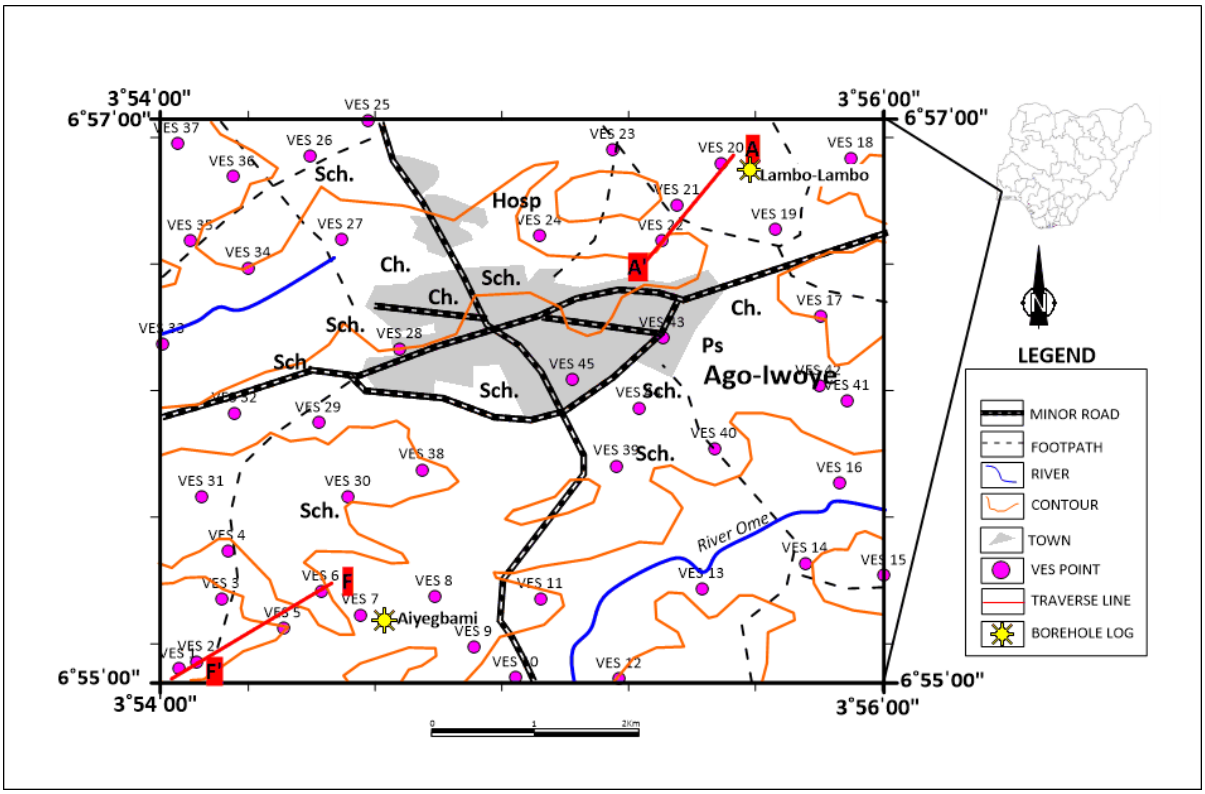

Figure 1: The map of the study area indicating established vertical electrical sounding (VES) points.

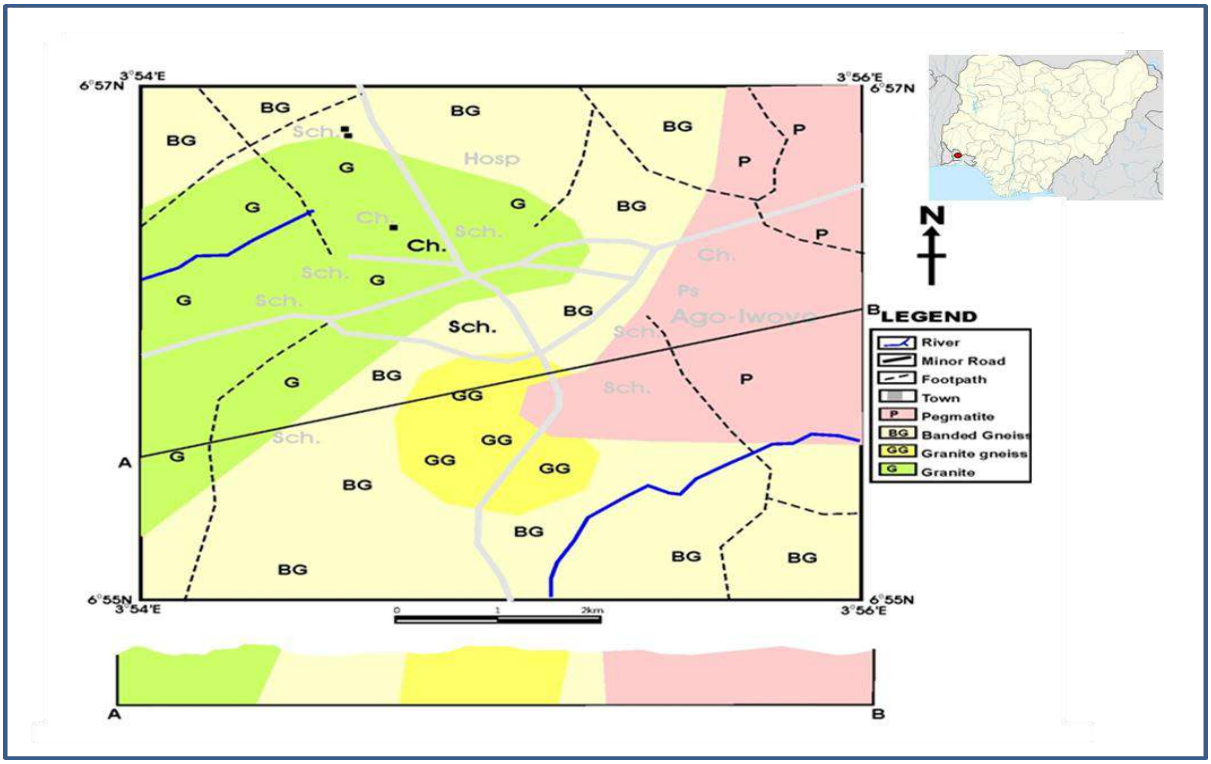

Figure 2: Geological map of the study area indicating various rock types present.

MATERIALS AND METHOD

The acquisition phase of this research entails the establishment and collection of VES data of forty five (45) points in the study location (figure 1). The maximum current electrode spacing ($\frac{AB}{2}$) was 100m using the Ohmega Ω Resistivity Meter the Schlumberger array configuration. Current were passed into the subsurface from the resistivity meter through pair of current electrode and the potential difference was measured at the electrode current end thereby generating the resistance value of the subsurface lithological unit which was later product with the appropriate Geometric Factor (G.F) for Schlumberger array configuration with reference to Zohdy *et al*., (1974) formula (1) to generate the apparent resistivity of the subsurface. In attempt to convert the apparent resistivity to true resistivity, the partial curve matching approach was adopted, this entails the bi-logarithm plotting of apparent resistivity and current electrode spacing on the ordinate and abscissa respectively after which a curve will be generated by drawing the plotted points. The generated curve is matched with standardized series of curves that has been pre-calculated (Alfano, 1959; Crous, 1971; Zohdy, 1965; Flathe, 1963); this process is known as the curve matching technique in order to obtain the resistivity, depth and thickness of the entire respective layer in the subsurface. The depth and thickness information are converted to its true values by undergoing the computer iteration process using the 1-D WINRESIST computer software program to run inversion and generate model that reveal the true parameters of the subsurface (Ghosh, 1971). Quantitative interpretation approach was adopted using formula (2) taking into consideration the resistivity of the last layer and second to the last layer in order to determine the reflection coefficient of the established point.

Apparent Resistivity

$$\rho a) = \left(\frac{\left(\frac{AB}{2}\right)^2 - \left(\frac{MN}{2}\right)^2}{MN}\right) \times \pi \ldots\ldots\ldots\ldots\ldots (1)$$

ρa= resistivity (Ωm), AB = current electrode spacing (m), MN = potential electrode spacing (m), π =3.142)

The reflection coefficient was calculated with the formula:

$$r = \frac{(\rho n - \rho(n-1))}{(\rho n + \rho(n-1))} \ldots\ldots\ldots\ldots\ldots\ldots (2)$$

(r = reflection coefficient, ρ_n = resistivity of nth / last layer, ρ (n−1) = resistivity of above the nth layer)

Two (2) lithological log information of drilling recovery for Lambo-Lambo and Ayegbami (areas within the study area) were collected from Ogun State Ministry of Water Resources for two community wells previously dug in the study area as this will serves as a physical evidence for the confirmation of the underlying lithological layer in the study area.

RESULT AND DISCUSSION

The processing of the subsurface model generated reveal a total of six (6) lithological curve geometry with their percentage occurrence are mainly H (62%), KH (20%), HKH (2%), K (2%), QH (9%) and A (5%) type (Figure 3), with most established points having 3-4 inferred layers with varying resistivity and depth for VES 1-VES 4 are presented in Figure 4a-d respectively. Inferred lithological

Scientia Africana, Vol. 21 (No. 1), April, 2022. Pp 37-52 *https://dx.doi.org/10.4314/sa.v21i1.4*
© Faculty of Science, University of Port Harcourt, Printed in Nigeria *ISSN 1118 – 1931*

units from the derived resistivity values in relation to the geology of the study location showed presence of topsoil, weathered layer (clay, clayey sand and sand) and basement (fresh and fractured basement). Resistivity range for the topsoil layer is 33.4Ωm-2485.3Ωm indicating a clayey to Lateritic topsoil layer, weathered layer comprising of clay, clayey sand and sand reveal a resistivity range of 8.3Ωm-102.6Ωm, 100.0Ωm-130.0Ωm and 199.4Ωm-784.8Ωm respectively while the basement rock for fractured and fresh basements showed resistivity range of 123.3Ωm-952.4Ωm and 993Ωm-15308.5Ωm respectively. The layer thickness observed for each successive layer revealed topsoil layer thickness range of 0.6m-1.7 while that of the weathered layer range from 2.4m-51.3m indicating a relatively varying thickness region while the thickness of the basement could not be determined (infinity). The subsurface diagrammatic view indicating vertical variation in the lithology, depth, thickness and resistivity values is presented using the geoelectric sectional diagram of traversable VES points in the study area (Figure 5 and Figure 6). Traverse A-A' (Figure 5) and Traverse F –F' (Figure 6) revealed a gradual increase in the overburden thickness from the northeastern region to the southwestern region of the study area, the topsoil have almost the same thickness from VES 20 to VES 22 for Traverse A-A' and from VES6 to VES 1 for Traverse F – F' respectively. The hydrogeological implication of this subsurface layering geometry gives an indication that the highest overburden thickness to the basement rock for the two profiles is noticeable in the eastern ad northwestern region of the study location with about 9.1m and 11.3m respectively.

Geoelectric Parameters

Evaluation for groundwater potential in a typical basement environment has identified some important geoelectric layering parameters as determinant factors that gives clue to aquiferous layer within the subsurface lithological unit. The geoelectric parameters widely used include the basement resistivity, overburden thickness and reflection coefficient which is mostly functions of resistivity and depth variation in lithological units.

The sum total thickness of lithological units overlying the subsurface aquiferous zone in an established vertical electrical sounding point is regarded as the overburden thickness (i.e addition of the thicknesses of the weathered earth materials). The overburden thickness has established a direct correlation with groundwater potentiality whereby high overburden thickness areas are associated with high groundwater potential in this tropical basement region (Akinrinade *et al*., 2016). Overburden thickness in the study location range from 2.7m to 52.2m indicating a shallow to moderately deep basement rock occurrences and it also revealed an appreciable overburden capable of yielding a considerable amount of groundwater. The geospatial isopach map of the overburden thickness revealed that most areas possess thick overburden (>22m) except for some areas in the central and western areas of the map (Figure 7) which has lesser values. The basement resistivity is also capable of inferring regions underlined with hard/ crystalline rock (non-weathered underlying basement rocks) and weathered basement rock. Area

with weathered basement rock revealed a drop in resistivity value than region underlined by non-weathered rock as the non-weathered rock can imply regions of low area of groundwater potentiality. Basement resistivity values in the study location range from 123.3Ωm-49600Ωm indicating varying resistivity values of the underlying rock types of the established geology of the study area (Figure 8). The predominant geospatial representation revealed low resistivity (<10,000 ohm meter) which serves as an indicator that can favor water bearing aquiferous layer. The small portion at the eastern and northwestern parts of the map indicate fairly high resistivity (>10,000 ohm meter) which can be an indicative of low water bearing aquiferous layer. However, the bedrock resistivity values cannot be solely used in determining the water potential of an area because of its ambiguity (Olayinka and Mbachi, 1992). The reflection coefficient, which is the function of the bedrock resistivity and the resistivity of its overlying layer usually, gives better information on presence of fracture in the subsurface which harbors the accumulation of water in the basement terrain. The reflection coefficient value ranges from 0.62 to 0.92. The geospatial maps revealed that it is higher than 0.82 on most parts of the map except for some parts in the northern and central parts of the map where reflection coefficient values are lower which is about 0.62 which is favorable for high ground water yield encouraging exploitation (Figure 9). The geospatial map of overburden thickness, basement resistivity and reflection coefficient of the study area were stacked together to enhance parameter comparison in relation to the range of value in Figure 10.

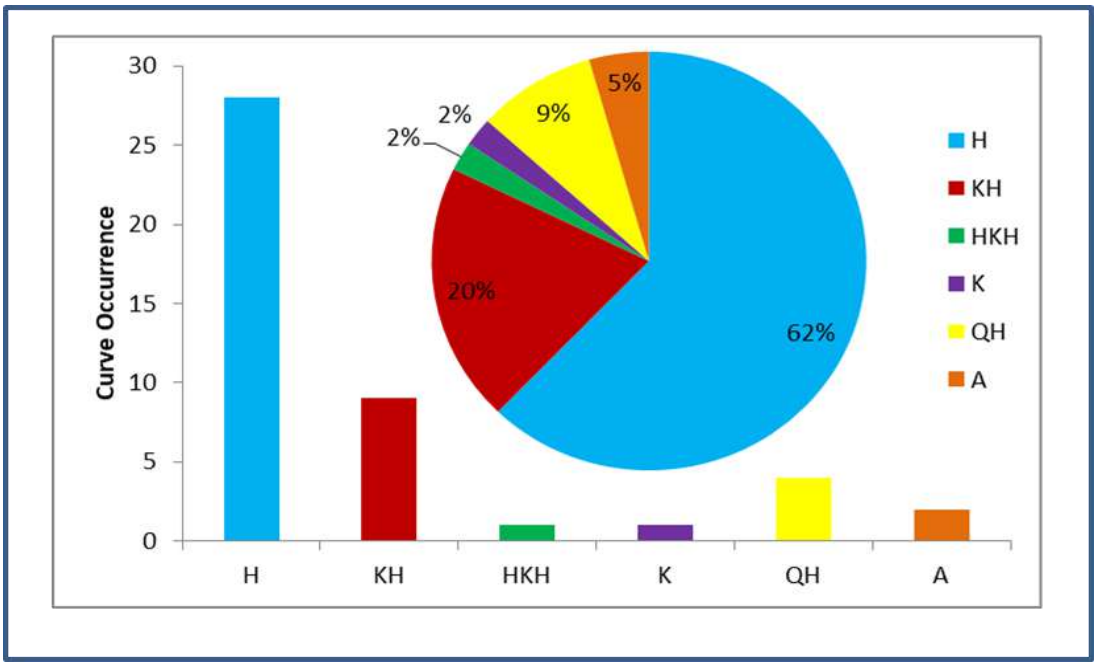

Figure 3:- Infographical summary of geophysical curve occurrence using bar and pie chart.

Scientia Africana, Vol. 21 (No. 1), April, 2022. Pp 37-52 *https://dx.doi.org/10.4314/sa.v21i1.4*
© Faculty of Science, University of Port Harcourt, Printed in Nigeria *ISSN 1118 – 1931*

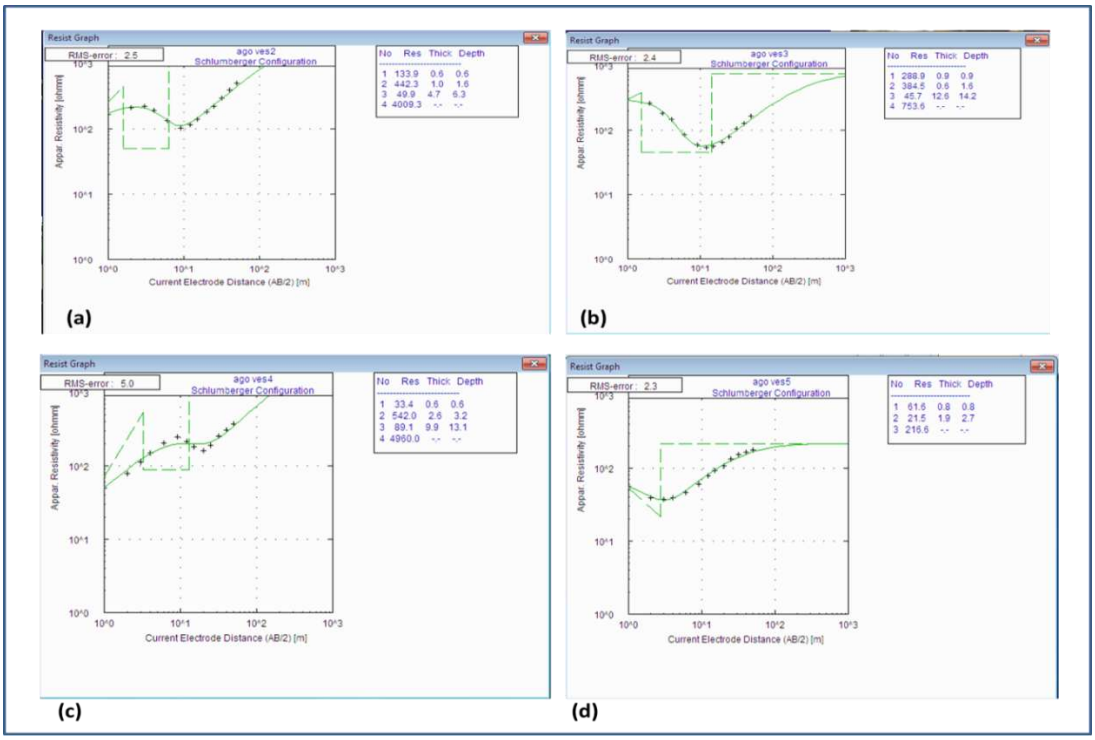

Figure 4a-d: - Generated iterated curve indicating geoelectric parameters (Resistivity, number of layers, thickness and depth for VES 1-4).

Table 1:- Geoelectric parameters of the VES points in the study area

VES Point	Basement Resistivity (Ωm)	Overburden Thickness (m)	Reflection Coefficient
VES 1	172.03	4.9	0.86
VES 2	4009.5	6.3	0.98
VES 3	753.6	14.2	0.89
VES 4	49600	13.1	0.96
VES 5	216.6	2.7	0.82
VES 6	2180.2	5	0.94
VES 7	3435.7	48.8	0.85
VES 8	1739	6.5	0.91
VES 9	618.4	3	0.91
VES 10	286.6	3.6	0.73
VES 11	285	8.4	0.85
VES 12	2331	23.8	0.95
VES 13	3868.1	20.6	0.90
VES 14	489.6	6.3	0.97
VES 15	1696	10.3	0.95
VES 16	1208	5.7	0.98
VES 17	3136.8	7.7	0.95
VES 18	6840.7	52.2	0.92
VES 19	966.8	6	0.94
VES 20	889.6	35.8	0.74

VES 21	3807.8	15.9	0.91
VES 22	2669.8	26.3	0.95
VES 23	880.9	8.8	0.69
VES 24	1440.1	6.7	0.64
VES 25	17746.4	19	0.99
VES 26	712.5	5.8	0.90
VES 27	1900	6.2	0.90
VES 28	1521.5	17.1	0.75
VES 29	1250.9	13.7	0.91
VES 30	746.3	4	0.90
VES 31	478.1	9	0.61
VES 32	158.3	12.1	0.98
VES 33	2898.7	44.4	0.86
VES 34	703.3	17.1	0.74
VES 35	5515.9	11.3	0.96
VES 36	1441	11.5	0.74
VES 37	916.2	7.2	0.64
VES 38	636.8	3.1	0.74
VES 39	1266	4.9	0.87
VES 40	21729.6	22.3	0.95
VES 41	1098.6	9.1	0.91
VES 42	1052.2	12.5	0.91
VES 43	952.4	5.1	0.83
VES 44	993	3.3	0.81
VES 45	123.3	7.3	0.70

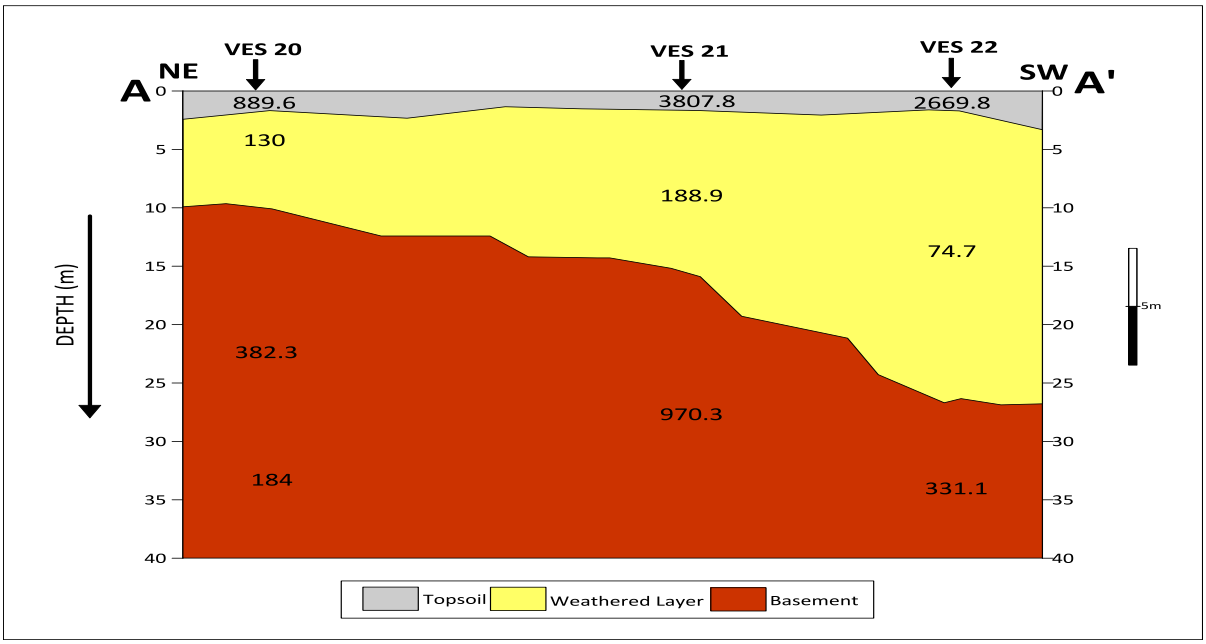

Figure 5:- The geoelectric section along traverse line A -A’

Scientia Africana, Vol. 21 (No. 1), April, 2022. Pp 37-52 https://dx.doi.org/10.4314/sa.v21i1.4
© Faculty of Science, University of Port Harcourt, Printed in Nigeria *ISSN 1118 – 1931*

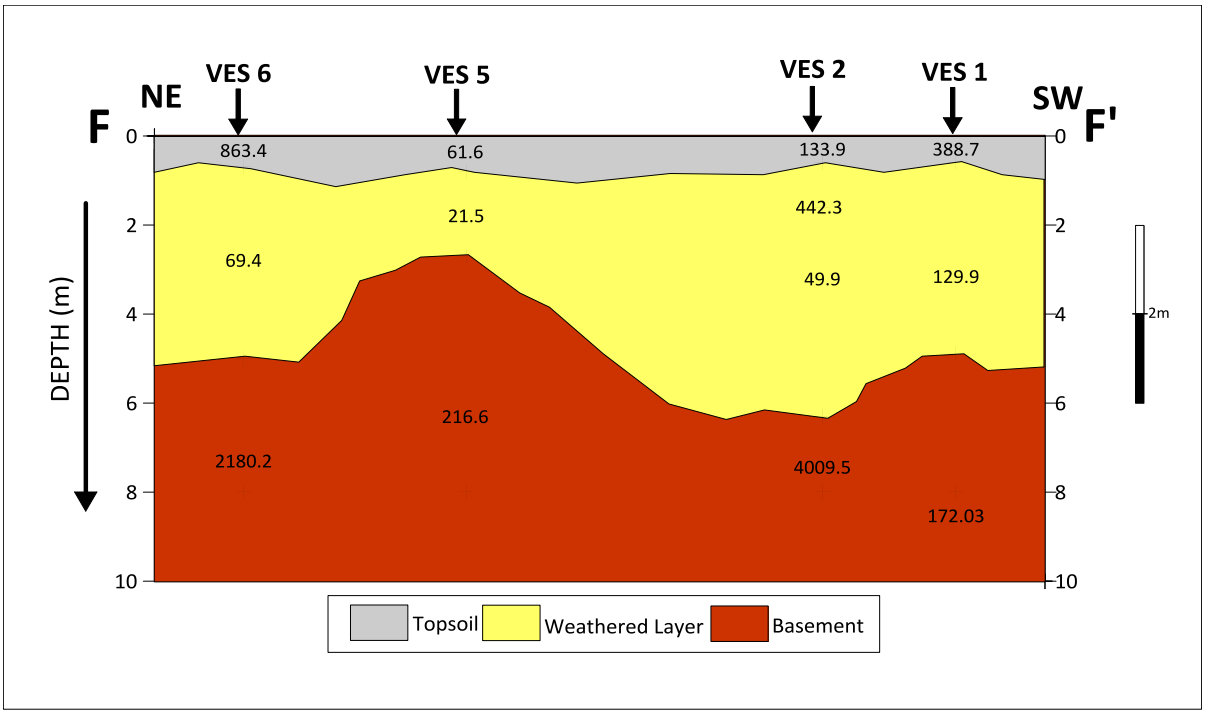

Figure 6:- The geoelectric section along traverse line F -F'

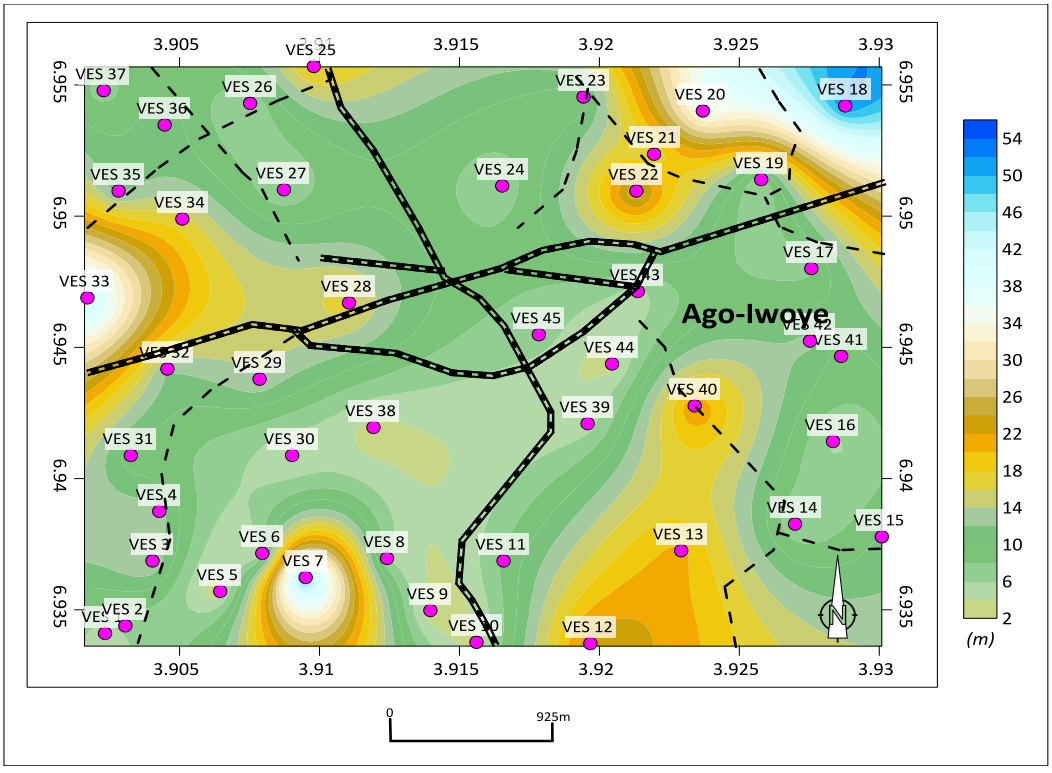

Figure 7: The Isopach map of the overburden thickness in the study location showing the VES points.

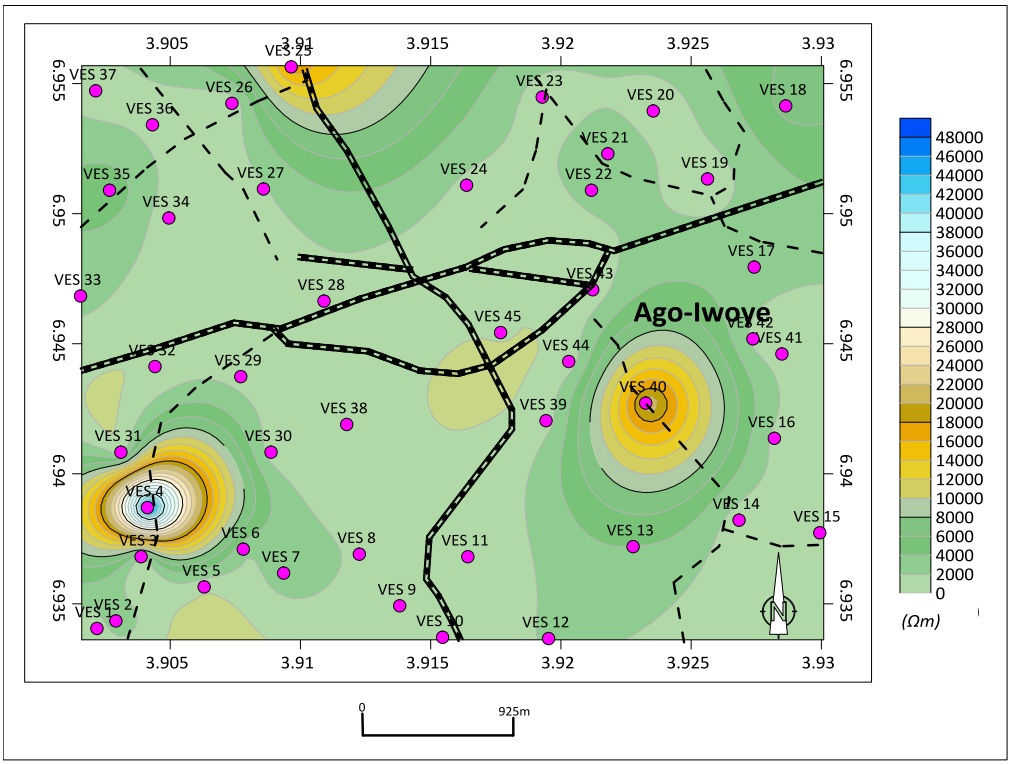

Figure 8:-Basement resistivity map of the study location showing the VES points.

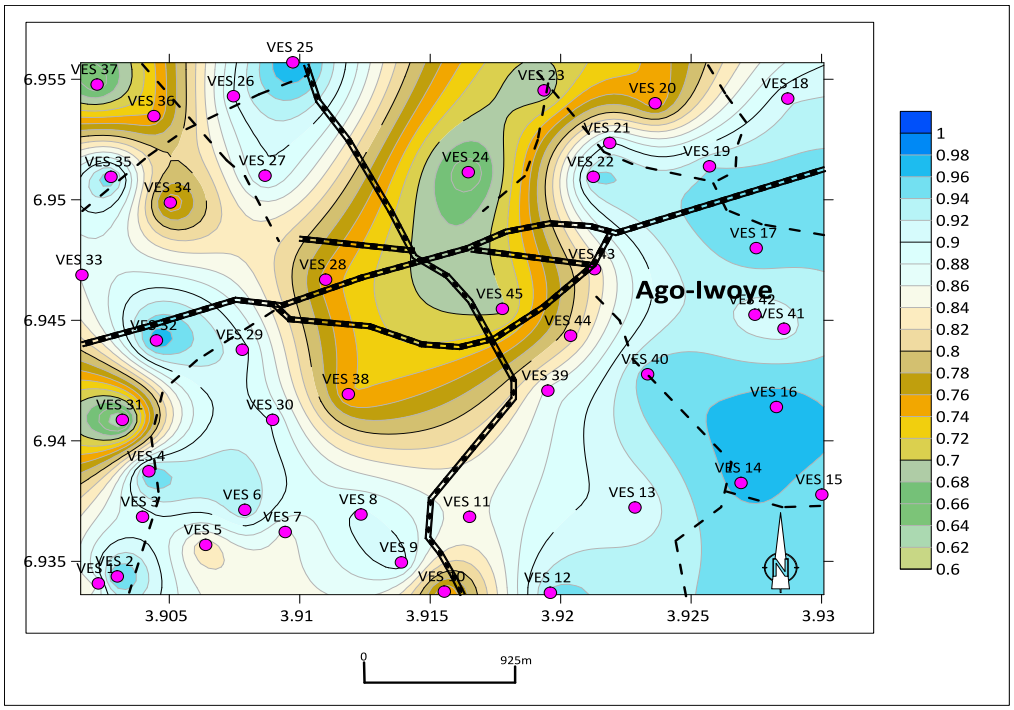

Figure 9:- Reflection coefficient of the study location.

Scientia Africana, Vol. 21 (No. 1), April, 2022. Pp 37-52 *https://dx.doi.org/10.4314/sa.v21i1.4*

ISSN 1118 – 1931

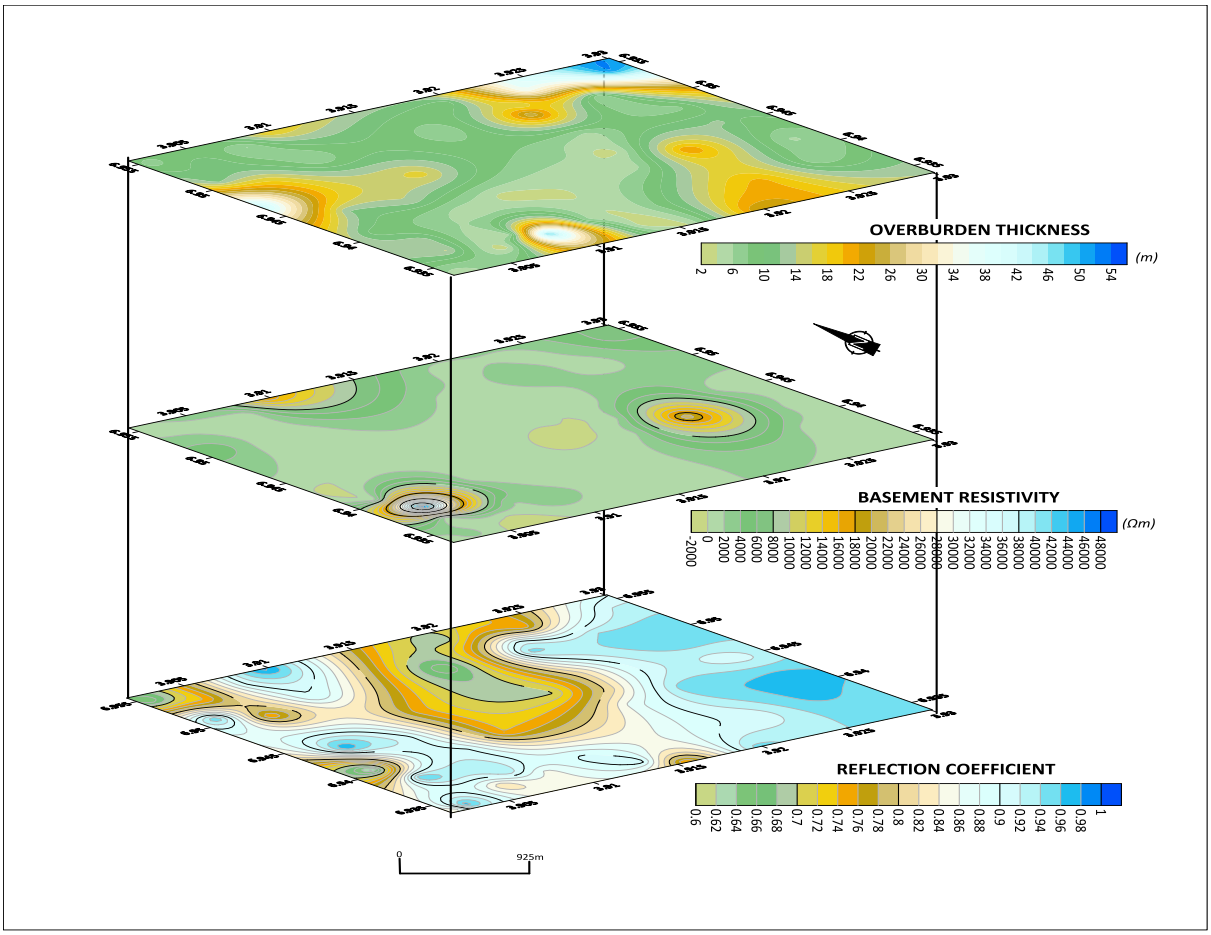

Figure 10:- Stacked map of overburden thickness, basement resistivity and reflection coefficient of the study area.

Delineation of Groundwater Potential Zones

Studying the condition of the basement rock underlying a crystalline basement environment is very essential in the delineation of groundwater potential. Hydrogeologically, they are relatively impermeable and they often have no primary porosity resulting from rock formation process, these characteristics (porosity and permeability) serves as the basis for which the hydrogeological potential of a rock is determined (Olayinka, 1996, Bayewu *et al*., 2017). The hydrogeologists therefore suggested that the major aquiferous zone in a crystalline terrain include fracture in the basement rock and tapping from the overlying weathered layer before the basement rock. The presence of fracture in rock is mainly due to post formation process (such as tectonics which involves series of tectonic movement's stages) capable of creating secondary porosity that in turn increases the groundwater potential of the rock. The weathered layer aquifer configuration resulted from the mineralogical framework of the rock undergoing weathering as weathering is more intense in rock containing ferromagnesian minerals than silicate rich mineral (Vinnarasi *et al*., 2021). These two important hydrogeological factors can be inferred from geoelectric parameters obtained using the electrical resistivity method considering the overburden thickness and

basement resistivity respectively and they can be incorporate to delineate the groundwater potential of the study location. On the basis of the integration of the overburden thickness and reflection coefficient, the groundwater potential of the study area is classified into three, which include area of high, moderate and low potential or yield (Table 2) and this parameters were carefully used to delineate the groundwater potential of each vertical electrical sounding point obtained in the study area (Table 3).

The groundwater potential of the study area reveals that groundwater potential is high in the northeastern and western part. Moderate groundwater potential region is noticeable in the western, and some part of Northeastern and southwestern part of the study location while the remaining part shows low groundwater potential (Figure 11). The potential yield delineation for low, moderate and high potential reveal a percentage of 58%, 17% and 2% respectively thereby indicating the study area can be characterized as low to moderate potential.

Lithological Log

Core sample recovery serves as a direct tool in hydro geophysical works and also other fields of geosciences as they are use as confirmation of geophysical method. Two (2) borehole logs was obtained at Lambo-Lambo and Ayegbami area of Ago-Iwoye with high materials recovery containing weathered materials in both well, with approximately high overburden thickness of >30m (Figure 12). Lambo-Lambo wells showed presence of clayey sand while it is absent in Ayegbami which showed mainly thickness of sand. This borehole has been giving a reasonable yield of water at an economic rate both in the wet and dry season which is due to the high overburden thickness of this area.

Table 2:- Groundwater Potential Classification Criteria (Bayewu *et al*., 2017)

	Overburden	**Reflection coefficient**	**Remarks**
1	<10	>0.8	Low groundwater yield
2	10--20	>0.8	Moderate groundwater yield
3	>20	<0.8	High groundwater yield

Table 3:- Groundwater yield potential classification of established VES point

VES point	**Overburden Thickness**	**Reflection Coefficient**	**Groundwater Yield potential**
VES 1	4.9	0.86	Low
VES 2	6.3	0.98	Low
VES 3	14.2	0.89	Moderate
VES 4	13.1	0.96	Moderate
VES 5	2.7	0.82	Low
VES 6	5	0.94	Low
VES 7	48.8	0.85	Moderate
VES 8	6.5	0.91	Low
VES 9	3	0.91	Low
VES 10	3.6	0.73	Low

Scientia Africana, Vol. 21 (No. 1), April, 2022. Pp 37-52 *https://dx.doi.org/10.4314/sa.v21i1.4*
© Faculty of Science, University of Port Harcourt, Printed in Nigeria *ISSN 1118 – 1931*

VES 11	8.4	0.85	Low
VES 12	23.8	0.95	Moderate
VES 13	20.6	0.90	Moderate
VES 14	6.3	0.97	Low
VES 15	10.3	0.95	Moderate
VES 16	5.7	0.98	Low
VES 17	7.7	0.95	Low
VES 18	52.2	0.92	Moderate
VES 19	6	0.94	Low
VES 20	35.8	0.74	High
VES 21	15.9	0.91	Moderate
VES 22	26.3	0.95	Moderate
VES 23	8.8	0.69	Low
VES 24	6.7	0.64	Low
VES 25	19	0.99	Moderate
VES 26	5.8	0.90	Low
VES 27	6.2	0.90	Low
VES 28	17.1	0.75	Moderate
VES 29	13.7	0.91	Moderate
VES 30	4	0.90	Low
VES 31	9	0.61	Low
VES 32	12.1	0.98	Moderate
VES 33	44.4	0.86	Moderate
VES 34	17.1	0.74	Moderate
VES 35	11.3	0.96	Low
VES 36	11.5	0.74	Moderate
VES 37	7.2	0.64	Low
VES 38	3.1	0.74	Low
VES 39	4.9	0.87	Low
VES 40	22.3	0.95	Moderate
VES 41	9.1	0.91	Low
VES 42	12.5	0.91	Moderate
VES 43	5.1	0.83	Low
VES 44	3.3	0.81	Low
VES 45	7.3	0.70	Low

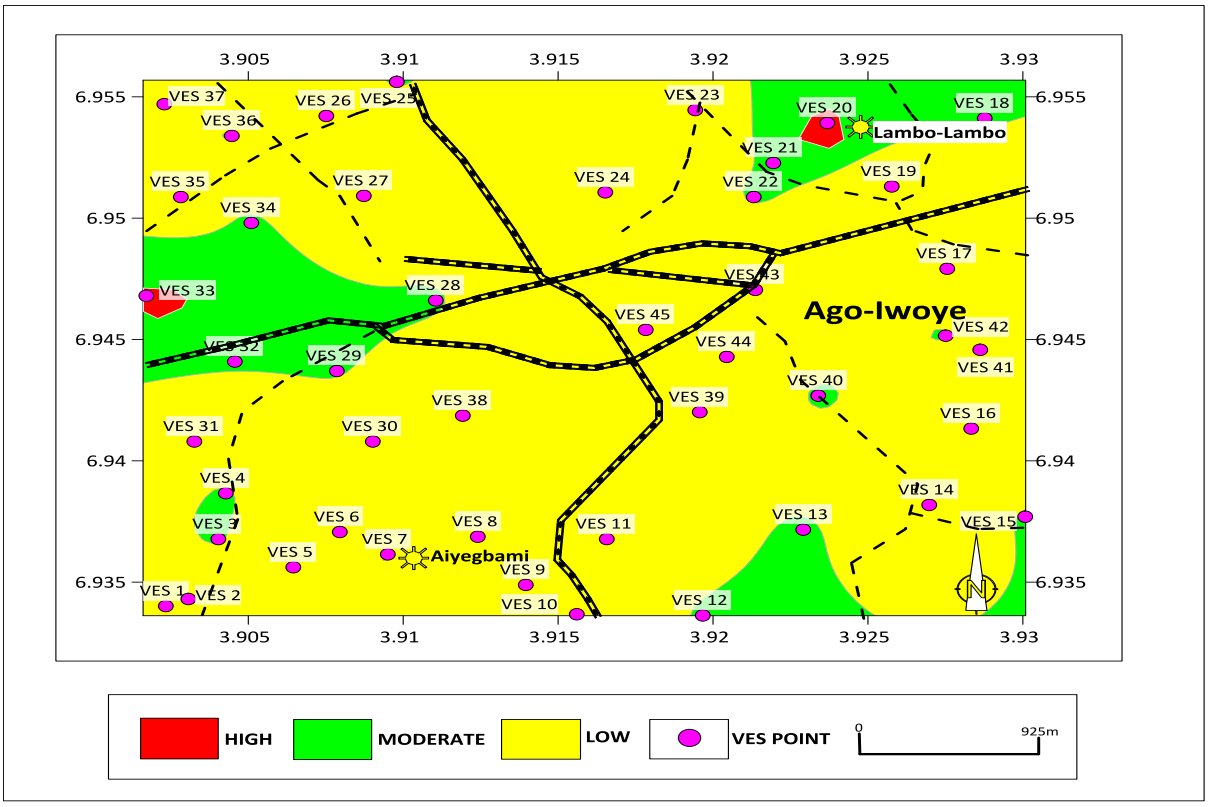

Figure 11:- Groundwater potential map of the study area.

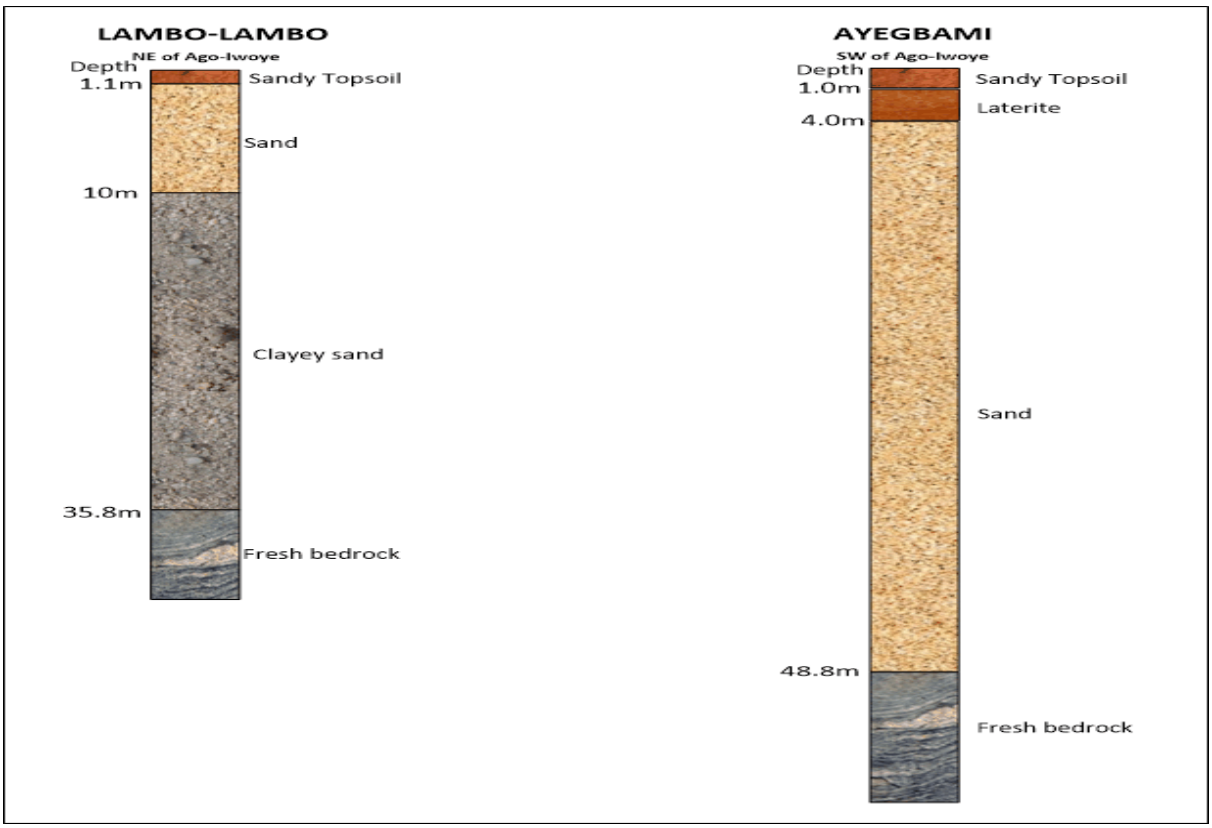

Figure 12:-The lithological log for borehole at Lambo-Lambo and Ayegbami in the study area

Scientia Africana, Vol. 21 (No. 1), April, 2022. Pp 37-52 *https://dx.doi.org/10.4314/sa.v21i1.4*
© Faculty of Science, University of Port Harcourt, Printed in Nigeria *ISSN 1118 – 1931*

CONCLUSION

Interpretation of results obtained from the geological information, geoelectric parameters and core lithology has revealed the condition of the subsurface and this has been used to infer the hydrogeological condition of the subsurface in the study area. The study area is predominantly of low yield based on the classification of groundwater yield potential for the study area. Fracturing and relatively moderate overburden increases the ground water potential in the eastern and western part of the study location. High aquiferous groundwater potential areas is only noticeable in the northeastern and western part of the study area as a local occurrence and this is due to the fracturing of the rock that has created secondary porosity by tectonism and also presence of overburden thickness to bedrock.

REFERENCES

Adeyemi, G.O. and R.O. Salami (2004) Some Geotechnical Properties of Two Termite-reworked Lateritic Soils from Ago-Iwoye, South-Western Nigeria Geotechnology, 133, pp. 35 – 41.

Akinrinade, O. J., and Adesina, R. B. (2016. Hydrogeophysical investigation of groundwater potential and aquifer vulnerability prediction in basement complex terrain–a case study from Akure, Southwestern Nigeria. Materials and Geoenvironment, 63(1), pp. 55-56.

Alfano, L., (1959) Introduction to the interpretation of resistivity measurements for complicated structural conditions: Geophysics Prospecting, 7, pp. 311-366.

Ariyo, S.O., Ajibade, O.M., Coker, J.O., Adeyemi, G.O., Oshagale, B. and Odugbesan, O.O. (2021) Hydrogeophysical Characterization of Aquifer for Groundwater Potential Evaluation at Ogbere, Southwestern Nigeria, Journal of Mining and Geology, 57(1), pp. 33-39.

Bayewu O. O., Oloruntola M. O., Mosuro G. O., Laniyan T. A., Ariyo S. O, Fatoba J. O. (2017) Geophysical evaluation of groundwater potential in part of southwestern Basement Complex terrain of Nigeria, Journal of Applied Water Science, 7, pp. 4615–4632.

Bayewu O.O., Oloruntola M O., Mosuro G.O., Laniyan T.A., Ariyo S.O., and Fatoba J.O. (2018) Assessment of groundwater prospect and aquifer protective capacity using resistivity method in Olabisi Onabanjo University campus, Ago-Iwoye, Southwestern Nigeria, NRIAG Journal of Astronomy and Geophysics, 7(2), pp. 347-360, DOI: 10.1016/j.nrjag.2018.05.002

Carruthers, R.M., (1985) Review of geophysical techniques for groundwater exploration in crystalline basement terrain: British Geological Survey, Regional Geophysics Research Group, Report, 85/3, pp 30.

Crous, C.M., (1971) Computer assisted interpretation of electrical soundings: Colorado School of Mines, Thesis T-1363.

Emenike, E.A., (2001) Geophysical exploration for groundwater in a Sedimentary Environment: A case study from Nanka over Nanka Formation in Anambra Basin, Southeastern Nigeria: Global Journal of Pure and Applied Sciences, 7(1), pp. 1-11.

Flathe, H. (1963) Five-layer master curves for the hydrogeological interpretation of geoelectric resistivity measurements above a two-story aquifer: Geophysical Prospecting, 11, pp. 471-508.

Ghosh, D.P. (1971) Inverse filter coeffecients for the computation of apparent resistivity standard curves for a horizontally stratified earth: Geophysical Prospecting, 19(4), pp. 769-775.

Haque, A., Salama, A., Lo, K., and Wu, P. (2021) Surface and Groundwater Interactions: A Review of Coupling Strategies in Detailed Domain Models. Hydrology, 8(1), pp. 35.

Olayinka, A. (1996) Carbon mineralization from poultry manure straw sawdust amended Alfisol. Ife Journal of Agriculture, 1, pp. 26-36.

Olayinka, A.I. and Olorunfemi, M.O. (1992) Determination of geoelectrical characteristics in Okene area and implication for borehole siting. Journal of Mining and Geology, 28, pp. 403-412

Olayinka, A.I., and Mbachi, C.N.C. (1992) A technique for the interpretation of electrical sounding from crystalline basement Areas of Nigeria. Journal of Mining and Geology, 27, pp. 63-69.

Olorunniwo, M.A., and M.O. Olorunfemi. (1987) Geophysical investigation for groundwater in Precambrian terrain, a case history from Ikare, Southwest Nigeria, Journal of African Earth Sciences, 6, pp. 787-796.

Vinnarasi, F., Srinivasamoorthy, K., Saravanan (2021) Chemical weathering and atmospheric carbon dioxide (CO_2) consumption in Shanmuganadhi, South India: evidences from groundwater geochemistry. Environ Geochemical Health, 43, pp. 771–790. https://doi.org/10.1007/s10653-020-00540-3 .

Zohdy, A. A. (1965) The auxiliary point method of electrical sounding interpretation, and its relationship to the Dar Zarrouk parameters. Geophysics, 30(4), 644-660.

Zohdy, A. A., Eaton, G. P., & Mabey, D. R. (1974) Application of surface geophysics to ground-water investigations.

Zohdy, A.A., Bisdorf, R.J., and Gates, J.S. (1994) A Direct Current Resistivity Survey of the Beaver Dam Wash Drainage in Southwest Utah, Southeast Nevada, and Northwest Arizona: U.S. Geological Survey Open-File Report, 94-676, pp. 87.

Scientia Africana, Vol. 21 (No. 1), April, 2022. Pp 53-66 *https://dx.doi.org/10.4314/sa.v21i1.5*
© Faculty of Science, University of Port Harcourt, Printed in Nigeria *ISSN 1118 – 1931*

ANTIMCROBIAL ACTIVITY OF EXTRACT OF *BRYOPHYLLUM PINNATUM* AND *CITRUS AURANTIFOLIA*ON SOME SELECTED PATHOGENS.

Itaman, V. O.,* Osaro-Matthew, R. C., and Umeojinkeya, B.O.
Department of Microbiology, Michael Okpara University of Agriculture, Umudike, Abia State, Nigeria.
**Corresponding author: Email: itamanvivien@yahoo.com*

Received: 11-11-2021
Accepted: 04-02-2022

ABSTRACT

The inhibitory properties of Bryophyllum pinnatum and lime juice on some selected microorganisms (Staphylococcus aureus,Streptococcus pyogenes, Escherichia coli, Klebsiella pneumoniae, Aspergillus niger and Candida albicans) were investigated. The various concentrations of the extracts were prepared by double dilution method while the ability of the various extracts to inhibit the growth of the pathogenic organisms was determined using the agar well technique. The highest in-vitro antimicrobial activity of methanolic extract of Bryophyllum pinnatum was (13.0±2.83^{a} mm at 200 mg/ml) against Klebsiella pneumoniae while the least antimicrobial activity was (10.5±2.12^{b} and 10.0±0.00^{e} mm at 200 mg/ml) against Streptococcus pyogenes and Candida albicans respectively. The lime juice extracts had the highest in-vitro antimicrobial activity was (11.0±0.00^{b} mm at 200 mg/ml) against Staphylococcus aureus while the least antimicrobial activity was (7.0± 0.0^{b} mm at 200 mg/ml) against Streptococcus pyogenes. The methanol and aqueous soluble plant extracts were active against all the test isolates but methanol extract of Bryophyllum pinnatum demonstrated greater inhibitory activity (MIC) on Staphylococcus aureus, Escherichia coli, Streptococcus species and Aspergillus niger at the range of 12.5 mg/ml. The lime juice extracts demonstrated greater inhibitory activity (MIC) on Escherichia coli at 12.5 mg/ml. The results in the findings showed that the methanolic and aqueous extracts of Bryophyllum pinnatum as well as lime juice extracts have broad-spectrum antimicrobial activity and can serve as natural therapeutic agent against some enteric pathogens.

Keywords: *Bryophyllum pinnatum,* inhibitory properties, microorganisms, methanol, aqueous.

INTRODUCTION

The plant kingdom consists of a variety of plants which are of immerse importance to humans and of valuable use in the treatment of various illnesses (Igbinosa *et al.*, 2009; Akinyeye *et al.*, 2014).The medicinal value of these plants lies on their chemical and phytochemical substances they contain. Different parts (bark, root, twig, fruit and leaves) of different plants have been studied and found to be sources of antimicrobial agents. Many of these indigenous medicinal plants are used as spices and food plants that are sometimes added to foods for pregnant and nursing mothers for medicinal purposes (Akinyeye *et al.*, 2014). Medicinal plants contain biologically active chemical substances such as saponins, tannins, essential oil flavonoids, alkaloids and other chemical which have curative properties. These complex chemical substances of different composition are found as secondary plant

metabolite in one or more of these plants (Kayode and Kayode, 2011).

Bryophyllum pinnatum belongs to the crassulaceae family and is commonly found in tropical Africa, India, China, America and Australia (Obaid *et al*., 2019). *Bryophyllum pinnatum* is used in ethnomedicine. The leaves and leaf juice have been used traditionally as anti-inflammatory, antipyretic, antimicrobial, anti-oxidant, antitumour, antidiabetic, anti-ulcer, antiseptic, hypocholosterolemic, and cough suppressant (Ali *et al*., 2013; Ghasi *etal*., 2011; Devbhuti *et al.,* 2012). The leaves or the whole plant are used as analgesic and generally for the treatment of ear ache, cough, asthma, diarrhoea, dysentery, jaundice, abscesses, ulcers, insect bites, heart troubles, epilepsy, arthritis, dysmenorrheal, whitlow and other ailments. (Ghasi *etal*., 2011). This wide range of traditional uses justifies its being called "life plant", "resurrection plant", "goodluck", love plant, cathedral bells or miracle leaf and is distinctive for the profusion of miniature plantlets that form on the margins of its Phylloclades, a trait it has in common with some other members of its genus (Ghasi *et al*., 2011). The plant is a good source of ascorbic acids, riboflavin, thiamine and niacin.

Citrus aurantifolia (Lime) belongs to the Citrus family. It is sour in taste and serves as a rich source of vitamin C and often used to accent the flavours of foods and beverages. Limes contain nutrients such as carbohydrates, sugar, soluble and insoluble fiber, sodium, vitamins, minerals, fatty acids and amino acids (Bina *et al*., 2010). Limes possess unique flavonoid compounds that have antimicrobial, antioxidant and anti-cancer properties (Tomotake, 2006). Limes are also effective in the treatment of stomach ache, colds, fevers, sore throats, sinusitis, bronchitis and asthma (Khan*et al*., 2012). The present study was designed to evaluate the antimicrobial activity and potency of*B.pinnatum* and *Citrusaurantifolia* leaf extracts respectively on pathogens.

MATERIALS AND METHODS

Collection of samples

Fresh plant of *Bryophyllum pinnatum* was collected from the horticulture department of the National Root Crop Research Institute (NRCRI), Umudike and was identified by Mrs Flora Mukah from the Department of Plant Science and Biotechnology, Michael Okpara University of Agriculture, Umudike. The lime fruit was purchased from Ndioru market at Umudike, Abia State, Nigeria and was washed with distilled water.

Preparation and extraction of the leaf extracts

The leaves of *Bryophyllum pinnatum* were washed severally to remove dirt, dried in shade at room temperature and ground to powder using electric blender of model W-BL5085M. Fifty (50) grams of the leaf powder was macerated in 500 ml of methanol and 500 ml distilled water (aqueous extract) for 24 hours, and centrifuged at 120 rpm to enable proper diffusion of the active ingredients. After that, the contents were filtered using Whatman's filter paper No 1. The filtrates were evaporated to dryness separately in a water bath and stored for analysis (Karabi and Sankar, 2015).

Preparation and extraction of *Citrus aurantifolia* juice extract

Scientia Africana, Vol. 21 (No. 1), April, 2022. Pp 53-66 https://dx.doi.org/10.4314/sa.v21i1.5
© Faculty of Science, University of Port Harcourt, Printed in Nigeria *ISSN 1118 – 1931*

Citrus aurantifolia fruits free from defects and decay were washed with distilled water to remove dirt and further sterilized with methanol to remove any form of contaminant. The fruits were aseptically cut with a sterile knife and the juice extracted. The extracted juice was stored in a sterile container at a temperature of 4°C to 8°C (Ugwu *et al.*, 2018).

Preparation of concentration of the extracts

One gram (1g) each of the methanol and aqueous crude extract of the plant was added to 5 ml of aqueous and methanol respectively to give a concentration of 200 mg/ml. Other concentrations of 150, 100, 50, 25 and 12.5mg/ml were prepared by double dilution method as described by Iqbal and Arina (2001). Also, the lime juice was diluted with distilled water to give concentrations of 200, 150, 100, 50, 25, and 12.5 mg/ml respectively.

Test microorganisms

Bacterial and fungal cultures: *Staphylococcus aureus, Streptococcus pyogenes, Escherichia coli, Klebsiella pneumoniae, Candida albicans* and *Aspergillus niger* were obtained from Microbiology Laboratory stocks in Michael Okpara University of agriculture, Umudike, Abia State, Nigeria. The test organisms were resuscitated and the bacteria identities confirmed using cultural, morphological and biochemical tests as described by Cheesbrough, (2006). The test fungi were identified and characterized based on their macroscopic and microscopic characteristics by comparing them to taxonomic guides (Barnett and Hunter, 1972; Cheesbrough, 2006). They were maintained at 4°C on agar slants.

Standardization of bacterial inoculum:

Suspension of microorganisms was made in nutrient broth and incubated at 37°C for 24 hours. Turbidity produced was adjusted using sterile normal saline to 0.5 MacFarland standards (10^8CFU/ml).

Antimicrobial properties of lime juice and plant extracts against test organisms

The ability of the various extracts to inhibit the growth of the bacterial and fungal pathogenic organisms was determined using the agar well diffusion technique. Standardized 50µl inoculum of each selected bacteria was aseptically inoculated onto Mueller-Hilton agar plates and the fungi on SDA plates using the spread plate method. A sterile cork borer of 5 mm diameter was used to make wells on the plates and 0.1ml of each varying concentrations of the plant extracts, lime juice and antibiotic control (Gentamycin/Ketoconazole), i.e. 200, 150, 100, 50, 25 and 12.5 mg/ml was dispensed into the wells. The plates were allowed to stand at room temperature for 30 minutes to allow for easy diffusion of the extract into the agar before being incubated at 37°C for 24 hours and room temperature (25^oC) for 72 hours for fungi. After incubation, the diameter of the zones of inhibition around each well was measured and recorded in millimeter representing the antimicrobial activities of the extracts (Ahmad and Beg, 2001).

Determination of Minimum Inhibitory Concentration (MIC)

The minimum inhibitory concentration (MIC) of both leaf extracts and lime juice

were determined for each of the test bacterial and fungal pathogen at varying concentrations of 200, 150, 100, 50, 25, 12.5, 6.25 and 3.125 mg/ml. One milliliter (1 ml) of nutrient broth was added and then one milliliter (1ml) of the standardized bacterial suspension was added. A tube containing nutrient broth only was seeded with the test organism to serve as control. It was incubated at 37^{o}C for 24 hours and then examined for growth by observing turbidity (Kaya *et al.,* 2012). For fungal cultures, prepared sabouraud dextrose broth was used. The tubes were incubated at 25^{o}C for 72 hours and then examined for growth by observing for turbidity (Kaya *et al.,* 2012). The lowest extract concentration that showed growth was read as the MIC.

Determination of Minimum bactericidal/ fungicidal Concentration (MBC AND MFC)

The minimum bactericidal concentration/ Fungicidal Concentration (MBC/MFC) of all the extracts on the bacteria and fungi were carried out according to Ajaiyeoba *et al*. (2003). One (1ml) of each of the MIC tube cultures which showed no growth was pipetted onto nutrient and sabouraud dextrose agar plates and incubated at 37^{0}C and 25^{o}C for 24 hours and 72 hours respectively. After incubation, the lowest concentration at which there was no single colony of bacteria on nutrient agar and fungi on sabouraud dextrose agar plates was taken as MBC and MFC.

Statistical Analysis

One-way analysis of variance (one-way ANOVA) by using the statistical package for social sciences (SPSS Inc, Chicago, USA) program version 17.0 was used to analyze all data collected. The significant difference between the variables at $p < 0.05$ was determined by Duncan test.Triplicate determinations were carried out and standard errors were calculated for all results.

RESULTS AND DISCUSSION

The antimicrobial activity of the methanol and aqueous extracts of *Bryophyllum pinnatum* (Table 1) showed that *Bryophyllum pinnatum*exhibited varying degrees of antimicrobial activities against the test isolates, with the methanolic extract of *Bryophyllum pinnatum* showing more activity than the aqueous extracts.

Table 1: Antimicrobial activity of the methanol and aqueous extracts of *Bryophyllum pinnatum* against test organisms

Test Organisms	Concentration (mg/ml)/Zone of Inhibition (mm)									
	Methanol					Aqueous				
	200mg/ml	100mg/ml	50mg/ml	25mg/ml	12.5mg/ml	200mg/ml	100mg/ml	50mg/ml	25mg/ml	12.5mg/ml
S. aureus	12.5±0.71^d	10.0 ±1.41^a	8.0±0.10^d	6.0±0.0^b	0.0±0.0^b	6.0± 0.0^c	0.0± 0.0^c	0.0± 0.0^b	0.0± 0.0^e	0.0± 0.0^a
S. pyogenes	10.5±2.12^b	7.5±0.71^b	3.0±1.24^b	0.0±0.0^c	0.0±0.0^b	7.0± 1.41^a	3.0± 4.24^a	0.0 ± 0.0^e	0.0± 0.0^c	0.0± 0.0^d
E. coli	11.0±1.41^c	8.5±0.71^b	6.5±0.71^c	0.0±0.0^c	0.0± 0.0^c	8.0± 0.0^c	3.0± 4.24^a	0.0± 0.0^c	0.0± 0.0^c	0.0± 0.0^b
K. pneumoniae	13.0± 2.83^a	10.0± 1.41^a	7.5± 2.21^a	7.5±2.21^a	0.0± 0.0^d	8.0± 0.0^c	0.0± 0.0^c	0.0± 0.0^a	0.0± 0.0^b	0.0± 0.0^c
Candida albicans	10.0± 0.0^e	8.5± 0.0^c	6.0± 0.0^e	0.0± 0.0^c	0.0± 0.0^c	8.5± 0.71^b	6.5± 0.71^b	0.0± 0.0^c	0.0± 0.0^a	0.0± 0.0^b
Aspergillus niger	10.5± 0.71^d	9.5± 0.71^b	7.0±1.41^b	0.0± 0.0^c	0.0± 0.0^e	9.0± 1.41^a	8.0± 0.0^c	6.0± 0.0^d	0.0± 0.0^c	0.0± 0.0^d

Values and means of triplicate analysis ± standard deviation. Means with different superscripts in the same column are significantly different($P \leq 0.05$).

Key:

- indicates no growth ; + indicates growth

Scientia Africana, Vol. 21 (No. 1), April, 2022. Pp 53-66 *https://dx.doi.org/10.4314/sa.v21i1.5*
© Faculty of Science, University of Port Harcourt, Printed in Nigeria *ISSN 1118 – 1931*

The antimicrobial activity of the lime juice (*Citrus auranifolia*) soluble extracts (Table 2) shows thatthe highest *in-vitro* antimicrobial activity (11.0±0.00^{b}mm) was exhibited by the lime juice extracts at the concentration of 200 mg/ml against *Staphylococcus aureus*, while the least antimicrobial activity (8.0±0.00^{b}mm) exhibited at the concentration of 200 mg/ml was against *Aspergillus niger* and *Candida albicans*.

Table 2: Antimicrobial activity of the lime juice (*Citrus auranifolia*) extract against test organisms

Test Organisms	Concentration (mg/ml)/Zone of Inhibition (mm)				
	200mg/ml	100mg/ml	50mg/ml	25mg/ml	12.5 mg/ml
Staphylococcus aureus	11.0 ± 0.0^{b}	7.5± 0.71^{a}	3.0±4.24^{a}	0.0± 0.0^{d}	0.0± 0.0^{d}
Streptococcus pyogenes	7.0± 0.0^{b}	0.0± 0.0^{c}	0.0± 0.0^{b}	0.0± 0.0^{b}	0.0± 0.0^{b}
Escherichia coli	9.5± 0.71^{a}	7.5± 0.0^{c}	0.0± 0.0^{b}	0.0± 0.0^{b}	0.0± 0.0^{e}
Klebsiella pneumoniae	10.5± 0.71^{a}	8.0± 1.41^{b}	3.0±4.24^{a}	0.0± 0.0^{c}	0.0± 0.0^{b}
Candida albicans	8.0± 0.0^{b}	0.0± 0.0^{c}	0.0± 0.0^{b}	0.0± 0.0^{e}	0.0± 0.0^{d}
Aspergillus niger	8.0± 0.0^{b}	0.0± 0.0^{c}	0.0± 0.0^{b}	0.0± 0.0^{c}	0.0± 0.0^{e}

Values and means of triplicate analysis ± standard deviation. Means with different superscripts in the same column are significantly different($P \leq 0.05$).

Key:

- indicates no growth

+ indicates growth

The zone of inhibition produced by the standard antimicrobial agent (Gentamicin and Nystanin) against the test microorganisms showed higher antimicrobial activities than the extracts of *Bryophyllum pinnatum* and *Citrus auranifolia*.

Table 3: Zone of inhibition (mm) of standard antimicrobial agent (Gentamicin and Nystanin) against the test organism's positive control

Test Organisms	Concentration (mg/ml)/Zone of Inhibition (mm)				
	200mg/ml	100mg/ml	50mg/ml	25mg/ml	12.5 mg/ml
Staphylococcus aureus	16.5 ± 2.12^{a}	14.5± 2.12^{a}	11.0±1.41^{b}	8.0± 1.0^{d}	6.0± 0.0^{b}
Streptococcus pyogenes	16.0 ± 1.21^{a}	13.5 ± 0.71^{e}	9.5± 0.51^{d}	7.0±1.31^{b}	0.0± 0.0^{b}
Escherichia coli	21.0 ± 1.48^{b}	17.0± 1.41^{c}	14.0± 1.52^{a}	9.0± 1.41^{a}	6.0± 00^{b}
Klebsiella pneumoniae	17.5± 0.71^{d}	15.0± 1.71^{b}	11.5± 0.71^{c}	9.0± 1.41^{a}	6.5± 0.71^{a}
Candida albicans	15.0± 1.41^{c}	12.0± 1.41^{d}	11.0± 0.70^{c}	7.0±1.31^{b}	0.0± 0.0^{b}
Aspergillus niger	13.0± 1.41^{c}	12.0± 1.41^{d}	9.5± 0.51^{d}	7.5±1.12^{c}	0.0± 0.0^{b}

Values and means of triplicate analysis ± standard deviation. Means with different superscripts in the same column are significantly different($P \leq 0.05$).

Key:

- indicates no growth

+ indicates growth

Table 4 and Table 5 shows the minimum inhibitory concentration (MIC) of *Bryophyllum pinnatum* and *Citrus auranifolia* extracts against test bacteria. Methanol and aqueous soluble plant extracts of *Bryophyllum pinnatum* were active against all the test isolates but the methanol extracts demonstrated greater inhibitory activity on *Staphylococcus aureus,*

Escherichia coli, Streptococcus pyogenes at the range of 12.5 mg/ml each. The *Citrus auranifolia* extract were active against all the test isolates but demonstrated greater inhibitory activity on *Escherichia coli* at the range of 12.5 mg/ml.

Table 4: Minimum inhibitory concentration of *Bryophyllum pinnatum* plant extract against test bacteria

Tests organisms/Extracts								
Concentration (mg/ml)	***Staphylococcus aureus***		***Streptococcus pyogenes***		***Escherichia coli***		***Klebsiella pneumoniae***	
	Methanol	Aqueous	Methanol	Aqueous	Methanol	Aqueous	Methanol	Aqueous
200	-	-	-	-	-	-	-	-
100	-	-	-	-	-	-	-	-
50	-	-	-	-	-	-	-	+
25	-	+	-	+	-	+	+	+
12.5	+	+	+	+	+	+	+	+
6.25	+	+	+	+	+	+	+	+
3.125	+	+	+	+	+	+	+	+
MIC Value (mg/ml)	**12.5**	**25.0**	**12.5**	**25.0**	**12.5**	**25.0**	**25.0**	**50.0**
Control	**6.2**		**3.1**		**3.1**		**6.2**	

Key: – indicates no growth + indicates growth, MIC = Minimum Inhibitory Concentration, Control = Gentamicin

Table 5: Minimum inhibitory concentration of Lime juice (*Citrus auranifolia*)against test bacteria

Tests organisms				
Concentration (mg/ml)	***Staphylococcus aureus***	***Streptococcus pyogenes***	***Escherichia coli***	***Klebsiella pneumoniae***
200	-	-	-	-
100	-	-	-	-
50	+	-	-	+
25	+	+	-	+
12.5	+	+	+	+
6.25	+	+	+	+
3.125	+	+	+	+
MIC Value (mg/ml)	**50.0**	**25.0**	**12.5**	**50.0**
Control	**6.2**	**3.1**	**3.1**	**6.2**

Key:
– indicates no growth
+ indicates growth
MIC = Minimum Inhibitory Concentration
Control = Gentamicin

The minimum inhibitory concentration (MIC) of the *Bryophyllum pinnatum* and *Citrus auranifolia* extracts against test fungi are shown in Tables 6 and 7.Aqueous soluble extracts of *Bryophyllum pinnatum* showed greater inhibitory activity at the range of 12.5 mg/ml against *Aspergillus niger*. *Citrus auranifolia* extract was active against all the test fungi at the

Scientia Africana, Vol. 21 (No. 1), April, 2022. Pp 53-66 *https://dx.doi.org/10.4314/sa.v21i1.5*
© Faculty of Science, University of Port Harcourt, Printed in Nigeria *ISSN 1118 – 1931*

range of 25 mg/ml.The antibiotics Nystatin (control) showed lesser inhibitory activities on *Candida albicans* and *Aspergillus niger* at the range of 6.25 mg/ml.

Table 6: Minimum inhibitory concentration of *Bryophyllum pinnatum* Plant extract against test Fungi

Tests organisms/Extracts				
Concentration (mg/ml)	***Candida albicans***		***Aspergillus niger***	
	Methanol	Aqueous	Methanol	Aqueous
200	-	-	-	-
100	-	-	-	-
50	-	+	-	-
25	+	+	-	+
12.5	+	+	+	+
6.25	+	+	+	+
3.125	+	+	+	+
MIC Value (mg/ml)	**25.0**	**50.0**	**12.5**	**25.0**
Control	**6.2**		**6.2**	

Key: – indicates no growth + indicates growth, MIC = Minimum Inhibitory Concentration, Control = Nystatin

Table 7: Minimum inhibitory concentration of Lime Juice extract against test Fungi

Tests organisms		
Concentration (mg/ml)	***Candida albicans***	***Aspergillus niger***
200	-	-
100	-	-
50	-	-
25	+	+
12.5	+	+
6.25	+	+
3.125	+	+
MIC Value (mg/ml)	**25.0**	**25.0**
Control	**6.2**	**6.2**

Key: – indicates no growth + indicates growth, MIC = Minimum Inhibitory Concentration, Control = Nystatin

The minimum bactericidal concentration (Table 8) revealed that the methanol extracts of *Bryophyllum pinnatum* showed greater activity against *Staphylococcus aureus, Streptococcus pyogenes* and *Klebsiella pneumoniae* at 100 mg/ml, when compared to the aqueous plant extract. Table 9 revealed that the soluble extracts of lime juice were active against all the test bacteria, but showed greater activity against *Staphylococcus aureus*, *Streptococcus pyogenes* and *klebsiella pneumoniae* at 100 mg/ml each.

Table 8: Minimum bactericidal concentration of the *Bryophyllum pinnatum* extract against test bacteria

Tests organisms/Extracts								
Concentration (mg/ml)	***Staphylococcus aureus***		***Streptococcus pyogenes***		***Escherichia coli***		***Klebsiella pneumoniae***	
	Methanol	Aqueous	Methanol	Aqueous	Methanol	Aqueous	Methanol	Aqueous
200	-	-	-	-	-	-	-	-
100	-	+	-	+	+	+	-	+
50	+	+	+	+	+	+	+	+

25	+	+	+	+	+	+	+	+
12.5	+	+	+	+	+	+	+	+
6.25	+	+	+	+	+	+	+	+
3.125	+	+	+	+	+	+	+	+
MBC Value (mg/ml)	**100**	**200**	**100**	**200**	**150**	**200**	**100**	**200**
Control	**6.2**		**3.1**		**3.1**		**6.2**	

Key: – indicates no growth + indicates growth, MBC = Minimum Bactericidal Concentration, Control = Gentamicin

Table 9: Minimum bactericidal concentration of the Lime Juiceextract against test bacteria

Tests organisms				
Concentration (mg/ml)	***Staphylococcus aureus***	***Streptococcus pyogenes***	***Escherichia coli***	***Klebsiella pneumoniae***
200	-	-	-	-
100	+	+	+	+
50	+	+	+	+
25	+	+	+	+
12.5	+	+	+	+
6.25	+	+	+	+
3.125	+	+	+	+
MBC Value (mg/ml)	**150**	**150**	**200**	**150**
Control	**6.2**	**3.1**	**3.1**	**6.2**

Key: – indicates no growth + indicates growth, MBC = Minimum Bactericidal Concentration, Control = Gentamicin

The minimum fungicidal concentration as shown in Table 10 revealed that the methanol and aqueous soluble extracts of *Bryophyllum pinnatum* were active against all the test isolates with the aqueous extracts showing greater antifungal activity against *Candida albicans* at the range of 100 mg/ml. The minimum fungicidal concentration revealed that the soluble extracts of lime juice were active all the test isolates but showed greater antifungal activities against *Aspergillus niger* at the range of 50 mg/ml (Table 11).

Table 10: Minimum fungicidal concentration of the *Bryophyllum pinnatum* extract against test fungi

Tests organisms/Extracts				
Concentration (mg/ml)	***Candida albicans***		***Aspergillus niger***	
	Methanol	Aqueous	Methanol	Aqueous
200	-	-	-	-
100	-	+	-	-
50	+	+	+	-
25	+	+	+	-
12.5	+	+	+	+
6.25	+	+	+	+
3.125	+	+	+	+
MFC Value (mg/ml)	**100**	**200**	**100**	**25**
Control	**100**		**100**	

Key: – indicates no growth + indicates growth, MFC = Minimum Fungicidal Concentration, Control = Nystatin

Scientia Africana, Vol. 21 (No. 1), April, 2022. Pp 53-66 *https://dx.doi.org/10.4314/sa.v21i1.5*
© Faculty of Science, University of Port Harcourt, Printed in Nigeria *ISSN 1118 – 1931*

Table 11: Minimum fungicidal concentration of the Lime Juiceextract against test fungi

Tests organisms		
Concentration (mg/ml)	***Candida albicans***	***Aspergillus niger***
200	-	-
100	+	-
50	+	-
25	+	+
12.5	+	+
6.25	+	+
3.125	+	+
MBC Value (mg/ml)	**200**	**50**
Control	**100**	**100**

Key: – indicates no growth + indicates growth, MFC = Minimum Fungicidal Concentration, Control = Nystatin

The present study showed that the methanolic and aqueous extracts of *Bryophyllum pinnatum* exhibited variable degrees of antimicrobial activities against the test isolates investigated. The extent of sensitivity of the test organisms to the plant extracts was shown by the clear zones of inhibition produced by the extracts after the period of incubation. The highest *in-vitro* antimicrobial activity of (13.0 $\pm$2.83^{a} mm at 200 mg/ml) was exhibited by the methanolic extract of *Bryophyllum pinnatum* against *Klebsiella pneumoniae* while the least antimicrobial activity (10.5$\pm$2.12^{b} mm at 200mg/ml) was against *S. pyogenes*(Table 1). This study revealed that the methanol extract of *B. pinnatum* was most effective against the test organisms than the aqueous solvents. This is in-line with the assertion of Akinnibosun and Edionwe (2015), that methanol gives a higher antimicrobial effects than other extracting solvent such as aqueous and acetone. The highest *in-vitro* antimicrobial activity of (8.0$\pm$ 0.0^{c} mm at 200 mg/ml) was also exhibited by the aqueous extract of *Bryophyllum pinnatum* against *E. coli*and *K. pneumoniae* while the least antimicrobial activity (6.0$\pm$0.00^{c}mm at 200 mg/ml) was against *Staphylococcus aureus. Aspergillus niger*showed the highest susceptibility (10.5$\pm$ 0.71^{d} at 200 mg/ml) while *Candida albicans*showed the lowest susceptibility (10.0$\pm$ 0.0^{e} at 200 mg/ml) (Table 1).

The result also revealed that the highest *in-vitro* antimicrobial activity of (11.0$\pm$0.00^{b} mm at 200 mg/ml), was exhibited by the lime juice extracts against *Staphylococcus aureus*, while the least antimicrobial activity of (7.0$\pm$0.00^{b}mm at 200 mg/ml) was exhibited against *Streptococcus pyogenes. Aspergillus niger* and *Candida albicans* exhibited susceptibility of (8.0$^{a}\pm$ 0.0^{b} at 200 mg/ml) each(Table 2). The more significant inhibition was observed with a higher extract concentration which could be due to the stronger extraction capacity of methanol. This is in agreement with the observations of Ammara*et al*., (2009), who concluded that the stronger extraction capacity of methanol could have been responsible for the higher antimicrobial activity, although the observed differences were not statistically significant ($p \geq 0.05$). The stronger extraction capacity of methanol for *Bryophyllum pinnatum* could have been responsible for the higher antibacterial and antifungal activities as the biologically active components in the plant could have

been enhanced in the presence of methanol (Ammara*et al*., 2009).

The antimicrobial activity could be attributed to the presence of phenolic compounds which have been detected in this plant extract to include: saponin, tannins, alkaloids, bryophyllin and other secondary metabolites which are antimicrobial (Okwu and Josiah, 2006;Giteru *et al*., 2015). Aromatic phenolic compounds, flavonoids, saponin, tannin, steroids, curammin, bryophyllin and alkaloids have been confirmed to be strongly antagonistic to Gram positive and Gram negative human pathogens, especially *Staphylococcusaureus*, *Klebsiella pneumoniae*, *Salmonella typhi*, *Pseudomonas aeruginosa*, *Escherichia coli* and *Bacillus subtilis* (Adegoke *et al*., 2010). The plant *B. pinnatum* has also been reported to have very numerous medicinal applications ranging from its use in the treatment and management of inflammation, glycaemia, diabetes, cancer, headache, dysentery, smallpox, *convulsion*, arthritis and spasms (Theophil *et al*., 2006). Researchers have asserted that the phenolic compounds in the plant may be responsible for its therapeutic, antiseptic, antifungal or bactericides as well as antiviral and antitumor activities (Okwu and Josiah, 2006). The zone of inhibition produced by the standard antimicrobial agent (Gentamicin and Nystanin) against the test microorganisms showed higher antimicrobial activities than the extracts of *Bryophyllum pinnatum* and *Citrus auranifolia*.

The minimum inhibitory concentration (MIC) of the methanol and aqueous extracts was read as the lowest extract concentration that showed growth. The results showed that growth of the isolates was inhibited by both the aqueous and methanol extracts between the concentrations of 12.5 mg/ml and 50 mg/ml(Table 4 and Table 6). The MIC of the lime juice was observed to be between the concentrations of 12.5 mg/ml and 50 mg/ml for the bacterial isolates (Table 5) and 25mg/ml for the fungal isolates (Table 7).

The minimum bactericidal concentration revealed that the methanol soluble extracts of *Bryophyllum pinnatum* showed greater activity against *Staphylococcus aureus, Streptococcus pyogenes* and *Klebsiella pneumoniae* at 100 mg/ml, when compared to the aqueous plant extract (Table 8). The lime juice extracts were active against *Staphylococcus aureus, Streptococcus pyogenes,* and *Klebsiella pneumoniae* at 150 mg/ml (Table 9) while the minimum bactericidal concentration varied inhibition activity. This is in agreement with the study by Lawrence *et al*., (2016) who reported that the MBC of both the methanol and aqueous extracts of *Bryophyllum pinnatum* was at 100 mg/ml concentration and the bactericidal activity of both extracts was higher against *Streptococcus* sp. than *Staphylococcus* sp. This confirms the earlier observation that antibacterial activity of both the methanol and aqueous extracts were more pronounced against *Streptococcus* sp. than against *Staphylococcus* sp. Lawrence *et al*., (2016) also stated that a higher antibacterial activity was again observed against the isolates with the methanol extract than the aqueous extract which reveals a correlating increase in antibacterial activity with increase in extract concentration.

Scientia Africana, Vol. 21 (No. 1), April, 2022. Pp 53-66 https://dx.doi.org/10.4314/sa.v21i1.5
© Faculty of Science, University of Port Harcourt, Printed in Nigeria *ISSN 1118 – 1931*

In this present study, the lime juice and the methanol and aqueous soluble plant extracts of *Bryophyllum pinnatum* were active against all the test isolates but its methanol extract demonstrated greater inhibitory activity. The substances used in this study were more effective against the test organisms when compared to previous report by Akinnibosun and Edionwe (2015), who also worked on *Bryophyllum pinnatum* and *Citrus auranifolia*. This could be due to differences in the plant material, extraction method and the extracting solvent used.

The sensitivity of the test isolates to methanolic extracts of the plants is at variance with the findings of Obi and Onuoha (2000), who described ethanol as the best solvent for the extraction of bioactive substances from plants. The ability of the methanolic extract of *Bryophyllum pinnatum* to be more effective than that of the aqueous extract could be linked to the fact that, the active antimicrobial agent in the leaves are more soluble in methanol and as such, it is able to extract the antimicrobial constituents from the leaf (Okwu and Josiah, 2006).

Investigation of the antimicrobial activity of limejuice alone and in combination with other herbs has been investigated (Rodriguez *et al*., 2000;Onyeagba *et al*., 2004; Bina *et al*., 2010) and lime juice has been found to have high antimicrobial activity. The inhibitory effect of extracts of *B. pinnatum against* pathogenic strains makes the plant apotential drug development candidate fortreatment of ailments caused by thesepathogens.

CONCLUSION

The results of this finding indicates that the bacterial and fungal growth inhibition, evidenced by MIC and MBC values of both methanolic and aqueous extracts of *Bryophyllum pinnatum* as well as lime juice extracts have broad-spectrum antimicrobial activity when compared to the standard antibiotics used in this study, hence can serve as natural therapeutic agent against some enteric pathogens. Based on the findings of this research, methanol extract of *Bryophyllum pinnatum* demonstrated greater antimicrobial activity on *Staphylococcus aureus, Escherichia coli, Streptococcus pyogenes*, while the lime juice extracts demonstrated greater antimicrobial activity on *Streptococcus pyogenes*, and *Klebsiella pneumoniae*. Antimicrobial activity of these plants has been related to the presence of bioactive phytochemicals in parts of the plant. Hence, *B. pinnatum* leaves and lime juice could be useful in the treatment of infant respiratory infections and a potential source of antibacterial agents and raw material for the pharmaceutical industry if adequately explored.

REFERENCES

Adegoke, A.A., Iberi, P.A., Akinpelu, D.A., Aiyegoro, O.A. and Mboto, C.I. (2010). Studies on phytochemical screening and antimicrobial potential of *Phyllanthus amarus* against multiple antibiotic resistant bacteria. *International Journal of Applied Research in* Natural Products, **3** (3):6 - 12.

Ahmad, I. and Beg, A. (2001). Antimicrobial and photochemical studies on 45 Indian medicinal plants against multi-drug resistant human

pathogens. *J. Ethnopharmocol*., **74**:113 – 123.

Ajaiyeoba, E.O., Onocha, P.A., Nwozo, S.O. and Sama, W. W. (2003). Antimicrobial and cytotoxicity evaluation of *Buchholzia coriacea* stem bark. *Phytotherapy,* **74**: 706-709.

Akinnibosun, F. and Edionwe, O. (2015). Evaluation of the Phytochemical and Antimicrobial potential of the Leaf Extracts of *Bryophyllum pinnatum* L. and *Citrus aurantifolia* Sw. and their Synergy. *J. Appl. Sci. Environ. Manage*, **19** (4): 611 – 619.

Akinyeye, A.J., Solanke, E.O. and Adebiyi, I.O. (2014) Phytochemical and antimicrobial evaluation of leaf and seed of *Moringa oleifera* extracts. *Int J Res Med Sci.,***4**: 1 – 5.

Ali, E. A. (2013). The chemical constituents and pharmacological effects of Bryophyllum calycinum. A review. *International Journal of Pharma Sciences and research,***4**(12): 171 – 176.

Ammara, H., Salma R., Farah, D. and Shahid, M. (2009). Antimicrobial activity of some plant extracts having hepatoprotective effects. *Journal of Medicinal Plant Research,* **3**(1): 20-23.

Barnett, H. L. and Hunter, B. B. (1972). Illustrated genera of Imperfect Fungi, Burgress Publishing Company, Minneapolis, Minnesota. 241pp.

Bina, L., Tista, P., Anjana, S. and Kayo, D. (2010). Study of antimicrobial activity of lime juice against *Vibrio cholera. Scientific World,***8**: 44-48.

Cheesbrough, M. (2006). District Laboratory Practice in Tropical Countries. Cambridge University Press, 434pp.

Devbhuti, D., Gupta, K. and Devbhuti, P. (2012). Studies on antitumour activity of *Bryophyllum calycinum* Salisb. Against Ehrlich ascites carcinoma in swiss albino mice. *Journal of Pharma Sci Tech.,* **2**(1):31 – 33.

Ghasi, S., Egwuibe, C., Achukwu, P. and Onyeanusi, J. (2011). Assessment of the medical benefit in the folkloric use of *Bryophyllum Pinnatum* leaf among the Igbos of Nigeria for the treatment of hypertension. *Afr. J. Pharm. Pharmacol.,***5**: 83-92.

Giteru, S., Coorey, R., Bertolatti, D., Watkin, E., Johnson, S. and Fang, Z. (2015). Physicochemical and antimicrobial properties of citral and quercetin incorporated kafirin-based bioactive films. *Food chemistry*, **1:**168:341-7.

Igbinosa, O.O., Igbinosa, E.O. and Aiyegoro, O.A. (2009). Antimicrobial activity and phytochemical screening of stem bark extracts from *Jatropha curcas* (Linn). *Afr. J. Pha Pharmacol.,***3**: 58-62.

Iqbal, A. and Arina, Z. (2001). Antimicrobial and phytochemical studies on 45 Indian medicinal plants against multi-drug resistant human pathogens. *Journal of Ethnopharmacology*, **74**: 113 – 123.

Karabi, B. and Sankar, N. (2015). Antibacterial activity of *Bryophyllum pinnatum* against *pseudomonas aeruginosa* isolated from UTI. *International Journal of Life Sciences and Pharma Research*, **4**: 184 – 188.

Kaya, O., Akcam, F. and Yayh, G. (2012). Investigation of the in vitro activities of various antibiotics against *Brucella melitensis* strains. *Turkish Journal of Medical Sciences,* **42** :145-148

Scientia Africana, Vol. 21 (No. 1), April, 2022. Pp 53-66 *https://dx.doi.org/10.4314/sa.v21i1.5*
© Faculty of Science, University of Port Harcourt, Printed in Nigeria *ISSN 1118 – 1931*

Kayode, A. A. and Kayode, O. T. (2011). Some medicinal values of Telfairia occidentalis: A review. *American Journal of Biochemistry and Molecular Biology*,**1**: 30-38.

Khan, P. R., Gali, P. R. Pathan, P., Gowthan, T. and Pasupuleti, S. (2012). In vitro antimicrobial activity of *Citrus aurantifolia* and its phytochemical screening. *Live Sciences feed*, **1**(2): 13 – 16.

Lawrence, B. E., Godwin, A.O., Chuks, A. A. and Bassey, V.E. (2016). Antibacterial potential of *Bryophyllum pinnatum* leaf extracts on bacteria obtained from infected infant respiratory tract. *British Journal of Pharmaceutical Research*, **10** (6): 1 – 8.

Obaid, O.H. and Reddy, S.K. and Sridhar, S. S. (2019). Callus induction and plant regeneration from *Bryophyllum* leaves and salt stress effect on callus content of bryophilin A and bryophilin C. *Plant Archives*, **19**(2):1483-1485.

Obi, V. and Onuoha, C (2000). Extraction and characterization methods of plants and plants products. In: Biological and agricultural techniques. Ogbulie, J. N and Ojaiko, O.A. (eds). Websmedia publishers, Owerri, Nigeria. pp. 271-286.

Okwu, D.E. and Josiah, C. C. (2006). Evaluation of the chemical composition of two Nigerian medicinal plants. *African Journal of Biotechnology*, **5**(4):357-361.

Onyeagba, R.A., Ugbogu, O.C., Okeke, C.U. and Iroakasi, O.O. (2004). Studies on the antimicrobial effects of garlic (*Allium sativum* Linn), ginger (*Zingiber officinale* Roscoe) and lime (*Citrusaurantifolia* Linn). Africa Journal of Biotechnology, **3** (10): 552 – 554.

Rodriguez, A., Sandstrom, A., Ca, T., Steinsland, H., Jensen, H., and Aaby, P. (2000). Protection from cholera by adding lime juice to food results from community and laboratory studies in Guinea-Bisau, West Africa. *Tropical journal of Medical International Health*, **5**(6): 418-422

Theophil, D.D., Agatha, F.L., Nguelefack, T.B., Asongalem, E.A. and Kamtchouing, P.P. (2006). Anti-inflammatory activity of leaf extracts of *Kalanchoe crenata.Indian Journal ofPharmaceuticals*, **38**:115-117.

Tomotake, H., Koga, T., Yamato, M., Kassu, A. and Ota, F. (2006). Antimicrobial activity of citrus fruits juices against Vibrio species. Iida Women's Junior College, Nagana, Japan, *Nutritional Science Vitamin*. **52**(2): 157-160.

Ugwu, G.C., Okanya, C.L., Egbuji, J.V., Okwo, J.I., Nnamonu, E.I. and Eyo, J.E. (2018). Comparative nephroprotective effects of extracts of *Buchholzia coriacea* on some biochemical parameters in carbon tetrachloride-induced toxicity in *Rattus novergicus*. *Dhaka Univ. J. Pharm. Sci*., **17**(2): 227-235.

Scientia Africana, Vol. 21 (No. 1), April, 2022. Pp 67-76 https://dx.doi.org/10.4314/sa.v21i1.6
© Faculty of Science, University of Port Harcourt, Printed in Nigeria *ISSN 1118 – 1931*

MANLY TRANSFORMATION IN QUANTILE REGRESSION: A COMPARISON OF TWO TRANSFORMATION PARAMETER ESTIMATORS

[1]Nwakuya, M. T. and [2]Nkwocha, C. C.
[1&2]Department of Mathematics and Statistics, University of Port Harcourt
Email: [1]maureen.nwakuya@uniport.edu.ng, and [2]chibueze.nkwocha@uniport.edu.ng

Received: 05-02-2022
Accepted: 30-03-2022

ABSTRACT

This study implements the Manly transformations for normalization of variables in quantile regression analysis.The transformation parameter was estimated using two different methods namely; the maximum likelihood estimation (MLE) method and the two-step estimation method by Chamberlain and Buchinsky(CBTS).The transformation parameters obtained using the two different methods were used for the Manly transformation of data with outliers and data without outliers. The methods were applied to a quantile regression analysis at different quantiles (0.25, 0.50, 0.75, 0.95). Based on our findings, for data without outliers, the 25th quantile model was seen to be the best fit model compared to the other quantiles for the CBTS method with AIC=-43.46279, BIC=20.75212 and MSE=0.70956, while for the MLE the 50th quantile model was seen to be the best fit model with AIC=-348.3657, BIC=20.13548, and MSE=0.00864. Considering data with outliers the 25th quantile model was still seen to be the best fit model compared to the other quantiles for the CBTS method with AIC=-48.5671, BIC=21.8321 and MSE=0.92341, while for the MLE the 50th quantile model was still seen to be the best fit model with AIC=988.6763, BIC=710.09, and MSE=690.7965. Comparison of both methods for data without outliers the study concludes that the estimation of the transformation parameter using the MLE produced better results with lower AIC, BIC and MSE at all quantiles and for data with outliers the study concludes that the estimation of the transformation parameter using CBTS produced better results with lower AIC, BIC and MSE results as is shown in table (3.5) and table (3.6) respectively.

Keywords: Manly Transformation, Quantile Regression, Maximum Likelihood EstimationandChamberlain and Buchinsky Two Stage (CBTS) method.

INTRODUCTION

Conventional regressions assume that the covariates effects are constant across the population, which in most cases is not true . Quantile regression is an effective method to estimate not only the center, but also the lower or, upper tail of the conditional distribution of interest. An important advantage of quantile regression is its flexibility to describe the complete relationship between response and predictors. The Gaussiandistribution provides the foundation for most statistical methodological frameworks. As a result, statisticians and academics have noticed the widespread use of mappings that 'Gaussianize' data since Box and Cox (1964) released their seminal normalization transformation. Box and Cox (1964) transformation method is among the exponential family transformation, likewise the manly transformation method and Yeo-Johnson transformation amongst others. The Yeo-Johnson transformation

was introduced by Yeo and John (2000) as an extension of the Box-Cox transformation to accommodate negative response values since the Box-Cox transformation is restricted to only positiveresponse values. Manly (1976) stated that an exponential transformation is quite effective at turning a skewed unimodal distribution into a nearly symmetric normal distribution.More recently, Watthanacheewakul (2020) proposed a modified BoxCox transformation as an appropriate method to transform right-skewed data to become normal.These methods mentioned above employ the use of maximum likelihood method in estimating their transformation parameter and it can be particularly sensitive to outliers.Chamberlain (1994) and Buchinsky (1994) proposed a two stage method(CBTS) for estimating the transformation parameter in quantile regression, this method incorporates the equi-variance property of quantiles. Quantile regression has been seen to be robust tooutliers (outliers are data points that differ significantly from other observations).QR models can detect heterogeneous effects of covariates at different quantiles of the outcome, but also offer more robust and complete estimates compared to the mean regression, when the normality assumption violated or outliers and long tails exist. These advantages make QR attractive and are extended to apply for different types of data, including independent data, time-to-event data and longitudinal data Huang, Q (2017). In this work we tried to implement the CBTS and maximum likelihood method in estimating the transformation parameter for manly transformation in a quantile regression analysis, using data without outliers and data with outlier in other investigate the robustness of the CBTS to outliers and compare its results to that of maximum likelihood estimation (MLE) method.

QUANTILE REGRESSION

Linear regression analysis confines the covariates effects to be centered across the population of the response. This confinement might give an incomplete picture and thus can lead to possibly wrong conclusions as soon as all assumptions of the classical linear regression model are not met. Quantile regression (QR) has given a solution to; how to go further question, in regression analysis. This solution was proposed by Koenker and Bassett (1978). They introduced a new method labelled “quantile regression” that allows the estimation of the entire distribution of the response variable conditional on any set of linear covariates. In other words, the calculationof a single value, the conditional mean, is replaced by the computation of a whole set of numbers for the conditional quantileswhich are able to give a more complete picture of the underlying interrelations. QR framework that has pervaded the applied economics literature is based on the conditional quantile regression method. It is used to assess the impact of a covariate on a quantile of the outcome conditional on specific values of other covariates. In most cases, conditional quantile regression may generate results that are often not generalizable or interpretable in a policy or population context. In contrast, the unconditional quantile regression method provides more interpretable results as it marginalizes the effect over the distributions of other covariates in the model Borah and Basu (2013). QR

Scientia Africana, Vol. 21 (No. 1), April, 2022. Pp 67-76 https://dx.doi.org/10.4314/sa.v21i1.6
© Faculty of Science, University of Port Harcourt, Printed in Nigeria *ISSN 1118 – 1931*

methods have the potential to deepen and expand the existing quantitative evidence from more common mean-based analyses Wei et al (2019). Chernozhukov et al (2022) describe several new methods for speeding up quantile regression computations when it is desirable to estimate a large number of distinct quantiles.Quantile regression is being in many areas of research, Nwakuya (2020) applied a Bayesian ordinal quantile regression approach in assessing the mental health of undergraduate students based on Age.

To present the mathematical notations, consider a classical linear regression model:

$$y_i = x_i'\beta + e_i \qquad i = 1, \dots, n \qquad (1)$$

Where $y_i$is the response variable, $x_i$is the covariates, $\beta \sim N(\beta, (X^T X)^{-1}\sigma^2)$ is the covariates effect and $e_i \sim N(0, \sigma_e^2)$ is the error term. Assume that the expected value of the error term conditional on the covariates is zero $(E(e_i|x_i) = 0)$, then the conditional mean ofy_i with respect to $x_i$is

$$E(y_i|x_i) = x_i'\beta \qquad (2)$$

The covariates effect β can be estimated by the well-known method of least squares:

$$\hat{\beta} = \underset{\beta \in \mathbb{R}^k}{argmin} \sum_i (y_i - x_i'\beta)^2 \qquad (3)$$

A solution to equation (3) is given by$\hat{\beta} = (X'X)^{-1}X'y$.

Assume that $y_i = x_i'\beta_\tau + e_{i,\tau}$and that not the expected value, but the τ-th quantile of theerrorterm conditional on thecovariatess is zero$(Q_\tau(e_{i,\tau}|x_i) = 0)$. Then it is ready to see that the τ-th conditional quantile of y_i with respect to $x_i$can be written as:

$$Q_\tau(y_i|x_i) = x_i'\beta_\tau \qquad (4)$$

hence for any τ in the interval (0, 1), the parameter vector β_τ can be estimated by:

$$\widehat{\beta_\tau} = \underset{\beta_\tau \in \mathbb{R}^k}{argmin} \left\{ \sum_{i \in \{i | y_i \geq x_i'\beta_\tau\}} \tau |y_i - x_i'\beta_\tau| + \sum_{i \in \{i | y_i < x_i'\beta_\tau\}} (1-\tau)|y_i - x_i'\beta_\tau| \right\} \qquad (5)$$

$$\therefore \widehat{\beta_\tau} = \underset{\beta_\tau \in \mathbb{R}^k}{argmin} \sum_i \rho_\tau (y_i - x_i'\beta_\tau) \qquad (6)$$

Where the check function is $\rho_\tau(e) = e\left(\tau - I(e < 0)\right), \quad 0 < \tau < 1$

METHODOLOGY

This section describes the Manly transformation and the two methods for estimating the transformation parameter, namely the Chamberlain and Buchinsky two step**(CBTS)** method and the maximum likelihood Method (MLE). The analysis was done using the Iris data from R that comprises of 150 data points with four factors namely sepal length, sepal width, petal width and petal length of plants. In the analysis the data was transformed using the manly transformation. But the transformation parameter lambda was estimated using the CBTS and MLE. The estimated lambdas were then used in the manly transformationfor data without outliers and for data with an outlier. Three methods of model comparison criteria (MSE, AIC AND BIC) were used in this work. These methods were also discussed in this section. Finally the next section presented the results and conclusion.

Manly Transformation

The family of transformation applied over a long period can be used for data transformation for any population so that the transformed data can be normally distributed. Let y be a random variable

distributed as non-normal and Y^* be the transformed value of y and λ the transformation parameter. Box-Cox(1964) gave a simple modified form of the power transformation to avoid discontinuity at $\lambda = 0$. He considered;

$$Y^* = \begin{cases} \frac{y^\lambda - 1}{\lambda} & ,\lambda \neq 0 \\ lny & ,\lambda = 0 \end{cases} \quad for\ y > 0 \quad (7)$$

This equation () is known as the Box-Cox transformation. Manly (1976), proposed a one parameter exponential transformation as an alternative to Box Cox transformation because it allows negative y values.The transformation by Manly is given as:

$$Y^* = \begin{cases} \frac{\exp(\lambda y) - 1}{\lambda} & ,\lambda \neq 0 \\ y & ,\lambda = 0 \end{cases} \quad (8)$$

Where λ is the transformation parameter, Y* is the transformed response variable and *y* is the observed response variable and it is restricted to be positive. It has been found that this transformation is quite effective in turning skewed unimodal distribution into nearly symmetric distributions but is not quite useful for bimodal or U-shaped distribution, WatthanacheewakulL.(2014).Traditional remedies for deviation from normality include employing a more appropriate distribution as well as transforming data to near-normality. Zhu, and Melnykov (2018), merged both approaches by introducing a mixture model with components derived from the multivariate Manly transformation and this mixture models show good performance in modeling skewness and have excellent interpretability.

Maximum Likelihood Estimation of transformation parameter

Maximum Likelihood Estimation (MLE) approach involves forming an assumption about the underlying probability distribution function (pdf) that generates the observed data set, and then estimating parameters of the assumed distribution. The steps in the estimation process typically involve two steps;

-Specification of a probability distribution for u_i .

-Computation and maximisation of the likelihood function.

Thepdfof each transformed observation takes the following form:

$$f(y^*|\mu, \delta^2) = \frac{1}{(2\pi\sigma^2)^{1/2}} e^{-\frac{1}{2\sigma^2}(y^* - \mu)^2} \quad (9)$$

Where y^* is the transformed observation, μ is the mean and σ^2 is the variance. The Manly likelihood function in relation to the original observations is given by

$$L(\mu, \sigma^2, \lambda/y) = \frac{1}{(2\pi\sigma^2)^{\frac{n}{2}}} \exp\left\{-\frac{1}{2\sigma^2}\left[\frac{e^{-\lambda y} - 1}{\lambda} - \mu\right]^2\right\} . J(y^*; y) \quad (10)$$

Given that, $J(y^*; y) = \Pi \left|\frac{\partial y^*}{\partial y}\right|$

Given that λ is the transformation parameter.The maximum likelihood estimate of transformation parameter is obtained by solving the likelihood equation below;

$$\frac{d}{d\lambda} \ln L(\lambda) = \frac{-n\left[\sum e^{2\lambda y_i} y_i - \sum \frac{1}{n}(e^{\lambda y_i})(e^{\lambda y_i} y_i)\right]}{\sum (e^{2\lambda y_i}) - \sum \frac{1}{n}(e^{\lambda y_i})^2 + \frac{n}{\lambda} + \sum y_i} = 0 \quad (11)$$

Lakhana Watthanacheewakul (2020).

Scientia Africana, Vol. 21 (No. 1), April, 2022. Pp 67-76 https://dx.doi.org/10.4314/sa.v21i1.6
© Faculty of Science, University of Port Harcourt, Printed in Nigeria *ISSN 1118 – 1931*

Chamberlain and Buchinsky Two Step (CBTS) Estimation

The two-step estimation was proposed by Chamberlain (1994) and Buchinsky (1994). They suggested the following numerically attractive simplification in form of a two-step procedure (CBTS) which exploits the equivariance property of quantiles inother to estimate the parameters. The procedure is as follows:

First estimate $\beta_\tau(\lambda)$ conditional on λ by solving the minimization problem;

$$\hat{\beta}_\tau(\lambda) = arg\min_{\beta} n^{-1} \sum_{i=1}^{n} \rho_\tau\left(y_{\lambda i}\bar{g}_{y_\tau} - x'\beta\right) \quad (12)$$

Secondly estimate λ_τ by solving the minimization problem;

$$\hat{\lambda}_\tau = \min_{\lambda \in \mathbb{R}} n^{-1} \sum_{i=1}^{n} \rho_\tau \left(y_i - (\lambda x'\hat{\beta}_\tau(\lambda) + 1)^{-1/\lambda}\right) \quad (13)$$

Conditioned on the assumption that, $\lambda x'\hat{\beta}_\tau(\lambda) + 1 > 0$

In implementing this procedure, for this paper we assume that $\lambda x'\hat{\beta}_\tau(\lambda) + 1$ is strictly positive.

Comparison Criteria

Akaike's Information Criteria (AIC)

One of the most commonly used information criteria is AIC. The idea of AIC (Akaike, 1973) is to select the model that minimises the negative likelihood penalised by the number of parameters as specified in the equation.

$$AIC = -2 \log (L) + 2p \quad (14)$$

Where L refers to the likelihood under the fitted model and p is the number of parameters in the model. Specifically, AIC is aimed at finding the best approximating model to the unknown true data generating process and its applications.

Mean Squared Error (MSE):

The MSE measures the average of the square deviation between the fitted values with the actual data observation. The mean-squared error is determined by the residual sum of squares resulting from comparing the predictions $\hat{y}$ with the observed outcomes **y**:

$$MSE = \sum_{i=1}^{N} (y_i - \hat{y}_i)^2 \quad (15)$$

Bayesian information criteria (BIC)

Another widely used information criteria is the BIC. BIC is derived within a Bayesian framework as an estimate of the Bayes factor for two competing models; Schwarz (1978), Kass and Rafftery (1995). BIC is defined as:

$$BIC = -2 \log (L) + p \log (n) \quad (16)$$

RESULTS

Table 1: Results Summary from CBTS Method Without Outlier

	25%	50%	75%	95%
Intercept	**-0.4262978**	-1.1070109	-1.0729753	-1.4473967
Sepal.Width	**0.4825532**	0.6367298	0.6305471	0.8335235
Petal.Length	**0.5252625**	0.6922661	0.7355744	0.8442709
Petal.Width	**-0.4123057**	-0.6922661	-0.6829649	-0.5766708

AIC	**-43.46279**	-5.406937	66.48484	347.9554
BIC	**20.75212**	20.95704	21.51937	29.68686
MSE	**0.70956**	0.91450	1.47683	9.64432

From table 3.1the model of best fit using the model selection criteria is the 25% quantile model, because it has the smallest AIC, MSE and BIC values compared to other quantile results.

Table 2: Results Summary fromMLEMethod without Outlier

	25%	50%	75%	95%
Intercept	1.63385	**1.84461**	2.01079	2.42655
Sepal.Width	0.65597	**0.65916**	0.63587	0.63186
Petal.Length	0.69066	**0.71928**	0.77466	0.63337
Petal.Width	-0.51315	**-0.59353**	-0.67459	0.31060
AIC	-286.0308	**-348.3657**	-284.3705	-138.5484
BIC	20.18337	**20.13548**	20.18494	20.41898
MSE	0.01983	**0.00864**	0.02027	0.14169

From table 3.2 the model of best fit using the model selection criteria is the50% quantile model, because it has the smallest AIC, MSE and BIC values compared to other quantile results.

Table 3: Results Summary fromCBTSMethod With an Outlier

	25%	50%	75%	95%
Intercept	**-10.6789**	-22.7312	-26.6612	-31.4693
Sepal.Width	**7.33456**	8.01567	8.92617	22.67813
Petal.Length	**7.89651**	8.82614	9.67813	22.98165
Petal.Width	**-7.58671**	-9.68120	-9.87110	-8.07623
AIC	**-48.56710**	-6.78234	78.23412	505.6624
BIC	**21.8321**	22.03489	24.89412	33.6712
MSE	**0.92341**	2.3867	3.69812	8.77631

From table 3.3the model of best fit using the model selection criteria is the 25% quantile model, because it has the smallest AIC, MSE and BIC values compared to other quantile results.

Table 4: Results Summary fromMLEMethod With an Outlier

	25%	50%	75%	95%
Intercept	-24.83032	**-44.21738**	-49.53094	-40.6526
Sepal.Width	9.39032	**14.15994**	15.41346	13.90437
Petal.Length	10.28397	**15.00064**	17.52720	18.89159
Petal.Width	-8.33953	**-14.57947**	-16.82453	-16.4337
AIC	1001.26	**988.6703**	992.0208	1026.736
BIC	771.2872	**710.809**	726.412	910.355
MSE	751.2447	**690.7965**	706.3695	890.3125

Scientia Africana, Vol. 21 (No. 1), April, 2022. Pp 67-76 *https://dx.doi.org/10.4314/sa.v21i1.6*
© Faculty of Science, University of Port Harcourt, Printed in Nigeria *ISSN 1118 – 1931*

From table 3.4The model of best fit using the model selection criteria is the50% quantile model, because it has the smallest AIC, MSE and BIC values compared to other quantile results.

Table 5: Model comparison using AIC, BIC and MSE at different quantile for CBTS and MLE Method Without Outlier.

	MLE with Manly Transformation			TwoStage(CBTS)Estimation		
T	AIC	MSE	BIC	AIC	MSE	BIC
25%	**-286.0308**	**0.3752726**	**20.18337**	-43.46279	0.8423644	20.75212
50%	**-348.3657**	**0.3048652**	**20.13548**	-5.406937	0.9562941	20.95704
75%	**-284.3705**	**0.3773553**	**20.18494**	66.48484	1.21525	21.51937
95%	**-138.5484**	**0.6135492**	**20.41898**	347.9554	3.105531	29.68686

From table (3.5) above based on the AIC, MSE and BIC the maximum likelihood technique gave lower values at all quantiles, making it the preferred method.

Table 6: Model comparison using AIC, BIC and MSE at different quantile for CBTS and MLE Method With An Outlier.

	MLE with Manly Transformation			**Two Stage (CBTS)Estimation**		
Quantile	**AIC**	**MSE**	**BIC**	**AIC**	**MSE**	**BIC**
25%	1001.26	751.2447	771.2872	**-48.5671**	**0.92341**	**21.8321**
50%	988.6703	690.7665	710.809	**-6.78312**	**2.3867**	**22.03489**
75%	992.0208	706.3695	726.412	**78.23412**	**3.69812**	**24.89412**
95%	1026.736	890.3125	910.355	**505.61123**	**8.77631**	**33.66712**

From table (3.6) above based on the AIC, MSE and BIC the CBTS gave lower values at all quantiles, making it the preferred method.

DISCUSSIONS

Given the results above, the summary result of the CBTS for data without outliers showed that the 25th quantile model was of best fit with an AIC of -43.46279, BIC of 20.75212 and MSE of 0.70956. While the 50th quantile model was the best fit for the MLE method with AIC of -348.3657, BIC of 20.13548 and MSE of 0.00864. The results from data with outliers still showed that the 25th quantile model was the model of best fit for CBTS method with AIC of -48.56710, BIC of 21.321 and MSE of 0.92341 and for the MLE method, the 50thquantile still appeared the best fit with AIC of 988.6763, BIC of 710.809 and MSE of 690.7965. Now considering the MLE method alone for both data with outliers and data without outliers, it was observed that the AIC, BIC and MSE for data without outliers were very small compared to that of data with outliers, exposing the outlier sensitivity of MLE. The comparison of the CBTS and MLE methods at both cases showed that MLE produced smaller AIC, BIC and MSE at all quantiles for data without outliers. While the CBTS produced smaller AIC, BIC and MSE at all quantiles for data with outliers.

CONCLUSIONS

Data transformation plays a vital role when it comes to normalization of variables in statistical analysis;the study was performed using Manly data transformation for normalizing of the response variables in quantile regression analysis.The Manly transformation parameter was estimated using two different methods namely; the maximum likelihood estimation (MLE) method and the two-step estimation method by Chamberlain and Buchinsky(CBTS).The methods were applied to a quantile regression analysis at different quantiles (0.25, 0.50, 0.75, 0.95). Based on our findings, the CBTS method showed that the 25^{th} quantile model was the best fit for the data with outliers and without outliers, while the MLE method showed the 50^{th} quantile as the model of best fit at both scenarios. The comparison of the two estimation methods revealed that for data without outliers the MLE performed better but for data with outliers the CBTS performed better. These observations can lead us to conclude that in agreement to literature the MLE is very sensitive to outliers while the CBTS is robust to outliers.

REFERENCES

Akaike, H. (1973). Information Theory and an Extension of the Maximum Likelihood Principle. In: Petrov, B.N. and Csaki, F., Eds., International Symposium on Information Theory, pp 267-281.

Borah, B, J. and Basu, A. (2013).Highlighting Differences Between Conditional and Unconditional Quantile Regression Approaches Through an Application to Assess Medication adherence

Buchinsky, M. (1994). Changes in the US wage structure 1963-1987: Application of quantile regression. Econometrica: Journal of the Econometric Society, 62(2), pp 405-458.

Box G. E. P. and Cox D. R. (1964). An Analysis of Transformation (with Discussions). Journal of the Royal Statistical Society, Ser. B; 26(2), 211-252

Chamberlain, G. (1994). Quantile Regression, Censoring, and the Structure of Wages.Advances in Econometrics: Sixth World CongressVol. 1, pp 171-209. Cambridge University Press.

Chernozhukov, V., Fernández-Val, I. &Melly, B. (2022).Fast algorithms for the quantile regression process. Empir Econ 62**,** 7–33. https://doi.org/10.1007/s00181-020-01898-0

Huang, Q., Zhang, H., Chen, J. and He, M. (2017). Quantile Regression Models and Their Applications: A Review. Journal of Biometrics & Biostatistics 08(03). DOI: 10.4172/2155-6180.1000354

Kass, R. E., & Raftery, A. E. (1995). Bayes factors. Journal of the american statistical association, 90(430), 773-795.

Koenker, R., & Bassett, G. (1978). Regression Quantiles. Econometrica, 46(1), 33–50. https://doi.org/10.2307/1913643

Manly, B. F. (1976). Exponential data transformations. Journal of the Royal Statistical Society: Series D,The Statistician, 25(1), 37-42.

Nwakuya, M. T. (2020). Assessment of Mental Health of Undergraduate

Scientia Africana, Vol. 21 (No. 1), April, 2022. Pp 67-76 *https://dx.doi.org/10.4314/sa.v21i1.6*
© Faculty of Science, University of Port Harcourt, Printed in Nigeria *ISSN 1118 – 1931*

Students Based on Age: A Bayesian Ordinal Quantile Regression Approach. Quarterly Journal of Econometrics Research6(1), 12-17.

Wei, Y., Kehm, R.D., Goldberg, M. and Terry, M. B. (2019). Applications for Quantile Regression in Epidemiology. Curr Epidemiol Rep **6,** 191–199. https://doi.org/10.1007/s40471-019-00204-6

Yeo, I. K., & Johnson, R. A. (2000). A new family of power transformations to improve normality or symmetry. Biometrika, 87(4), 954-959.

Zhu, X. and Melnykov, V. (2018).Manly transformation in finite mixture modeling.Computational Statistics & Data Analysis; 121: 190-208. DOI:10.1016/j.csda.2016.01.015

WatthanacheewakulL.(2014). A New Family of Transformations for Lifetime Data.Proceedings of the World Congress on Engineering, Vol1 WCE 2014, July 2-4, London UK.

WatthanacheewakulL.(2020). Modified Box-Cox Transformation and Manly Transformation with Failure Time Data; https://pdfroom.com/books/modified-box-cox-transformation-and-manly-transformation-with failure-time-data/8Pe5xkNZ2nN

Scientia Africana, Vol. 21 (No. 1), April, 2022. Pp 77-86 *https://dx.doi.org/10.4314/sa.v21i1.7*
© Faculty of Science, University of Port Harcourt, Printed in Nigeria *ISSN 1118 – 1931*

REMOVAL OF BTEX FROM REFINERY WASTE USING HDTMAC-MODIFIED OGWUTA SOURCE CLAY: ADSORPTION EQUILIBRIUM AND THERMODYNAMIC INCLINATIONS

Agha, I. I.[1], Ibezim-Ezeani, M. U.,[2] and Obi, C.[2]*
[1]Department of Chemistry, Nnamdi Azikiwe University, Awka, Anambra State, Nigeria
[2]Department of Pure and Industrial Chemistry, Faculty of Science, University of Port Harcourt, P.M.B. 5323, Choba, Port Harcourt. Rivers State, Nigeria.
***Corresponding Author Email:**chidi.obi@uniport.edu.ng

Received: 01-03-2022
Accepted: 30-03-2022

ABSTRACT

The possible non-compliance of refineries to the demands of environmenteal protection laws has led to the discharge of poorly treated and contaminated wastewater to the environment. Carcinogenic compoiunds such as benzene, toluene, ethylbenzene, and xylene (BTEX) find their way to the ecosystem. This study is aimed at investigating the isotherm and thermodynamics of the uptake of BTEX using hexadecytrimethylammonium chloride (HDTMAC)-modified natural Ogwuta clay. Batch adsorption process was used at different BTEX concentrations and at temperatures of 303°K, 313°K and 323°K. Langmuir, Freundlich, Dubinin-Radushkevich (D-R), and Tempkin models were used to describe the process while changes in enthropy (ΔS)*, enthalpy* (ΔH)*, and Gibbs free energy* (ΔG) *of the process were evaluated. The maximum monolayer coverage capacity* (q_m) *of 1.83, 0.92, 0.86 and 0.69 mg/g of BTEX was lower than the calculated values of 4.94, 2.64, 2.76 and 2.20 mg/g respectively, implying uptake of pollutants through other mechanisms. The Dubinin-Radushkevich monolayer coverage range of 0.81-2.66 mg/g agreed with the monolayer coverage of the Langmuir model but with energy less than 1 kJ/mol. Freundlich adsorption intensities for BTEX were 1.64, 1.41, 1.11 and 1.22 respectively and* R^2 *values of not less than 0.99 for each pollutant showed that the model best fits the process. Results of the thermodynamic parameters showed that the process was more feasible at increased temperature, endothermic and lead to increased randomness at the solid-liquid interface. This study has presented hexadecyltrimethylammonium chloride-modified Ogwuta source clay as a veritable adsorbent for organic pollutant decontamination both from laboratory and real-life sources.*

Keywords: BTEX**,** Batch reactor system, isotherm, adsorption, hexadecyltrimethylammonium chloride

INTRODUCTION

Refineries are plants engaged in complex multiple operations aimed at transforming crude oil into more useful products. Some of the operations such as light and heavy coking, cracking, desalting, cooling, stripping, etc heighten the demand for water i.e. making refineries larger comsumer of water relative to other industries. Pingping *et al*. (2018) found out that 1.9 gallons (7.19 L) of

water are required to process 1 gallon (3.79 L) of crude thereby generating categories of waste water such as the desalter effluent, sour water, tank bottom draws and spent caustic. This wastewater gets contaminated in the course of operations due to contact with crude.

Mahdi *et al*. (2021) observed gross negligence to the demands of the environmental regulations on the management of petroleum refinery effluents (PRE) in most developing countries. Therefore, many of these industries discharge inadequately treated wastewater into the environment. This discharge allows for the introduction of pollutants such as heavy metals, synthetic materials, aromatic and polyaromatic hydrocarbons, to the environment which in most cases far exceed permissible limits (Obi and Woke, 2014). Netai *et al*. (2013) noted that phenols and some other aromatic compounds such as BTEX (benzene, toluene, ethylbenzene and xylene) are priority pollutants since exposure to them can cause cancer, irritation of mucosal membrane, disruption of liver, and kidney functions, etc in humans; creating an unpleasant taste and odour in drinking water. Thus a great deal of concern has been raised globally to remove these pollutants from refinery effluents in particular and other industrial effluents in general into the fragile ecosystem, and it has become obligatory for industries to properly treat their wastewater effluent to ensure safe disposal to the environment (Taghreed and Muftah, 2018).

Over the years, several methods have been adopted in an attempt to remove organic contaminants from aqueous phase. They include; chemical precipitation, ion exchange, electrodeposition, solvent extraction, membrane separation, reverse osmosis and adsorption process. Gopinathan et *al.* (2017) remarked that in general, adsorption is a far less energy-intensive unit operation. Consequently, several types of materials such as activated carbon, carbonized maize tassels, banana pitch, cassava waste, coal and clay minerals have been researched to adsorb organic pollutants from aqueous solutions (Okoro and Abii, 2011).

Hexadecyltrimethylammonium chloride (HDTMAC) is an eco-begnin cationic surfactant emanating from the organic chloride group of cetytrimethylammonium (Inya *et al*., 2021). It is a quaternary ammonium salt with molecular formula $C_{19}H_{42}N.Cl$ and highly soluble in aqueous phase.

Clays are layered phyllosilicates with very small particle size of less 2 μm. Structurally, they have a net negative charge due to the isomorphous substitution of silicon ion by aluminum ion in the tetrahedral layers or likely substitution of aluminum ion by magnesium ion. Thus, cations such as sodium, potassium and calcium may be attracted to the mineral surface to neutralize the layer charge (Ivana *et al.*, 2014). This underscores the hydrophilicity of clay and reduces its application in an organic medium. To improve its

Scientia Africana, Vol. 21 (No. 1), April, 2022. Pp 77-86 https://dx.doi.org/10.4314/sa.v21i1.7
© Faculty of Science, University of Port Harcourt, Printed in Nigeria *ISSN 1118 – 1931*

application, clays are modified with suitable organic surfactants (Leyva-Ramos *et al.*, 2021; Padmaja *et al.*, 2018, Bhattacharyya and Mandof, 2014). Hence, the need for the modification of Ogwuta Source clay situated at Iyi Ogo Afikpo, Ebonyi State for real-life application.

In this work, adsorption thermodynamics of refinery wastewater BTEX unto natural Ogwuta clay modified with hexadecyltrimethylammonium chloride (HDTMAC) was investigated considering the significance of adsorption isotherm in wastewater treatment as it provides valuable insights into the application of design.

MATERIALS AND METHOD

All the chemicals used for the purpose of this work were of analytical grade. A 0.1 M HCl and 0.1 M NaOH stock solutions were used to adjust the pH of samples of the wastewater collected from the observation tank of Port Harcourt Refining Company (PHRC), Eleme using specialized bottles called "Bassey and God Investment" (BGI) to prevent evaporation given the volatility of the pollutants. The concentration of the sample before and after sorption was measured using Agilent 6890N Gas Chromatography (AR, 3130). The hexadecyltrimethylammonium chloride clay was crushed with an iron roller to fine particle sizes. These clay particles were sieved through a 63 µm sized mesh and stored in a glass bottle.

Adsorption Process

Batch adsorption process was employed using 250 ml conical flasks to determine the adsorption efficiency of the HDTMAC-modified clay. Results of the refinery wastewater showed the following initial concentrations of 20.38 ppm benzene, 11.13 ppm ethylbenzene, 13.17 ppm toluene, and 9.56 ppm xylene. It was used without further treatment. A 0.2 g of the organoclay was added to 50 ml of BTEX wastewater solution and by the aid of a magnetic stirrer, the mixture was stirred until equilibrium reached. The suspension was filtered and the filtrate was analysed by GC-MS. The adsorption capacity of BTEX in the solid, q_e (mg/g), was evaluated using the expression:

Adsorption Capacity (q_e)

$$= \frac{(C_o - C_e)}{M} \times V \qquad (1)$$

Where, C_o is the initial BTEX concentration (mg/L), C_e is the concentration (mg/L) at equilibrium, V is the volume (L) of the solution and M is the mass (g) of the adsorbent.The concentration of the BTEX in the wastewater was varied by serial dilution.

Adsorption Isotherm Studies

To describe the relationship between the amounts of BTEX molecules adsorbed on the HDTMAC-modified ogwuta clay, the following isotherm models were employed to provide insight into sorption mechanism, surface properties, and the affinity of pollutants.

Temkin Model: This was employed to explain possible indirect chemical interaction between the adsorbate and the adsorbent. It assumes that the fall in energy as the process continues is linear rather than logarithmic within intermediate concentrations. The linear form of the equation is expressed as:

$$q_e = \frac{RT}{b} \ln K_T + \frac{RT}{b} \ln C_e \qquad (2)$$

Where, values of the constants K_T, provides the information about the binding energy and b, is a measure of the heat of adsorption.

Langmuir Model: This model gives the fractional coverage on an adsorbent at constant temperature. It assumes uniform energy of adsorption on the surface of the adsorbent. The equation for this analysis is expressed as:

$$\frac{C_e}{q_e} = \frac{1}{q_m K_L} + \frac{C_e}{q_e} \qquad (3)$$

Where, q_m is the monolayer uptake capacity, K_L is Langmuir constant related to intensity of adsorption, and other parameters remain as decribed above.

Freundlich Model: The Freundlich isotherm model was employed to describe multilayer adsorption on a heterogeneous adsorbent surface. The model is described by:

$$\ln q_e = \ln K_F + \frac{1}{n} \ln C_e \qquad (4)$$

Where, the values of the constants, K_F (Lg^{-1}) which indicates the adsorption capacity and measures the favourability of adsorption, and $\frac{1}{n}$shows the extent of adsorption intensity.

Dubinin-Radushkevich Model: This model was applied to categorize adsorption process into physical, chemical or ion exchange (Morunmradi, 2012). The linear form of the expression is as follows:

$$\ln q_e = \ln q_m - \beta_\varepsilon{}^2 \qquad (5)$$

Where, q_m(mg/g) is the theoretical sorption capacity, β (kJ/mol) is related to the mean adsorption energy, and ε (Polanyi Potential) is equal to:

$$\varepsilon = RT\ln\left(1+\frac{1}{C_e}\right) \qquad (6)$$

The mean adsorption energy E is related to β by:

$$E = \frac{1}{\sqrt{2\beta}} \qquad (7)$$

The energy value specifies the type of adsorption process. For $E < 8$ $kJmol^{-1}$, the process is physical. If $8 < E < 16$ $kJmol^{-1}$, the process occurred through ion exchange. While for $E > 16$ $kJmol^{-1}$, the process involves chemical interaction (Dada *et al.*, 2012).

Thermodynamic Evaluations

The thermodynamic studies were investigated by carrying out the effect of temperature on the adsorption of BTEX unto HDTMA-modified Ogwuta source clay at 30°C, 40°C and 50°C respectively. The thermodynamic parameters of changes in enthalpy (ΔH), Gibbs free energy (ΔG) and entropy (ΔS) were calculated using the following equations (Nourmoradi *et al.*, 2013):

$$K = \frac{q_e}{C_e} \qquad (8)$$

Scientia Africana, Vol. 21 (No. 1), April, 2022. Pp 77-86 https://dx.doi.org/10.4314/sa.v21i1.7
© Faculty of Science, University of Port Harcourt, Printed in Nigeria *ISSN 1118 – 1931*

$$\ln K = \frac{\Delta S}{R} - \frac{\Delta H}{RT} \quad (9)$$

$$\Delta G = \Delta H - T\Delta S \quad (10)$$

Where, K is the distribution coefficient and is related to the Langmuir constant $K_L = (\frac{q_e}{C_e})$ which is dimensional with common units (L/g) (Hong. *et al.*, 2009), C_e is the equilibrium concentration (mg/L) and R the universal gas constant ($8.314 Jmol^{-1}K^{-1}$).

RESULTS AND DISCUSSION

Temkin Analysis

The result obtained by plotting q_e against $\ln C_e$ was presented in Table 1. As can be seen, the binding energy K_T (L/g) for benzene, toluene, ethylbenzene, and xylene were 0.869, 0.756, 0.802 and 0.712 respectively. With high b > 0 values of 355.41, 687.64, 550.88 and 839.00 J/mol respectively for BTEX and coefficient of correlation of over 0.98 for each of the pollutant, which suggests that the process involves chemical interaction (Nimibofa *et al*., 2017).

Langmuir Analysis

The total monolayer capacity of the adsorbent, q_m and the Langmuir constant K_L, obtained from the slope and intercept of a plot of $\frac{C_e}{q_e}$ against C_e was presented in Table 1. The equilibrium parameter, $R_L = \frac{1}{1+(1+K_L C_e)}$, a dimensionless quantity related to the separation factor was also presented in Table 1. Given that R_L reveals the adsorption nature of being unfavourable ($R_L > 1$), linear ($R_L = 1$), and favourable ($0 < R_L < 1$ or irreversible ($R_L = 0$)) (Davoud *et al.*, 2017). The values of BTEX lying between 0.174 - 0.287 show that adsorption process was favourable. However, the maximum monolayer coverage capacity q_{max} of 1.83, 0.92, 0.86 and 0.69 mg/g for BTEX was lower than the calculated equilibrium capacity values of 4.94, 2.64, 2.76 and 2.20 mg/g respectively. This difference, according to Dada *et al.*, (2012) may have been due to further uptake of pollutants by other mechanisms.

Freundlich Analysis

The sorption bond between pollutant and adsorbent would be relatively strong if n values obtained were greater than 1 (Nournmradi *et al.*, 2013). By extension, the value measures the extent of fitness of the model to the adsorption process. Therefore the n values of 1.64, 1.41, 1.11 and 1.22 respectively for BTEX showed that they were suitably adsorbed by HDTMAC-modified ogwuta source clay. This agrees with the observation made by Sharmasarkar *et al.* (2000) in the removal of BTEX using montmorillonite organoclays. The measure of the favourability was determined by the value of K_F. Favourable values lie between 1 - 20 Lg^{-1} (Nimibofa *et al.*, 2017). Therefore with the values of K_F in Table 1 lying between 4.31 and 10.6 shows that the model favours and fits the process.

Dubinin-Radushkevich Analysis

The values of the D-R parameters for the adsorption of BTEX onto HDTMAC-modified clay were

presented in Table 1. The q_m range of 0.81 - 2.66 mg/g agreed with the monolayer coverage of the Langmuir values as well as mean adsorption energy less than 1 $kJmol^{-1}$. This process showed that the three models of Langmuir, Freundlich, and D-R were favored. However, the values of the regression coefficient (R^2) showed that Freundlich's model best fits the experimental data.

Table 1: Parameters for Langmuir, Freundlich, D-R and Temkin isotherm models for adsorption of BTEX using HDTMAC-clay

Isotherm	Parameter	Adsorbate			
		Benzene	Toluene	Ethylbenzene	Xylene
Langmuir	K_L	0.335	0.530	0.344	0.507
	q_{max}	1.83	0.92	0.86	0.69
	R^2	0.985	0.997	0.982	0.994
	R_L	0.174	0.207	0.287	0.263
Freundlich	K_F	10.6	4.71	8.67	4.31
	n	1.64	1.41	1.11	1.22
	R^2	0.998	0.997	0.998	0.999
D-R	q_m	2.16	1.08	1.07	0.81
	E($kJmol^{-1}$)	0.41	0.71	0.41	0.50
	R^2	0.912	0.889	0.898	0.917
Temkin	b_T	355.41	687.64	550.08	839.10
	K_T	0.869	0.756	0.802	0.712
	R^2	0.990	0..997	0.993	0.998

Thermodynamic Analysis

The values of the thermodynamic parameters were obtained from the plot of lnK versus $\frac{1}{T}$, with the entropy change ($Jmol^{-1}K^{-1}$) obtained from the intercept and the change in enthalpy ($Jmol^{-1}$) obtained from the slope as shown in Figures 1-4 and Table 2. The negative values of the change in Gibbs free energy $(\Delta G)$for temperatures of 303, 313 and 323 K for the removal of BTEX using HDTMAC-Clay showed that the adsorption process was thermodynamically feasible as well as spontaneous (Nourmoradi *et al.*, 2012; 2013, Konggidinata *et al.*, 2017). The values of ΔG for benzene adsorption were found to decrease from -531 $Jmol^{-1}$ at 303 K to -407 $Jmol^{-1}$ at 323 K which indicates that the adsorption process became more feasible at higher temperatures (Nourmoradi *et al.* 2017; Kumar *et al.*, 2016). The calculated values for change in enthalpy ΔH for the BTEX were all positive, which indicates that the process was endothermic. Also the positive values of entropy ΔS of 177.2, 95.9, 91.6 and 85.6 $Jmol^{-1}K^{-1}$ of BTEX reflect the affinity of organic contaminants and the increasing randomness at the solid-liquid interface.

Scientia Africana, Vol. 21 (No. 1), April, 2022. Pp 77-86 *https://dx.doi.org/10.4314/sa.v21i1.7*
© Faculty of Science, University of Port Harcourt, Printed in Nigeria *ISSN 1118 – 1931*

Table 2: Thermodynamic parameters for BTEX removal using HDTMAC-Clay

	ΔS (Jmol^{-1}K^{-1})	ΔH (Jmol^{-1})	$\Delta G(Jmol^{-1})$ 303 K	313 K	323 K
B	177.2	53151.4	-531.0	-2302.8	-4074.5
T	95.90	29182.2	-112.2	-847.2	-1806.6
E	91.60	27619.1	-141.8	-1058.0	-1974.2
X	85.60	26322.1	-385.3	-470.7	-1326.0

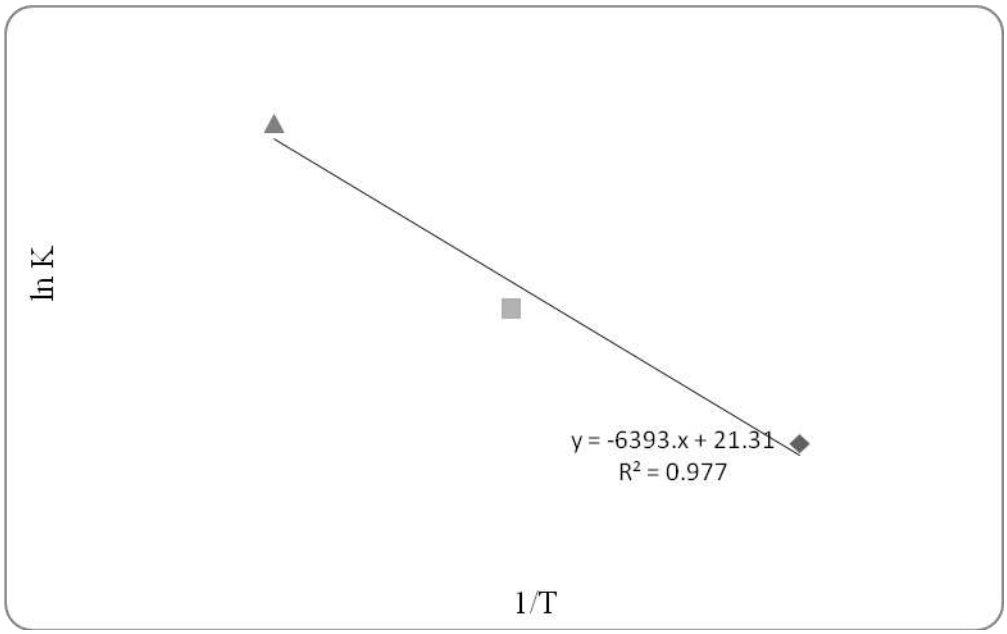

Figure 1: Plots of lnk versus 1/T for effect of temperature on benzene uptake

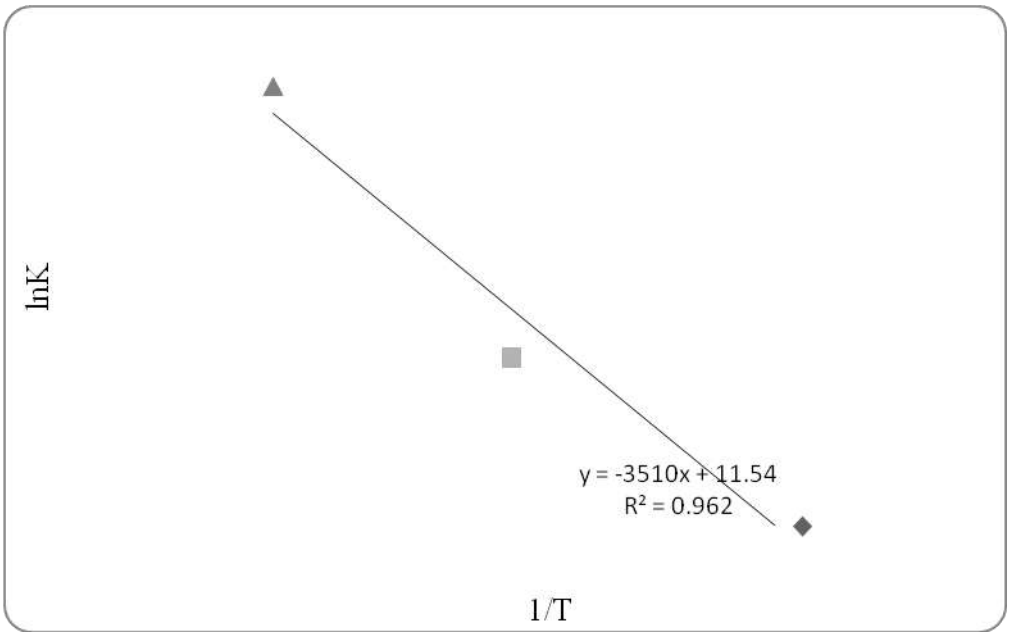

Figure 2: Plots of lnk versus 1/T for effect of temperature on toluene uptake

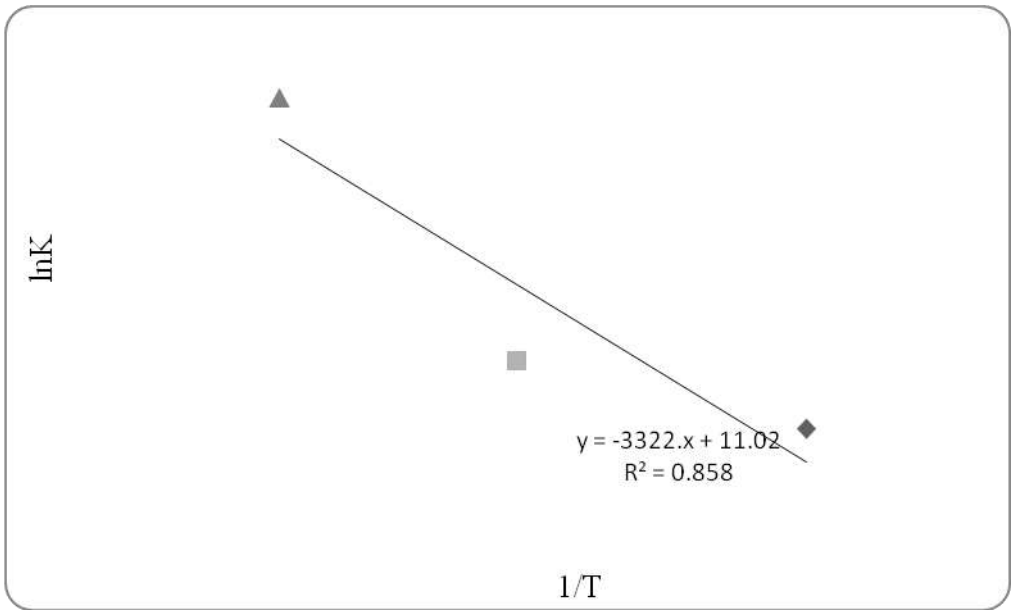

Figure 3: Plots of lnk versus 1/T for effect of temperature on ethylbenzene uptake

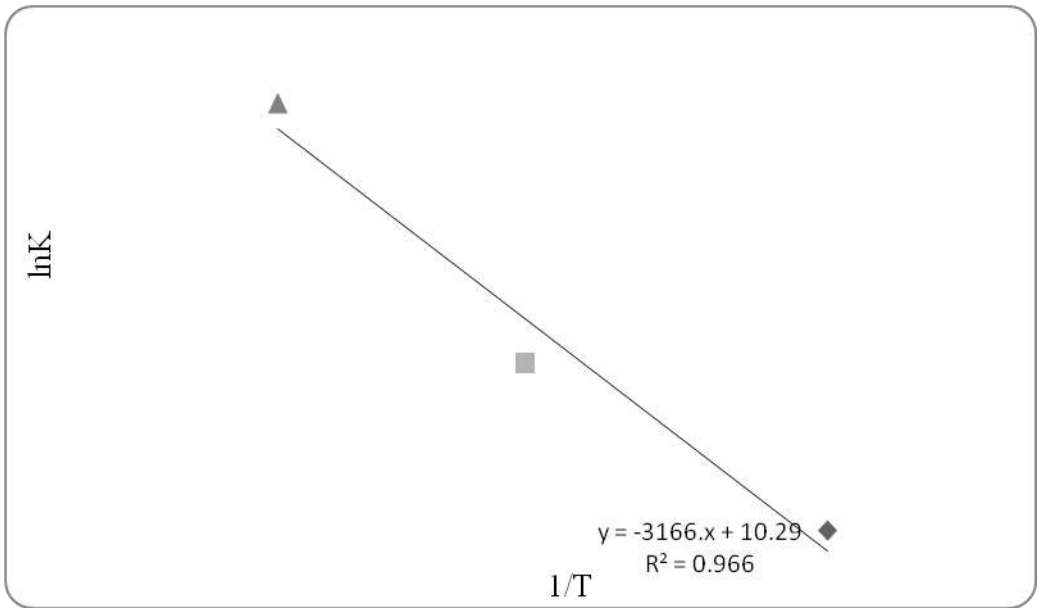

Figure 4: Plots of lnk versus 1/T for effect of temperature on xylene uptake

CONCLUSION

The removal of BTEX from refinery wastewater was carried out using hexadecyltrimethylammonium chloride modified Ogwuta source clay. Langmuir, Freundlich, Dubinin-Radushkevich, and Temkin adsorption models were adopted to understand the pollutant-adsorbent interface interactions. The Temkin constants suggest some degree of chemical interaction as much as the D-R values agreed with the Langmuir theoretical monolayer coverage capacity. However, the values are at variance with the experimental data and the energy of adsorption was found to be less than 1 kJ/mol. The Freundlich model with R-squared value for each

Scientia Africana, Vol. 21 (No. 1), April, 2022. Pp 77-86 https://dx.doi.org/10.4314/sa.v21i1.7
© Faculty of Science, University of Port Harcourt, Printed in Nigeria *ISSN 1118 – 1931*

of the pollutant not less than 0.999 was found to be the best fit for the process. The changes in enthalpy and Gibbs free energy showed that the adsorption process was endothermically favorable and spontaneous. Hence, this study has presented hexadecyltrimethylammonium chloride modified Ogwuta source clay as a veritable adsorbent for organic pollutant decontamination both from laboratory and real-life sources.

Conflicts of Interest

The authors declare that no conflict of interest(s) exist.

REFERENCES

Bhattacharya, S., & Mandof, A. (2014). Studies on preparation and analysis of organoclay nanoparticles. *Research Journal of Engineering Sciences, 3*(3), 10-16.

Hong, S., Wen, C., He, J., Gan, F., & Ho, Y. S. (2009). Adsorption Thermodynamics of Methylene Blue unto Bentonite. *Journal of Hazardous Materials*, *167*; 630-633.

Agha, I. I., Ibezim-Ezeani, M. U., & Obi, C. (2021): Physicochemical Properties of Organophilic Clay Developed Using Hexadecyltrimethylammonium Chloride (HDTMAC) Modifier. *International Research Journal of Pure & Applied Chemistry*, *22*(9): 20-30. Doi: 10.9734/IRJPAC/2021/v22i930431

Kumar, G., Sen, S., & Bhattacharyya K. G. (2016). Adsorption of Crystal Violet on Raw and Acid-treated Montmorrilinite K10 in Aqueous Suspension. *Journal of Environmental Management,171*; 1-10.

Mahdi, N. R., Ali, J. J., & Abdulaziz, J. A. (2021). Treatment of Petroleum Refinery Effluent and Wastewater in Iraq: A Review. *Material Science Engineering*, *1058*. Doi: 10.1088/1757-899x/1058/1/012072

Taghreed, A., & Muftah, E. (2018). Organic Contaminants in Refinery wastewater: Characteriztion and Novel Approach for Biotreatment; Recent Insights in Petroleum Science and Engineering. Doi: 10.5772/intechopen.72206

Gopinathan, R., Bhowal, C., & Galapati C. (2017). Thermodynamic study of some basic dyes adsorption from aqueous solution on activated carbon and new correlations. *Journal of Chemical Thermodynamics*, *107*; 182-188.

Padmaja, M., Bhavani, R., Pamila, R. (2018). Adsorption of cadmium from aqueous solutions using low cost materials: A review. *International Journal of Engineering and Technology*,*7*(4.2); 26-29.

Leyva-Ramos, R., Jacobo-Auara, A., & Marinez-Costa, J. I. (2021). Organoclays: Fundamentals and applications for removing toxic pollutants from water solution. In: Moreno-piraja J, C., Giraldo-Gutierrez L., Gomez-Granadoz F. (eds) Porous Materials. Springer, *Cham.*, Doi. Org/10.1007/978-3-030-65991-2_13.

Pingpung, S., Amgad E., Micheal W., Jeonghoo, H., & Robert J. H. (2018). Estimation of US refinery water consumption and allocation to refinery products. *Fuel*, *221*; 542-557.

Dada, A. O., Olalekan, P. A., and Olatunya, A. (2012). Langmuir, Freundlich Temkin and Dubinin-Radushkevich isotherm studies of equilibrium sorption of Zn^{2+} unto phosphoric acid modified rice husk. *Journal of Applied Chemistry*, *3*(1); 38-45

Davoud B., Ferdps L., Hossein A., & Ali J. (2017). Langmuir, Freundlich, Temkin and Dubinin-Radushkevich isotherms studies of equilibrium sorption of ampicillin unto montmorillonite nanoparticles. *Journal of Pharmaceutical Research International*, *20*(2); 1-9.

Ivana, S., Stanisa, S., Ivan, S., & Dragoljub, G. (2014). Industrial application of clay and clay minerals. Earth Sciences in the 21st Century, Nova Science Publishers Inc. New York.

Kongjidinataa, M. I., Cjao, B., Lian, Q., Subramaniam, R., Zappi, M., 7 Gang, D. D. (2017). Equilibrium, kinetic and thermodynamic studies for adsorption of BTEX unto ordered mesoporous carbon (OMC). *Journal of Hazardous Materials,336*; 249-259.

Netai, M., Lydia, C., David, S., & Mathew, M. (2013). Adsorption of phenol from aqueous solution using carbonized maize tassels. *British Journal of Applied Sciences and Technology,3*(3); 649-661.

Nimibofa, A., Augustus, N., & Donbebe, W. (2017). Modelling and interpretation of adsorption isotherms. *Journal of Chemistry, 2017*; 67-77.

Nourmoradi, H., Avospour, M., Ghasiemian, N., Heidari, M., Moradnejedi, K., & Mohammadi, F. (2017). Surfactant modified montmorillonite as a low cost adsorbent for 4-Chlorophenol: Equilibrium, kinetic and thermodynamic study. *Journal of Taiwan Institute of Chemical Engineering, 59*; 244 -251.

Nourmoradi, H., Khiadani, M., & Nikaeen, M. (2013). Multi-component adsorption of benzene, toluene, ethylbenzene, and xylene from aqueous solutions by Montmorillonite modified with tetradecyl trimethyl ammonium bromide. *Journal of Chemistry, 2013*(1-4); 1-10.

Nourmoradi, H., Khiadani, M., & Nikaeem M. (2012). Removal of benzene, toluene, ethylbenzene and xylene from aqueous solutions using montmorillonite modified with nonionic surfactants: Equilibrium, kinetic and thermodynamic study. *Chemical Engineering Journal, 191*; 341-348.

Obi, C., & Woke, J. (2014). The removal of phenol from aqueous solution by *Colocaciaesculenta* araesia Linn Schott. *Journal of Soil Science and Environmental Management, 3*(6); 50-58.

Okoro, I. A & Abii, T. (2011). Sorption models of cadmium (II) ion onto edible fruit wastes. *American Journal of Scientific and Industrial Research, 2*(3), 386-390.

Sharmasarkar, S., Haynes, W., & Vance G. (2000). BTEX sorption by montmorillonite organoclays. *Water, Air and Soil Pollution, 19*(1-4); 257-273.

Scientia Africana, Vol. 21 (No. 1), April, 2022. Pp 87-100 *https://dx.doi.org/10.4314/sa.v21i1.8*
© Faculty of Science, University of Port Harcourt, Printed in Nigeria *ISSN 1118 – 1931*

TERRESTRIAL MOLLUSCS SPECIES RICHNESS AND DIVERSITY IN GASHAKA - GUMTI NATIONAL PARK, TARABA STATE , NIGERIA.

Ogorode, I. O.
Department of Animal and Environmental Biology, University of Port Harcourt,
P.M.B 5323, Choba, Port Harcourt, Nigeria
israelogorode@gmail.com

Received: 14-01-2022
Accepted: 20-03-2022

ABSTRACT

To assess the biodiversity of terrestrial molluscs in Gashaka-Gumti National Park, a four plot (20 x 20m) each within the park were sampled by searching the forest floor, tree trunk, fallen logs, root facies, and vegetation for the presence of mollusks. The species found were collected by hand picking.A total of 819 specimens comprising 22 species belonging to six molluscan families were collected from four plots. Each plot yielded between 8 to14 species (Mean:10, Standard Deviation:2.71) and 33 to 683 individuals (Mean:204.75, Standard Deviation :319.09). The most abundant species in the park was Curvella sp. represented by 683 individuals (79.4%) of the total sampled species. The most abundant family is Streptaxidae represented by 8 species (36.4%) of the total sample.The sample intensity was 37.22 while the Inventory Completeness is 79.31%. Eleven (11) species occurred as singleton across plots while ten (10) species occurred as doubleton across the four plots sampled.The Whittaker Index is 4.00. The rarefaction curve nearly reached an asymptote as sampling stopped. The nonparametric estimator Chao 2 and jackknife 2 were 28.05 and 33.99 of all sample collected. The dendogram of similarity by plots using Bray-Curtis similarity of index show the close relationship of two plots in terms of species. It shows that there is no significant difference between plots. Plot 1 and 4(P=0.4329), Plot 2 and 3 (P=0.9595), Plot 1 and 3 (P=0.2390), Plot 2 and 4 (P= 0.78). In conclusion, the family Subulinidae has the most abundant individuals with 733 individuals representing 89.4% while Streptaxidae occur as the most abundant family with 8 species of the total sample.

Keywords: Species Richness, Species Diversity and Species Abundance.

INTRODUCTION

The land mollusks is one of the numerous species of mollusks that live on land; as opposed to sea snails and freshwater snails, they are terrestrial gastropods that have shells (those without shells are known as Slugs). Majority of the land mollusks are pulmonates (they have lungs and breathe air) while a majority belong to much more ancient lineage where their anatomy includes gills and an operculum. These operculate land snails (snails with gills and opeculum) live in habitat or micro habitats that are sometimes (or often) damp or wet such as in Moss (Encyclopedia Britannic, 2009). Around 85,000 extant species of molluscs are recognized ((Gray, 2014). The number of fossil species is estimated between 60,000 and 100,000 additional species. Estimates of accepted described living species of molluscs vary from 50,000 to a maximum of 120,000 species (Chapman, 2009). Hazprunar (2001) identified an estimate of about 93,000 named species including

23% of all named marine organisms (Hancock, 2008). It has been found that there are about 200,000 living species of mollusks in total, (Chapman, 2009).Molluscs are second to arthropods in number of living species (Ponder and Lindberg, 1997) . They include snails, slugs and other gastropods; clams and other bivalves; squids and other cephalopods; and other lesser-known but similarly distinctive sub-groups. The majority of species still live in the oceans, from the seashores to the abyssal zone, but some form a significant part of the freshwater and terrestrial ecosystems. Mollusks are extremely diverse in tropical and temperate regions but can be found at all latitudes (Gilbert *et al.,* 2006). About 80% of all known mollusks species are gastropods (Ponder and Lindberg, 1997). They have the following characteristic features: They are unsegmented triploblastic coelomates, usually bilaterally symmetrical, body soft and fleshy and divided into head, ventral muscular foot and visceral hump, presence of mantle with a body cavity of homocoel (Taylor *et al*.,2002). The land mollusks (snails) species richness in some tropical rainforest has been assessed recently by some authors (Schilthuizen and Rutges,2001). In most ecosystem investigated so far in South-west Nigeria and other parts of tropical Africa, the dominant molluscan family is usually the *Streptaxidae* followed by either *Subulinidae* or *Urocyclidae* (Winter and Guttenberger,1998; Tattersfield, 1998; Oke and Alohan, 2002,2004,2006; Seddon *et al*.,2005, and Fontain *et al*., 2007). Changes in the abundance and distribution of individual species in recent decades have been widely documented as species have responded to land use pressures and climate change (Oke and Chokor, 2009). Rainforest destruction usually result in reduced abundances, diversities and ultimately local extinction of species or to changes in community structure of species composition (Lydeard *et al*.2004, Schilthuizen *et al*.2005; Oke *et al*, 2008). Today, 75% of the world's food is generated from only 12 plants and five animal species. Animals provide some 30% of human requirement for food and agriculture and 12 percent of the world's population live almost entirely on products from animals (FAO,1999b). The tropical rainforest is important due to the quantity and diversity of life they support. They cover only 70% of the earth's land area, but at least 50% of terrestrial (FAO, 1999b). The influence of forest on biodiversity are global, reaching for beyond national borders, in both space and time. Despite the loss of primary covers, secondary forest reserve harbour a substantial amount of biodiversity. This has been justified by studies of diverse ecosystem using birds and arthropods as indicator species (Vandermeer and Perfecto,1997, Castelletta, et.al,2000; Dunn,2004). The tropical rainforest is threatened with widespread deforestation and degradation of natural habitat for agricultural purposes resulting in the loss of species (Castelletta et al , 2000 and Brooks,2013). Due to the ongoing process of species loss in agricultural landscape, maintaining biodiversity has become a challenge. Agro-bio diverse traditional agro-ecosystem help in the production and availability of food and environmental conservation through stable and diverse production system. Modern mono-cultural systems, uniform crop activities and

Scientia Africana, Vol. 21 (No. 1), April, 2022. Pp 87-100 *https://dx.doi.org/10.4314/sa.v21i1.8*
© Faculty of Science, University of Port Harcourt, Printed in Nigeria *ISSN 1118 – 1931*

agrochemical input, have contributed in eroding agricultural biodiversity and degraded other natural resources, contributing to serious economic loss and human suffering (Thrupp,, 1998). Previous studies on tropical land snails have concentrated on primary forest or forest reserve and have revealed high level of species richness, low densities and considerable heterogeneity in richness and species composition among plots within the study area. Winters and Guttenberger, 1998, Schilthuizen and Rutjes,2001; Alohan and Oke, 2004; Oke and Alohan,2004.). Land snail species richness declined with increasing activity and disturbance. Anthropogenic effect reducing land snail biodiversity includes: habitat modification, urbanization and land use practices have strong negative effects on land snail diversity (Graveland *et al*., 1994, Orstan *et al*., 2005, Lange,2000, Oke and Alohan, 2006). In Gashaka-Gumti National Park, human activities ranging encroachment, improper land-use practices and exploitation of land snails occurred and may cause a decline in the biodiversity of land snails including species composition. It then becomes necessary to conduct this study with an aim to ascertain or assess the biodiversity of terrestrial molluscs in the Gashaka- Gumti National Park.

MATERIALS AND METHODS

Study Area

The Study was conducted in both Gashaka-Gumti National Park with a total area cover of 6,402km² with a coordinate of 6º 55¹N, 11º 13¹E / 6.917ºN, 11.217ºE). Gashaka is a local Government area in Taraba State with its headquarters in Serti. The Northern Gumti sector of the park is relatively flat and covered with woodlands and grass lands while the southern Gashaka sector is a more mountainous and contains vast expanses of rainforest as well as area of woodland and montane grassland. The altitude ranges from 457 metres (1499feet) in the North and 2419m (7936ft) in the south.

Figure 1: Map of Local Government in Taraba State

Figure 2: Coordinate Map of Gashaka Gumti National Park in Serti, Taraba State

Sampling Method

Land mollusks samples were collected from the study area using a combination of direct search and later sieving techniques (Tattersfield,1996). This was carried out three (3) consecutive times between June, 2016, September, 2016, April, 2017 and June, 2017. This method was designed to detect both large sized tang that often occur in low density and micro species that are often cryptic and litter dwelling (De winter and Guttenberger,1998). Direct search technique involves examining all potential molluscan microhabitats that can be assessed such as fallen trunk, rotten logs, tree bark and buttresses, deep litter beds and hard surfaces by hand picking in a plot of over 30m×30m. While the litter sieving techniques involves collection of litters and top soil loosened with hand fork. Four plots from different location of the area were sampled, and at each plot we searched intensively for mollusk (5 persons per plot, 3 times daily). In addition, the author collected an average of 5litres of leaf litters and top soil in total of about 80 bags, from different randomly selected sites (1m×lm each) within each plot and labeled with the locality name, date and plot of collection and tied to prevent snails from escaping.

All live specimens were preserved in 70% alcohol. Fieldwork was not undertaken at night because of the difficulties this would have entailed, including adequate access and searching of sites, and safety issues related to the habitat types sampled. Slugs were not considered and the sampling methods would not be suitable to determine slug abundance. All specimens were identified and lodged in the Egborge's Museum in the Department of Animal and Environmental Biology, University of Benin.

Statistical Analysis

The diversity was measured as overall species richness(S) and Whittaker's index (I), which is the total number of species recorded(S) divided by the mean number of species per site (α), providing a measure of diversity difference between sites (Schilthuizen and Rutjes, 2001). The true diversity was estimated by performing 100 randomizations on the data and calculating(S) using the Chao2 and second-order jack knife richness estimators in the program Estimate S7.5 (Colwell, 2006). We defined sample intensity as the ratio of individuals to species number, and inventory completeness as the percentage of the observed number of species over the expected number of species as estimated by Chao2 or Jack2 (Coddington et al., 1996; Soberon et al., 2007). Statistical analyses were performed using the PAST software (Hammer et al., 2001). Hierarchical clustering (Bray-Curtis similarity measure) was used to identify natural groupings among the sampled sites according to similarities in their species composition. The non-parametric one-way Analysis of Similarity (ANOSIM; Clarke, 1993) was used to test for statistical differences in species composition between clusters. From ANOSIM, if R>0.75 groups are well separated, if R>0.5 groups are overlapping but clearly different, and if R>0.25 groups are barely separable (Lovell et al., 2010).

RESULT ANALYSIS

A total of 819 individuals comprising 22 species belonging to six molluscan families were collected from four plots in Gashaka

Scientia Africana, Vol. 21 (No. 1), April, 2022. Pp 87-100 https://dx.doi.org/10.4314/sa.v21i1.8
© Faculty of Science, University of Port Harcourt, Printed in Nigeria *ISSN 1118 – 1931*

Gumti National Park. Each plot yielded between 8 and 14 Species (Mean 10, Standard deviation, 2.71) and between 33 and 683 Individuals (Mean 204.75, Standard deviation 319.09)

The species collected from all sample plots are listed in Table 1, percentage abundance of species and individuals across sampled locations are shown in Table 2, while species richness and diversity of land mollusks in the park are found in Table 4.From Table 1, plot 4 yielded the most (683 Individual) representing 83.4% of the total number of individual species encountered, *Curvella sp* appear to be the species that is more in number with 650 individuals representing 79.4% of the total number of individual species encountered . From Table 3, the family *Subulinidae* has the most abundant individuals with 733 individuals representing 89.4% while *Streptaxidae* occur as the most abundant family with 8 species of the total sample.

Table 1: List of Land mollusks collected from Gashaka-Gumti National Park, Taraba State, Nigeria. Families and species are arranged alphabetically.

	ACHATINIDAE	**PLOT 1**	**PLOT 2**	**PLOT 3**	**PLOT 4**	**TOTAL**
1	*Limicolaria flammea*	0	2	0	8	**10**
2	*Limicolaria sp*	0	0	0	2	**2**
	CERASTIDAE					
3	*Rachistia sp*	1	1	0	0	**2**
	STREPTAXIDAE					
4	*Gulella cf gemmia*	2	0	0	0	**2**
5	*Gulella angloria*	1	0	0	0	**1**
6	*Gulella monodon*	0	5	0	0	**5**
7	*Ptychotrema anceyi*	4	0	0	0	**4**
8	*Ptychotrem acomplicatum*	0	1	0	0	**1**
9	*Ptychotrema martense*	0	2	1	0	**3**
10	*Streptostele sp.*	0	0	0	1	**1**
11	*Tomostele musaecola*	1	0	0	0	**1**
	SUBULINIDAE					
12	*Curvella sp*	0	17	24	609	**650**
13	*Kempiochoncha sthulmani*	2	0	2	2	**6**
14	*Pseuduglessula sp*	2	0	3	0	**5**
15	*Subulona striatella*	12	0	0	29	**41**
16	*Subulona involute*	1	1	24	5	**31**
17	*Opeas sp.*	0	0	0	0	**0**
	UROCYCLIDAE					
18	*Gymnarion sp*	4	3	4	3	**14**
19	*Thapsia sp*	4	0	0	24	**28**
20	*Trochozonite adansonia*	0	1	0	0	**1**
21	*Trochozonite hystrix*	3	0	3	0	**6**
22	*Trochozonite sp*	1	0	0	0	**1**

	VERONUCELLIDAE					
23	*Pseudoveronicella sp*	2	0	2	0	**4**
	Total Number of Individual	**40**	**33**	**63**	**683**	**819**
	Total Number of Species	**14**	**9**	**8**	**9**	

Table 2: Percentage Abundance of Species and Individual in Gashaka Gumti National Park

Family	**Number of Species**	**Number of Individual**	**% Species**	**% Individuals**
Achatinidae	2	12	9.09	1.46
Cerastidae	1	2	4.55	0.24
Streptaxidae	8	18	36.4	2.19
Subulinidae	5	733	22.7	89.49
Urucyclidae	5	50	22.7	6.11
Veronucellidae	1	4	4.55	0.49
Total	**22**	**819**	**100**	**100**

Table 3: Species Richness and Diversity of Land Mollusks in Gashaka Gumti National Park, Taraba State, Nigeria

Number of Individuals	819
Number of Species	22
Number of Plots	4
Range per Plot	8 – 14
Mean Number of Species per Plot	10
Standard Deviation	2.71
Mean Number of Individual per Plot	204.75
Standard Deviation	319.09
Whittaker Index(S)	4
Sample Intensity (S/sp)	37.22
Singletons	11
Doubletons	10
Inventory Completeness	79.31%
Margalef	0.4472
Shannon_H	0.6256
Evenness	0.4673
Simpson I-D	0.2946

The sample rarefaction curve (Fig. 5) nearly reached an asymptote when sampling stopped and the number of species was not different from that obtained by non-parametric estimator. The Chao 2 and Jackknife estimator was 28.05 and 33.99 of all sample collected. The Sample

Scientia Africana, Vol. 21 (No. 1), April, 2022. Pp 87-100 *https://dx.doi.org/10.4314/sa.v21i1.8*
© Faculty of Science, University of Port Harcourt, Printed in Nigeria *ISSN 1118 – 1931*

Intensity was 37.22 while the Inventory Completeness was 79.31%. The Whittaker Index was 4.00 indicating high differentiation among plots.

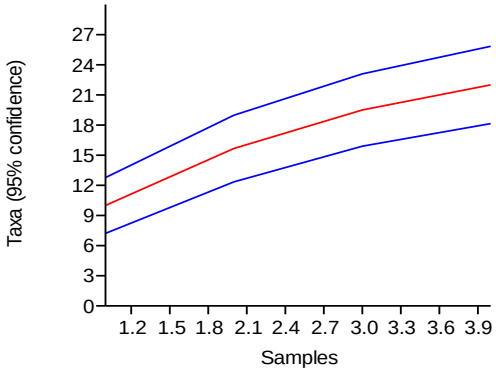

Figure 5: Rarefaction Curve showing the rate of Species accumulation across Sampling Plot

The species rank abundance for land mollusks in the four plots (Figure 6) shows the presence of some rare species. The moderately high diversity is borne out of the fact that some species exist in the sample. The dendogram of similarity by plots using the Bray - Curtis similarity index (Figure 7) show the close relationship two plots in terms of species. The cluster analysis is grouped into two group (Figure 8). The similarity between plots revealed that there is no significant difference between plots as shown below. Plot 1 and 4 (P = 0.4329), Plot 2 and 3 (P = 0.9595), Plot 1 and 3 (P = 0.2390), Plot 2 and 4 (P = 0.78).

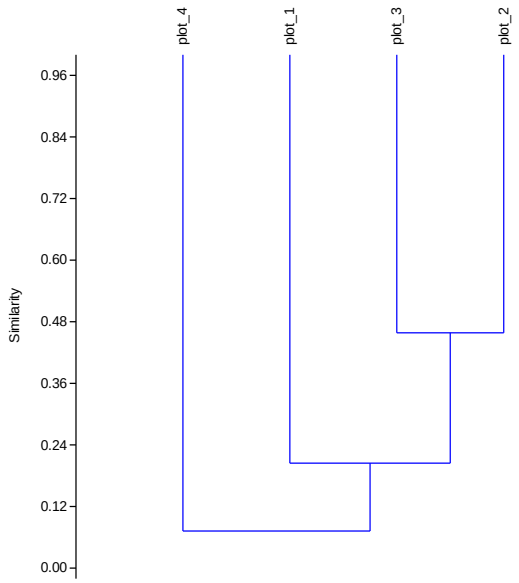

Figure 7: Dendrogram of similarity by plots using Bray-Curtis similarity index.

Plate 1

3cm 6cm

Plate 2: Semi-slug *Gymnarion* sp. (Urocyclidae) Slug, *Pseudoveronicella* sp. (Veronicellidae)

8cm

Plate 3:*Subulona sp*

9.5cm

Plate 4: *Callistoplepa sp*

9cm

Plate 5: *Subulina sp*

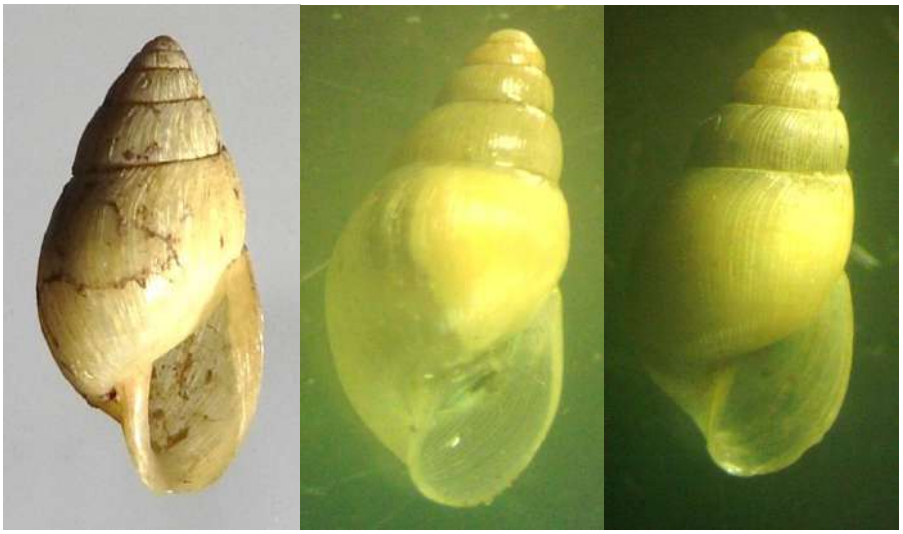

6cm 6.5cm 5.5cm

Plate 6: *Curvella sp*

Scientia Africana, Vol. 21 (No. 1), April, 2022. Pp 87-100 https://dx.doi.org/10.4314/sa.v21i1.8
© Faculty of Science, University of Port Harcourt, Printed in Nigeria *ISSN 1118 – 1931*

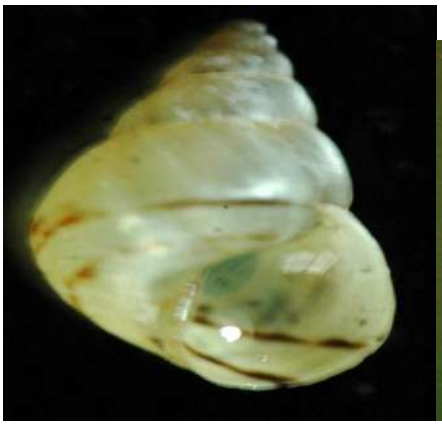

9cm

Plate 7: *Rachistia sp*

7cm

Plate 8: *Tomostele sp.*

5.5cm 6.5cm 8cm

Plate 9: *Gullela sp*

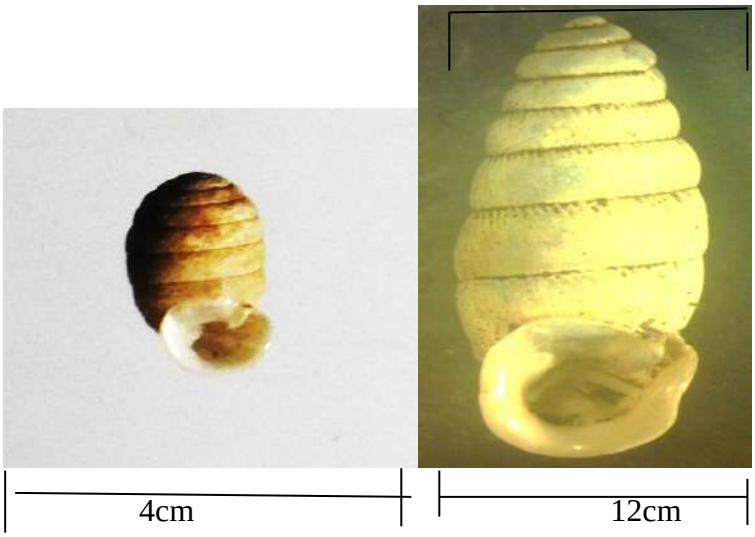

Plate 11: *Phychotrema sp* Plate 12:*Ptychotrema anceyii*

DISCUSSION

Identify the species of land mollusks in Gashaka Gumti National Park

A total of 819 individuals comprising 22 species belonging to six molluscan families were collected from four plots in Gashaka Gumti National Park. Each plot yielded between 8 and 14 Species. In comparison, the number of land snail species recorded in this study (GGNP) , North Eastern Nigeria is higher than the ones recorded in South Eastern Nigeria with 242 individuals in Obudu Cattle Ranch, 425 individuals in Odukpani and 636 individuals in Oban Hills Sector, all in Cross River State, Nigeria (Oke *et al*., 2004 & 2007). Also, the species from Oban Hills were collected from 24 sampling plots in Ehor, Edo State, Nigeria. (Oke and Alohan, 2004), 38 species and 1258 individuals were recorded from nine 20 metres squared plot in a tropical rainforest (Oke and Alohan, 2002). Moreover, 35 species and 316 individuals were collected from five 20 metre squared plots in Okomu National Park, Edo State, Nigeria. This also agrees with the record for Sebah, Malaysian Burneo in (Schiltuizen and Rutjes,2001) and more than half of the species recorded for Cameron, Texas (De-winter and Gittenberger,1998) The researcher can therefore infer that GGNP is one of the richest area in Northern Nigeria with high biodiversity site and may be compared with other places in the world.

Estimating the species richness, abundance and species composition of land mollusks in Gashaka Gumti National Park.

The most abundant species in the Park was *Curvella sp*. reported by 683 individuals (79.4%) and most dominant family was *Streptaxidae* reported by 8 species. Gashaka Gumti National Park is made of primary forest but there are open patches which allow the sun to penetrate some areas of the forest floor. This open patches may be due to illegal logging of timber or other agricultural activities. This may account for the reason why *Curvella sp* dominate the area since they can resist

Scientia Africana, Vol. 21 (No. 1), April, 2022. Pp 87-100 https://dx.doi.org/10.4314/sa.v21i1.8
© Faculty of Science, University of Port Harcourt, Printed in Nigeria *ISSN 1118 – 1931*

harsh weather and moderate temperature to a great extent compared to the *arachnida*who prefer very humid environment.(Dillon,, 2000) Environmental variability is one of the primary characteristics of natural selection. The distribution of mollusks species and of higher taxa depends on the antiquity of the group, its power of dispersal, its adaptability to environmental variables and the effects, if any, of isolation. (Fretter and Peake, 1978). The *Streptaxidae*, on the other hand, has more number of species, 8 species of the total sampled. This may be attributed to the fact that they are diverse and well distributed in most habitats. The dominance of the Carnivorous *Streptaxidae* in various biodiversity location has been established. Twenty three species, 159 individuals from 52 species and 425 individuals in Odukpani, Cross River State, Nigeria (Oke *et al.*,2007).Oke and Alohan (2004), in spite of low abundances, recorded a total of 25 species and 323 individuals in 7 molluscan families in the land snail diversity of a patch of Cocoa Plantation in Usen, Edo State, The carnivorous *Streptaxidae* dominated in numerous of individual (55%) and diversity of species (36%), (Oke and Ugiagbe, 2007). The land mollusks fauna in a single squared kilometre of undisturbed tropical rainforest in Okomu National Park, Edo State, Nigeria was surveyed and this yielded a total of 1442 individual mollusks belonging to 46 species in 11 molluscan families. In number and diversity, *Streptaxidae* was the most dominant family consisting 33% of the total number of species collected and 35% of the total number of individuals (Oke and Alohan, 2006). Looking at the molluscan survey carried out by Oke *et al* (2008), on the land mollusks diversity in a patch cultivated with Oil Palm (*Elaisguinensis*) in Egbeta, Edo State, Nigeria yielded 22 species and 833 individuals in 6 molluscan families from 10 plots. The detrivores *Subulinidae* dominated the land molluscan fauna in number of individuals (42%) and diversity (27%). From the fore-going environmental variables determine the poor dispersal ability of land snails(Baur & Baur,1993::Schilthuizen & Lombaerts, 1994) but more to it is that small snail species can exhibit extensive distribution range (Nekola et.al, 2009: Nekola, 2014)

CONCLUSION

This study will contribute to knowlege in the following ways: Provide an annotated checklist of land mollusks collected from Gashaka Gumti National Park, Provide information on the species richness and diversity pattern of the land mollusks of Gashaka Gumti National Park, Highighting information on the abundance of *Curvella sp*. in Gashaka Gumti National Park.. Knowledge on land snail of the area has been made known and the different kind of species present in the area.

REFERENCES

Baur, A. and Baur, B. (1993) Daily movement patterns and dispersal in the land snail Arianta arbustorum. Malacologia.35,89.98.

Brooks, R. (2013). A slow passion. Snail; My Garden and Me. London Bloomsbury

Castelleta, M, Sodhi, N.S and Sobring, R. (2000).Heavy extinction of forest avifauna in Singapore Lessons for Biodiversity Conservation in South

East Asia. *Conservation Biology*.**4**:1870-1880.

Chapman, A.D (2009). Numbers of living species in Australia and the world. 2nd edition. *Australian Biological Resources Study*. Canberra.

Clarke K. R (1993. Non Parametric multivariate analysis of change in community structure.*Australian Journal of Ecology*. **18**: 117-143.

Colwell R K & Coddington JA 1994. Estimating terrestrial biodiversity through extrapolation. Philos Trans R. Soc. (B, 345: 101-118.

De Winter, A.J. and Guttenberger, E. (1998). The land snail fauna of a square kilometre patch ofrainforest in South Western Cameroon: High Species Richness, Low abundances and Seasonal fluctuations .*Malacologia*. **40:**231-250.

Dillon, R.T (2000). The Ecology of Freshwater Mollusca. Cambridge University Press

Dunn, R.R. (2004). Recovery of faunal communities during tropical forest Generation .*Conservation Biology*.**18:**302-309.

FAO (Food and Agriculture Organization) (1999b)State of the world's forest . 1999 FAQ

Encyclopaedia Britinnica, (2009) Integument (Mollusca.) Ultimate Reference Suite DVD

Fontaine. B, Gargominy, O. and Neubert, E. (2007).Land Snail diversity of the Savannah/forest mosaic in Lope National Park, Gabon.*Malacologia*.**49(**2):313-338.

Gilbert, G., Okusu, A., Lindgren,A.R., Huff, S.W.,Schrodi, M. and Nishiguchi., M. K. (2006). Evidence for a clade composed of molluscs with serially repeated structures: Monoplacophorans are related to Chitons. *Proceedings of the National Academy of Science* of the United States of America. **103**(20):7723-7728.

Graveland, J. and VanderWal, R. (1994). Decline in Snail abundance due to Soil Acidification which causes eggshell defects in forest Passerines.*Oecologia*.**105**: 351-360.

Gray, R.(2014). A new critical estimates of named species-level diversity of the recent Mollusca. *American Macological Bulletin*, **32** (2), 308-322

Hammer O, Harper DAT & Ryan PD 2011. PAST: Paleontological statistics software for education anddata analysis. Paleontological Electronica, **4**(1): 1-9.

Hannock R. (2008). Distribution and Taxonomy of Molluscs in some Northern parts of Nigeria.

Hazprunar,G (2001). Mollusca (Mollusks) Encyclopedia of Life Sciences. John Wiley and Sons Limited.

Lange, C.N.(2000). Environmental Factors Influencing Land Snail diversity in ArabukoSokoke forest, Kenya. *African Journal Ecology*.**41**: 352 – 355.

Lovell, S. Hamer, M. Slotow, R. and Herbert, D (2010). Assessment of Sampling Approaches for a multi-taxa invertebrate survey in a South African Savanna-mosaic ecosystem *Australian Ecology* **35:** 357-370

Lydeard, C.,Cowie, R.H., Ponder,W. F.,Bogan, A. E.,Bouchet, P., Clark, S. A.,Cunnings, K. S., Frest, T.J., Gargominy, O., Herbert, D. G., Hershler, R., Perez, K.E., Roth, B., Seddon, M., Strong, E. E. and

Scientia Africana, Vol. 21 (No. 1), April, 2022. Pp 87-100 https://dx.doi.org/10.4314/sa.v21i1.8
© Faculty of Science, University of Port Harcourt, Printed in Nigeria *ISSN 1118 – 1931*

Thompson, F.G. (2004). The global decline of non-marine mollusks .*Bioscience*.**54**:321-330.

Nekola, J.C., Coles, B.F. & Bergthorsson, U. (2009) Evolutionary pattern and process within the Vertigo gouldii (Mollusca: Pulmonata, Pupillidae) group of minute North American land snails. Molecular Phylogenetics and Evolution,53, 1010–1024. doi:10.1016/j.ympev.2009.09.012.

Nekola, J.C. (2014) North American terrestrial gastropods through each end of a spyglass. Journal of Molluscan Studies,80, 238–248. doi:10.1093/mollus/eyu028.

Oke, O. C., Alohan, F. I. and Abhulimen, W. (2007). Land Snail Diversity in a Threatened Limestone Formation in Odukapni, Cross River State, *Nigeria Global Journal of Pure and Applied Sciences.* **13**(4): 487-492.

Oke, O. C. and Alohan, F. I. (2002).The Land Snail Diversity in a Square Kilometre of Tropical Rainforest in Ehor, Edo State. Nigeria. Modest Species Richness, High Abundance and Local Homogeneity. *Journal of Environment, Science and Health*.**5**: 39 - 43.

Oke, O.C and Alohan, F.I. (2004). Land Snail Diversity in a Patch of Rainforest in Cross River National Park: High Species Richness Abundance and Heterogeneity. *Nigerian Journal of Applied Science*.**22**:166 -173.

Oke, O. C. and Alohan, F. I. (2006).The land Snail diversity in a Square Kilometre of Tropical Rainforest in Okomu National Park, Edo State, Nigeria. *African Science*.**7**: 135 - 142.

Oke, O.C. and Chokor, J. U. (2009).Land Snail Population in a Shade and Full Sun Cocoa Plantation in South Western Nigeria, West Africa.*African Scientist*.**10**(1): 19 – 29.

Oke, O.C. and Chokor, J.U. (2009).The Effect of Land Use on Snail Species Richness and Diversity in the Tropical Rainforest of South Western Nigeria.*African Scientist*. **10(2)**: 95-108.

Oke, O.C., Alohan, F.I., Uzibor, M.O. and Chokor, J.U. (2008).Land Snail Diversity and Species Richness in an Oil Palm Agro forest in Egbeta, Edo State, Nigeria.*Bioscience*.**20:**249-256..

Oke, O.C.and Ugiagbe, O.O.(2007).Land Snail Diversity in a Patch of Cocoa Plantation in Usen, Edo State, Nigeria. *Great Journal of Pure Applied Science*.**13:**481-485.

Ponder, W.F. and Lindberg, D.R. 1997. Towards a phylogeny of gastropod molluscs: an analysis using morphological characters. *Zoological Journal of the Linnean Societ*y **119**:83–265.

Seddon, M., Appleton, C., Van Damme, D. and Graf, D. 2011. Freshwater molluscs of Africa: diversity, distribution, and conservation. In: Darwall et al. 2011. The Diversity of Life in African Freshwaters: Under Water, Under Threat. An analysis of the status and distribution of freshwater species Throughout mainland Africa. Cambridge, United Kingdom and Gland, Switzerland: IUCN.

Chilthuizen, M. & Lombaerts, M. (1994) Population structure and levels of gene flow in the mediterranean land

snail Albinaria corrugate (Pulmonata, Clausiliidae).Evolution,48, 577–3586.

Schilthuizen, M. and Rutjes, H.A. (2001). Land Snail Diversity in a Square Kilometre of Tropical Rainforest in Sabah, Malaysian Borneo. *Journal of Molluscan Studies.***67**: 417-423.

Tattersfield, P. (1996) Local Patterns of Land Snail Diversity in a Kenyan Rainforest. *Malacologia*.**38**:161-180.

Taylor, D.J, Green, N. P. O and Stout, G. W (2002). Biological Science. Third Edition. CambridgeUniversity Press. Pp 15

Thrupp,L.A (1998).The Central Role of Agricultural Biodiversity: Trend and Challenges. In Conservation and Sustainable Use of Agricultural Biodiversity, Manila. CIP-UPWARD in partnership with GTZ,IDRC,IPGRI and SEARICE.

Vandermeer, J., Perfecto, I. (1997).The Agro ecosystem: A Need for the Conservation Biologist's Lens. *Conservation Biology*.**11**: 1 - 3.

Scientia Africana, Vol. 21 (No. 1), April, 2022. Pp 101-114 https://dx.doi.org/10.4314/sa.v21i1.9
© Faculty of Science, University of Port Harcourt, Printed in Nigeria *ISSN 1118 – 1931*

EFFECT OF ETHANOL EXTRACT OF THE FRUITING BODIES OF *PLEOROTUS OSTREATUS* ON THE SERUM HEPATO-SPECIFIC ENZYME MARKERS AND LIVER HISTOLOGY OF HIGH SUCROSE-HIGH FAT DIET-STREPTOZOTOCIN INDUCED DIABETIC RATS

Onuoha, S. C.[1], Okoroh, P. N.[2*], Uwakwe, A. A.[1], Monago-Ighorodje, C. C.[1], and Okari, K. [3]

[1.]*Department of Biochemistry, Faculty of Science, University of Port Harcourt Choba, Rivers State, Nigeria.*
[2.]*Department of Medical Biochemistry, Faculty of Basic Medical Sciences, Gregory University, Uturu, Abia State, Nigeria .*
[3.]*Department of Medical Biochemistry, Faculty of Basic Medical Sciences, University of Port Harcourt, Choba, Nigeria.*
*Corresponding Author. Email: pnokoroh@gmail.com , p.okoroh@gregoryuniversityuturu.edu.ng ,

Received: 28-10-2021
Accepted: 26-03-2022

ABSTRACT

The effect of ethanol extract of the fruiting bodies of Pleurotusostreatus on the serum hepato-specific enzyme markers and liver histology were determined in high sucrose-high fat diet-streptozotocin induced diabetic rats. The pharmacological model was 20% High Sucrose (HS) + 20% High Fat Diet (HFD) + 35mg/kg body weight (intraperitoneal) Streptozotocin (STZ) induced diabetic rat model, with the fruiting body ethanol extracts administered orally at 50, 150 and 300mg/kg b.w. After 6 weeks of treatment, alkaline phosphatase activity (ALP) of the treated groups and the reference treatment groups were significantly ($p<0.05$) higher than the D group but after the 9th week of treatment, the ALP activity of the diabetic groupstreated with fruiting body ethanol extract at 50mg/kg b.w., 150mg/kg b.w. and the reference treatment group were significantly lower ($p<0.05$) than the D group. All the treated groups had aspartate amino transferase activity that was significantly higher ($p<0.05$) than the D group at the end of 3 weeks but at the end of the 6th week of treatment, the AST activity of all the treated groups was significantly lower than the D group ($p<0.05$). At the end of the first 3 weeks of treatment, the alanine amino transference (ALT) activity of the diabetic group treated with fruiting body ethanol extract at 150mg/kg b.w. was significantly ($p<0.05$) lower than the D group. After 6 weeks of treatment, ALT activity of all the treatment groups as well as the reference treatment groups were significantly lower ($p<0.05$) than the D group but the values of the diabetic group treated with fruiting body ethanol extract at 150mg/mg b.w. and diabetic group treated with metformin hydrochloride at 150mg/kg b.w. were not significantly different ($p>0.05$) from the normal control. At the end of 9 weeks of treatment, the ALT activity of the diabetic group treated with fruiting body ethanol extract at 300mg/kg b.w. and diabetic group treated with fruiting body ethanol extract at 50mg/kg b.w. were significantly lower ($p<0.05$) than the D group although not significantly different than the normal control.The extract at 300mg/kg b.w. reversed the fatty liver and periportalinflammation caused by HS-HFD-streptozotocin induced diabetes in the rats to normal, indicating dose dependent protective effects of the extract against HS-HFD-streptozotocin induced hepatotoxicity alterations. The reduction in the serum levels of these liver enzymes by the extract suggests that they may be used to reverse the incidence of liver function test irregularities common in diabetic patients. The results suggest that ethanol extract of fruiting bodies of Pleurotusostreatus may be employed in the management of liver diseases associated with diabetes mellitus.

Keywords: Serum hepatospecific-enzyme markers, liver histology, Streptozotocin, diabetes, rats, high fat diet

INTRODUCTION

Diabetes mellitus has been reported as a burden of disorder in the structure and function of biological systems (Jamaludinet al., 2016). According to Okorohet al., (2021), the disease is a major factor in the endocrine region of the biological system responsible for the crisis in the metabolism of biomolecules such as fats, carbohydrates and proteins. Diabetes mellitus has been reported to be linked with abnormalities in the liver such as abnormal glycogen deposition, non-alcoholic fatty liver disease, fibrosis, cirrhosis, abnormal increase in liver enzymes levels, acute liver disease etc. (Guvenet al., 2006) When too much fat accumulates in the liver, insulin resistance may be critical causing serious irregularities in metabolism (Levinthal and Tavill, 1999). The liver is one of the major organs in the body that suffers the negative effects of hyperglycemia-induced oxidative stress (Bugianesiet al., 2005; Palsamyet al., 2010). Diabetes mellitus has been implicated in histopathological changes in the liver such as micro vesicularsteatosis and macro vesicularsteatosis (Mukhlif et al.,2020). Diabetes mellitus is a contributory factor to impaired vision, stroke, kidney failure, cardiovascular diseases (WHO, 2016), its prevalence has been on the increase particularly among middle- and low- income nations like Nigeria. The World Health Organization has stated that diabetes mellitus will be the 7^{th} leading cause of deaths by 2030. The implication is that diabetes mellitus presents a major challenge to researchers and health care systems around the globe. Diabetes mellitus is defined as a group of metabolic diseases of endocrine origin caused by high glucose level in the blood over a prolonged period because of complete or relative lack of insulin resulting from the impairment of insulin secretion, insulin action or both (WHO,2014). Its symptoms include osmotic diuresis, increased thirst, hunger, and high concentration of lipids in the blood (WHO, 2013).High blood sugar level as a result of insulin resistance causes alteration in the metabolism of fats, proteins and carbohydrates resulting to non-alcoholic steatohepatitis, cirrhosis and hepatocellular carcinomas (Jamaludinet al.,2016).Diabetes has been indicated to cause pathological changes in the liver (Lucchesiet al., 2015). Alanine aminotransferase, aspartate amino transferase and alkaline phosphatase are biomarkers of hepatocyte damage and are involved in various reactions in the liver. Hepatocyte injury has been revealed by the levels of AST and ALT in the plasma or serum andhigh levels of ALP indicate biliary tree obstructions (Lee et al., 2012). Synthetic drugs such as sulfonylurea, biguanides and thiazolidinedionesused to treat diabetes are expensive and have side effects (Lee et al., 2012).

Pleurotusostreatus belongs to the family of mushrooms known as *Pleurotaceae* (Kuo, 2005).*P.ostraetus* is also called tree oyster mushroom (Stamets, 2000). The people from Japan call it Hiratake which means flat mushroom (Hall,2010).The Igbo-speaking people of South-East Nigeria, call it Eroatakata because it has very tough texture on mastication (Akpajaet al., 2003). The mushroom has quality nutritional value, numerous medicinal properties and many other beneficial effects. It has been used as food and as means of treating ailments by numerous people all over the globe for many years (Finimundyet al.,

Scientia Africana, Vol. 21 (No. 1), April, 2022. Pp 101-114 *https://dx.doi.org/10.4314/sa.v21i1.9*
© Faculty of Science, University of Port Harcourt, Printed in Nigeria *ISSN 1118 – 1931*

2013). *P. ostreatus* is rich in dietary fiber, sterol, proteins, macro-minerals and trace-elements. It has been reported that the macro fungi, due to the presence of mychochemicals in them coupled with their antioxidative properties may be used to cure ailments associated with viruses, bacteria, high cholesterol level in blood, it has hematological characteristics as well as the capacity to enhance immune functions (Finimundyet al., 2013; Markopoulosetal., 2012). This is because it is a source of important mineral nutrients such as selenium, potassium, magnesium, copper, calcium, vitamins like riboflavin, niacin, vitamin D,tocopherol, vitamin C, folic acid, vitamin K and dietary fiber to humans (Maria et al., 2014). The present study was conducted to determine the effect of ethanol extract of the fruiting bodies of organically cultivated *P.ostreatus* on the serum hepato-specific enzyme markers and liver histology of HS-HFD-streptozotocin induced diabetic rats.

MATERIALS AND METHODS

Preparation of High Calorie Density Diet

High calorie density diet was prepared according to formulation by Okorohet al., (2021) as shown below;

Table1: High Sucrose-High Fat Diet (HS-HFD %)

Composition	Proportion (%)
Normal diet	60.0
Sucrose	20.0
Lard	20.0
Total	**100.0**

* Diet was prepared daily to avoid microbial contamination and fed to the animals *ad libitum*, throughout the period of the experiment.

Collection of Mushroom Materials and Preparation of Mushroom Ethanol Extracts

Pleurotusostreatus fruiting bodies were obtained from the samples cultivated using organic supplements at the Research Unit Demonstration Farm of the University of Port Harcourt, Rivers State, Nigeria. Ethanol extract of *P.ostreatus* was prepared according to the method reported by Okorohet al. (2021)

Collection of Experimental Animals, Induction of Diabetes and Determination of Blood Glucose and Body Weight

A total of 54 normoglycemic female Wistar albino rats were used for this study. The animals were purchased from the Animal House, Department of Biochemistry, Faculty of Science, University of Port Harcourt, kept and maintained in a house that is well-ventilated, having a 12hour light / 12hour dark cycle in propylene cages, at room temperature. Food and water were adequately given to the animals. The animals were acclimatized to laboratory conditions, 7days prior to starting of experiment. After acclimatization of the animals for a period of 7 days, the nine animals in Normal control group were placed on normal diet of guinea growers mash diet while the other rats in the remaining five groups (n=9) were fed with High Sucrose-High Fat Diet (HS-HFD) throughout the experimental period. The forty-five rats (n=9 rats/group) in the other five groups were placed on HS – HFD for 21 days, fasted overnight and induced diabetes using a single intraperitoneal injection of streptozotocin (35mg/kg bw). Stroptozotocin (Sigma, USA) at a dose of

35mg/kgbw was prepared in fresh and cold normal saline solution and administered immediately to the animals. The animals were first weighed using an electronic scale (TH 500) and their base line fasting blood glucose level taken using Fine Test Auto-coding™ Premium Blood Glucose Monitoring System and Blood Glucose Strips via tail vein cut before they were injected with streptozotocin (Okorohet al.,2021).

Experimental Design

The experimental model was 20% High Sucrose (HS) + 20% High Fat Diet (HFD) + 35mg/kg body weight (intraperitoneal) streptozotocin (STZ) induced diabetic rat model .The Metformin HCl and ethanol extract were given once daily(1ml per animal) by intragastric gavage to the reference treatment and experimental groups respectively at doses 150mg/kg b.w., 50mg/Kg b.w, 150mg/kg b.w. and 300mg/kg b.w. respectively while the normal control received saline solution for 88days. The rats (3 from each group) were sacrificed after 3, 6 and 9 weeks of treatment. Blood samples and liver were collected for analysis. The extracts and metformin HCl (reference drug) were kept in plastic bottles with cap tightly sealed before and after each use, stored in the refrigerator, protected from direct sunlight to prevent spoilage throughout the time of animal treatment. (Okorohet al.,2021). Ethical guidelines for the use of animals (Mary and Paul, 2016) was followed in this research

Determination of Serum Hepato Specific Enzyme Markers and Liver Histopatology

Alkaline phosphatase activity , alanine transaminase activity and aspartate transaminase in the serum were estimated using Randox test kits (Randox Laboratories Test Crumlin, England, UK) (Reitman & Frankel, 1957).Histopathology was carried out at the Department of Anatomical Pathology, University of Port Harcourt Teaching Hospital. Small pieces of liver tissues were collected in 10% formalin for proper fixation. These tissues were processed and embedded in wax of paraffin. Sections of about 5µm in thickness were cut, mounted on slide and stained with hematoxylin and eosin. The sections were then observed under light (Opticphot -2, Nikon, Tokyo, Japan) at x200 and x400 magnifications respectively.

Statistical Analysis

Data was statistically analyzed by a one way analysis of varience (ANOVA) using SPSS/PC + package. Multiple comparisms of differences between means were conducted using Fisher's Least Significance Difference (LSD). Significance was accepted at a p-value of less than 0.05.

RESULTS AND DISCUSSIONS

The initial and most important biomarkers in assessing liver injury include the levels of serum ALT, AST and ALP (Longo et al., 2011).The results of this scientific study (Table 1, Table 2 and Table 3, respectively) revealed that the extracts of *P.ostreatus* at all doses significantly ($p< 0.05$) lowered ALP level after 3 weeks of treatment, while *Pleurotusostreatus*extract

Scientia Africana, Vol. 21 (No. 1), April, 2022. Pp 101-114 *https://dx.doi.org/10.4314/sa.v21i1.9*
© Faculty of Science, University of Port Harcourt, Printed in Nigeria *ISSN 1118 – 1931*

(POE) at 50 and 150mg/kg significantly ($p<0.05$) reduced ALP levels of the treated rats after 9 weeks. The ALT activity was significantly ($p<0.05$) lowered after 3 weeks of treatment with extract dose of 150mg/kg. It was also significantly ($p<0.05$) lowered after 6 weeks of treatment at all doses of POE, and reduced ALT activity was observed after 9 weeks of treatment with extract doses of 300 and 50mg/kg respectively. The AST levels were significantly ($p<0.05$) reduced after 6 weeks of treatment by extracts at 50 and 300mg/kg doses respectively. Diabetes has been indicated to cause pathological changes in the liver (Lucchesiet al., 2015). Alanine aminotransferase, aspartate amino transferase and alkaline phosphatase are biomarkers of hepatocyte injury and these enzymes are involved in various reactions in the liver. Hepatocyte injury has been revealed by the levels of AST and ALT in the plasma or serum. A high level of ALP indicates biliary tree obstructions (Lee et al., 2012). Haris (2005), in a clinical study reported that people suffering from type 2 diabetes mellitus show more liver function test irregularities when compared to the individuals that are normal. The reduction in the activities of these liver disease marker enzymes in the serum by *P.ostreatus*ethanol extracts suggests that they may be used to reverse the incidence of liver function test irregularities common in diabetic patients. The AST/ALT ratio is vital in medical diagnosis for elevated transaminases to differentiate between the causes of liver damage. An AST/ALT ratio equal to 1 may be sign of acute viral hepatitis or drug related liver toxicity while an AST/ALT ratio higher than 1 means that there is liver cirrhosis (Nyblom et al., 2006).

The mushroom extract at a dose of 150mg/kg b.w. was more effective in lowering ALP, AST and ALT levels compared to metformin hydrochloride (reference standard drug) after 3 weeks of treatment. The extract at a dose of 300mg/kg b.w. was less effective than the reference standard drug in lowering ALP and AST but the effect of the extract and the reference standard drug in lowering ALT level was comparable.

After 6weeks of treatment, the extract at a dose of 150mg/kg b.w. was more effective than the reference standard drug in lowering AST and ALT levels but the extract at 300mg/kg was less effective than the reference standard drug in lowering ALT level.

However, after 9 weeks of treatment, the extract at 300mg/kg b.w. was only more effective in lowering ALT level compared to the reference standard drug.

The reduction in the serum levels of these liver enzymes by the mushroom extract observed in this study suggests that they may be used in place of metformin hydrochloride to reverse the incidence of liver function test irregularities common in diabetic patients

Table 2: Effect of ethanol extract of the fruiting bodies of *Pleurotusostreatus* on the serum hepato-specific enzyme markers of HS-HFD-Streptozotocin induced diabetic rats after three weeks of treatment.

Treatment group	Magnitude			
	Alkaline phosphatase activity (U/L	**Aspartate transaminase activity (U/L)**	**Alanine transaminase(U/L)**	**AST:ALT ratio**
NC	90.47 ± 21.32^{a}	49.67 ± 2.52^{af}	11.67 ± 1.53^{a}	4.26±1.34
DC	209.67 ± 18.50^{b}	31.67 ± 3.79^{a}	10.00 ± 2.00^{ad}	3.17±2.11
D+POE_{50}	84.26 ± 8.65^{a}	67.33 ± 9.02^{bf}	16.33 ± 208^{b}	4.12±1.94
D+POE_{150}	49.43 ± 18.36^{ce}	$53/00\pm13.53_{cf}$	7.0 ± 1.00^{cd}	7.57±1.00
D+POE_{300}	108.16 ± 17.24^{a}	56.00 ± 20.00^{df}	10.00 ± 2.00^{ad}	5.6±2.35
D+MET_{150}	52.80 ± 2.69^{de}	54.00 ± 4.58^{ef}	10.00 ± 2.00^{ad}	5.4±2.35

Values are means ± SD, n=9per group. Values in the same column with different superscripts are significantly different at $p<0.05$. NC=normal control, DC=diabetic control, D+POE_{50}, D+POE_{150} , D+POE_{300} , D+MET_{150} are diabetic groups treated with *Pleurotusostreatus* extracts and metformin at different doses.

Table 3: Effect of ethanol extract of the fruiting bodies of Pleurotusostreatus on the serum hepato-specific enzyme markers of HS-HFD-Streptozotocin induced diabetic rats after six weeks of treatment.

Treatment group	Magnitude			
	Alkaline phosphatase activity (U/L	**Aspartate transaminase activity (U/L)**	**Alanine transaminase(U/L)**	**AST:ALT ratio**
N	92.23 ± 6.99^{a}	38.33±2.52	8.67 ± 1.15^{a}	4.4
D	94.10 ± 8.05^{a}	54.67±10.79	14.0 ± 3.61^{bd}	3.9
D+POE_{50}	99.60 ± 11.90^{af}	51.67±16.26	13.67 ± 1.53^{cd}	3.7
D+POE_{150}	101.53 ± 13.37^{ag}	43.67±8.02	8.67 ± 1.54^{a}	5.0
D+POE_{300}	99.50 ± 11.45^{ah}	51.67±4.73	11.00 ± 1.73^{ad}	4.6
D+MET_{150}	113.60 ± 11.43^{bfgh}	55.33±11.93	9.00 ± 2.65^{a}	6.1

Values are means ± SD, n=9, per group. Values in the same column with different superscripts are significantly different at $p<0.05$. NC=normal control, DC=diabetic control, D+POE_{50}, D+POE_{150} , D+POE_{300} , D+MET_{150} are diabetic groups treated with *Pleurotusostreatus* extracts and metformin at different doses.

Table3: Effect of ethanol extract of the fruiting bodies of *Pleurotusostreatus* on the serum hepato-specific enzyme markers of HS-HFD-streptozotocin induced diabetic rats after nine weeks of treatment.

Treatment group	Magnitude			
	Alkaline phosphatase activity (U/L	**Aspartate transaminase activity (U/L)**	**Alanine transaminase (U/L)**	**AST:ALT ratio**
N	100.37 ± 0.12^{a}	39.67 ± 1.53^{a}	10.67 ± 0.58^{a}	3.7
D	106.40 ± 11.86^{ac}	46.67 ± 5.88^{af}	12.67 ± 2.52^{ad}	3.6
D+POE_{50}	103.63 ± 16.13^{ad}	66.33 ± 10.97^{bg}	11.00 ± 1.00^{a}	6.0
D+POE_{150}	105.17 ± 4.56^{ae}	66.00 ± 2.65^{cg}	14.00 ± 1.73^{bde}	4.7
D+POE_{300}	120.43 ± 0.12^{bcdef}	59.20 ± 17.49^{dfg}	9.00 ± 1.00^{a}	6.6
D+MET_{150}	103.20 ± 12.73^{af}	72.67 ± 6.35^{eg}	16.33 ± 1.53^{ce}	4.4

Scientia Africana, Vol. 21 (No. 1), April, 2022. Pp 101-114 *https://dx.doi.org/10.4314/sa.v21i1.9*
© Faculty of Science, University of Port Harcourt, Printed in Nigeria *ISSN 1118 – 1931*

Values are means ± SD, n=9, per group. Values in the same column with different superscripts are significantly different at $p<0.05$. NC=normal control, DC=diabetic control, D+POE_{50}, D+POE_{150} , D+POE_{300} , D+MET_{150} are diabetic groups treated with *Pleurotusostreatus* extracts and metformin at different doses.

Histopathological changes of *P.ostreatus*ethanol extract in HS-HFD-streptozotocin induced diabetic rats were investigated as shown in the histologic section of the liver in plates 1-6. In diabetes mellitus, the liver has been a major organ of focus because of its critical role in carbohydrate and lipid metabolism as well as blood sugar regulation and detoxification functions. In some diabetic incidences, manifestations in the changes in the liver hepatocytes have been reported (Singh et al., 2017). The histologic section of the diabetic rat's revealed fatty liver and periportal inflammation compared to the normal control which showed normal histological features of the liver. Treated diabetic rats (POE_{50} group), (POE_{150} group) and the reference treatment group (MET_{150}) also manifested fatty change in hepatocytes and periportal inflammation. This may imply that the treatment at these dosages could not reverse these complications. Kumeet al., (1994) also reported the accumulation of fat into hepatocytes in streptozoticin induced diabetic mice. Fatty changes in hepatocytes were also reported by Noman (2009) in the work on histopathological liver changes in streptozoticin induced diabetic mice. However, an interesting finding in this study is that there was no obvious histologic change in the liver of diabetic rats treated with extracts at dosage level of 300mg/kgb.w. This clearly showed that the extract at this dose reversed to the control the fatty liver and periportal inflammation the liver caused by HS-HFD-streptozotocin induced diabetes. The reason for this hepatoprotective effect of the extract may be due to the pharmacological activities of this mushroom against insulin resistance and hyperlipidemia as a result of the presence of bioactive substances of medicinal value in the macro fungi such as the steroids. This study therefore has shown that *Pleurotusostreatus* extract may dose dependently act as a bio protective agent against HS-HFD-Streptozotocin induced hepatotoxicity alterations indicated in this study normal.

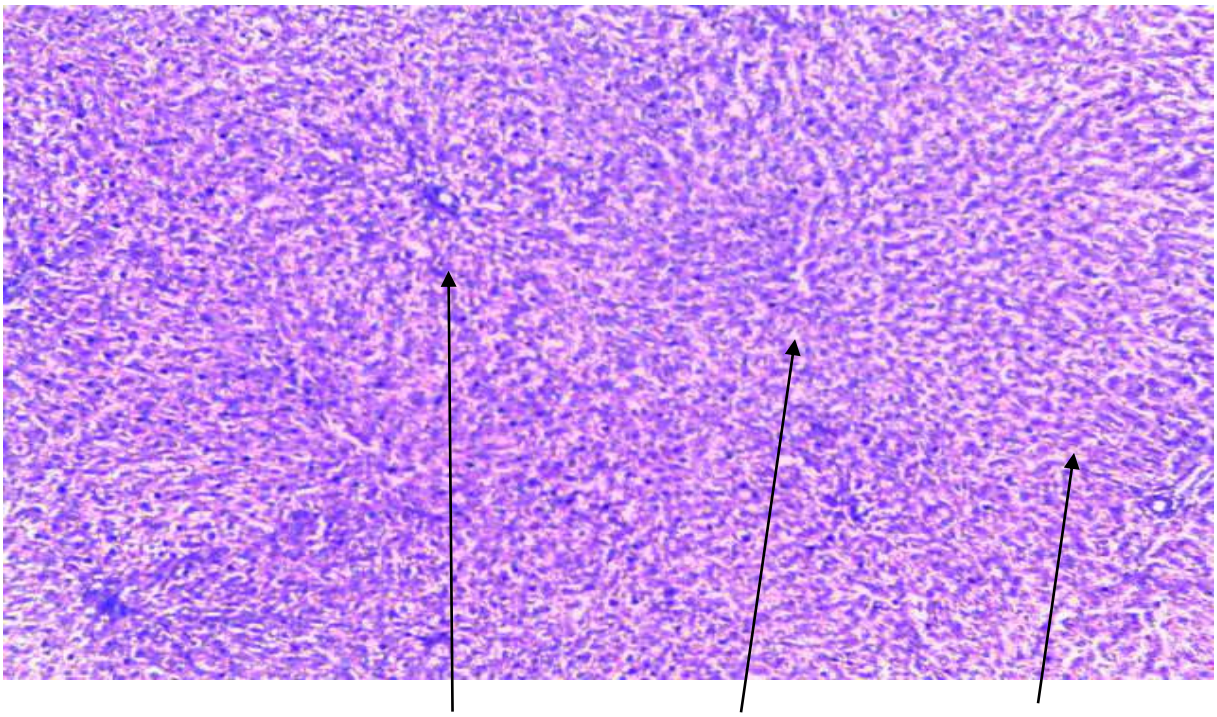

Group N Liver H&E X 200

Plate 1: Histologic section of the liver of normal rats showing normal histologic features.

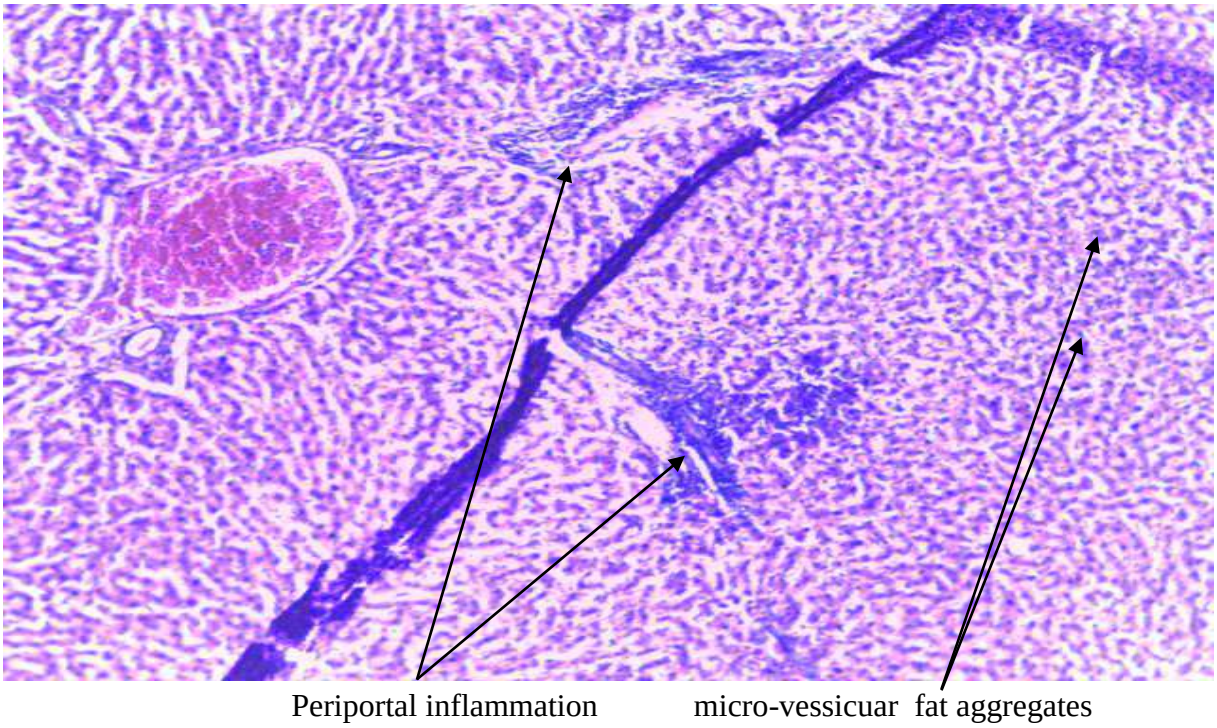

Group D Liver H &E X 400

Plate 2: Histologic section of the liver of diabetic rats showing inflammation and fatty change

Scientia Africana, Vol. 21 (No. 1), April, 2022. Pp 101-114 *https://dx.doi.org/10.4314/sa.v21i1.9*
© Faculty of Science, University of Port Harcourt, Printed in Nigeria *ISSN 1118 – 1931*

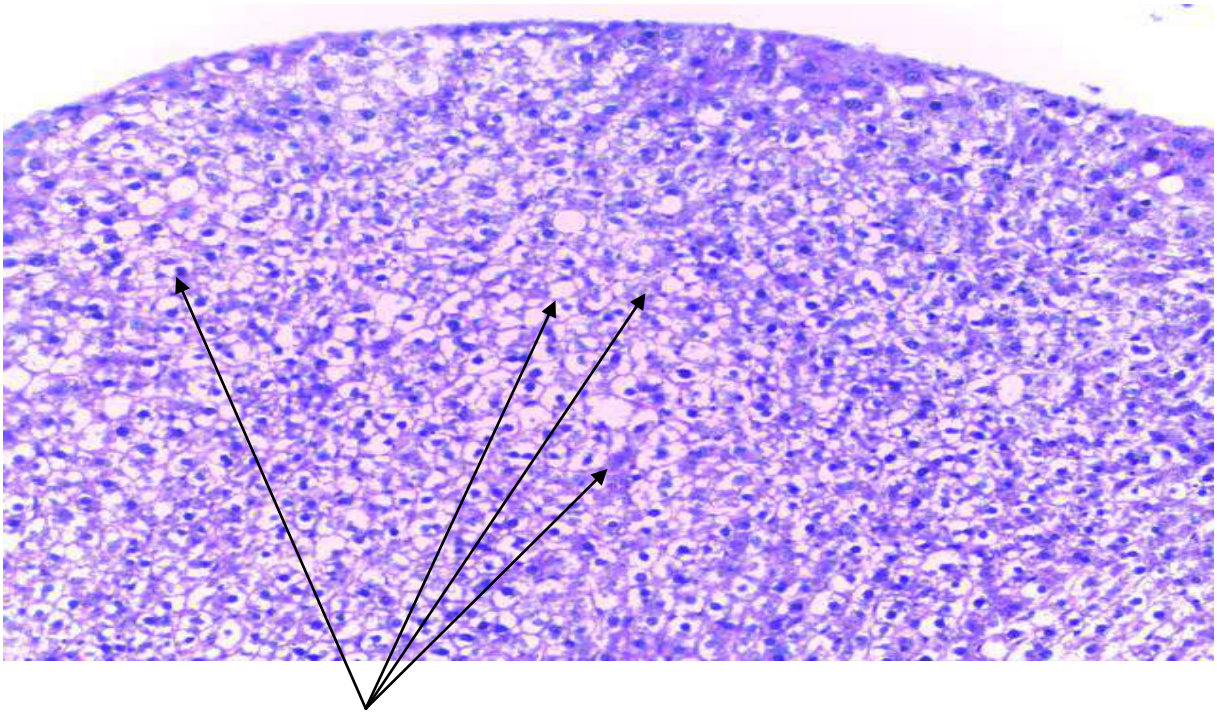

Fat vessicles

Group D+POE$_{50}$Liver H &E X 200

Plate3: Histologic section of the liver of diabetic rats treated with extracts at dosage of 50mg/kg indicating marked fatty change in hepatocytes

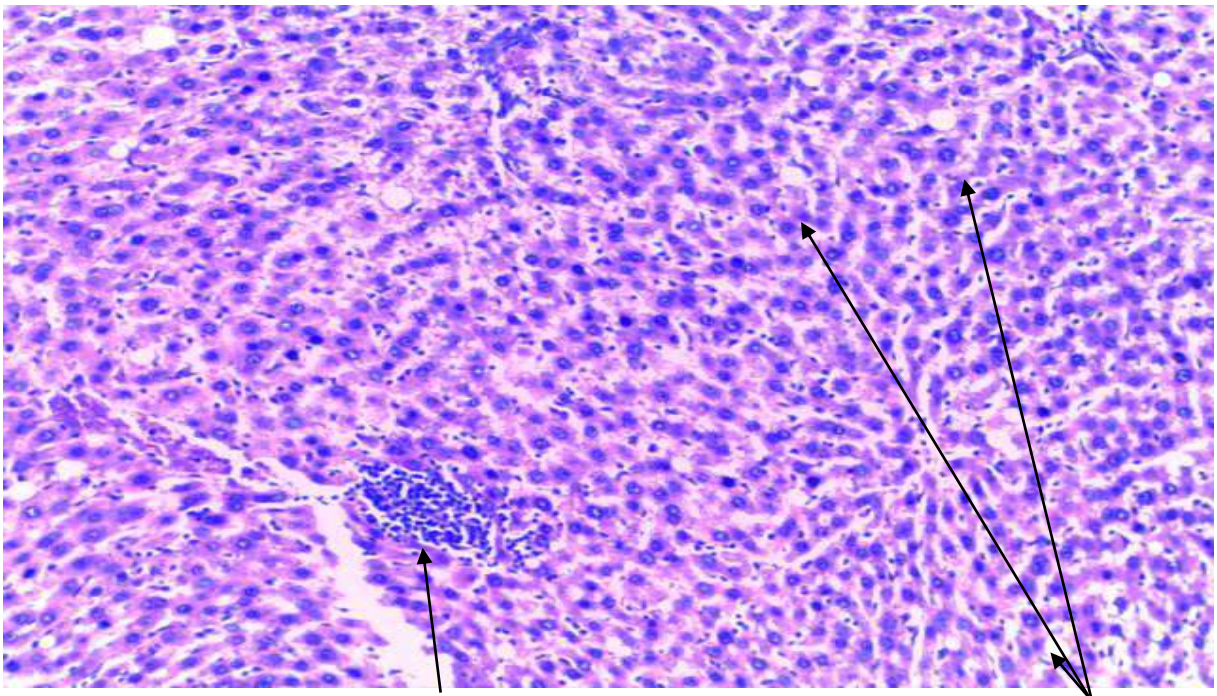

Inflammatory cells fat cells

Group D+POE$_{150}$ Liver H&E X 400

Plate4: Histologic section of the liver of diabetic rats treated with extracts at dosage of 150mg/kg showing fats cells and inflammatory cells within the liver parenchyma.

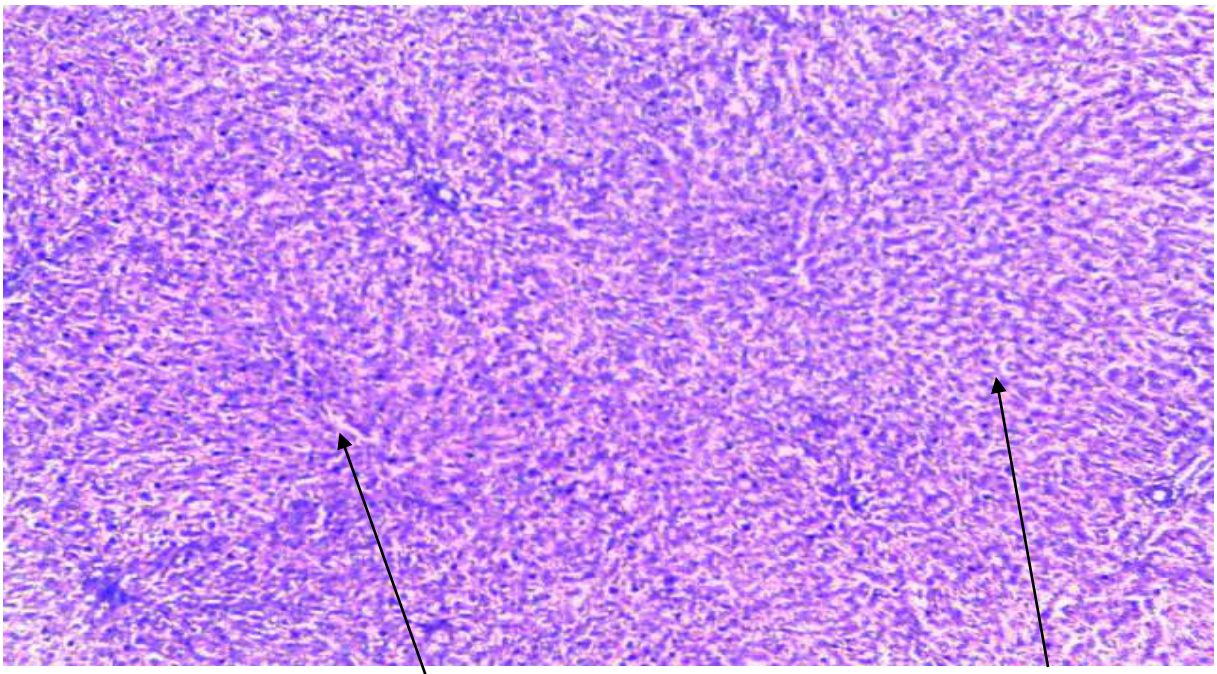

Group D+POE$_{300}$ Liver H &E X 200

Plate5: Histologic section of the liver of diabetic rats treated with extracts at dosage of 300mg/kg highlighting no obvious histologic changes.

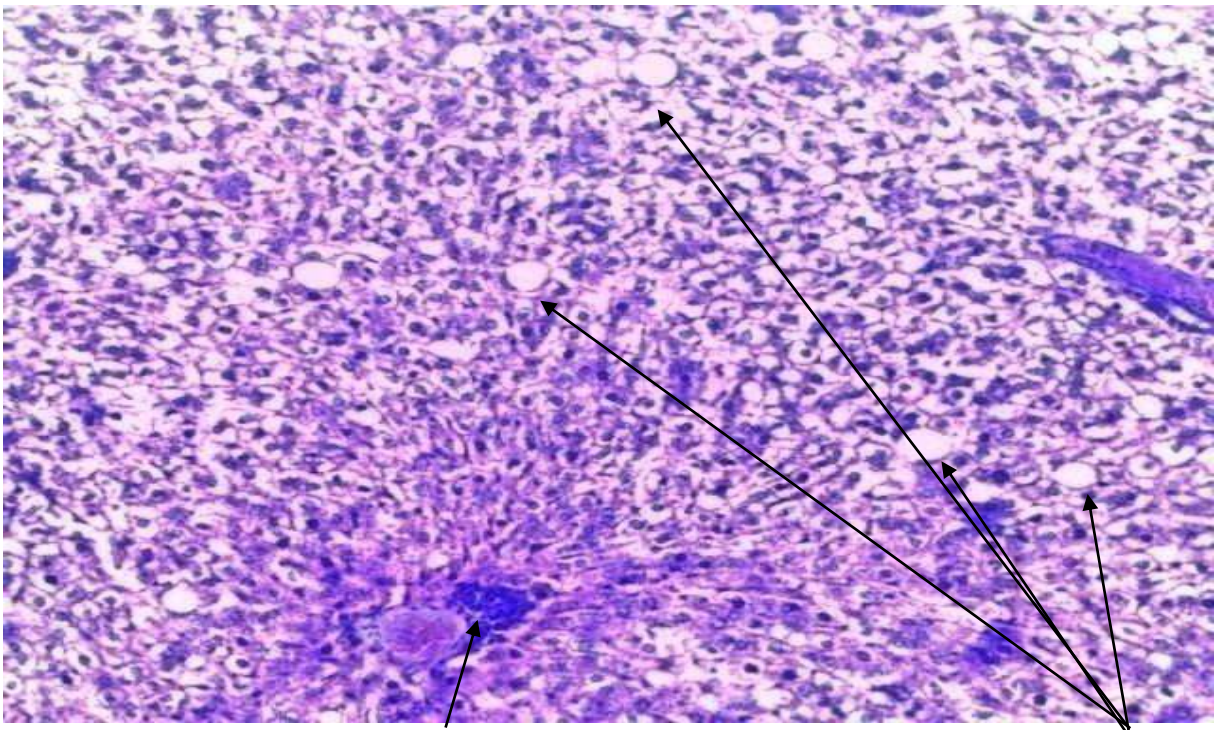

Group D+MET$_{150}$Liver H &E X 400

Plate6: Histologic section of the liver of diabetic rats treated with metformin HCl (150mg/kg) showing marked fatty change and periportal inflammation.

Scientia Africana, Vol. 21 (No. 1), April, 2022. Pp 101-114 *https://dx.doi.org/10.4314/sa.v21i1.9*
© Faculty of Science, University of Port Harcourt, Printed in Nigeria *ISSN 1118 – 1931*

CONCLUSION

The results in this study showed that ethanol extracts of P.ostreatus time and dose dependently caused a reduction in the serum levels of liver enzymes (ALP, ALT and AST) suggesting that they may be used to reverse the incidence of liver function test irregularities common in diabetic patients. The extracts reversed the fatty liver and periportal inflammation pathological insults on the liver caused by HS-HFD-Streptozotocin induced diabetes in the rats to normal, indicating dose dependent bio protective features of the extract against HS-HFD-Streptozotocin induced hepatotoxicity alterations. The results suggest that ethanol extract of organically cultivated *Pleurotusostreatus* may be employed in the management of liver diseases associated with diabetes mellitus.

Acknowledgements

The authors thank the Chancellor, Gregory University, Uturu, Abia State, Professor Gregory IykeIbe for building and equipping the Biochemistry Laboratory to standard for research. Authors are thankful to the Head and the entire Staff of Biochemistry research unit, Gregory University, Uturu, Abia State, Nigeria, for their immense support geared towards achieving this scholarly research work.

Competing Interests

The authors hereby declare that there was no conflict of interest or financial inducement which may have negatively influenced them in writing this scholarly article

Authors' Contributions

P.N.O. and S.C.O. designed the study, drafted the manuscript and carried out the experiments; K.O. collected resource materials and conducted statistical analysis; A.A.U and C.C.M supervised laboratory work, revised and edited the manuscript. The authors read and approved the manuscript.

REFERENCES

Akpaja, E. O., O. S., Isikhuemhen, O.S. & Okhuoya, J.A. (2003). Ethnomycology and usage of edible and medicinal mushrooms among the Igbo people of Nigeria. *International Journal of Medicinal Mushroom*: **14** (5) 313-319.

Bugianesi, E, McCullough, A.J.& Marchesini, G. (2005). Insulin resistance; A metabolic pathway to chronic liver disease. *Hepathology*. 42:987-1000.

FiniMundy, T. C., Gambato, & G. Fontana (2013) Aqueous extracts of lentinulaedodes and *Pleurotussajor-caju* exhibit high antioxidant capability and promising in vitro antitumor activity, *Nutrition Research*, **33** (1): 76-84.

Guven, A, Yavuz, O, Cam, M, Ercan, F, Bukan, N,&Comunoglu, C, et al. (2006). Effect of melatonin on streptozotocin-induced diabetic liver injury in rats.*ActaHistochemica*; 108;85-93

Hall, Ian, R. (April 2010). "Growing mushroom:L the commercial reality" (PDF). Lifestyle farmer. Auckland, New Zealand: Rural press: 42-45. Retrieved 26, January 2012.

Hamlton, H. K. (1987). Professional guide to diseases. An up to date

Encyclopedia of illness, disorders and their treatment, 2nd ed., spring House corporation book division, USA pp 691-715.

Harris, E. H. (2005). "Elavated liver function tests in type 2 diabetes," *Clinical Diabetes*, vol. 23, Hass, B, Ecksterin, N; Pfeifer, V; Mayer, P;

Jamaludin Mohamed, A.H. NazratunNafizah, A.H, Zariyantey, & S.B. Budin (2016).Mechanism of diabetes-induced liver damage: The role of oxidative stress and inflammation. Sultan *Qaboos University Medical Journal*. 16(2): e132-e141.

Kume, E., Ohmachi, Y. Hagaki, S. Tamura, K. &Dio, K. (1994): Hepatic changes of mice in subacute phase of streptozotocin induced diabetes. *Journal of Experimental and Toxicological Pathology*,46, 368-374.

Kuo, M. (2005, February). Pleurotusostreatus: The oyster mushroom. Retrieved from the mushroom expert. Come web site: http://www.mushroomexpert.com/pleurotusostreatus.html.

Lee I. M., Shiroma E. J. Lobelo F, Puska P, Blair S. N &Katzmarzyk P. T. (2012). "Effect of physical inactivity on major non-communicable diseases worldwide: an analysis of burden of disease and life expectancy" *The Lancet* 380(9838): 219-29.

Lee, T. H., Kim, W. R. &Poternucha, J. J. (2012). "Evaluation of evaluated liver enzymes".*Clinics in liver disease* 16(2): 183-198.

Levinthal, G.N., &Tavill, A.S. (1999).Liver disease and diabetes mellitus.Clinical Diabetes. ; 17:73

Longo, D.L., Fauci, A.S., Kasper, D.L., Hauser, S.L., Jameson, J.L. & Loscalzo, J. (2011). Harrisson's Principles of Internal Medicine. 18th ed. Vol.2. New York, USA: McGraw Hill.

Lucchesi, A.N., Cassettari, L.N., & Spadella, C.T.(2015) Alloxan-induced diabetescauses morphological an ultrastructural changes in rat liver that resemble the natural history of chronic fatty liver disease in humans. *Journal of Diabetes Research.* 2015:494578

Makropoulou, M., Aligiannis, N., Gonou-Zagou, Z., Pratsinis, H, Skaltsounis, A.L. &Fokialakis, N. (2012). Antioxidant and cytotoxic activity of the wild edible mushroom Gompliusclavatus. *Journal of Medicinal Food*, 15(2):216 -221.

Maria, E. V., Talia, &O'ctavio, P., (2014). Edible Mushrooms: Improving Human Health and Promoting Quality life. *International Journal of Microbiology*.Volume, 2015, Article ID 376387, 14 pages.

Mary, A.V., & Paul, L. (2016). Introduction: Global laws, Regulations, and Standards for Animal Research, *ILAR Journal*, 57(3): 261-265.

Mukhlif, Z.F., Rahim, S.M.&JumaaJamal M.N. (2020). The effect of diabetes on the Histological parameters in alloxan induced diabetes male rats.*Prensa Med Argent*, 106(6):264

Nanji, A. A., French, S. W & Freeman, J. B. (1986). Serum Alanine Aminotransferases, Ratio and Degree of fatty liver in morbidly obese patients, *Enzyme*, **36**: 266-269.

Norman, D.S.(2009). Histological liver changes in streptozotocin induced

Scientia Africana, Vol. 21 (No. 1), April, 2022. Pp 101-114 *https://dx.doi.org/10.4314/sa.v21i1.9*
© Faculty of Science, University of Port Harcourt, Printed in Nigeria *ISSN 1118 – 1931*

diabetic mice. *International Medical Journal Malaysia.* 8(1): 1-4

Norman, A. W. (2008). From Vitamin D to hormone D: fundamentals of the vitamin D endocrine system essential for good health. *The American Journal of ClinicalNutrition*, **88** (2): 4915-4995.

Nyblom, H., Bjornsson, E., Simren, M., Aldenborg, F. Almer, S. & Olsson, R.(2006).The ALT/AST ratio as an indicator of cirrhosis in patients with PBC. *Liver International* 26(7) :840 – 5

Okoroh, P.N., Sam Onuoha, A.A.Uwakwe & C.Y. Ukegbu (2021). Effect of ethanol extract of the fruiting bodies of Pleurotusostreatus on serum lipid profile and atherogenic indices of HFD-STZ induced diabetic rats. *Asian Journal of Research in Biochemistry*. 9(2):11-21

Palsamy, P., Sivakumar, S., & Subramanian, S. (2010). Resveratrol attenuates hyperglycemia-mediated oxidative stress, proinflammatory cytokines and protects hepatocytes ultrastructure in streptozotocin-nicotinamide-induced experimental diabetic rats. *Chemico- Biological Interactions* ; 186:200-10

Stamet, P. (2000). "Chapter 21: Growth parameters for gourmet and medicinal mushroom species" growing gourmet and medicinal mushroom = ShokuyooyobiyakuyoKinoko no sabia (3rded.) Berkeley, California, USA: Ten speed press, pp. 308-315 ISBN 978-1- 58008-175-7.

Singh, S., Osna, N.A., &Kharbanda, K.K.(2017). Treatment option for alcoholic and non alcoholic fatty liver disease: Are view. *World Journal of Gastroenterology*, 23 (36):6549-6570

World Health Organization (2016).Global report on diabetes. Pp. 26-27. ISBN 978-92-4-156525-7.

Scientia Africana, Vol. 21 (No. 1), April, 2022. Pp 115-122 *https://dx.doi.org/10.4314/sa.v21i1.10*
© Faculty of Science, University of Port Harcourt, Printed in Nigeria *ISSN 1118 – 1931*

COMMUNITY WASTE MANAGEMENT AND ITS HEALTH IMPACT ON OBALENDE AND LAFIAJI VILLAGES OF LAGOS ISLAND

Joseph, J.C[1], Udochukwu, U.[1*], Ehinmitan, E.[2], Omorodion, E.[3], and Tom-Otu, M.O.[1]
[1]*Department of Biosciences, Salem University Lokoja, Nigeria*
[2]*Department of Microbiology, Federal University of Agriculture Abeokuta*
[3]*Advanced Space Technology Labouratory, Obafemi Awolowo University, Ile-Ife, Osun State*
*E-mail: rev.dr.ud@gmail.com

Received: 27-10-2021
Accepted: 20-03-2022

ABSTRACT

Managing municipal solid waste in cities has become a serious challenge which could result in the accumulation of heavy metals in the environment. Against this background, the municipal solid waste management practices in peri-urban communities (Obalende and Lafiaji Village) of Lagos Island and the impact of heavy metals in soil were studied. This study aims at examining the present municipal waste management practices in Lagos Islandandhowthey can beimproved upon. Random sampling was used to administer 100 questionnaires to household while the different heavy metal concentrations in the soil samples were determined using Buck 200 Atomic Absorption Spectrophotometer (AAS). About 58 % of the respondents are aware of solid waste management while LAWMA (50%) and Cart pushers (40%) were the two main options for waste disposal. The wastes were mainly composed of food wastes, plastics/pet bottles and nylon. Although majority of the respondents (67%) have a waste bin/bag assigned to their houses, about 74% do not sort their wastes. The concentrations of the heavy metals (Co, Zn, Ni, and Mn) in the soil samples were higher in Obalende and Lafiaji village, where wastes were dumped indiscriminately on roadsides. SWOT analysis revealed the need for improving environmental awareness in order to minimize the threat of low sorting of wastes. Also, opportunities exist for recycling plastics/pet bottles and nylon while wastes from food materials could benefit agriculture through composing. This study suggests that more environmental awareness, policies and better administration are needed to improve the status of waste management in peri-urban communities of Lagos Island.

Keywords: Peri-Urban Communities, Waste Management, Heavy Metals, Health Impact, Lagos

INTRODUCTION

The increase disposal of solid waste in our environment has become a challenge in today's waste management programme. This is mainly due to the increasing generation of such solid waste and the burden posed on the municipal budget. In addition to the high costs, the solid waste management is associated with lack of understanding of different factors that affect waste management system (Dasgupta, 2013). Municipal solid waste management is an important issue in today's world as it deals with budget allocations of local municipality, public acceptance and adverse impacts on environment (Ramakrishna, 2013). In developing countries, a waste management system encompasses planning,

engineering, organization, administration, financial and legal aspects of activities associated with generation, growth, storage, collection, transport, processing and disposal in an environmentally compatible manner adopting principles of economy and aesthetics (Dasgupta, 2013). Lagos is experiencing rapid urbanization. This rapid increase in population leads to rapid industrialization, urbanization and economic growth, which are the main factors of increased solid waste generation worldwide (Bandara, 2013). The waste generated by urban residents is expected to get almost doubled from 3.5 million metric tons/day in 2002 to 6.1 million metric tons/day in 2025, and a total of $375 billion will be spent for its management in 2025 (Sawyer *et al.,* 2003). It has been a local government responsibility to provide the service of urban solid waste management. In developing countries, government makes budgets for solid waste management; however only small percent of the waste is managed (Simon, 2008). Therefore, management procedures of municipal waste in many developing countries are rather chaotic and need to be analysed and strengthened further (Bandara, 2013; Udochukwu *et al.,* 2017b).

Municipal solid wastes of developing countries often contains the wastes that is produced from residential and industrial (non-processed wastes), commercial and institutional sources with the exception of hazardous (which include medical, mineral and radioactive wastes) and universal wastes, construction and demolition wastes, and liquid wastes such as water, waste water, industrial processes (Tchobanoglous *et al.,* 2002). Furthermore, market wastes, yard wastes, street sweepings and few cases of liquid wastes as sewage sludge are also added to municipal solid waste categories (Simon, 2008). The composition of municipal solid waste is higher in most of its characteristics when compared to that of developed countries with respect to density, moisture content, organic matter and dust (Blight and Mbande, 1996). The local authorities are responsible for urban waste management in Lagos city and practice several methods of disposal such as open dumping, composting, land filling, incineration, direct and indirect recycling. However, due to some limitations such as high operation and management cost, poor understanding of the process, economically viable, environmentally friendly and socially acceptable methods are limited in use. Therefore, it appears that most of the waste disposal practices can adversely affect the environment, such as open dumping on land and water bodies, direct combustion and so forth. These poor methods leads to several environmental crises such as contamination of surface and groundwater, soil and air pollution and heavy metal contamination in particular (Sawyer *et al*., 2003; Udochukwu *et al*., 2017c).

Heavy metals are found in electrical wastes, municipal solid and from degradation of organic wastes (Esarru *et al*., 2003). They can also be found in the disposal of household wastes, hazardous wastes, non-hazardous industrial wastes and other chemical by products (Marine *et al*., 2005). Several studies have showed that collection, storage, transportation and final disposal of solid wastes are a major problem in urban cities and areas (Okot-okumu and Nyenje, 2011). Cities in East and North Africa as well as most

Scientia Africana, Vol. 21 (No. 1), April, 2022. Pp 115-122 *https://dx.doi.org/10.4314/sa.v21i1.10*
© Faculty of Science, University of Port Harcourt, Printed in Nigeria *ISSN 1118 – 1931*

developing countries are also facing the same problems. The main reason of these problems is attributed to the poor economy of these areas which accounts for the low achievement in solid waste management (Okot-okumu and Nyenje, 2011). Heavy metals are often referred to as trace metals, occurring naturally in low concentrations in organisms. They are not biodegradable and do not undergo ecological cycling (Duribe *et al*., 2007). Some metals are essential to life but they are toxic at thigh level of dose (Ukpebor and Unigbe, 2003). The accumulations of heavy metals in soil have since become a threat to vegetation and animals which ultimately affect the quality of human life through the food chain. This study focused on the community waste management and its health impact on Obalende and Lafiaji villages of Lagos Island. The major objective of this study is to investigate the existing municipal solid waste management practices in Lagos Islandandtorecognizefactors that areliableforineffectivemanagement.

MATERIALS AND METHODS

Study Area

The study area covered two (2) Wards in the Local Government Area of the State.

Ijeh in Obalende: and Lafiaji Village in Ilado/Eti-osa.

Study Approach

Data were collected through soil analysis and structural questionnaire. A sample size of 100 respondents for the questionnaires and two (2) composite soil samples were collected from each of the two sampling locations.

Questionnaire

Primary data sources were utilized to examine the waste management system in Lagos urban and suburb. The research design used for the questionnaire consisted mainly of two parts. In the first part, a group of research questions were formulated aiming at diagnosing the strengths, weaknesses, opportunities and threats of urban and suburb waste management in Lagos State. Second, a detailed SWOT analysis was performed based on the research questions developed. Answers to those questions were abstracted by analysing information obtained from questionnaires distributed randomly among residents of the sampled locations.

Soil Sample Collections

The survey carried took into consideration population, types of income and types of houses. The questionnaires were distributed randomly in the selected locations in Eti-Osa Local Government Area. A total of two (2) Soil samples were also collected in polyethene bags, carefully labelled according to the sampled area and taken to the laboratory in iceberg for soil physico-chemical and heavy metal analysis. The Ph, electrical conductivity, Lead, Cobalt, Copper, Zinc, Iron, Cadmuim, Nickel and Manganese were analysed (Udochuku *et al.*, 2017a)

Statistical Analysis

Analysis of variance (ANOVA) for completely randomised design was used to test the difference between the treatments. Means of significant differences were separated using Duncan's new multiple-range test. Differences were considered statistically significant at a P-value of <0.05. All statistical analysis was carried

out on SPSS version 23.0, IBM, USA. The data collected through the questionnaires was analysed using statistical methods such as simple percentages, charts (bar charts and pie charts). The simple percentages were computed using the equation:

$X/Y \times 100\%$

Where X= Number of observations

Y= Total population

100%= Total percentage

RESULTS

Table1: Soilpropertiesand heavy metalconcentrations insoil

Parameters	Ijeh	Lafiajivillage	Control
pH	7.850 ±0.05bc	7.400 ±0.10a	7.900±0.00bc
EC (µScm^{-1})	197.000±3.00d	584.500±4.50e	87.000±1.00a
Pb(mg/kg)	0.017 ±0.00c	0.033 ±0.00d	0.007 ±0.00a
Co(mg/kg)	0.050 ±0.04a	0.011 ±0.00a	0.005 ±0.00a
Cu (mg/kg)	5.442 ±0.00d	5.635 ±0.00e	2.926 ±0.01a
Zn (mg/kg)	7.517 ±0.00e	6.967 ±0.03d	3.745 ±0.05a
Fe(mg/kg)	49.022 ±0.01c	66.846 ±0.13e	20.151±0.01a
Cd (mg/kg)	ND	ND	ND
Ni(mg/kg)	0.036 ±0.00b	0.017 ±0.01a	0.015 ±0.00a
Mn(mg/kg)	0.034 ±0.00d	0.013 ±0.00bc	0.008 ±0.00a

ND-NOTDETECTED

Table 2: Percentage respondents by sex

Sex	Percentage
Male	58%
Female	42%

Table 3: Percentage respondent by age

Age group	Percentage
18-28	43%
29-39	36%
40-40	16%
51-61	1%
62 and above	3%

Table 4: Respondents by Family Size

Family size	Percentage
Living alone	9%
1 to 2	27%
3 to 5	43%
Above 5	20%

Table 5: Respondents Awareness of Waste Management

Have you ever heard of solid waste management?	
YES	58%
NO	42%
If YES, in what way?	
In School	27%
On Television	31%
In Public meeting	24%
On Radio	18%

Table 6: Type of Waste Generated

Types of Waste	Percentage
Nylon	24%
Paper/cardboard	8%
Metal/Aluminum	3%

Scientia Africana, Vol. 21 (No. 1), April, 2022. Pp 115-122 *https://dx.doi.org/10.4314/sa.v21i1.10*
© Faculty of Science, University of Port Harcourt, Printed in Nigeria *ISSN 1118 – 1931*

Plastics/pet bottles	30%
Food waste	34%
Others	1%

Table 7: House Hold with Waste Container

Responds	Percentage
YES	67%
NO	33%

Table 8: Respondents That Sort Their Waste

Responds	Percentage
YES	36.14%
NO	73.86%

DISCUSSION

The results of the physico-chemical analysis showed that the soil samples across the locations were slightly alkaline while the range of EC was much larger (Table 1). Increased EC has been associated with polluted soils andcompounds or elements such as nitrates, potassium, sodium, chloride, sulfate and ammonia (Zhang *et al.*, 2018). Higher EC in soil samples from rural communities as oppose to the urbancommunities suggest higher concentration of pollutants in the former. These pollutants mayinclude heavy metals. This conforms to the report of Iranpour et al. (2014) that heavy metalpollutioninsoilsisusually associatedwith higherelectricalconductivity. The highest concentration of most of the heavy metals was observed in Obalende.These were Co, Zn, Ni and Mn whileLafiajivillagehadthehighestlevelofCu andFe.This buttress theimproper waste management system observed in Lafiaji village, in which wastes aredumped indiscriminately on roadsides.

Heavy metal concentrations from the results were generally lower than permissible limits set by the European Union (EU) and United Nations Environment Programme (UNEP) for agricultural soils (David *et al.*, 2019). These limits are Fe 50,000mg/kg, Mn 2000mg/kg, Pb 100mg/kg, Zn 300mg/kg, Cd 3mg/kg, Co 50mg/kg, Cr 100mg/kg, Mn 50mg/kg. The concentrations of Pb varied between 0.01 and 0.04mg/kg while the range of values for Fe was 20.14 – 66.98 mg/kg. Both were lower than the permissible limits of 1.60 and 400 mg/kg recommended for soil by FEPA (1997). Also, the range of Cu and Ni, 2.92-5.64 and 0.01-0.04 respectively were lower than the limits of 10.10 mg/kg and 35 mg/kg, respectively (FEPA, 1999). The fact that cadmium was undetected in the soil samples also implies that it's muchlowerthanthe0.80mg/kglimitsetbyFEPA for Nigerian soil (FEPA, 1999). Compared to heavy metals concentration in soils from Odo-oba in Ogbomosho, (Adagunodo*et al.*, 2018), and electronic waste site (Jiang *et al.*, 2019), the levels of heavy metals in this study was much lower. However, there port in this study was similar to that of school playgrounds in Port Harcourt Metropolis, Rivers State (Okereke and Amadi, 2017). Cadmium is usually present in high concentration in soil ecosystems polluted with wastes from metal and mining industry (Šrut *et al.*, 2019). The undetectable level of Cd in the soil may be attributed to the area of sampling which were not close to mining industries or farmlands. The significantly

higher levels of Cu, Zn, Fe, Mn indicates additional source of the metallate in the studied soil which must have accumulated over time (Udochukwu *et al*., 2016a).

A total of 100 questionnaires were administered and 88 was recovered which amount to 88 %of the sampled population. The respondents consist of 58 % female and 42 % male which shows that women participate more in the study. The study also discovered that married people, between the age range of 18-50, educated and employed, living in either a two bedroom flat or in a self-contained apartment with the average household size of 3-5 persons generates more waste and the sampled population included all formal and non-formal residences in the sampled locations without distinction. Many socio-economic and other variables influence the rate ofwaste generation however, in this study; we assumed that all sections of different incomegroups havebeen covered during therandomsampling. The results in (Table 5) shows that 58% oftherespondents are aware of solid wastemanagement and they got to know about it either in school, on television, in public meetingsand on radio. Rahji and Oloruntoba, (2009), suggested that increasing the awareness of thepeoplemay haveapositiveimpactontheir attitudetowards theenvironment. From the study in (Table 6), it was discovered that food waste, plastic/pet bottles and nylonare mostly generated by the respondents and this was in line with Ogwueleka (2009), whoreported that solid waste in Nigeria are more corrosive, weighty and are saturated with waterthan those in industrialized nations, hence, a different solid waste management approach isrequired while Imam *et al* (2008) argues that since the waste composition in Abuja shows that a large percentage of the waste generated are organic in nature, compaction trucks may not be appropriatefor their disposal. The study also showed in (Table 7) that majority of the respondents (67 %) have a wastebin/bag assigned to their houses where they dump their waste and this implies that majority ofthem in the studied locations dispose their waste lawfully while minority dispose their waste unlawfully either on the roadside, gutter/canal or other illegal methods, a habit which will eventually results in health hazards in the sampled locations overtime.

CONCLUSION

Waste management requiresthe contributions from government, businessmen, politicians, religious organizations, civil servants and the public at large. All these must be brought together by government policy and legislation to work together to tacklewaste problems. Thus, to ensure the sustainability of Lagos state and other cities in Nigeria, there is a need for an effective solid waste management policy with a comprehensive and coordinated planning which will be combined withadequate legislation, fiscal provision, public involvement and awareness to bringabout the expected improvement in the quality of our urban space.

REFERENCES

Adagunodo, T.A., Sunmonu, L.A., Emetere, M.E. (2018). Heavy metals' data in soils foragriculturalactivities. *Datain Brief*. 18,1847–1855.

Bandara N. J. G. J. (2008). Municipal solid waste management - The Sri Lankan case. In Proceedings of the

Scientia Africana, Vol. 21 (No. 1), April, 2022. Pp 115-122 *https://dx.doi.org/10.4314/sa.v21i1.10*
© Faculty of Science, University of Port Harcourt, Printed in Nigeria *ISSN 1118 – 1931*

Conference on Developments in Forestry and Environment Management in Sri Lanka, Colombo, Sri Lanka.

Blight G.E, Mbande C.M. (1996). Some problems of waste management in developing countries. *Journal of Solid Waste Technology and Management*. 23(1):19-27.

Dasgupta, T.(2013). Sustainable municipal solid waste management of Bhopalcity. *International Journal of Scientific Engineering and Technology*. 2(11):1103-1106.

David, E., Eleazu, C., Igweibor, N., Ugwu, C., Enwefa, G., Nwigboji, N., (2019). Comparative study on the nutrients, heavy metals and pesticide composition of some locally produced and marketed rice varieties in Nigeria. *Food Chemistry*. 278,617–624.

Duribe, J. O., Wuegbuand, M. O. C and Gwurugw, J. N. (2007). Heavy metal pollution and human *biotoxic Effects, physics*. 2.P111-119.

Esarru, S., Polonivelu and Kuri, J. (2003). Assessment of Heavy metals in municipal solidwasteDumpsite. *Work on landfill management*. P139-145.

Federal Environmental Protection Agency (FEPA)(1997).Guidelines and standard for environmental impact assessment in Nigeria.pp. 87–95.

Federal Environmental Protection Agency (FEPA) (1999). National Guidelines and Standards for Soil Quality in Nigeria. FEPA, Rivers State Ministry of Environment and Natural Resources, PortHarcourt.

Henry, R.K. Youngsheng, Z. and Jun, D. (2006). Municipal solidwaste management challenges in developing countries–Kenyancasestudy.*WasteManagemen.* 26,92-100.

Imam, A., Mohammed, B., Wilson, D.C., Cheeseman, C.R.(2008). Solid Waste ManagementinAbuja, Nigeria. *WasteManagement*. 28, 468–472.

Iranpour, I, lakzian, A. and Khorasani, R. (2014). Effects of Cadmium and Organic Matter on Soil pH, Electrical Conductivity and their Roles in Cadmium Availability in Soil. *Journal of Middle East Applied Science and Technology*. 18 643-646.

Jiang,B.,Adebayo,A.,Jia,J.,Xing,Y.,Deng,S.,Guo,L.,Liang,Y.,Zhang,D. (2019). Impacts of heavy metals and soil properties at a Nigeriane-waste site on soil microbial community.*Journal of Hazardous Materials.*362, 187–195.

Marine, W. L., B, Gabrial land T.T, mathy, (2005). Heavy metals binding of municipal solid wasteland Fill Leachates, *Chemo. Phe*. 60, P260-215.

Ogwueleka, T. (2009). Municipal Solid Waste Characteristics and Management in Nigeria.

Okereke, C.J., Amadi, P.U. (2017). Accumulation and risk assessment of heavy metal contentsin school playgrounds in Port Harcourt Metropolis, Rivers State, Nigeria. *Journal of Chemical Health and Safety*. 24, 11–22.

Okot-Okumu, J,R. Nyenje, (2011). Habitat International. 35,537–543.

Rahji, M. A. Y., Oloruntoba, E.O. (2009). Determinants of Households' Willingness-To-Payfor Private Solid Waste Management Services in Ibadan, Nigeria. *Waste Managementand Research, the journal of international solid waste*

and Public Cleansing Association Iswa. 27(10), 961–965.

Ramakrishna V. (2013). Lifecycle assessment model for integrated solidwaste management.

Sawyer NC, McCarty LP, Parkin FG. (2003). Chemistry for environmental engineering and science. *Ser. Knowl. Pap*. No.15.World Bank,p.116.

Simon AM. (2008). Analysis of activities of community based organizations involved in solid waste management. Investigating Modernized Mixtures Approach: The case of Kinondoni Municipality, Dares Salaam, Tanzania [M.Sc.thesis], Wageningen University and Research Centre, Wageningen, Netherlands;2008.

Šrut,M.,Menke,S.,Höckner,M.,Sommer,S. (2019). Earthworms and cadmium–Heavymetal resistant gut bacteria as indicators for heavy metal pollution in soils? *Ecotoxicology and Environmental Safety*. 171, 843–853.

Tchobanoglous G, KreithF. (2002). Handbook of solid waste management. McGraw-Hill, New York, United States.

Udochukwu, U, Ehinmitan, E. and Dave-Omoregie, A. O. (2016b). Microbial Waste Conversion and Comparative Biogas production from the Rumen Content of Cow and the Intestinal Waste content of Pigs. *Nigerian Journal of Microbiology*. 30(2): 3395-3340.

Udochukwu, U., Atuanya, E.I. and Abidemi, J. M. (2017a). Ecotoxicological Effects of Plastic Enriched Composting Waste on Soil Biological Sentinels. *Nigerian Journal of Scientific Research.* 16(1): pp 34-40.

Udochukwu, U., Atuanya, E.I. and Abidemi, J. M. (2017b). Ecotoxicological Effects of Plastic-Enriched Composting Waste on Soil Biological Sentinels. *Nigerian Journal of Scientific Research.* 16(1): pp 34-40.

Udochukwu, U., C.C. Chikere and P. G. Olannye (2017c). Comparative Biosurfactant Production by Actinomycetes Isolated from Hydrocarbon Contaminated Soil, Plastic Enriched Composting Waste and Ikpoba River Sediment in Benin City. *Nigerian Journal of Microbiology*. 31:3859-3866

Udochukwu, U., Inetianbor J., Omorotionmwan F.O., and Okpuruka N.S. (2016a). "Quality of Restaurants in Lokoja Metropolis and Its Public Health Impact." *American Journal of Microbiological Research*. 4(2): 51-55. doi: 10.12691/ajmr-4-2-1.

Ukpebor, E.C,C.A.Unigbe, (2003).Heavy metals Concentration in the Sub Solid refusedumpsites in Benicity, *Ghas.sci.* 43, P9-15.

Zhang L., Zhu G., Ge X., Xu, G. and Guan, Y. (2018). Novel insights into heavy metalpollution of farmland based on reactive heavy metals (RHMs): Pollution characteristics,predictive models, and quantitative source apportionment. *Journal of Hazardous Materials*,360:32–42.

Scientia Africana, Vol. 21 (No. 1), April, 2022. Pp 123-132 *https://dx.doi.org/10.4314/sa.v21i1.11*
© Faculty of Science, University of Port Harcourt, Printed in Nigeria *ISSN 1118 – 1931*

PETROPHYSICAL EVALUATION FOR DEVELOPMENT OF A MARGINAL OIL FIELD IN THE ONSHORE NIGER DELTA, NIGERIA

***Ugwu, U P., Okengwu, K O. and Jones, A. E.**
Department of Geology, University of Port Harcourt.
*Corresponding author; e-mail- ugwuudoka@yahoo.com

Received: 22-11-2021
Accepted: 20-03-2022

ABSTRACT

Petrophysical evaluation was conducted on an onshore marginal field in Niger Delta with the aim of evaluating the rock and fluid properties to boost hydrocarbon production in the field. Five well logs suite from five wells and core log data for two wells were utilized for this study. Petrophysical properties evaluated included; porosity, net to gross, formation factor, irreducible water saturation, permeability, water saturation, hydrocarbon saturation and pay thickness. The well logs suite contained the following logs: Gamma ray log for lithology identification; Resistivity log for fluid type discrimination and determination of water saturation; Density log for porosity determination; and Neutron log in combination with density log for hydrocarbon types. A total of seven reservoir sands (, Sand A, B, C, D, E, F and G) were identified and correlated across all five wells on the basis of gamma ray and resistivity log motifs. The reservoir gross thicknesses ranged from 62.55 to 228.50 ft, shale volume from 7.0 to 24.60%, net to gross from 0.76 to 0.93%, effective porosity from 20.78 to 26.22%, water saturation from 35.80 to 62.30% and permeability ranged from 545.94 to 2821.97 mD. This shows that the reservoirs are of good quality for hydrocarbon productionacross the field.

Keywords: Petrophysics, Shale Volume,Porosity, Permeability, Reservoir,Well Logs, Hydrocarbon

INTRODUCTION

A reservoir is one which by virtue of its porosity and permeability is capable of containing a reasonable quantity of hydrocarbon if entrapment conditions are right, and can also release hydrocarbon at a satisfactory rate when the reservoir is penetrated by a well (Etu-Efeotor, 1997).

Reservoir quality analysis is the application of available data in the description of the reservoir in terms of its cleanliness (shale volume), amount of fluid it can hold (porosity) and produce (permeability), fluid saturation (oil, gas, water), net-to-gross, etc. Reservoir quality assessment at the well scale is often accomplished through petrophysics.

Petrophysics is the study of the physical and chemical properties of rocks and their contained fluids (Canon, 2017). Defining petrophysical properties such as permeability, fluid saturation, areal extent, thickness of reservoir and porosity is very vital to the oil and gas industry. Majority of hydrocarbons produced in the Niger Delta is gotten from the accumulations in the pores of porous and permeable rock bodies. These ‘spaces’ are a function of the porosity of the rock which is a very important petrophysical parameter. Fluid saturation is how much of oil, water or gas

is present in the pore spaces of the rock and is very essential to determine the distribution of fluids in the reservoir (Darling, 2005).

The porosity along with hydrocarbon saturation determines the quantity of hydrocarbon reserves enclosed in the reservoir. Thickness is also a significant petrophysical parameter in the estimation of hydrocarbon volume. In some reservoirs, the thickness of some rock beds such as shale which has almost no recoverable oil due to their low permeability must be calculated and removed from the gross thickness to get the thickness of the productive beds (Canon, 2017). Areal extent is also required in the estimation of hydrocarbon volume. It is considered as the areal extent of the reservoir and it is determined from seismic. All these show that the determination of these petrophysical parameters is a crucial process in the evaluation of hydrocarbon volume. These properties depend on a host of other properties such as the mineralogy of the rock, pore size and the nature of the fluid itself.

The objectives of the research include: the evaluation of the petrophysical properties of reservoirs in UPX field and the identification of fluid types and their saturations levels within the hydrocarbon bearing reservoirs.

The well data utilized for this study includes well header, well deviation, well logs (gamma ray, resistivity, neutron and density logs). Well headers were used to define the locations of the wells. Well Deviations were used to show the trajectory of the individual wells. Gamma ray log was used for lithology identification and correlation as well as estimating shale volume. Resistivity log was used for fluid discrimination and estimating water and hydrocarbon saturation. Density log was used for total porosity estimation. Total porosity and shale volume were used for estimating effective porosity. Permeability was calculated using water saturation, effective porosity, formation factor and irreducible water saturation. Density and Neutron logs were used in combination for discriminating between types of hydrocarbons. The software utilized for visualization and interpretation is Schlumberger Techlog.

Scientia Africana, Vol. 21 (No. 1), April, 2022. Pp 123-132 *https://dx.doi.org/10.4314/sa.v21i1.11*
© Faculty of Science, University of Port Harcourt, Printed in Nigeria *ISSN 1118 – 1931*

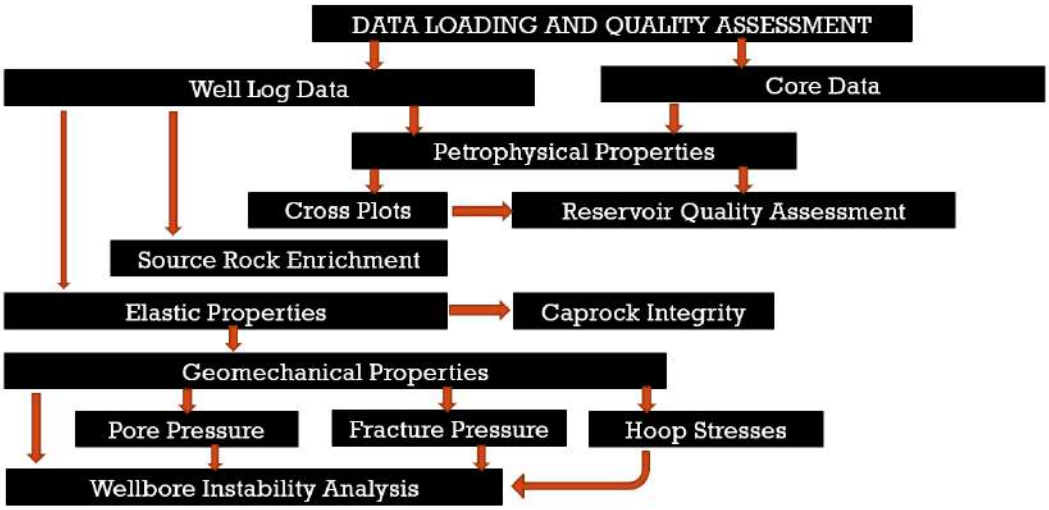

Figure 1: Methodology Flowchart adopted for formation evaluation in UPX Field

Petrophysical Analysis

Four main petrophysical parameters are important in defining any reservoir quality, which include: shale volume (Larinov, 1969), total and effective porosity (Dresser Atlas, 1979), Net to Gross (NTG), permeability (Owolabi et al., 1994) and water saturation (S_w). Various equations applicable to the Niger Delta formations were utilized for their computation and are presented as follows;

$$Vsh = 0.083 \times (2^{(3.7 \times GR_{index})} - 1) \quad (1)$$

$$GR_{index} = \frac{GR_{log} - GR_{min}}{GR_{max} - GR_{min}} \quad (2)$$

$$\Phi t = \frac{\rho_{ma} - \rho_{log}}{\rho_{ma} - \rho_{fl}} \quad (3)$$

$$\emptyset_E = (1 - Vsh) \times \emptyset_T \quad (4)$$

$$Net - to - gross = \frac{NH}{GH} \quad (5)$$

$$S_w = \sqrt{\frac{R_o}{R_t}} \quad (6)$$

$$K(mD) = 307 + 26552(\emptyset_e^2) - 34540\ (\emptyset_e \times S_{wirr})^2 \quad (7)$$

$$S_{wirr} = \left[\frac{F}{2000}\right]^{1/2} \quad (8)$$

$$F = \frac{0.62}{\emptyset^{2.15}} \quad (9)$$

$GR_{log} = GR log reading of formation$

$GR_{min} = GR sand baseline$

$GR_{max} = GR\ shale\ baseline$

$\rho ma = density\ of\ the\ rock\ matrix$

$Density\ of\ sand = (2.65g/cm^2)$

$\rho log = \ formation\ bulk\ density\ from\ log$

$\rho fl = \ Density\ of\ contained\ fluid$

$\emptyset_E \ = \ Effective\ porosity$

$\emptyset_T = \ Total\ Porosity$

$Vsh \ = \ Volume\ of\ shale$

$NH = Net\ thickness$

$GH = Gross\ thickness$

$S_w = water\ saturation$

$R_o = Resistivity\ of\ the\ oil\ leg$

$R_t = True\ resistivity\ reading$

$K(mD) = permeability\ in\ milliDarcy$

$S_{wirr} = irreducibe\ water\ saturation$

$F \ = \ Formation\ Factor$

RESULTS AND DISCUSSION

Petrophysical properties (total porosity, effective porosity, water saturation and permeability) calculated using various empirical models defined within the Schlumberger Techlog environment. The results showing derived petrophysical properties for reservoir sands A, B, C, D, E, F and G are presented in Table 1.0 and summarized in Table 2.0. Figure 3.0 is a histogram plot showing the average reservoir petrophysical properties for reservoir sands identified across UPX field. Porosity and permeability results provided from special core analysis for UPX-01 and UPX-05 wells were compared with log derived porosity and permeability results obtained from empirical modelling using various equations and presented in Table 4.0 and Figures 4.0 and 5.0 respectively.

Shale Volume

As a reservoir rock become shalier, it will be more difficult to store and produce hydrocarbons. On average, shale volumes recorded are 7.0%, 10.8%, 8.8%, 4.8%, 24.6%, 7.6% and 10.0% in Sand A, B, C, D, E, F and G reservoirs respectively (Table 2.0). High shale volume lowers the quality of a reservoir and prevents flow of hydrocarbons to a well. Generally, all reservoir sand bodies have less than 25% shale volumes (on average) which signify that there is less resistance to the flow of fluids within the reservoir rock. This shows that only a minor amount of the reservoir sands are dirty, hence, about 70% of the reservoir sands are clean and can be produced of hydrocarbon.

Net to Gross

On average, net to gross ratio are; 93% 89%, 91% 95%, 75%, 92% and 90% in Sand A, B, C, D, E, F and G (Table 2.0).

Scientia Africana, Vol. 21 (No. 1), April, 2022. Pp 123-132 *https://dx.doi.org/10.4314/sa.v21i1.11*
© Faculty of Science, University of Port Harcourt, Printed in Nigeria *ISSN 1118 – 1931*

These results show that all identified reservoir sand packages have >70% clean sand volumes, indicating that the reservoirs are clean enough for hydrocarbon production, provided they are hydrocarbon bearing.

Total and Effective Porosity

On average, total porosities are 26.84%, 25.46%, 26.22%, 24.56%, 25.16%, 21.52% and 21.22% accordingly (Table 2.0). The porosity that is responsible for flow and accumulation in a reservoir is the effective porosity. The average effective porosities derived from density log are 26.22%, 24.64%, 25.8%, 24.12%, 24.68%, 21.16% and 20.78%. According to Levorsen (1967), rocks have negligible porosity when < 5%, poor porosity when >5-10%, good porosity when >10-20%, very good when >20-30%, and excellent when >30. Based on this classification scheme, the average total effective porosity recorded for all reservoir rock units in UPX field are classed as having very good porosities for hydrocarbon production. The results of effective porosity obtained from special core analysis conducted on UPX-01 (at a depth ranging from 5002.30 to 5048.60 ft) and UPX-05 (at a depth ranging from 5539.60 to 5562.20 ft) ranged from 20.40% to 22.50% and 24.41% to 27.50% respectively. Results of effective porosity obtained from density logs for UPX-01 and UPX-05 at same cored depth intervals ranged from 19.22% to 22.28% and 21.44% to 25.56% respectively. The error difference between core derived porosity and log derived porosity ranged from 0.45 to 3.23%. A plot of depth against core and log derived porosities for UPX-01 and UPX-05 wells revealed similar trends with minimum differences. The low difference between these porosity values suggests that the density tool is a very good tool for porosity determination in UPX field.

Permeability

The results of permeability obtained from special core analysis conducted on UPX-01 (at a depth ranging from 5002.30 to 5048.60 ft) and UPX-05 (at a depth ranging from 5539.60 to 5562.20 ft) ranged from 920.54 to 1045 mD and 4105 to 5022 mD respectively (Table 2.0). Results of log permeability obtained using Owolabi et al (1994) empirical model for UPX-01 and UPX-05 at same cored depth intervals ranged from 2895 to 6430 mD and 6223 to 8955 mD respectively. Results of log permeability obtained using Wylie and Rose (1950) empirical model for UPX-01 and UPX-05 at same cored depth intervals ranged from 853 to 1677 mD and 4098 to 5354.87 mD respectively. Results of log permeability obtained using Timur (1968) empirical model for UPX-01 and UPX-05 at same cored depth intervals ranged from 85.67 to 365.80 mD and 293.51 to 694.56 mD respectively.

A plot of depth against core and log derived permeability using various empirical models for UPX-01 and UPX-05 revealed that Owolabi's model greatly overestimated permeability values by approximately 206%, Timur's model underestimated permeability values by approximately 84%, whereas Wylie and Rose's model exceeded core permeability values by approximately 7%. Bear in mind that permeability is the most difficult reservoir property to be estimated using empirical models. Surprisingly, Wylie and Rose's empirical model gave reasonable permeability values which closely match permeability values obtained from special

core analysis. Hence, Wylie and Rose's empirical model was used for determination of permeability values across UPX field.On average, the results of reservoir permeability calculated using Wylie and Rose mathematical model are 2821.97 mD, 2475.18 mD, 2405.98 mD, 1829.13 mD, 2184.7 mD, 831.09 mD and 545.94 mD for sand A, B, C, D, E, F and G. Both Levorsen (1967) and Rider (1986) classified reservoir quality based on permeability values as follows; < 10 mD (poor to fair), >10-50 mD (moderate), >50-250 mD (Good), >250-1000 mD (very good) and >1000 mD (excellent). Based on this classification scheme, reservoir Sand A, B, C, D, E, F and G are classed as having very good to excellent reservoir quality. These values are typical of Niger Delta reservoirs. Hence, fluid flow within these reservoir units will occur with ease because of the relatively high permeability values.

Fluid saturation

Water saturation obtained from hydrocarbon bearing reservoirs are 99.72%, 41.20%, 98.94%, 62.30%, 34.80%, 40.45% and 48.75% for Sand A, B, C, D, E, F and G accordingly. This leads to a corresponding hydrocarbon saturation of 0.28%, 58.8%, 0.6%, 37.70%, 65.20%, 59.55% and 51.25% for Sand A, B, C, D, E, F and G respectively. Sand A and sand C are predominantly water with very little or no hydrocarbons present. These hydrocarbon saturation values are good for reservoir development.

CONCLUSION

This study has shown that the reservoir intervals evaluated in UPX fields have the necessary requirement to be termed good reservoir rocks for production. The reservoir rocks are of good to excellent quality and can be produced with minimum stress because of low shaliness, high net to gross, good to excellent effective porosity and permeability, good hydrocarbon saturation values.

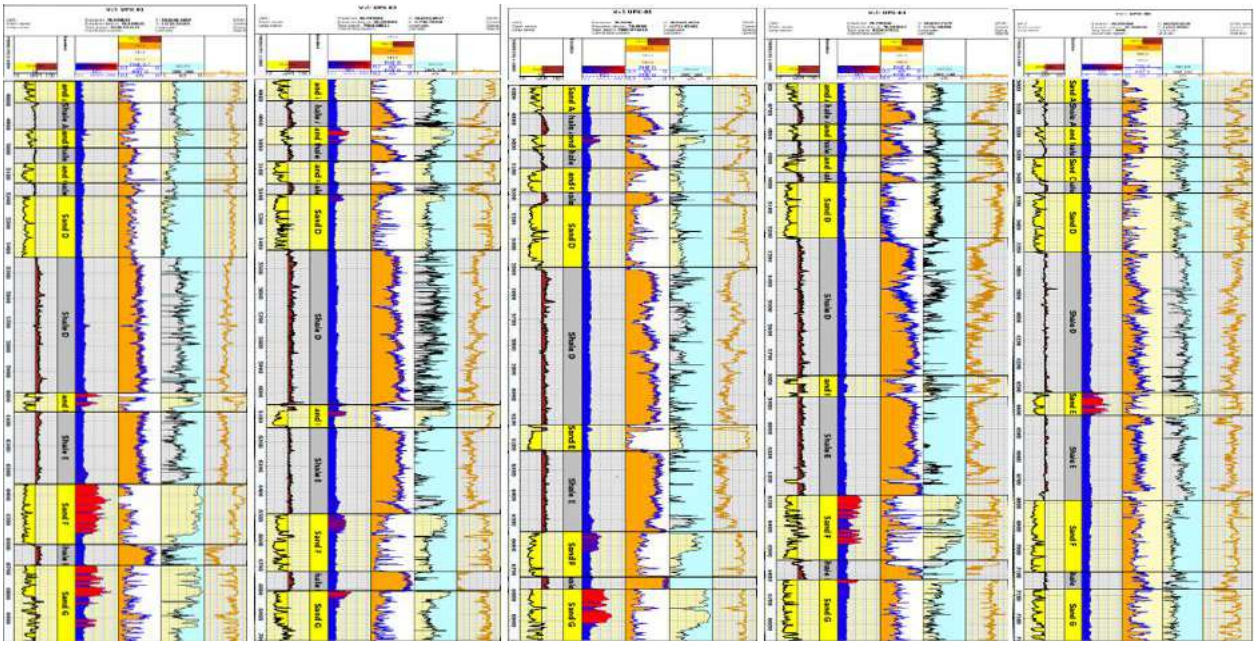

Figure 2: Results of petrophysical evaluation conducted on five wells in UPX field

Scientia Africana, Vol. 21 (No. 1), April, 2022. Pp 123-132 *https://dx.doi.org/10.4314/sa.v21i1.11*
© Faculty of Science, University of Port Harcourt, Printed in Nigeria *ISSN 1118 – 1931*

Table 1: Results of petrophysical evaluation conducted on five wells in OPX oil field

Well	Reservoir	Top (Ft)	Base (Ft)	Gross (Ft)	Net (Ft)	NTG	Vsh (%)	Total Porosity (%)	Effective Porosity (%)	Water Saturation (%)	Permeability (mD)
UPX-01	Sand A	4801.67	4890.51	88.84	85.80	0.96	4.00	25.80	25.20	99.90	1598.39
UPX-02	Sand A	4801.67	4887.45	85.78	78.75	0.92	8.00	29.00	28.40	99.80	3356.37
UPX-03	Sand A	4844.56	4954.85	110.29	100.08	0.91	9.00	26.20	25.70	99.50	1916.00
UPX-04	Sand A	4669.94	4749.59	79.65	75.89	0.95	5.00	26.30	25.80	99.50	2984.63
UPX-05	Sand A	5037.56	5141.72	104.16	94.44	0.91	9.00	26.90	26.00	99.90	4254.44
UPX-01	Sand B	4997.73	5071.26	73.52	70.52	0.97	3.00	24.30	23.50	57.60	998.28
UPX-02	Sand B	4991.61	5065.13	73.52	58.41	0.79	21.00	29.20	28.30	22.50	6530.70
UPX-03	Sand B	5043.69	5101.89	58.21	53.42	0.92	8.00	24.80	24.30	43.50	1371.27
UPX-04	Sand B	4838.43	4905.83	67.40	64.88	0.96	4.00	23.30	22.50	98.10	876.30
UPX-05	Sand B	5242.81	5322.46	79.65	65.50	0.82	18.00	25.70	24.60	97.20	2599.36
UPX-01	Sand C	5135.59	5215.24	79.65	73.65	0.92	8.00	22.70	22.30	97.80	669.76
UPX-02	Sand C	5132.53	5224.43	91.90	86.16	0.94	6.00	28.70	28.30	99.90	3043.65
UPX-03	Sand C	5175.42	5270.38	94.97	88.46	0.93	7.00	24.80	24.50	98.80	1456.02
UPX-04	Sand C	4967.10	5037.56	70.46	62.37	0.89	11.00	26.70	26.30	98.70	2195.65
UPX-05	Sand C	5374.54	5481.76	107.22	94.22	0.88	12.00	28.20	27.60	99.50	4664.83
UPX-01	Sand D	5267.32	5515.46	248.14	237.32	0.96	4.00	20.40	20.00	99.30	289.27
UPX-02	Sand D	5267.32	5490.95	223.63	213.76	0.96	4.00	25.20	24.80	62.30	1278.47
UPX-03	Sand D	5322.46	5570.60	248.14	239.74	0.97	3.00	24.40	24.00	99.90	1039.32
UPX-04	Sand D	5077.38	5304.08	226.70	220.45	0.97	3.00	25.30	25.00	98.80	1547.22
UPX-05	Sand D	5530.78	5785.04	254.27	228.27	0.90	10.00	27.50	26.80	98.20	4991.36
UPX-01	Sand E	6063.82	6143.47	79.65	56.50	0.71	29.00	29.80	29.30	33.60	6534.36
UPX-02	Sand E	6115.90	6210.87	94.97	77.27	0.81	19.00	26.10	25.70	51.70	1520.13
UPX-03	Sand E	6198.61	6302.77	104.16	87.42	0.84	16.00	26.40	26.20	99.70	1734.79
UPX-04	Sand E	5864.69	5950.47	85.78	44.19	0.52	48.00	21.40	20.80	99.10	542.24
UPX-05	Sand E	6388.55	6486.58	98.03	87.00	0.89	11.00	22.10	21.40	19.10	592.00
UPX-01	Sand F	6434.50	6679.58	245.08	230.00	0.94	6.00	25.00	24.70	22.30	2067.26
UPX-02	Sand F	6557.04	6792.92	235.89	221.37	0.94	6.00	22.60	22.20	55.30	762.07
UPX-03	Sand F	6624.43	6805.18	180.75	168.59	0.93	7.00	18.90	18.60	51.40	236.35
UPX-04	Sand F	6351.78	6615.24	263.46	220.65	0.84	16.00	21.40	21.00	32.80	680.09
UPX-05	Sand F	6854.19	7163.60	309.41	301.91	0.97	3.00	19.70	19.30	99.40	409.68
UPX-01	Sand G	6762.29	7126.84	364.55	306.15	0.84	16.00	23.00	22.40	37.90	775.83
UPX-02	Sand G	6869.51	7077.82	208.31	181.48	0.87	13.00	22.40	22.00	56.90	687.85
UPX-03	Sand G	6854.19	7059.44	205.25	190.63	0.93	7.00	22.30	21.90	30.80	588.33
UPX-04	Sand G	6694.89	6952.22	257.33	248.83	0.97	3.00	17.90	17.70	69.40	265.70
UPX-05	Sand G	7237.13	7460.76	223.63	200.00	0.89	11.00	20.50	19.90	99.10	412.01

Table 2: Average petrophysical properties for reservoir rocks in UPX field

Reservoir Interval	Gross (Ft)	Net (Ft)	NTG (Ft)	Vsh (%)	Total Porosity (%)	Effective Porosity (%)	Sw (%)	Permeability (mD)
Sand A	93.74	86.99	0.93	7.00	26.84	26.22	99.72	2821.97
Sand B	70.46	62.55	0.89	10.80	25.46	24.64	41.20	2475.18
Sand C	88.84	80.97	0.91	8.80	26.22	25.80	98.94	2405.98
Sand D	240.18	227.91	0.95	4.80	24.56	24.12	62.30	1829.13
Sand E	92.52	70.48	0.75	24.60	25.16	24.68	34.80	2184.70
Sand F	246.91	228.50	0.92	7.60	21.52	21.16	40.45	831.09
Sand G	251.82	225.42	0.90	10.00	21.22	20.78	48.75	545.94

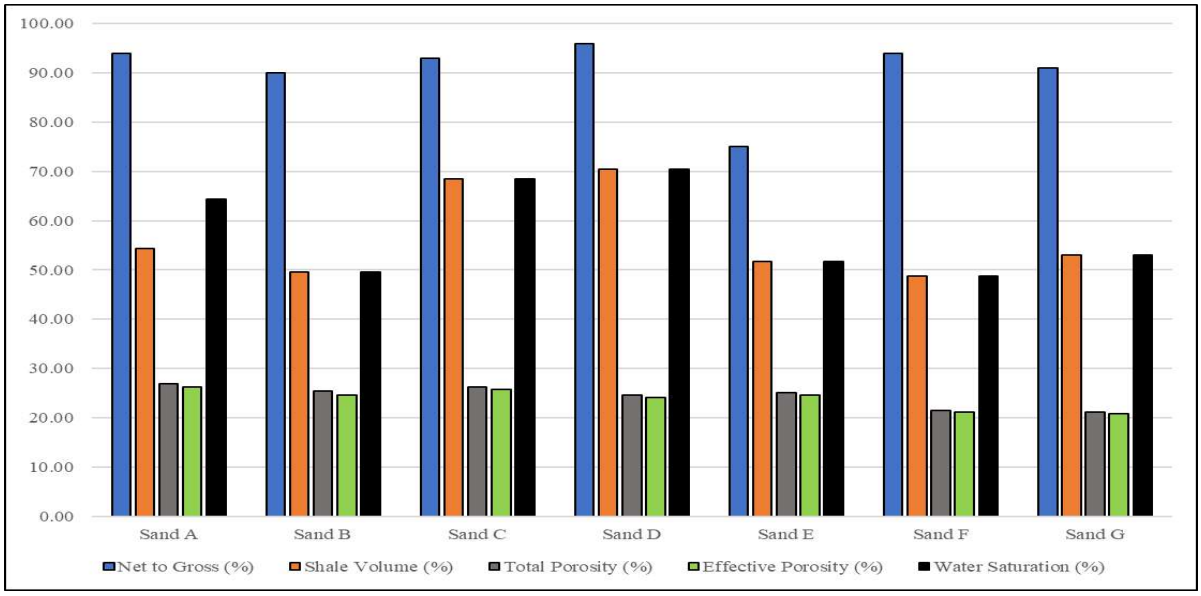

Figure 3: Histogram plot showing reservoir petrophysical properties across UPX field

Table 3: Results of routine core analysis compared with log analysis using empirical models

Well	Depth (m)	Core Effective Porosity (%)	Well log Effective Porosity (%)	Core Permeability (mD)	Permeability (Owolabi et al, 1994)	Permeability (Wylie and Rose, 1950)	Permeability (Timur, 1968)
UPX-01	5002.30	21.40	20.34	1023.43	6430.00	1387.00	325.40
UPX-01	5008.40	22.30	21.55	1050.66	5920.00	1677.00	223.67
UPX-01	5011.60	22.50	22.28	920.54	3986.00	853.00	114.65
UPX-01	5023.40	20.40	19.22	1045.00	3548.00	1137.00	365.80
UPX-01	5034.80	21.80	20.67	935.54	2895.00	1020.00	85.67
UPX-01	5048.60	20.66	20.12	1034.60	4043.41	1022.00	169.87
UPX-05	5539.60	25.56	24.56	5022.00	8435.00	4098.00	694.56
UPX-05	5543.30	24.67	21.44	4830.20	6223.00	4558.00	449.56
UPX-05	5549.50	26.22	24.89	4453.60	8130.00	4128.00	613.65
UPX-05	5553.40	27.50	25.56	4105.00	7940.00	4562.00	445.87
UPX-05	5558.70	24.41	24.86	4645.55	8955.00	4362.00	329.40
UPX-05	5562.20	25.92	24.76	5160.00	7320.00	5354.87	293.51

Scientia Africana, Vol. 21 (No. 1), April, 2022. Pp 123-132 *https://dx.doi.org/10.4314/sa.v21i1.11*
© Faculty of Science, University of Port Harcourt, Printed in Nigeria *ISSN 1118 – 1931*

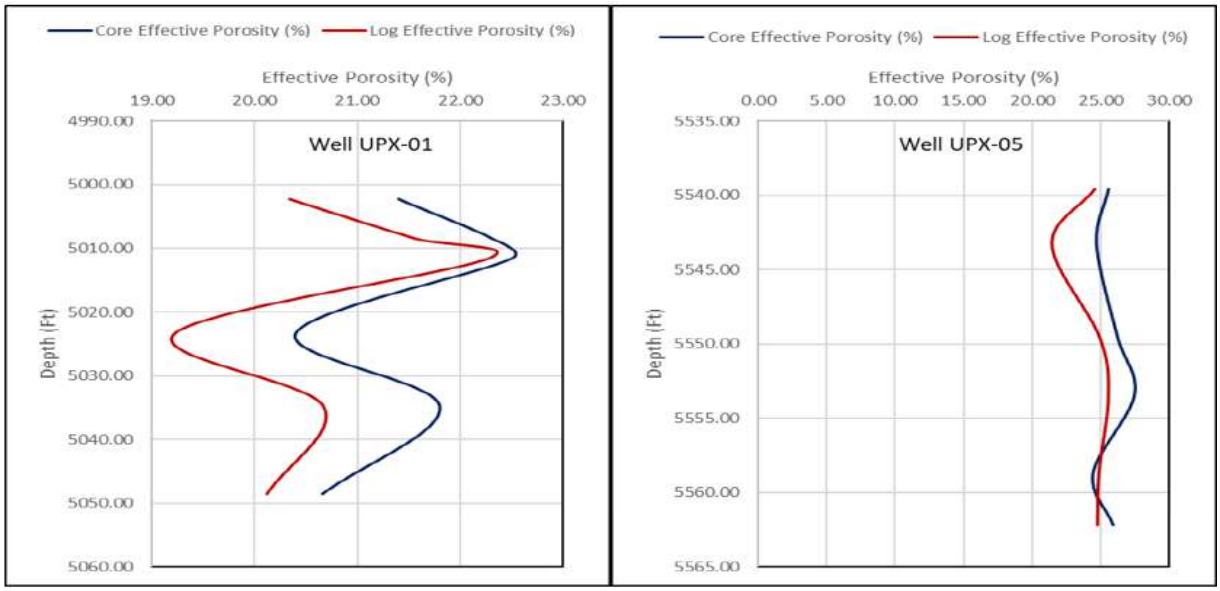

Figure 4: Results of core derived porosity vs density log porosity for UPX-01 and UPX-05 wells

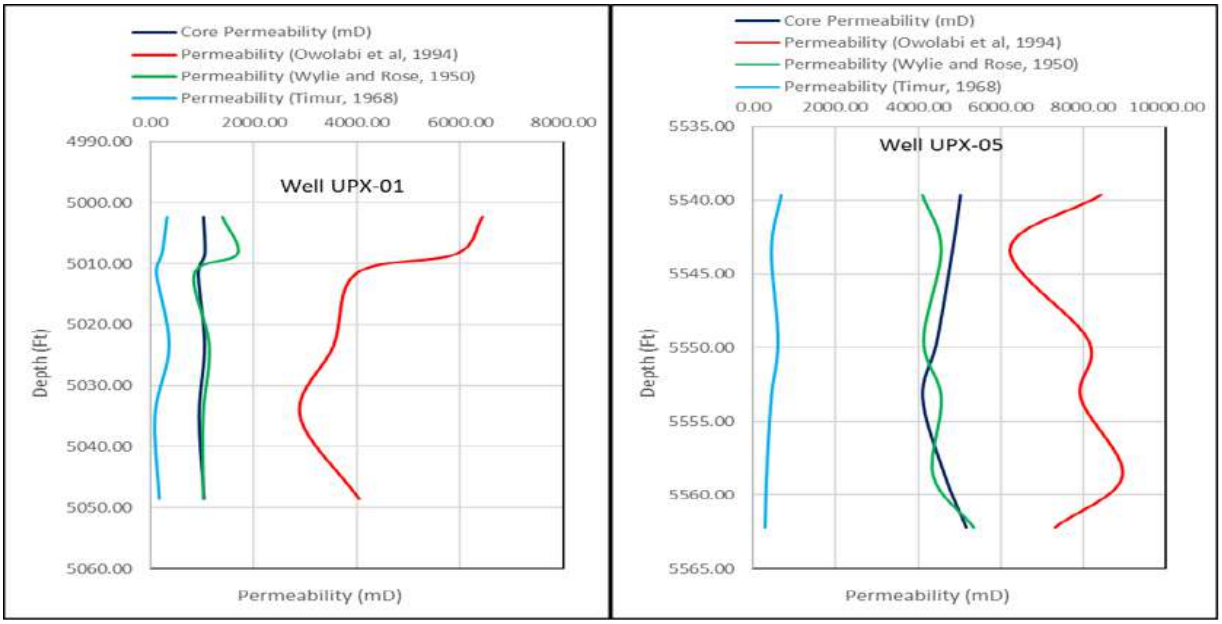

Figure 5: Results of core permeability versus log permeability for UPX-01 and UPX-05 wells

REFERENCES

Cannon, S. (2017). Petrophysics: A practical guide. John Wiley and Sons Ltd, UK. SBN 978-1-118-74674-5.

Darling T. (2005). Well Logging and Formation Evaluation. Elsevier Science & Technology, Gulf Publishing, Oxford, United Kingdom

Dresser Atlas (1979). Log Interpretation Charts, Dresser Industries Inc., Houston, Texas: p.107

Etu-Efeotor, J. O., (1997): Fundamentals of Petroleum Geology. Paragraphics: Port Harcourt.

Larionov, V. (1969). Borehole Radiometry: Moscow, U.S.S.R., Nedra.

Levorsen, A. I. (1967). The geology of petroleum. Freeman, San Francisco, second edition, 724p.

Owolabi, O.O., Longjohn, T.F., Ajienka J.A. (1994). An empirical expression for permeability in unconsolidated sands of eastern Niger Delta: J. Pet. Geol. 17(1): 111-116.

Rider, M.H. (1986).The Geological Interpretation of Well Logs. 2nd Ed. Whittles Publishing: Caithness.

Schlumberger (1974). Log Interpretation Charts, Schlumberger Educational Services, New York, 83p.

Timur, A. (1968). An Investigation of Permeability, Porosity and Residual Saturation Relationship for Sandstone reservoirs. Log Analyst, 9: 8.

Wyllie, M.R.J., and Rose, W.D. (1950). Some theoretical considerations related to the quantitative evaluation of the physical characteristics of reservoir rock from electrical log data: J.Pet. Tech., p.189.

Scientia Africana, Vol. 21 (No. 1), April, 2022. Pp 133-148 https://dx.doi.org/10.4314/sa.v21i1.12
© Faculty of Science, University of Port Harcourt, Printed in Nigeria *ISSN 1118 – 1931*

SEQUENCE STRATIGRAPHIC FRAMEWORK OF 'AKOS' FIELD, NIGER DELTA

[*1]Umukoro, A. G. and [2]Okengwu, K. O.
[*1]World Bank Centre of Excellence, University of Port Harcourt, Nigeria.
https://orcid.org/0000-0003-1262-7188. Email: akporjevweumukoro@gmail.com
[2]Department of Geology, University of Port Harcourt, Nigeria.
[*]Corresponding Author: +234 803 667 1300. Email:kingsley.okengwu@uniport.edu.ng

Received: 13-11-2021
Accepted: 20-03-2022

ABSTRACT

The aim of this study is to investigate the sequence-stratigraphic framework of a hydrocarbon prospect of 'AKOS' Field, Niger Delta, using well logs, and 3-D seismic data. To achieve this, the researchers identify the various sand/shale and seismic facies, build a sequence-stratigraphic framework of the oilfield, and assess the petroleum play of identified system tracts. A fault analysis reveal twelve (12) fault sets (Fault 1-12) mapped across the seismic volume. These faults are picked on an increment of 50 and examined for consistency using time slice and variance attributes. Faults-1 and 2 are major faults. The other ten (10) are minor faults. The mapped faults are normal growth faults common in the Niger Delta, as most trend approximately E-W direction. Sequence-stratigraphic analysis of the prospect based on chronostratigraphic correlation reveal two (2) sequences. Sequence-1 is between Sequence Boundary (SB) 0 to SB-1. Sequence-2 is between SB-1 to SB-2. Results from interpreted and analyzed system tracts reveal all three (3) present in Sequence-1. However, the Lowstand System Tract (LST) is absent in Sequence-2. The Lowstand Systems Tracts (LST) identified by shallowing and coarsening-upward succession, and progradational and aggradational parasequence sets are major hydrocarbon-producing intervals within the oilfield. The Transgressive Systems Tract (TST) typified by dirtying-upward seal the Lowstand Reservoirs. The upper section of the Highstand Systems Tracts (HST) has reservoir potential.

Keywords: Facies, Faults, Sequence, Sequence Boundary (SB), System tracts.

INTRODUCTION

Seismic stratigraphy involves establishing stratigraphic surfaces via identifying various reflection terminations, thus understanding the seismic facies relationship. Sequence stratigraphy applies both time and relative base-level changes to understand and identify facies migration. It is necessary to predict the vertical and horizontal distribution of depositional sequences, their system tracts, and facies during exploration and development of sandstone reservoirs. Sequence stratigraphy is an indispensable tool in basin-wide geologic analysis with widespread applications, especially aiding an understanding of the relationship between sea-level changes and sediment supply (Catuneanu, 2002). It also assists in correlating locally recognized depositional sequences.

The Niger Delta consists of a regressive sequence of clasts of deltaic and marine origin. It consists of three primary lithofacies- marine shale within the Akata Formation at the bottom, followed by a

stacked sequence of Agbada Formation, and non-marine alluvial (continental) sands within the Benin Formation at the top. Weber and Daukoru (1975) report the cyclic nature of sedimentation of paralic deposits. Their study results suggest a complete cycle consisting of thin fossiliferous transgressive marine sands followed by an offlap sequence commencing with marine sediments, and another transgression possibly terminating the cycle.

Doust and Omatsola (1990) recognize six depobelts: Offshore megastructures (Late Miocene), Coastal Swamp (Middle-Late Miocene), Central Swamp II (Middle Miocene), Central Swamp I (Early Miocene-Middle Miocene), Greater Ughelli (Oligocene - Early Miocene), and the Northern delta (Late Eocene - Early Miocene). These are distinguished by Ozumba (1999) while developing a stratigraphic framework of the Western Niger Delta using wireline log data and foraminifera acquired from four wells drilled within the Central-Swamp and Coastal depobelts. The results conclude that sequences formed during the Late Miocene are thicker than those of the Middle Miocene period.

Going by the seismic stratigraphy concept alongside a chart of the global sea-level cycle, one may assume eustasy as the primary driving influence behind the formation of sequences at every stratigraphic cyclicity level. The new stratigraphic methodology highlights seismic stratigraphy and the global sea-level cycle chart as an inseparable package (Catuneanu, 2002). As seismic stratigraphy evolved to sequence stratigraphy over time, there was a better understanding of the latter while combining outcrop and well-log data.

The study objective is to delineate sequence boundaries from their system tracts, correlate the reservoir sand bodies within the oilfield, predict sand body characteristics that form potential reservoirs, and infer the depositional environment of sand bodies within the oilfield through the combination of two stratigraphic tools; wireline well-logs, and seismic dataset.

MATERIALS AND METHODS

The dataset for this study include well-log, seismic covering about 110 sq. km, deviation, and check shot for six wells. Schlumberger's PETREL™ software is used in this study to aid well-log interpretation and well-to-well correlation.

Two approaches of structural and stratigraphic principles are applied to carry out the seismic interpretation. Firstly, the observation of reflection terminations against a planar or curvilinear trend to guide seismic structural interpretation. Then, analyzing seismic data attributes such as lithofacies, erosion, paleotopography, bedding patterns, thicknesses, spacing, paleobathymetry, and gross depositional environments to guide stratigraphic interpretation.

RESULTS AND DISCUSSION

Structural Interpretation

Schlumberger's Petrel™ software is used for seismic interpretation. The study investigators generated time structure maps from the horizons and the time domain maps were depth converted using the time-depth relationship derived from the check-shot data

Scientia Africana, Vol. 21 (No. 1), April, 2022. Pp 133-148 *https://dx.doi.org/10.4314/sa.v21i1.12*
© Faculty of Science, University of Port Harcourt, Printed in Nigeria *ISSN 1118 – 1931*

Fault Interpretation

The study investigators mapped twelve (12) fault sets (Fault 1-12) across the seismic volume. These faults were picked on an increment of 50 and examined for consistency using time slice and variance attribute. The mapped faults are normal growth faults common with the Niger delta. Almost all the faults trend approximately E-W. Two (2) sets: Fault 1 and 2 are major while the other ten (10) are minor (Figures 1 and 2).

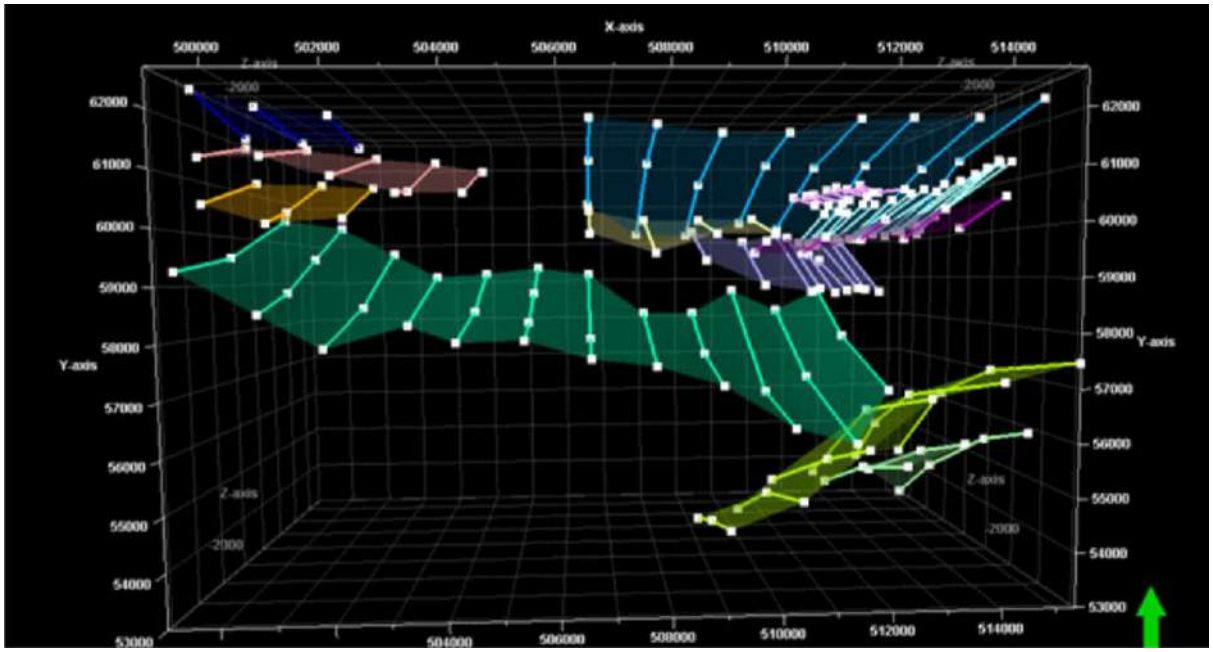

Figure 1: Fault interpretation as displayed on a 3D window

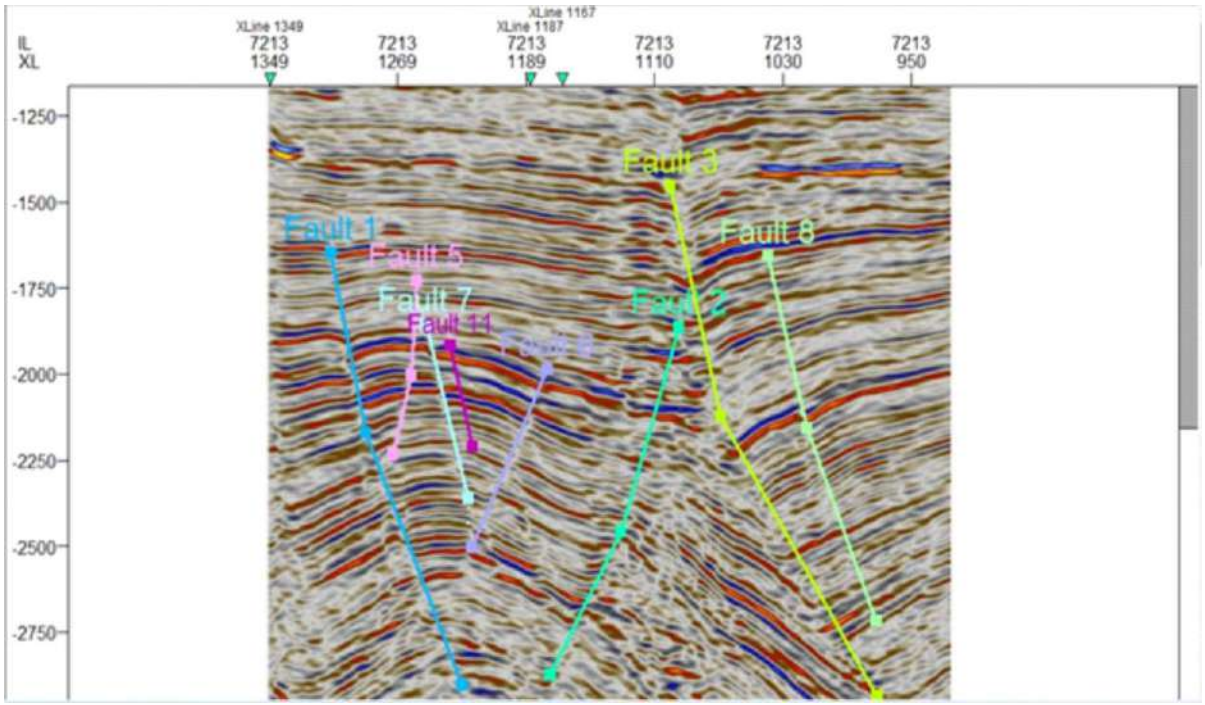

Figure 2: Seismic section Inline 7213 showing some of the interpreted faults

Well Correlation

A well-to-well correlation was done to establish the continuity and lateral extent of important stratigraphic surfaces. This was achieved using a lithology sensitive log (GR) and Resistivity log in six wells (Figure 3). By using four wells through the NW-SE strike line, it was possible to carry out another correlation for intervals that are potentially hydrocarbon-bearing. To achieve this, a shale baseline was established and areas to the left of the baseline were taken to be sand, and zones where the sand corresponded to a high resistivity log reading were assumed potentially hydrocarbon-bearing (Figure 4).

Well-to-seismic Calibration

The researchers generated a synthetic seismogram from the AKOS-1 well, helping to tie well-to-seismic data. Differences in the domains of well and seismic datasets were less pronounced. A combination of sonic and density logs and then matching them to the seismic information produced acoustic impedance attributes within the well.

The researchers obtained a sufficiently good match in calibrating the well to seismic trace (Figure 5).

Horizon Interpretation

The study investigators identified the stratigraphic surfaces on the oil well logs, mapped them on the seismic volume, and interpreted these surfaces on both in-lines and cross-lines on an increment of 5 (Figure 6). Next, they converted horizons to time structure maps (Figures 7 - 12) using the convergent interpolation method. Time structure maps were then converted to depth structure maps using the mathematical relationship obtained by plotting the time-depth relationship derived from the check shot data (Figure. 13). Figures 14 - 19 show the resulting depth structure maps.

The isopach maps of the resulting system tracts showed changes in the thickening and thinning directions (Figures 20 – 24).

Scientia Africana, Vol. 21 (No. 1), April, 2022. Pp 133-148 https://dx.doi.org/10.4314/sa.v21i1.12
© Faculty of Science, University of Port Harcourt, Printed in Nigeria *ISSN 1118 – 1931*

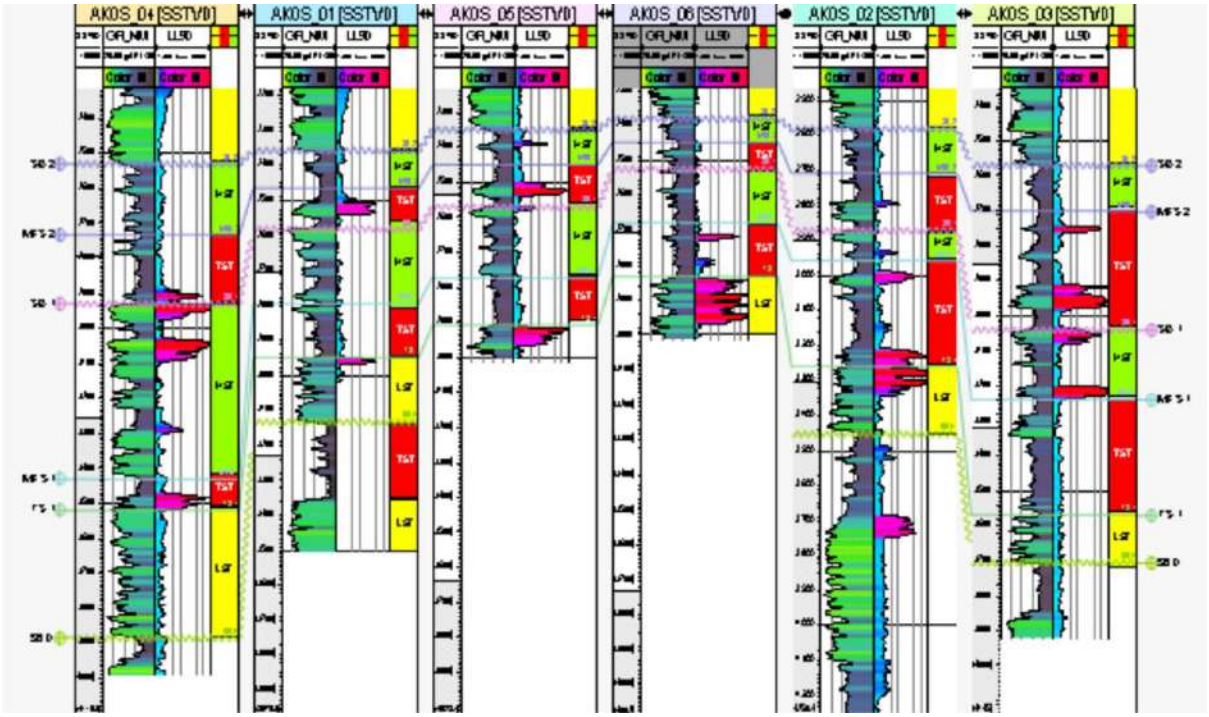

Figure 3: Correlation of Wells across 'AKOS' Field showing important surfaces and systems tracts

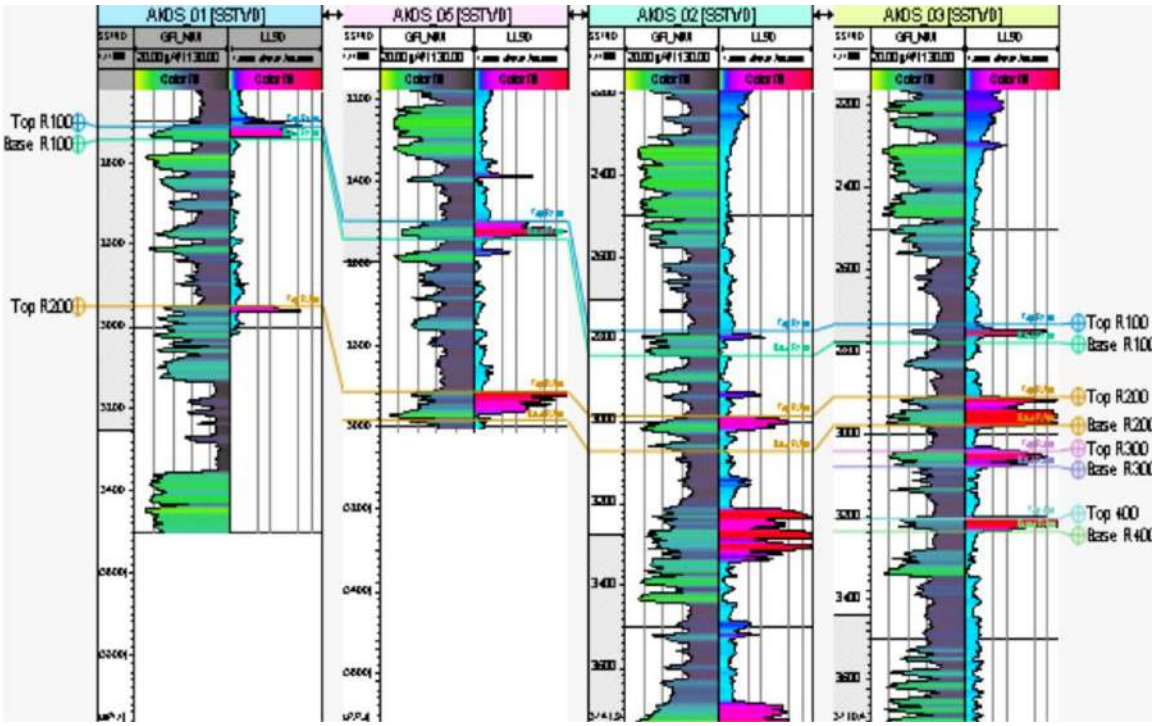

Figure 4: Well correlation panel showing the potential hydrocarbon-bearing intervals across the four wells

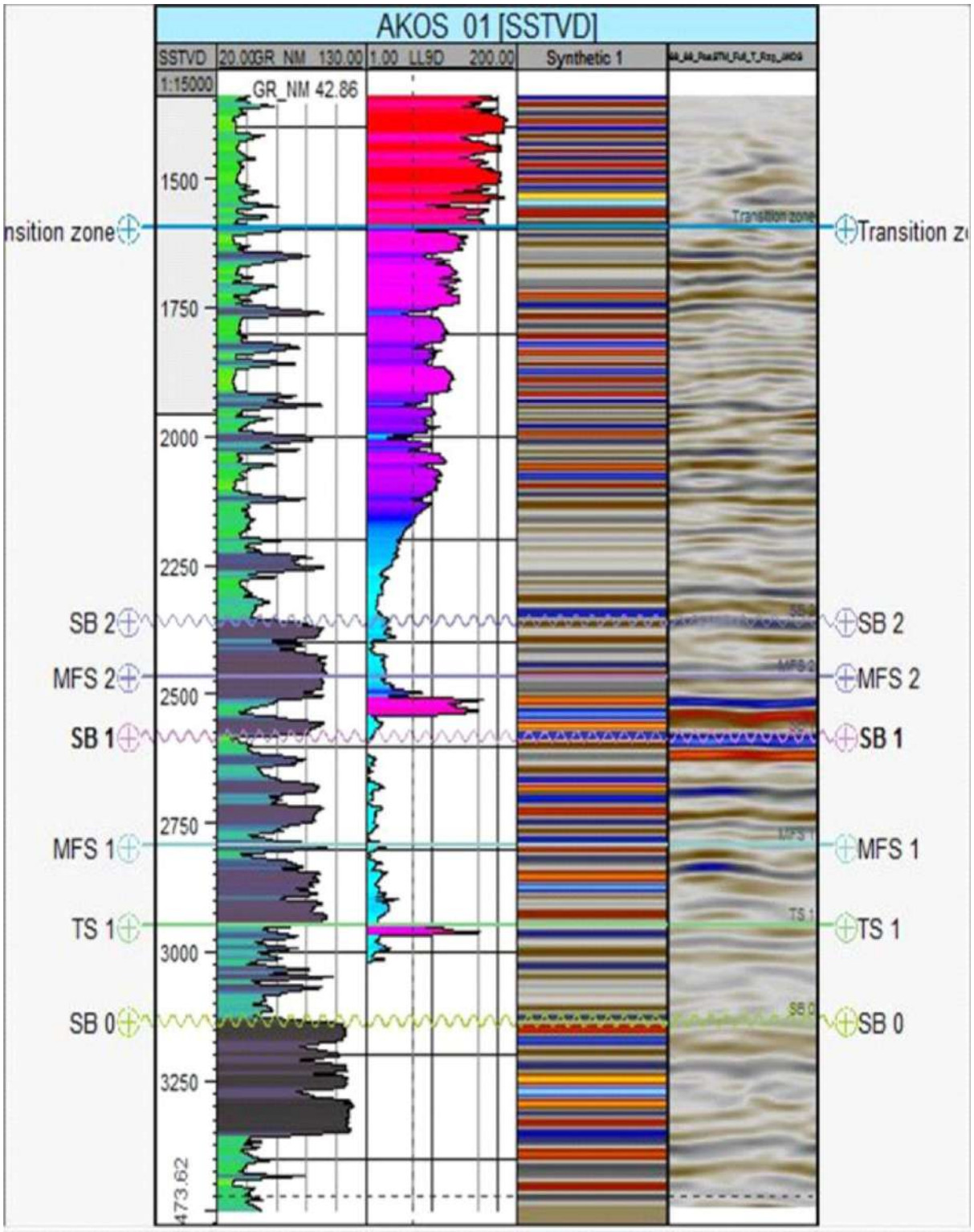

Figure 5: Synthetic seismogram for well AKOS 01

Scientia Africana, Vol. 21 (No. 1), April, 2022. Pp 133-148 *https://dx.doi.org/10.4314/sa.v21i1.12*

ISSN 1118 – 1931

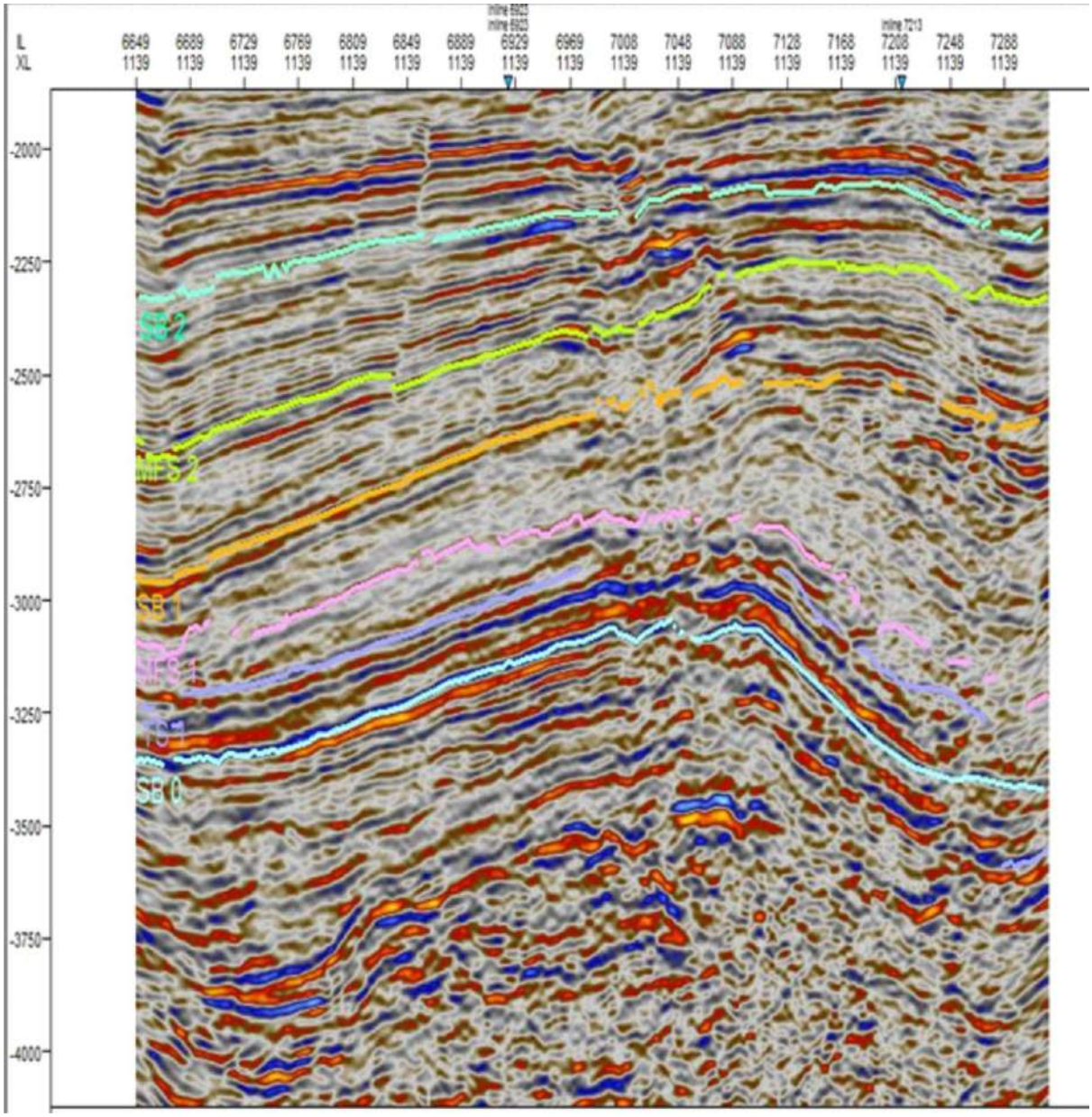

Figure 6: Seismic section along cross-line 1139 showing the interpreted surfaces

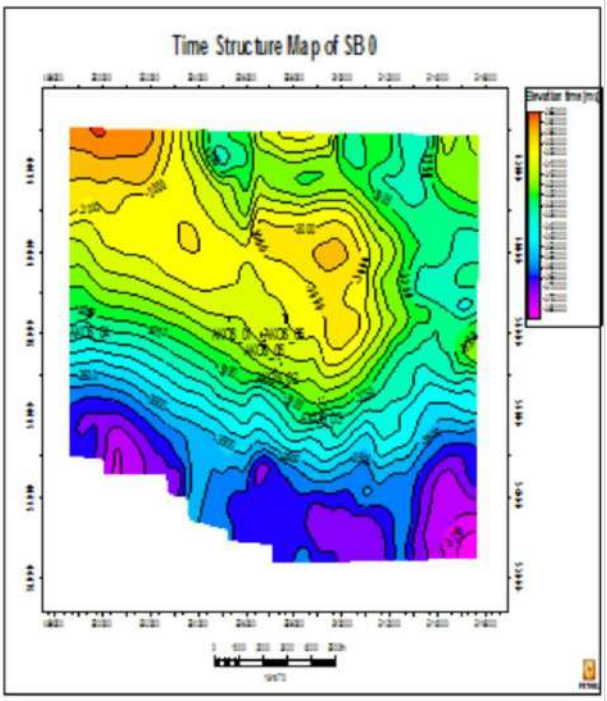

Figure 7: Time structure Map of SB 0

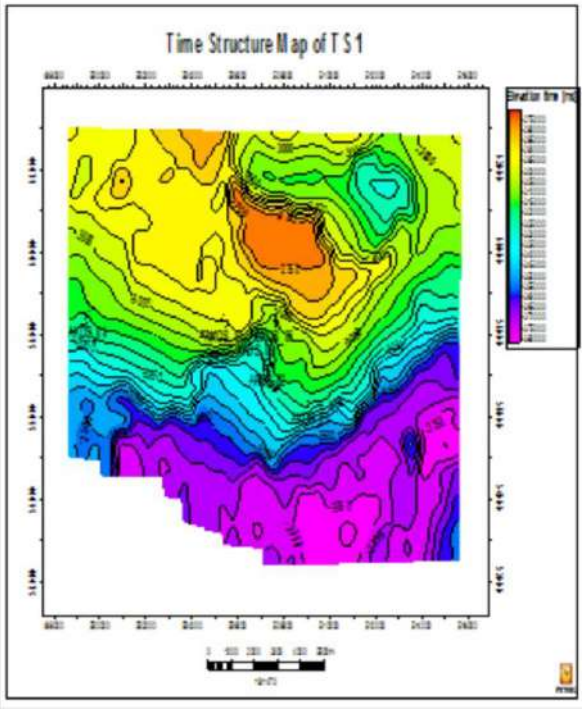

Figure 8: Time structure Map of TS 1

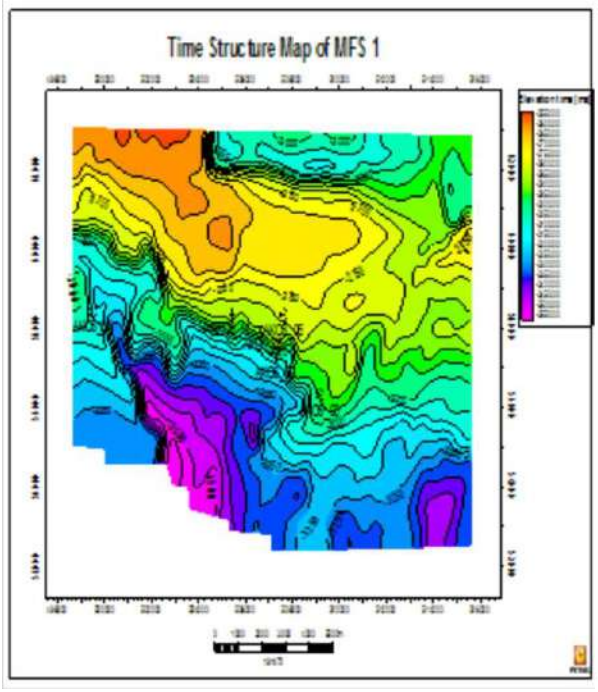

Figure 9: Time structure Map of MFS 1

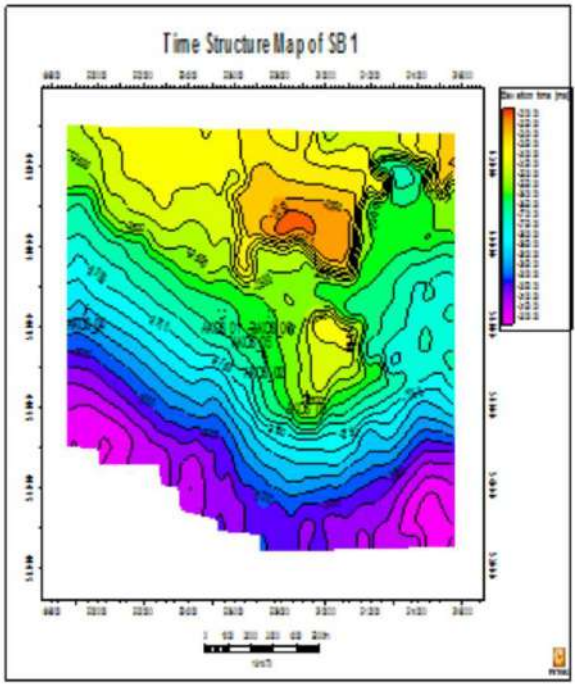

Figure 10: Time structure Map of SB 1

Scientia Africana, Vol. 21 (No. 1), April, 2022. Pp 133-148 *https://dx.doi.org/10.4314/sa.v21i1.12*
© Faculty of Science, University of Port Harcourt, Printed in Nigeria *ISSN 1118 – 1931*

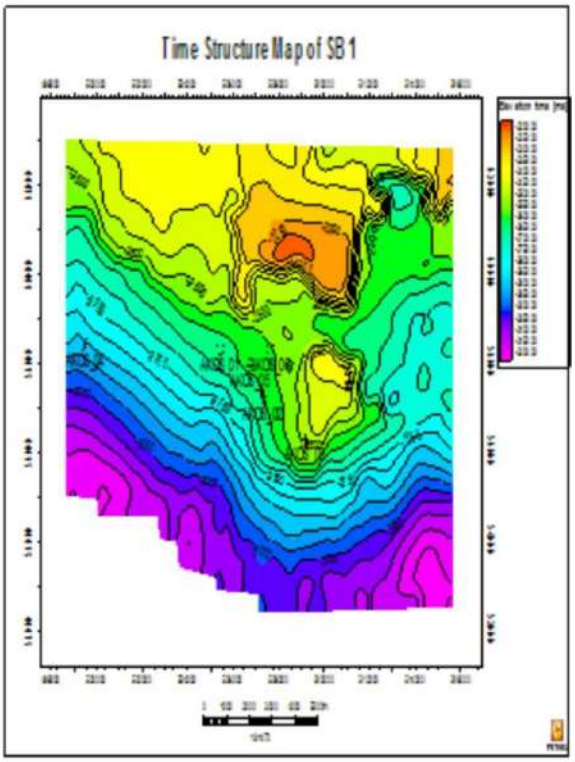

Figure 11: Time structure Map of MFS 2

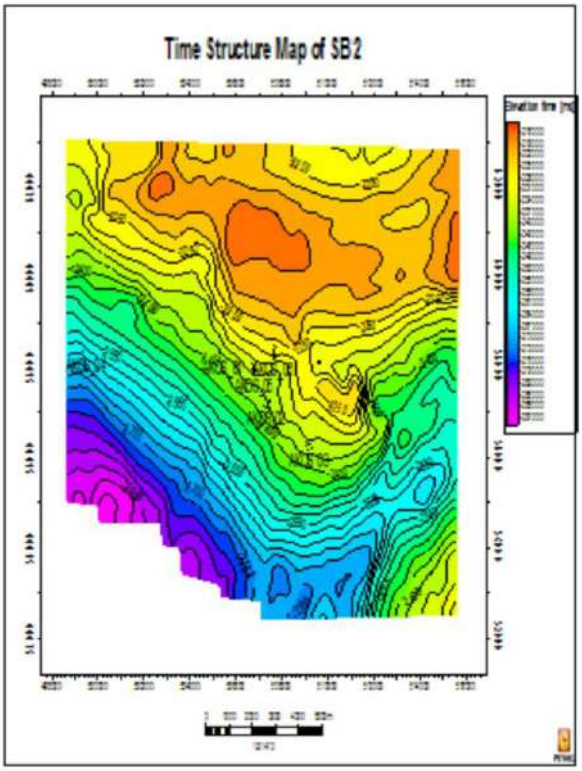

Figure 12: Time structure Map of SB 2

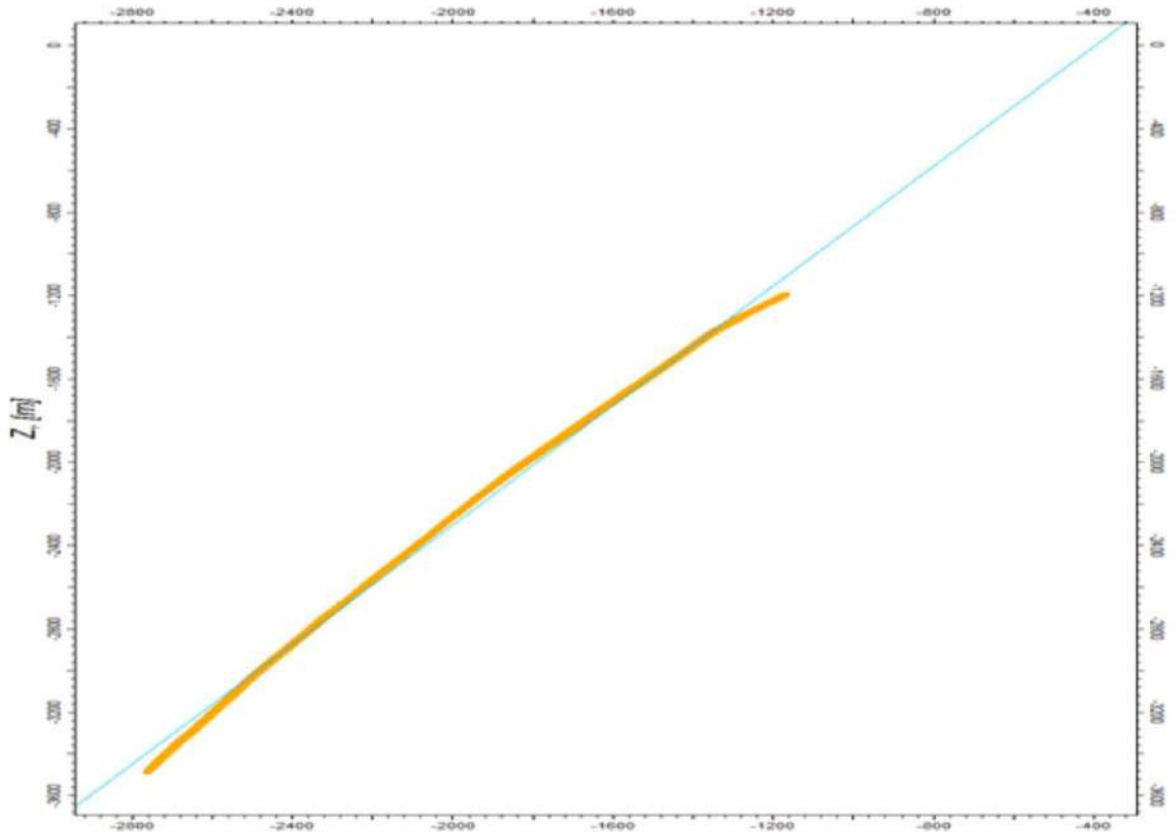

Figure 13: TWT Vs. Depth Linear Function Plot for Time-Depth Conversion (The resulting equation is: Y = 1.43464 * X + 568.571)

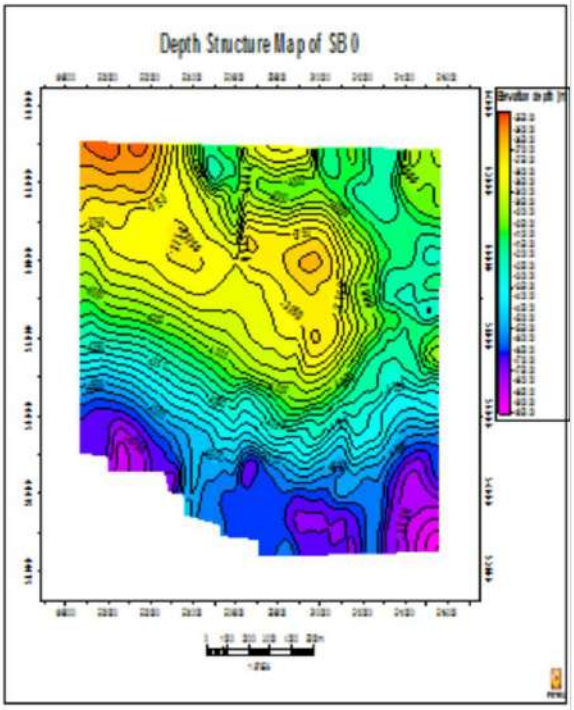

Figure 14: Depth structure Map of SB 0

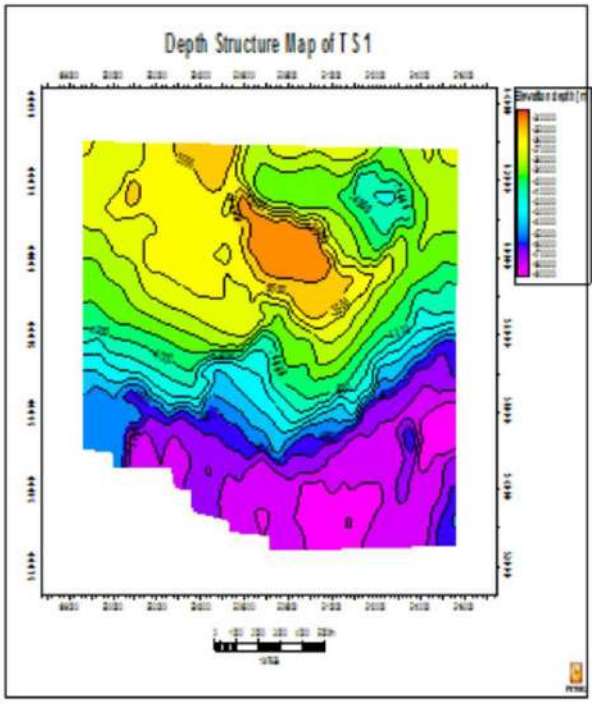

Figure 15: Depth structure Map of TS 1

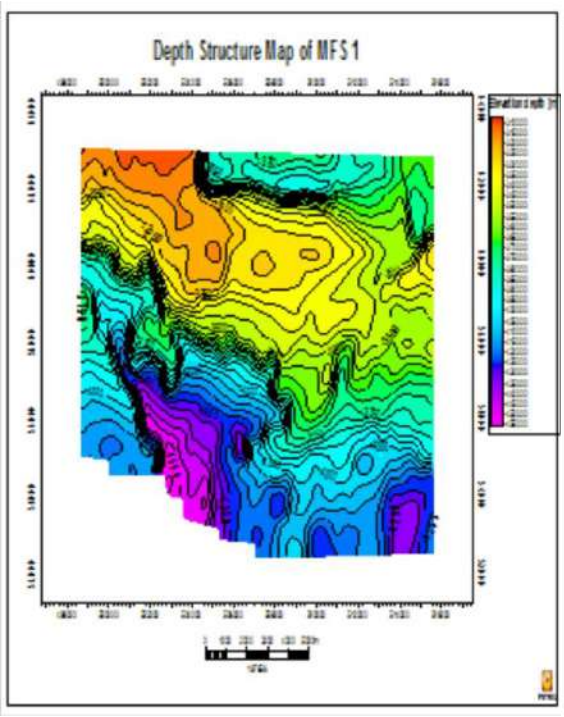

Figure 16: Depth structure Map of MFS1

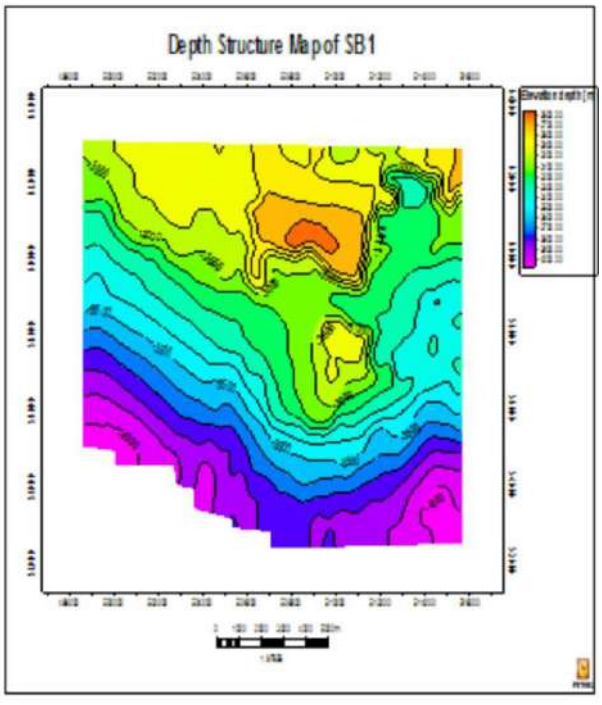

Figure 17: Depth structure Map of SB1

Scientia Africana, Vol. 21 (No. 1), April, 2022. Pp 133-148 *https://dx.doi.org/10.4314/sa.v21i1.12*
© Faculty of Science, University of Port Harcourt, Printed in Nigeria *ISSN 1118 – 1931*

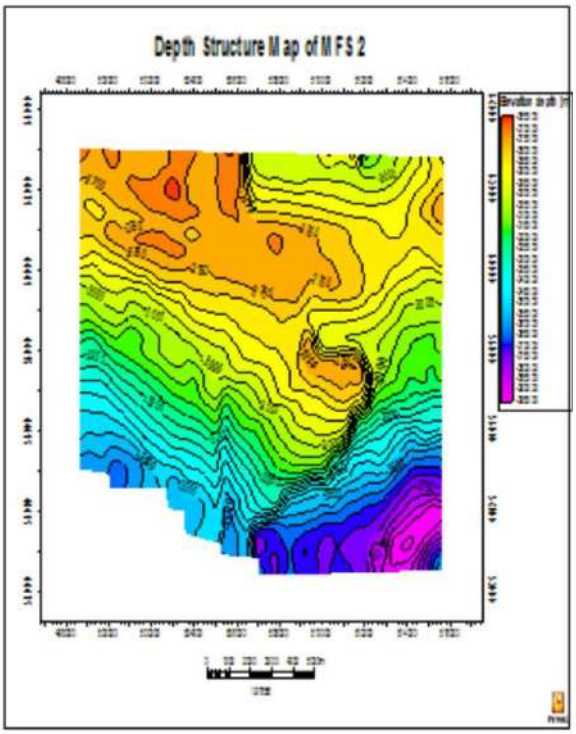

Figure 18: Depth structure Map of MFS 2

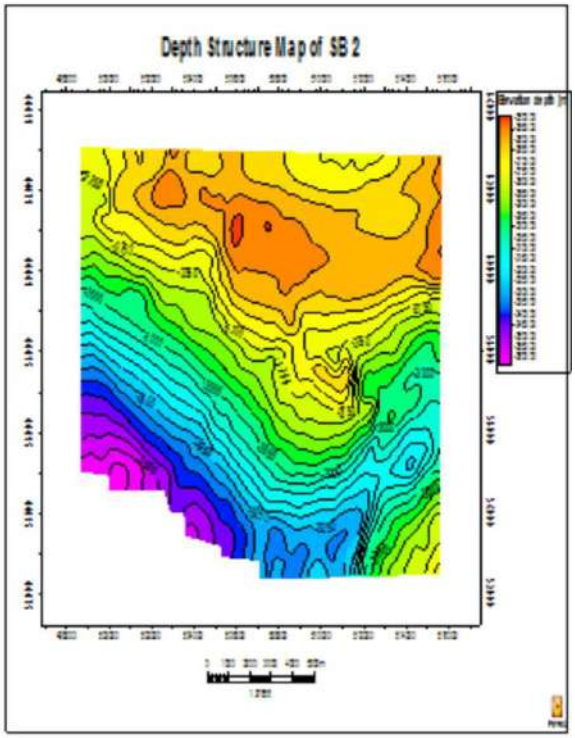

Figure 19: Depth Structure Map of SB 2

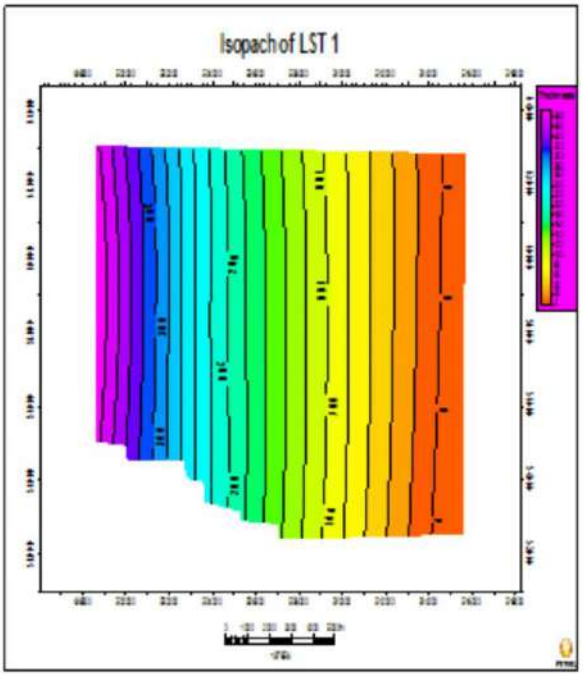

Figure 20: Map showing variation in thickness across LST1

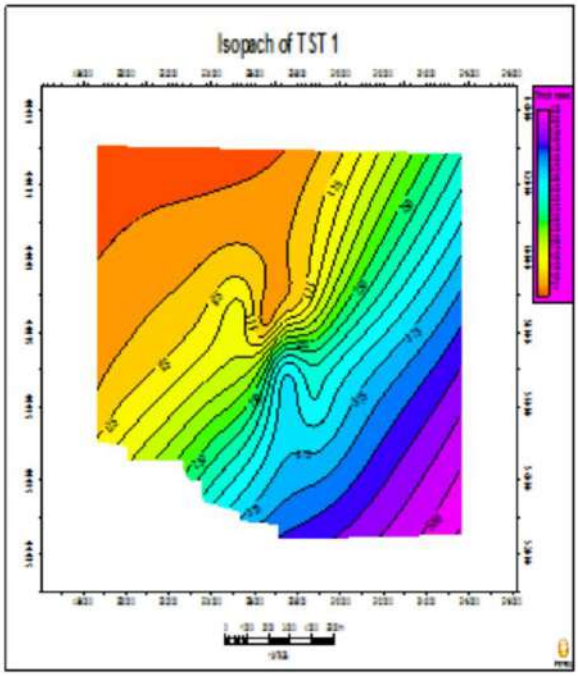

Figure 21: Map showing variation in thickness across TST 1

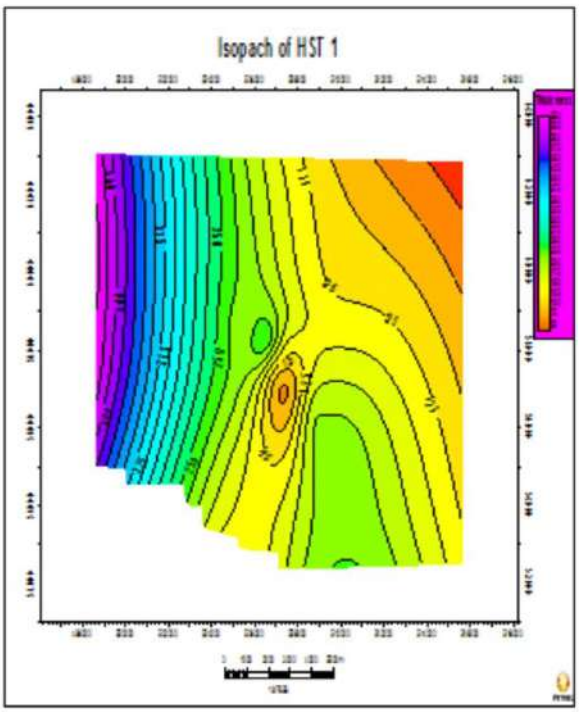

Figure 22: Map showing variation in thickness across HST 1

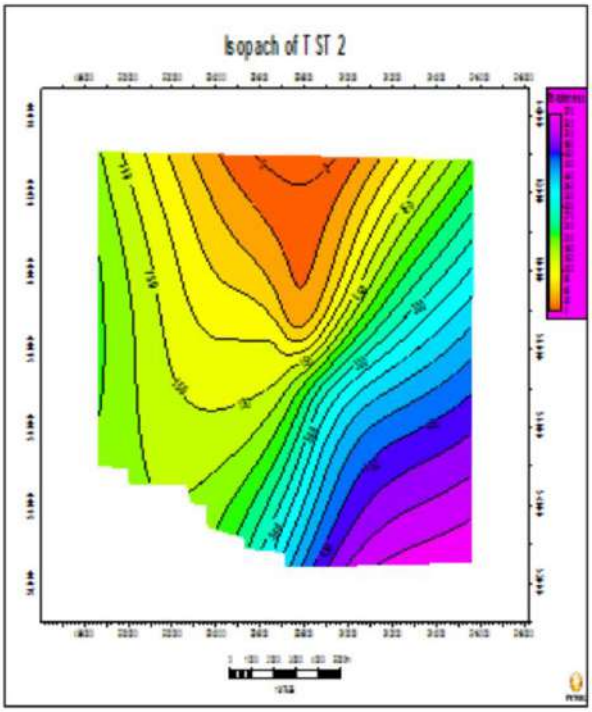

Figure 23: Map showing variation in thickness across TST 2

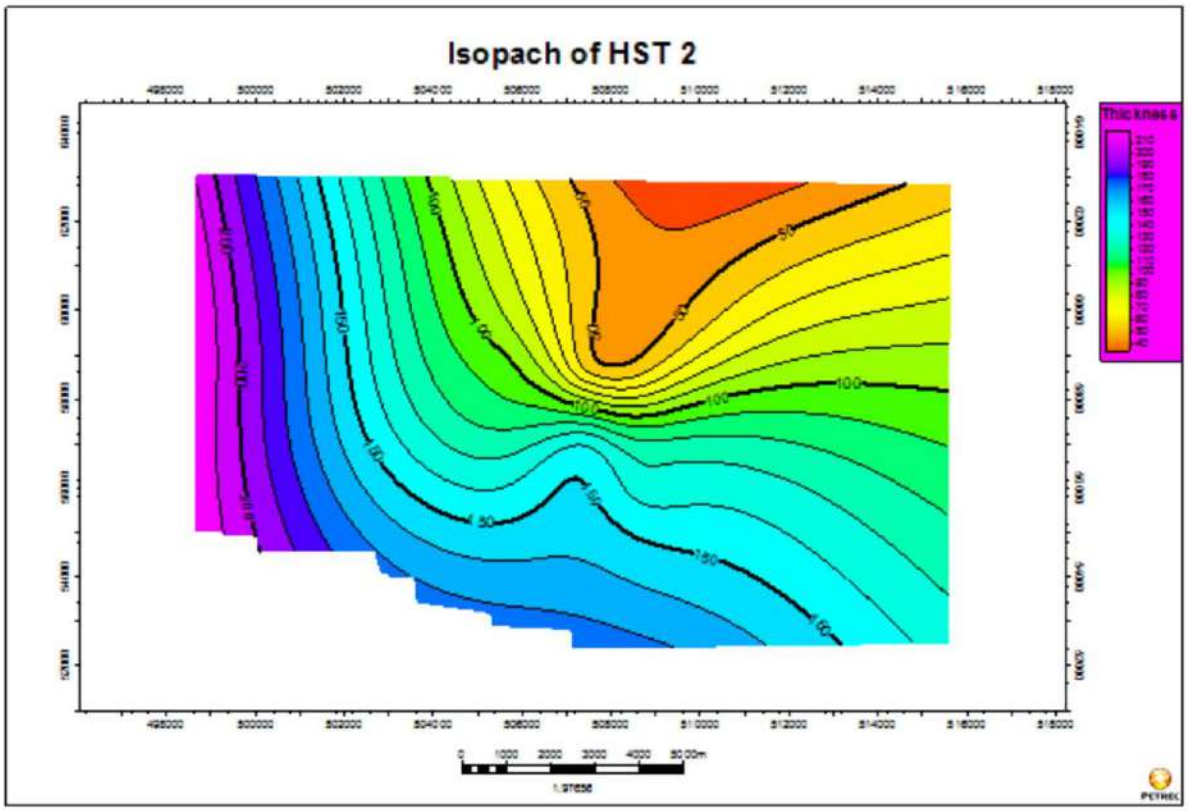

Figure 24: Map showing variation in thickness across HST 2

Scientia Africana, Vol. 21 (No. 1), April, 2022. Pp 133-148 *https://dx.doi.org/10.4314/sa.v21i1.12*
© Faculty of Science, University of Port Harcourt, Printed in Nigeria *ISSN 1118 – 1931*

Sequence Stratigraphic Evaluation of 'AKOS' Field

Two (2) crucial sequences are identified based on the chronostratigraphic correlation. Sequence 1 covers the interval between SB 0 to SB 1. Sequence 2 covers SB 1 to SB 2 interval. All three (3) crucial systems tracts are present in sequence 1. The Lowstand system tract (LST) is absent in Sequence 2.

The Lowstand systems tract (LST) identified by a shallowing-upward, coarsening-upward succession and progradational and aggradational parasequence sets is the major interval producing hydrocarbon within the Field. The transgressive systems tract (TST), typified with a dirtying-upward succession seals the lowstand reservoirs. The upper section of the Highstand Systems Tracts (HST) has reservoir potentials. Based on the studied Systems Tracts and their positioning, the crucial reservoir-seal pair elements required for accumulation are present. Hence, 'AKOS' Field could be a viable hydrocarbon Field.

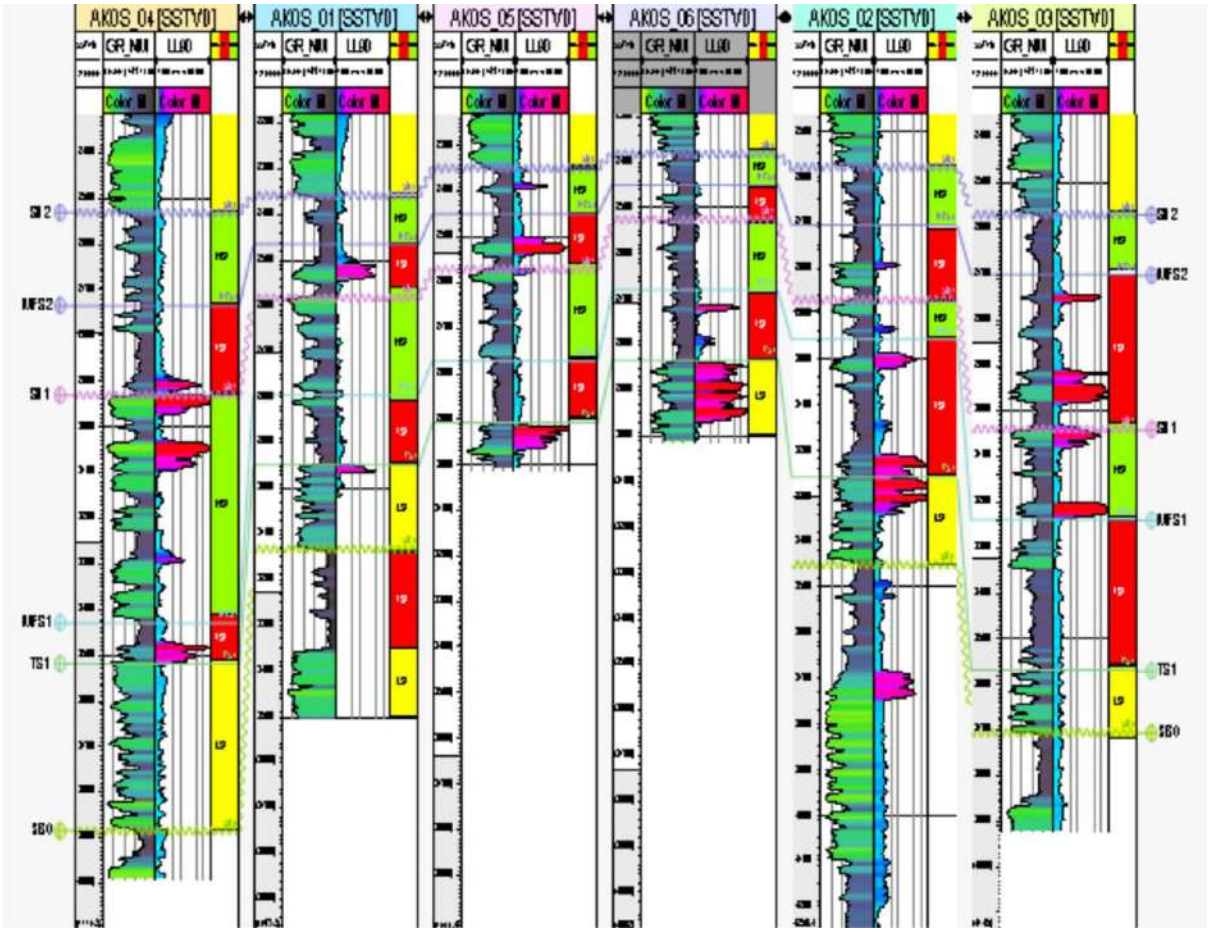

Figure 25: Sequence stratigraphic framework of 'AKOS' Field showing the identified systems tracts on Well correlation panel

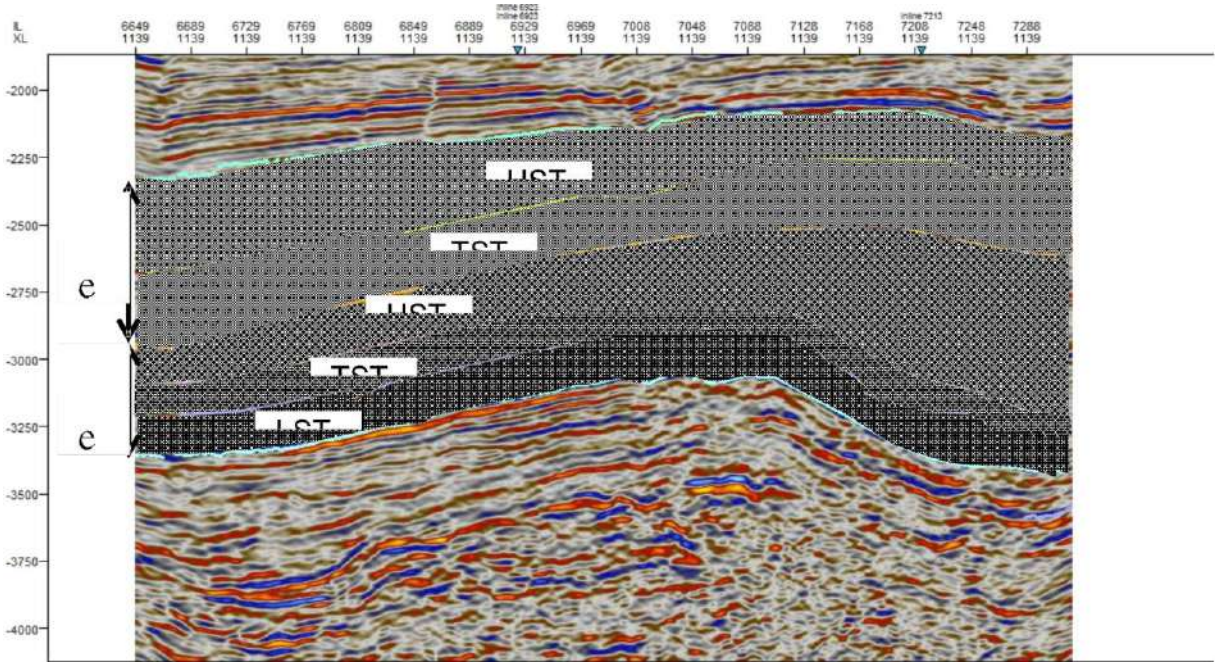

Figure 26: Sequence Stratigraphic framework of AKOS Field showing the identified system tracts in the two (2) sequences

CONCLUSION

From the analysis and interpretation of the available dataset, "AKOS" Field possesses good hydrocarbon potential with good reservoir-seal pairs. The research investigators identify leads. The identified potential reservoirs are laterally continuous. The reservoir units are considerably thick and can host commercially quantifiable hydrocarbon provided the petrophysical attributes of the reservoir rocks are effective for hydrocarbon accumulation.

The fault network serves a decisive role in the trapping style of the field due to its nature and connectivity. All the faults display a dominant E-W trend.

Sources of Funding: The research was funded by the authors.

Conflict of Interest: On behalf of all the co-authors, the corresponding author states that there is no conflict of interest.

REFERENCES

Allen, J. (1965). Coastal Geomorphology of Eastern Nigeria, Beach Ridge Barrier Island and Vegetated Tidal Flats. *Geol.EnMijnb*, *44*(1), 1-21.

Boggs, S. (Jr.) (2014).*Principlesof Sedimentology and Stratigraphy*. (4th ed.). Pearson Prentice Hall.

Bilotti, F. (2005).*Structural styles in the deep-water fold and thrust belts of the Niger delta*: *AAPG Bulletin*, *89*, 753-778.doi.org/10.1306/02170504074

Catuneanu, O. (2002). Sequence Stratigraphy Of Clastic Systems: Concepts, Merits, and Pitfalls, *Journal Of African Earth Sciences*, *35*(1), 1-43.doi.org/10.1016/S0899-5362(02)00004-0

Charles, W.B., and George, L.S. (1993).*Sequence Stratigraphy of the Lower Ordovician Praire Du Chien Group onthe Wisconsin Arch and in the Michigan Basin. AAPG*

Scientia Africana, Vol. 21 (No. 1), April, 2022. Pp 149-158 https://dx.doi.org/10.4314/sa.v21i1.13
© Faculty of Science, University of Port Harcourt, Printed in Nigeria *ISSN 1118 – 1931*

Bulletin,77, (1).doi:10.1306/bdff8b5a-1718-11d7-8645000102c1865d

Corredor, F., Shaw, J.H.,and Bilotti, F. (2005).*Structural styles in the deep-water fold and thrust belts of the Niger Delta. AAPG Bulletin*, *89(*6), 753-780.doi:10.1306/02170504074.

Damuth, J. E. (1994). Neogene gravity tectonics and depositional processes on the deep Niger Delta Continental Margin,*Marine and Petroleum Geology*, *11*(3), 320-346.Damuth, J. E. (1994). Neogene gravity tectonics and depositional processes on the deep Niger Delta continental margin. Marine and Petroleum Geology, 11(3), 320–346. doi:10.1016/0264-8172(94)90053-1

Doust, H.,and Omatsola, E. (1990). Niger delta: in J. D. Edwards and P.A.Santogrossi, eds., Divergent/passive margin basins: AAPG Memoir 48, 239-247.

Embry, A.F. (2009).*Practical Sequence Stratigraphy*. Canadian Society of Petroleum Geologists, 10-65.

Emery, D. and Myers, K., (Eds.). (1996): *Sequence Stratigraphy*. Blackwell ScienceLtd: London, Uk, 200-250.doi.org/10.1002/9781444313710

Evamy, B.D., Haremboure, J., and Kame, P. (1978).*Hydrocarbon habitat of tertiary Niger Delta.AAPG Bulletin*, *62*. 1-39. https://doi.org/10.1306/C1EA47ED-16C9-11D7-8645000102C1865D

Feely, M.H., Moore, T.C. (Jr)., Loutit, T.S., and Bryant, W.R. (2005).*Sequence Stratigraphy of Mississippi Fan Related To Oxygen Isotope Sea Level Index,AAPG*, *7*, 407-424.

Flint, S.S., and Hodgson, D.M. (2005). *Submarine slope systems: processes and products. Geological Society, London, Special Publications*, *244*(1), 1-6. https://doi.org/10.1144/GSL.SP.2005.244.01.01

Frazier, D. (1974). Depositional episodes: their relationship to the Quaternary StratigraphicFramework in the Northwestern portion of the Gulf Basin. Bureau of Economic Geology, University of Texas, Geological Circular 74-1, 28p.

Hospers, J. (1965).*Gravity Field and Structure of the Niger Delta, Nigeria, West Africa. Geological Society of American Bulletin*, *76*(4), 407. doi:10.1130/0016-7606(1965)76[407:GFASOT]2.0.CO;2

Hunt, D., and Tucker, M. (1992). Stranded Parasequences and the Forced Regressive wedge systems tract: deposition during base level fall. *Sedimentary Geology, 81(1-2),* 1-9.https://doi.org/10.1016/0037-0738(92)90052-S

Kendal, G.W.I., Johnson, J .G., Brown J.O., and Klapper, G. (1983).*Stratigraphy And Facies across Lower Devonian-Middle Devonian Boundary, Central Nevada*. *AAPG*, *67*(12), 2199p.https://doi.org/10.1306/AD460940-16F7-11D7-8645000102C1865D

Knox, G.J., and E.M., Omatsola. (1989).Development of the Cenozoic Niger Delta in Terms of the "Escalator regression" Model and Impact on Hydrocarbon Distribution. In: van der Linden, W.J.M., et al., Proceedings KNGMG Symposium on Coastal Lowlands, Geology, Geotechnology.

Kluwer Academic Publishers, Dordrecht, 181-202.

Kulke, H., (1995). Nigeria. In: Kulke, H., Ed., Regional Petroleum Geology of the World. Part II, Africa, America, Australia and Antarctica, Gebruder Borntraeger, Berlin, 143-172.

Lehner, P., and De Ruiter, P.A.C. (1977).*Structural history of Atlantic Margin of Africa:AAPG*, *61*, 961-981.https://doi.org/10.1306/C1EA43B0-16C9-11D7-8645000102C1865D

Liangqing, X., and Galloway, W.E. (1993).*Genetic Sequence Stratigraphy Framework, Depositional Style, and Hydrocarbon Occurrence of The Upper Cretaceous QYN Formations inthe Songliao Lacustrine Basin, Northeastern China.AAPG*, *7*, 407.https://doi.org/10.1306/BDFF8F42-1718-11D7-8645000102C1865D

Nichols, G. (2009).*Sedimentology and Stratigraphy*, (2nded.). Wiley-Blackwell.

Ozumba, B.M., 1999. Middle to late miocene sequence stratigraphy of the Western Niger Delta. *NAPE Bulletin*, *13*, pp.176-192.

Posamentier, H.W., and Allen, G.P. (1999).*Concepts and applications of Siliciclastic sequence stratigraphy*. SEPM.

Posamentier, H.W., and Kolla, V. (2003). Processes and reservoir architecture of deep water sinuous channels from the shelf edge to the basin floor, based on analyses of 3D seismic and sidescan imagery , in D. Hodgson, C.

Short, K. C., and A. J. Stauble. (1967). Outline of Geology of Niger delta: *AAPG*, *51*(5), 761-779.https://doi.org/10.1306/5D25C0CF-16C1-11D7-8645000102C1865D

Sloss, L., Moore, R.C., McKee, E.D., Muller, S.W., Spieker, E.M., Wood, H.E., Krumbein, W.C., and Dapples, E.C. (1949). Integrated facies analysis, In: Longwell, C.R., (ed.).SEDIMENTARY FACIES IN GEOLOGIC HISTORY: Geological Society America, Memoir 39, 93-113.

Stacher, P. (1995). Present understanding of the Niger delta hydrocarbon habitat, in Oti, M. N. and Postma, G. (Eds.). Geology of deltas: Rotterdam, A.A. Balkema, 257-267.

Vail, P. R., R. M. Mitchum, and S. Thompson (1977). In Seismic stratigraphy and global changes of sea level, part 3: Relative changes of sea level from coastal onlap, in C. W. Payton, ed. Seismic stratigraphy—Applications to hydrocarbon exploration: AAPG Memoir 26, p. 63-97.

Weber, K.J. and Daukoru, E.M. (1975).PETROLEUM GEOLOGY OF THE NIGER DELTA: Proceedings of the 9th World Petroleum Congress, Tokyo, *2*, 209-221

Wheeler, H.E., and Murray, H. (1957). Base level control patterns in cyclothemic sedimentation: AAPG Bulletin, vol. 41, 1985-2011.

Xiao, H., and Suppe, J. (1992).*Origin of Rollover*. *AAPG Bulletin*, *76*, 509-529.

Scientia Africana, Vol. 21 (No. 1), April, 2022. Pp 149-158 *https://dx.doi.org/10.4314/sa.v21i1.13*
© Faculty of Science, University of Port Harcourt, Printed in Nigeria *ISSN 1118 – 1931*

PHYTOCHEMICAL SCREENING AND PROXIMATE ANALYSIS OF THE LEAF EXTRACTS OF *VITEX DONIANA*

***Ushie, O. A., Longbap, B. D., Azuaga, T.I., Iyen, S. I., Ugwuja, D. I and Ijoko, R. F.**
Department of Chemical Science, Federal University, Wukari, Taraba State, Nigeria.
* Correspondence Author: ushie@fuwukari.edu.ng or afiushie@yahoo.com

Received: 20-11-2021
Accepted: 20-03-2022

ABSTRACT

The method of cold maceration was used in the extraction by serial exhaustive extraction method which involves successive extraction with solvents of increasing polarity from a non-polar (hexane) to a more polar solvent (methanol) to ensure that a wide polarity range of compound could be extracted. The phytochemical screening of the crude extract of Vitex doniana showed that flavonoids, steroids, phlobatannins, alkaloids, saponins were found to be present. Alkaloids were detected in the methanol, n-Hexane, acetone and ethyl acetate extracts when Wagner`s reagent was used. Flavonoids were detected in the methanol, hexane and acetone extracts when treated with NaOH and was present in all extracts with the exception of methanol extract when treated with lead acetate. Acetone extract indicated the presence of phlobatannins, but phlobatannins was absent in the hexane, ethyl acetate, and methanol extracts. Proximate analysis for the leaves of Vitex doniana revealed moisture content (7.04%), crude fibre (8.12%), crude protein (51.80%), ash (5.5%) fat (16.33%) and carbohydrate (11.21%) indicating high nutritional value.

INTRODUCTION

The use of plants for the treatment of diseases and maintenance of good health has been well researched. Kamba and Hassan (2010) reported that plants and plant-based products are the bases of many modern pharmaceuticals used today for the treatment of various ailments. Modern society is now embracing the use of plants and plant-based products to meet societal health needs due to the fact that indiscriminate use of commercial antibiotics commonly utilized in the treatment of infectious diseases has led to the development of multiple drug resistance with attendant adverse effect on the host (Gupta *et al*., 2008). This emergence of pathogens resistant to antibiotics as a result of their excessive use in clinical and veterinary applications represents a serious public health concern (Keymanesh *et al*., 2009). The resistance of bacteria and fungi to these drugs is becoming increasingly important (Lagnika*et al*., 2012). This resistance has led to the search for plants with antibacterial and antifungal activity in recent years. Other factors responsible for the use of plants in traditional as well as in modern medicine include safety, cost effectiveness (Koche *et al*., 2011) and adulteration of synthetic drugs (Shariff, 2001). Such plants have been effectively used both in the treatment of infectious diseases to mitigated many of the side effects that are associated with synthetic antimicrobials (Perumalsamy and Ignacimuthu, 2000). The stem bark extract of *Vitex doniana* is used for the control of hypertension, treatment of stomach ache,

pains, disorders, indigestion and sterility (Ladeji and Okoye, 1996). It has also been used for the production of dyestuff for textile materials (Tadzabia, *et al*., 2013 and Aiwonegbe *et al.,* 2017).The search for more nutrition sources among forest products has called for the proximate analysis of *Vitex doniana* (Adejumo *et al.,* 2013). Most foreign drugs are expensive to purchase and may not be easy to find in our locality. Phytochemical screenings are usually considered as the first step toward the discovery of useful drugs in which the nature has taken as a potential source to its divers in plants (Obgbannia *et al.,* 2013).

There are still over a thousand species of plants which contain substances of medicinal and nutritional value which are yet to be discovered. *Vitex doniana* is one of the plants which have been used in traditional medicine for decades of years. This study is designed to enrich the available scientific proof on the phytochemistry and proximate analysis of *V. doniana* leaves. This work was initiated to justify the claims of the traditional uses of the plants by performing a test of the active component through phytochemical screening and also to ascertain the nutitional value of *V. doniana* through proximate analysis. The results obtained from this research are useful because the extracts of *V. doniana* prove that indeed *Vitex doniana* has nutritional value and the use of this plant for medicinal purposes is safe. To the best of our knowledge little or no work has been done on the plant *Vitex doniana* in Taraba, Nigeria. This work is designed to enrich the available scientific data on the phytochemistry and nutrient content *Vitex doniana* leaves. Hence, this paper reports the phytochemistry and nutrient content *Vitex doniana* leaves on some bacterial and fungal isolates. The aim of the study is to carry out preliminary phytochemical screening and proximate analysis on the leaves of *Vitex doniana* with a view of identifying the phytochemicals and nutrients content present.

MATERIALS AND METHOD

Sample Collection and Preparation

The leaves of *Vitex doniana* sample were collected from its natural habitat in the main town of Wukari Taraba state, Nigeria. The leaf sample was dried for two weeks at room temperature. The powdered plant sample part were store in an air tight labeled plastic container and were used for extraction purpose. The method of cold maceration was used in the extraction by serial exhaustive extraction method as described by Pavia, 1976. This involves successive extraction with solvents of increasing polarity from a non-polar (hexane) to a more polar solvent (methanol) to ensure that a wide polarity range of compounds could be extracted. The leaf extracts were prepared by soaking 100g of each of the sample in 250ml hexane for four days with frequent agitation until soluble matter was dissolved. The resulting mixture was filtered using filter paper and the filtrate was concentrated by evaporation using rotary evaporator. This was then kept in a vacuum oven overnight at room temperature to remove any residual solvent before the sample was weighed. The procedure was repeated on the residue using the following solvents; chloroform, ethyl acetate, acetone and ethanol sequentially in order of polarity. The extracts were kept in the refrigerator until required for testing.

Scientia Africana, Vol. 21 (No. 1), April, 2022. Pp 149-158 *https://dx.doi.org/10.4314/sa.v21i1.13*
© Faculty of Science, University of Port Harcourt, Printed in Nigeria *ISSN 1118 – 1931*

Phytochemical Screening

Phytochemical examinations were carried out for all the extracts using standard procedures to identify the constituents. Qualitative analysis of the crude extracts were carried out to identify the presence of the classes of secondary metabolites (alkaloids, anthraquinones, flavonoids, tannins, saponins, glycosides, cardiac glycosides, terpenes, steroids, phenol, etc) as previously described (Tiwari*et al*., 2011; Ushie and Adamu, 2013; Kendeson*et al*., 2019; Ushie *et al*., 2019)

Detection of Alkaloids

Extracts were dissolved individually in dilute hydrochloric acid and filtered and were subjected to Mayer's Test and Wagner's Test:

Mayer's Test

Filtrates were treated with Mayer's reagent (Potassium Mercuric Iodide). Formation of a yellow coloured precipitate indicates the presence of alkaloids.

Wagner's Test

Filtrates were treated with Wagner's reagent (Iodine in Potassium Iodide). Formation of brown/reddish precipitate indicates the presence of alkaloids.

Detection of Glycosides

Extracts were subjected to test Modified Born Trager's Test for glycosides.

Modified Born Trager's Test

Extracts were treated with ferric chloride solution and immersed in boiling water for about 5 minutes. The mixture was cooled and extracted with equal volumes of benzene. The benzene layer was separated and treated with ammonia solution. Formation of rose-pink colour in the ammoniacal layer indicates the presence of anthranol glycosides.

Detection of Saponins

Extracts were dissolved individually in dilute Hydrochloric acid and filtered and were subjected to **Froth Test** andFoam Test.

Froth Test

Extracts were diluted with distilled water to 20ml and this was shaken in a graduated cylinder for 15 minutes. Formation of 1 cm layer of foam indicates the presence of saponins.

Foam Test

0.5 gm of extract was shaken with 2 ml of water. If foam produced persists for ten minutes it indicates the presence of saponins.

Detection of Flavonoids

Extracts were subjected to Alkaline Reagent and Lead acetate for the detection of flavonoids

Alkaline Reagent Test

Extracts were treated with few drops of sodium hydroxide solution. Formation of intense yellow colour, which becomes colourless on addition of dilute acid, indicates the presence of flavonoids.

Lead acetate Test

Extracts were treated with few drops of lead acetate solution. Formation of yellow colour precipitate indicates the presence of flavonoids.

Detection of Tannins

A small quantity or the extract was mixed with distilled water and heated in a water

bath. The mixture was filtered and ferric chloride was added to the filtrate. A blue black or brownish green indicate the presence of tannins.

Detection of Anthraquinone

About 0.5g of the extrac**t** was boiled with 2ml HCI for few minutes in a water bath. The resultant solution was filtered and allowed to cool. Equal volume of chloroform was added to the filtrate. Few drops of 10% NH_3 solution was added to the mixture and heated. The formation of rose-pink colour indicated the presence of anthraquinone.

Detection of Terpenoids

The extract (0.2g) was mixed with 2ml chloroform, and 3ml concentrated H_2SO_4 was carefully added to form a layer. A reddish brown interface was formed which indicated the presence of terpenoids.

Detection of Phenol

To 1ml of leaf extract 2ml of distilled water was added followed by a few drops of 10% ferric chloride. Formation of blue or black colour indicates the presence of phenols.

Test for Phlobatannins

A portion of each extract was boiled with 1% aqueous HCI. The solutions were observed for a red deposit of precipitate taken as evidence for the presence of phlobatannins.

Test for Steroids

5 drops of concentrated H_2SO_4 was added to1ml of each extract in a test tube. The solutions were observed for a red colouration indicating the presence of steroids in the extracts.

Proximate Analysis of *Vitex doniana*

The powdered air dried leaves were taken for proximate analysis. The moisture, crude fibre, crude protein, ash, crude fat and carbohydrate of the samples were determined using the standard methods of the Association of Official Analytical Chemists (AOAC, 2000). All determinations were done in triplicates. The proximate values were reported in percentage. Determination of moisture content was done by weighing the sample in crucible and drying in oven at 105 0C, until a constant weight was obtained, determination of ash content was done by ashing at 550 ^{0}C for about 3 hours. The Kjeldah method was used to determine the protein content by multiplication of the nitrogen value with a conversion factor of 6.25. The crude fibre content of the samples was determined by digestion method and the crude fat was done by Soxhlet extraction method. Total Carbohydrate content was estimated based on the net difference between the other nutrients and the total percentage composition (100 %.).

Scientia Africana, Vol. 21 (No. 1), April, 2022. Pp 149-158 *https://dx.doi.org/10.4314/sa.v21i1.13*
© Faculty of Science, University of Port Harcourt, Printed in Nigeria *ISSN 1118 – 1931*

RESULTS

Table 1: Results of Preliminary Phytochemicals Screening from leaves of *Vitex doniana*

Phytochemicals	Reagents	HE	EAE	AE	ME
Flavonoids	Alkaline Test	+	+	+	-
	Lead acetate test	+	-	+	+
Alkaloids	**Mayer**	+	-	+	+
	Wagner	+	+	+	+
Steroids	**Extract+ H_2S0_4 + Acetic acid**	-	-	+	-
Tannins	**Extract + H_2O + $FeCl_3$**	+	-	-	+
Saponins	**Froth test**	-	-	+	+
	Foam test	+	-	+	+
Phlobatannins	**Extract+ 2% HCl**	-	-	+	-
Phenols	**Extract+ H_2O+ $FeCl_3$**	+	+	+	+

Key= HE= Hexane Extract, EAE= Ethyl Acetate Extract, ME= Methanol Extract, AE= Acetone Extract

Table2 Proximate Percentage (%) Compositions of leaves of *Vitex doniana*

S/N	Element	Mean (%)
1	Moisture content	**7.**04
2	Crude protein	51.80
3	Crude fibre	8.12
4	Ash	5.50
5	Fat	16.33
6	Carbohydrate	11.21

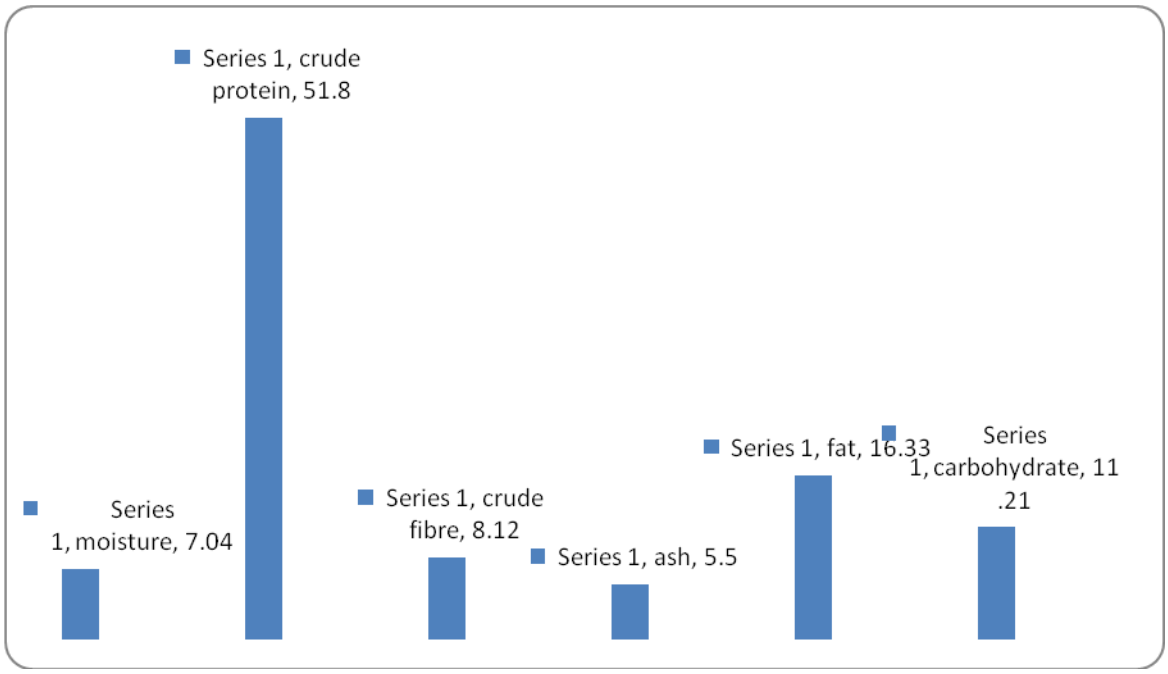

Figure 1: Histogram of Proximate % Composition of *Vitex doniana*

DISCUSSIONS

Preliminary Phytochemical Screening

The phytochemical screening of crude yields of *Vitex doniana* showed that flavonoids, steroids, phlobatannins, alkaloids, saponins were found to be present.

Tannins were found to be present in the methanol and hexane extracts. Hence, *Vitex doniana* can be a non-toxic and can they generate physiological responses in animals that consume them because of the presence of tannins (McDevitt *et al.*, 1996). The presence of tannin in the medicinal plant suggests that the *V. doniana* have muscle relaxant property and can be utilized for their analgesic, antispasmodic and bactericidal effects (Stray, 1998; Okwu and Okwu, 2004). Alkaloids were detected in the methanol, n-Hexane, acetone and ethyl acetate extracts. Alkaloids have been found to have microbiocidal effect and the major anti-diarrheal effect is probably due to their effects on the small intestine andantihypertensive antifungal, antiinflammatory, antifibrogenic effect (Ghosal *et al.*, 1996). Alkaloids in plants are used in medicine as anaesthetic agents (Herourat *et al.*, 1998). Flavonoids were detected in the methanol, hexane and acetone extracts. Hence, *Vitex doniana* can be used to modifythe body's reaction to allergens, virus and caranogens. It has been reported to show anti-inflammatory, antifungal, antibacterial and antimicrobial activities based on the literature (Cushnie and Lamb, 2005).

Vitex doniana is important in pharmacy due to the presence of steroidal compounds which has a relationship with sex hormones (Okwu, 2001). Saponins were found to be present in the methanol extract and acetone extract. The presence of saponins in the seeds can be useful in treating inflammation. Saponins have the

Scientia Africana, Vol. 21 (No. 1), April, 2022. Pp 149-158 *https://dx.doi.org/10.4314/sa.v21i1.13*
© Faculty of Science, University of Port Harcourt, Printed in Nigeria *ISSN 1118 – 1931*

property of precipitating and coagulating red blood cells. Some of the characteristics of saponins include formation of foams in aqueous solutions, haemolytic activity, cholesterol binding properties and bitterness (Rita *et al*., 2015). Also in nature, saponins appear to act as antibiotics that protect plants from microbes (Opara *et al*., 2019).

Phenols are present in the extracts of *Vitex doniana*, thus can normally be involved in defense against ultraviolet radiation or aggression by pathogens, parasites and predators, as well as causative to plants colours. They are ubiquitous in all plant organs and are therefore an integral part of the human diet (Dai and Mumper, 2010). Also, phenolic compounds can inhibit the absorption of amylase in the treatment of carbohydrate absorption, such as diabetes (Sales *et al*., 2012)

Proximate analysis is conventionally used to assess the food value of feed substance (AOAC, 2000). The proximate analysis of *Vitex doniana* also showed it to contain protein, ash and moisture in reasonable as well as carbohydrate, fat and oil and fibre (Table 2). The leaves contain a significant amount of fibers which is necessary for digestion and for effective elimination of wastes, and can lower the serum cholesterol, the risk of coronary heart disease, hypertension, constipation, diabetes, colon and breast cancer (Ishida *et al*., 2000). Ash content determined is considerable high which suggest that the selected plant seeds could be good sources of mineral elements (Ajayi and Ojelre, 2013). The ash content is a reflection of the amount of mineral elements present in the samples; therefore, the plants contained a good amount of minerals (Aborisade *et al*., 2017). The leaves of *Vitex doniana* contain reasonable amount of carbohydrates and are known to be important components in many foods. Carbohydrate constitutes a major class of naturally occurring organic compounds that are essential for the safeguarding and nourishment of life in plants and animals and also provide raw materials for many industries (Ebun-Oluwa and Alade 2007). The leaf is a good source of carbohydrate when consumed because it meets the Recommended Dietary Allowance values (FND,2002). The leaves of *V. doniana* also contain crude proteins as were revealed in the results. Jitendra *et al.*(2013) pointed out that among nutrients, the human body requires proteins as the most important compounds because they aid in building cells and tissues and help in repairing the tissues in the body. A high protein diet is recommended for those thinking of building body or muscles. Many versatile plant proteins are used as medicinal agents as they are produced by using molecular tools of biotechnology (Jitendra *et al.*, 2013).

CONCLUSION

From the results obtained from the analysis carried out on the leaves of this plant (*Vitex doniana*) we can conclusively say that this plant uncovers the possibility of it being a potent source of food nutrients and medicine. We can also conclude that since the leaves of *Vitex doniana* contains some significant phytochemicals such as flavonoids, phlobatannins, steroids, tannins, alkaloids, spaonins and phenols, it has some biochemical functions in the body and is an essential nutrient source. This plant is also a potent antibiotic and blood building agent as well as possesses medicinal value. Therefore, it could be

exploited for use in the formulation of cheap alternative antimicrobial drugs to cure or control human infectious diseases. This study has also showed that extracts of *Vitex doniana* contains significant levels of macro and micro nutrients i.e. carbohydrate, crude protein, crude fat, crude fibre, moisture, ash (minerals) therefore consumption of this plant is encouraged with exception of the aged due to the effect on the protein content in the liver of old people.

REFERENCES

Aborisade, A. B., Adetutu, A., Owoade, A. O. (2017).*Phytochemical and Proximate Analysis of Some Medicinal Leaves. Clinical Medicine Research*; 6(6): *209-214*

Adejumo, O. E., Kolapo, A. L., Folain, A. O(2012). *Moringa oleifera* Lam. (Moringaceae) grown in Nigeria: *In vitro antisickling activity on deoxygenated erythrocyte cells. Journal of Pharmacy and Bioallied sciences.4(2): 118-122*

Aiwonegbe, A. E., Iyasele, J.U. and Momodebe R. O. (2017).*Characterization ofa natural dye produced from the alcoholic extract ofAfrican black plum (Vitex doniana) fruit pulp using wool fabric. Proceedings ofthe 16th Annual International Conference of Nigerian Material Congress, Material Science and Technology Society ofNigeria (MSN)*. pp105- 109.

Ajayi, I. A. and Ojelere, O. O. (2013). *Phytochemical Screening, Proximate analysis and Anticancer Properties,Molecules.15(10): 7313–7352.*

AOAC 2000. *Association of Official Analytical Chemists; Official method of analysis. 15thEdn,cathatica*) seed. *PakistanJournal of Nutrition, 6: 345-348.*

Cushnie T. P. and Lamb A. J. (2005). Antimicrobial activity of flavonoids: *International Journal of Antimicrobial Agents. 26:343-356.*

Dai, J. and Mumper, R. J. (2010).*Plant Phenolics: Extraction, Analysis and their Antioxidant Different Plants of North-Eastern Region of India. Molecules 15, 7313-7352*

Ebun-Oluwa and Alade A. S. (2007). *Nutritional Potential of Berlandier Nettle spurge (Jatropha evaluation of chemicalcomponent of leaves stalks and stems of sweet potatoes (Ipomoea batatas poir).* Food Chem., 68: 359-367.

F. N. D. (2002). *Food and Nutrition Board, Institute of Medicines. National Academy of for the treatment of diarrhea in AIDS patients abstract. In program and Abstracts of the 36th Interscience conference on Antimicrobial Agents and Chemotherapy.American Society for Microbiology*, Washington, D. C.

Ghosal S., Krishna-Prasad B. N. and Laksmi V. (1996). Antiamoebic activity of Piper longum fruits against Entamoeba histolytica in vivo. *Journal of Ethnopharmacology.50:167-170.*

Gupta, C., Amar, P., Ramesh, G., Uriya, C. and Kumari, A. 2008.*Antimicrobial activity of some herbal oils against common food-borne pathogens. African Journal of Microbiology Research2, 258-261.*

Scientia Africana, Vol. 21 (No. 1), April, 2022. Pp 149-158 https://dx.doi.org/10.4314/sa.v21i1.13
© Faculty of Science, University of Port Harcourt, Printed in Nigeria *ISSN 1118 – 1931*

Herourat D, Sangwin R.S, Finiaux M.A, Sangwan-Norrel B.S. (1988).*Variationsin the leaf alkaloid content of androgenicdiploid plants of Daturuinnoxia, Planta medical Journal of Medicinal Plants Research .54:14-20.*

Ishida H, Suzuno H, Sugiyama N, Innami S, Todokoro T, Maekawa A (2000).*Nutritional evaluation of chemical Component of leaves stalks and stems of sweet potatoes* (*Ipomoea batatas* poir). *Food Chemistry, 68: 359-367*

Jitendra Y. Nehete, Rajendra S. Bhambar, Minal R. Narkhede,and Sonali R. Gawali (2013) *Natural proteins: Sources, isolation, characterization and applications. Pharmacognosy Reviews 7(14): 107–116.*

Kamba,A.S.and Hassan,L.G.(2010)..*Phytochemical screening and antimicrobial activities of Euphorbiabalasamifera leaves, stem and root against some pathogenic microorganisms. African Journal of Pharmacy and Pharmacology(1), 57-64.*

Kendeson A. C., Iloka S. G., Abdulkadir A. G., Ushie O. A**,**Abdu Z.,Jibril S. & John S. T. (2019). *Phytochemical Screening, Antimicrobial and Elemental Analyses of Crude Extracts from Cocos nucifera (Coconut) Shell. Dutse Journal of Pure and Applied Sciences (DUJOPAS), 5 (1b): 169 - 175.*

Keymanesh, K.,Hamedi. J., Moradi,S., Mohammadipanah, F.and Sardari, S (2009). *Antibacterial, antifungal and toxicity of rare Iranian plants. International Journal of Pharmaceutics.5, 82-85.*

Koche, D. K., Bhadange, D. G. and Kamble, K. D. (2011). *Antimicrobial activity of three medicinal plants. Bioscience Discovery 2(1), 69-71.*

Ladeji, O., Udo, F. V., Okoye, Z. S. C. 2004. *Activity ofaqueous extract ofthe bark of Vitex doniana on some Uterine Muscle Response to Drugs.Phytotherapy Research 19, 804 - 806.*

Lagnika, L., Amoussa,M., Adjovi, Y. and Sanni, A. (2012). *Antifungal,antibacterial and antioxidant properties of Adansoniadigitata and Vitexdoniana from Béninp harmacopeia.J. Pharmacog.and Phytotherapy*.4(4), 44-52.

McDevitt J. T., Schneider D. M., Katiyar S. K. and Edlind F. S. (1996). *Berberina: a candidate for the treatment of diarrhea in AIDS patients abstract. In program and Abstracts of the 36th Interscience conference on Antimicrobial Agents and Chemotherapy. American Society for Microbiology*, Washington, D. C.

Ogbonnia, S. O.; Mbaka, G. O.; Nwozor, A. M.; Igbokwe, H.N.;Usman, A.; Odusanya, P. A. (2013). *Evaluation of microbial purity and acute and sub-acute toxicities of a Nigerian commercial Polyherbal formulation used in the treatment of diabetes mellitus. British Journal of Pharmaceutical Research*3(4):948-962.

Okwu, D. E and Okwu, M. E. (2001). *Chemical composition of Spondia mombin plants. Journal* of *Sustainable*

Agriculture and *Environment 6, 140-147*.

Opara I.J., Ushie O. A., Aondoyima.I and Onudibia M.E. (2019**).** *Phytochemical Screening, Proximate and Vitamin Composition of Cucumismelo Seeds(Sweet Melon).International Journal of Research in InformativeScience Application & Techniques (IJRISAT). 3(1) 193122 – 193128*

Pavia, L.K. (1976). *A contemporary approach, Introduction to organic laboratory techniques, N.B. Saunders company Canada,46, 50, 358, 599 - 605.*

Rita N., Baruah K.K, Sarma S, Bhuyan R., Roy D.C and Mithu, D. (2015). *Phytochemical Screening of Different Plants of North-Eastern Region of India. Journal of Bioscience and Bioengineering 2: 9-11*

Sales P.M., Souza P.M., Simeoni L.A., Magalhães P.O., Silveira D (2012). *α-Amylase Inhibitor: A review of Raw Material and Isolated Compounds from Plant Source. J. Pharm. Sci. 15:141–183.*

Stray F (1998). *The natural guide to medicinal herbs and plants. Tiger Books International, London, pp. 12-16*

Tadzabia, K., Maina, H.M., Maitera, O.N. and Osunlaja, A.A. (2013). *Elemental and physiochemical screening of Vitex doniana leaves and stem bark in Hong Local Govt. Area of Adamawa State, Nigeria.InternationalJournal* of *Chemical Studies (3), 150 -156.*

Tiwari, P., Kumar, B., Kaur, M., Kaur, G., Kaur, H.(2011). *Phytochemical Screening and Extraction: A Review. Internationale Pharmaceutica Sciencia* 1(1):98-106.

Ushie O A and Adamu. H.M (2010). Phytochemical Screening of *Borreria verticillata* Leaves.- *Journal of Agriculture, Biotechnology and Ecology* 3(1), 108-117

Ushie, O. A., Abeng, F. E., Azuaga, T. I., Donatus, R. B., Ama, S. O. and Aikhoje, E. F. (2019). *Phytochemical Screening and Bioactivity of Chloroform, Acetone and Ethyl Acetate, Extracts of Haematostaphis Barteri***.** *FUDMA Journal of Sciences (FJS)3(4), pp 138 –143*

Scientia Africana, Vol. 21 (No. 1), April, 2022. Pp 159-174 *https://dx.doi.org/10.4314/sa.v21i1.14*
© Faculty of Science, University of Port Harcourt, Printed in Nigeria *ISSN 1118 – 1931*

PREDICTIVE HOSPITAL SITE SELECTION MODEL USING MACHINE LEARNING TECHNIQUES

Okengwu[1], U. A., Memmert[2], D., Rein[2], R. and Osuigbo,[3] E. N.
[1]Department of Computer Science, University of Port Harcourt, Port Harcourt, Nigeria
[2]Institute of Exercise Training and Sport Informatics, German Sport University, Cologne, Germany
[3]Department of Computer Science, Kenule Beeson Saro-Wiwa Polytechnic, Bori, Nigeria
*Corresponding Author: Email:ugochi.okengwu@uniport.edu.ng

Received: 09-02-2022
Accepted: 20-03-2022

ABSTRACT

Globally, countries are faced with healthcare challenges that vary from one to the next. While health service delivery challenges are more often seen in countries with a very high HumanDevelopment Index (HDI), inefficient healthcare intervention challenges attract more attention in those with a low HDI. Health systems and infrastructure interventions are major challenges for most countries in Africa. The conventional or traditional approach to situating hospitals has been subjected to the unreliable intuition of experts and perhaps biased by nepotism, favoritism, and tribalism of recognized interest. In this research, we prioritize health factors for hospital site predictions. A hospital is a healthcare intervention infrastructure that should meet the healthcare needs of people where it is located. Many hospital site selection researchers have considered other important factors such as geographical, economic, and socio-demographic factors. However, healthcare factors that will specifically address the healthcare needs of people in that locality have not been mentioned. This paper considers a robust, viable, reliable, and dependable approach to solve the specific problem of selecting the best location for building new hospitals based on the specific healthcare needs of the location for improved healthcare service delivery. We propose a supervised machine learning approach to predict the most suitable sites for building new hospitals. Support Vector Machine (SVM), K-Nearest Neighbours (KNN), Logistic Regression (LGR), and Decision Tree (DT) machine learning algorithm are used to predict the optimal location for hospital site selection on the basis of various attributes used in the dataset. The dataset was extracted from clinical exploratory data using parameters such as reproductive, maternal, newborn, and child health, Infectious diseases, Non-communicable diseases, Adequate sanitation, Service capacity, and access to essential medicines as a Universal Health Coverage (UHC) standard by World Health Organization (WHO). The model is implemented using Python programming language. The system will improve health systems and infrastructural interventions, thereby enabling efficient healthcare service delivery in developing countries, especially in Africa.

Keywords: Decision Tree (DT), Healthcare, Hospital site selection, K-Nearest Neighbours (KNN) Logistic Regression (LGR) Prediction, Support Vector Machine (SVM).

INTRODUCTION

Man-made difficulties have harmed Africa's healthcare systems over the years, affecting institutional, human resource, financial, technical, and political advancements (Roncarolo et al., 2013). The majority of low-HDI countries, particularly in Africa, are unable to achieve the minimum criterion for good healthcare systems and infrastructure. In resource-constrained countries, inadequate service

integration is connected to poor governance and human resource issues (Petersen et al., 2017; Marais and Petersen, 2015).

One key issue that has persisted over time is healthcare system inefficiency and infrastructure interventions, both of which have had a significant impact on the quality of healthcare service delivery. Cost, land availability, population, cultural concerns, manpower, proximity to man and natural elements, and access to inexpensive capital have all contributed to the difficulty of locating hospitals and healthcare institutions in various locations (Cynthia and Debra, 2011; Bob, 2012). These fundamental difficulties have had a significant impact on the availability of hospitals and medical centers for the general public. Because of the limited financial resources available to executive and administrative officers, further amenities have been completely neglected. These cost difficulties have also been exacerbated by a managerial or administrative officer's self-centered mindset, which has resulted in corrupt actions aimed at emptying public treasuries for personal gain. Although the land may appear to be available, due to the required size for establishing such hospitals, land availability can be a barrier. This can be tough to achieve in big cities with the required population size for siting hospitals, but less difficult in rural areas missing the fundamentals criteria fostering the siting of such establishment. The primary goal of hospital facilities is to provide health services within a specific geographic area in order to meet the healthcare needs of individuals (population size) who lack these services or who require more services. As a result, the population is critical in determining where hospitals should be located. The eventual location of medical institutions and their operational effectiveness might be determined by the cultural backdrop and background of a given community (Owen and Lawrence, 1996).

If hospital facilities are to function successfully, meeting the needs and desires of healthcare recipients, these elements cannot be overlooked. In fact, combining these criteria results in facilities that are strategically located to generate relevant money while providing essential services to the general public. As a result, the World Health Organization (WHO) developed a Universal Health Coverage (UHC) medical care standard to ensure that all people and communities have access to the health care they require without facing obstacles such as financial hardship, nepotism, or outright disregard.

In this study, an improved model that efficiently predicts optimal locations for situating hospitals using a supervised machine learning approach is developed. An efficient approach for situating the hospitals is undoubtedly a predominant challenge that has affected the quality of health service delivery in developing countries. Health systems and infrastructure are crucial components of a wider healthcare intervention approach, but if not placed correctly, they can disrupt the entire process. The conventional or traditional approach to situating hospitals has been subjected to the unreliable intuition of experts and perhaps biased by nepotism, favoritism, and tribalism of recognized interest. In this work, we propose a robust and efficient model for situating hospitals in optimal locations for

Scientia Africana, Vol. 21 (No. 1), April, 2022. Pp 159-174 *https://dx.doi.org/10.4314/sa.v21i1.14*
© Faculty of Science, University of Port Harcourt, Printed in Nigeria *ISSN 1118 – 1931*

improved healthcare service delivery. This approach will apply supervised machine learning algorithms using Support Vector Machine (SVM), K-Nearest Neighbours (KKN), Logistic Regression (LGR), and Decision Tree (DT) and select the best model for implementation.

LITERATURE REVIEW

Site Selection

Site selection is a research problem whose purpose is to find the best location that meets a set of criteria (Senvar et al., 2016). As proposed by Mohammed et al., site selection typically includes two primary stages: screening (identifying a set number of prospective sites from a wide topographical region given a scope of selection elements) and assessment (extensive evaluation of options to determine the most appropriate site) (2019). The two steps involve a large number of sometimes problematic factors. When you're going through the same situation, there are a variety of tools available to help you choose the best location. Expert Systems (ES) are used for well-defined and organized issues, whereas Decision Support Systems (DSS) are used for poorly organized situations or a combination of the two((Vafaei and ztayşi, 2014).

GIS with MCDM methodologies that can help with site selection in instances when the problem is poorly organized, meaning that leaders lack complete and reliable data on specifications, options, and outcomes (Boyac and Işman, 2021). Traditional GIS site selection methods rely on the transformation of powerful layers into a classified map, such as through the use of a Boolean model or Index Overlay activity.

Various hospital site selection scholars have embraced the comprehensive assessment of a hospital site and proposed a wide range of site selection standards that are largely dominated by topographical, financial, and socio-segment variables, with little regard for medical services needs evaluation. Separation from the arterial road, travel duration, tainting, land cost, and demographics were all factors evaluated by Vahinia et al. (2008). Soltani and Marandi (2011) looked at the distance to major streets, distance to other clinical facilities, demography, and land size. Wu et al. (2007) analyzed population number, age, thickness, legislative methods, capital, work, and land while deciding on the best location for Taiwanese hospitals. Schuurman et al. (2006) also looked at the importance of the help region's socioeconomics and proximity to potential expansion, space-separated from movement time, and populace thickness.

In light of the lack of available literature addressing healthcare characteristics as a significant measure for selecting hospital sites, this study considers four significant qualities and additional sub-traits for analyzing the medical care requirements of a competitive clinic site in Rivers state. These factors are based on the World Health Organization's Universal Health Coverage (UHC) - Service Coverage Indicators (SCI) standard (WHO). UHC, according to Bloom et al. (2018), means that everybody can get the healthcare they need, when and where they need it, regardless of their financial situation.

Healthcare Interventions

The word "health intervention" refers to any activity taken with the goal of improving human health by preventing

disease, reducing the duration of an existing infection, or restoring capacity lost due to illness or injury (Glasziou et al., 2010). A wide range of new interventions, as well as new approaches for using mediations, are being developed to combat the major diseases that plague low- and middle-income countries. Some of these treatments cover both public health and clinical considerations, and include medications for acute and chronic conditions, antibodies, vector control, health education, behavior change systems, injury prevention, and better wellbeing planning and the board strategies that work on a variety of wellbeing-related activities (Clarke et al., 2019). Interventions might be best applied in populaces to decide their effect on working on the health of the populace utilizing a field trial assessment (Smit et al., 2020. Interventions can be grouped into two general classes:

i. Preventive interventions are those that keep the sickness from happening and in this manner diminish the frequency (new instances) of infection, vaccines, nutritional interventions, maternal and neonatal interventions, education and conduct change, environmental adjustments, vector, and transitional host control, medication for the avoidance of sickness, and Injury anticipation are on the whole instances of preventive medical care mediations (Clarke et al., 2019).
ii. Therapeutic interventions are those that treat, moderate, or delay the impacts of sickness when it is in progress, and in this way diminish the case casualty rate or lessen the inability or dismalnessconnected with a disease. Health systems and infrastructure interventions are all examples of therapeutic interventions (Clarke et al., 2019).
iii. A few interventions might make the two impacts. Other types of interventions are legislation, legitimate activity, tax collection, and sponsorships, Implementation research, and Complex interventions.

Universal Health Coverage (UHC) Framework

Universal Health Coverage (UHC) is a framework designed by the World Health Organization (WHO) to ensure that all individuals and networks have access to the healthcare they require without facing financial hardship. It encompasses the complete range of critical, high-quality health services, from prevention through treatment, rehabilitation, and palliative care for people of all ages (Bloom et al., 2018). These administrations want enough and capable healthcare practitioners with optimal abilities blend at the office, outreach, and community level, who are impartially disseminated, satisfactorily supported, and appreciate good work. UHC systems enable everyone to access health services that address the primary causes of illness and death, while also ensuring that the quality of those services is sufficient to improve the health of people who receive them. Protecting people from the financial consequences of paying for health services out of their own pockets reduces the risk that they will be forced into poverty because unexpected disease forces them to burn through their life investment funds, sell assets, or acquire - obliterating their prospects and, in many cases, those of their loved ones. Accomplishing UHC is one of the objectives the countries of the world set

Scientia Africana, Vol. 21 (No. 1), April, 2022. Pp 159-174 *https://dx.doi.org/10.4314/sa.v21i1.14*
© Faculty of Science, University of Port Harcourt, Printed in Nigeria *ISSN 1118 – 1931*

while taking on the SDGs in 2015 (Xu et al., 2015).

At the United Nations General Assembly High-Level Meeting on UHC in 2019, nations reiterated their commitment to achieving UHC. Nations agreed that UHC will make progress toward other well-being goals. Good health enables children to learn and adults to purchase support people in escaping poverty and provides the foundation for long-term financial success (Nygren-Krug, 2019).

WHO contributes to achieving the Thirteenth General Program of Work 2025 goal of 1 billion more people benefiting from UHC, while also contributing to the two other billion goals of 1 billion more people better protected from health crises and 1 billion more people benefiting from better health and prosperity? It also contributes to WHO's fundamental goal of the right to the most noteworthy achievable norm of wellbeing, to Health for All, and the SDGs.

Parameters for Measuring UHC

Checking the advancement towards UHC is conceivable and ought to zero in on two things:

i. The extent of a populace that can get to fundamental quality healthcare services (SDG 3.8.1).
ii. The extent of the populace that spends a lot of family income on healthcare (SDG 3.8.2).

Estimating value is additionally basic to comprehend who is as a rule left behind-where and why. Along with the World Bank, WHO has fostered a structure to follow the advancement of UHC by checking the two classifications, considering both the general level and the degree to which UHC is evenhanded, offering administration inclusion and monetary security to all individuals inside a populace, like poor people or those living in distant provincial regions. WHO involves sixteen fundamental healthcare services in four classes as signs of the level and value of inclusion in nations as displayed in Table 1:

Some data, like the number of pages of an article or catchphrases, some of the time didn't show up in the StArt tool. Hence, the analysts needed more data to decide if the article would be incorporated or avoided in stage 2. Subsequently, analysts investigated these articles physically in stage 3. In this stage, a few articles, for example, short papers and articles not written in English were found.

Table 1: Universal Health Coverage Attributes.

Attributes	Sub-attributes
Reproductive, maternal, newborn and child health (RMNC)	Family Planning Antenatal care Full child immunization Health-seeking behaviour for child illness
Infectious diseases (ID)	Malaria prevention and treatment Tuberculosis effective treatment

	Cholera Prevention and treatment
	HIV antiretroviral treatment
	Adequate sanitation
Noncommunicable diseases (ND)	Prevalence of raised blood pressure
	Mean fasting plasma glucose
	Cervical cancer screening
	Tobacco control
Service capacity and access (SCA)	Basic hospital access
	Health worker density
	Access to essential medicines
	Compliance with the International Health Regulations

CATEGORY 1: Reproductive, maternal, newborn and child health:

i. family planning
ii. antenatal and delivery care
iii. full child immunization
iv. health-seeking behaviour for pneumonia.

CATEGORY 2: Infectious diseases:

i. tuberculosis treatment
ii. HIV antiretroviral treatment
iii. use of insecticide-treated bed nets for malaria prevention
iv. adequate sanitation.

CATEGORY 3: Noncommunicable diseases:

i. prevention and treatment of raised blood pressure
ii. prevention and treatment of raised blood glucose
iii. cervical cancer screening
iv. tobacco (non-) smoking.

CATEGORY 4: Service capacity and access:

i. basic hospital access
ii. health worker density
iii. access to essential medicines
iv. health security: compliance with the International Health Regulations.

Every nation is interesting, and every nation might zero in on various regions, or foster their own specific manners of estimating progress towards UHC. In any case, there is likewise esteem in a worldwide methodology that utilizations normalized measures that are globally perceived so they are practically identical across borders and over the long run..

Study Area Evaluation

The area under investigation covers all Local Government Areas (LGAs) in Rivers State, an oil rich state located in the southern part of Nigeria. The area extends from 51023’ to 51029’ east and from 35044’ to 35048’ south. The study area and existing hospitals are shown in Fig 1. The research evaluates the healthcare needs of the study area and predicts optimal locations for new hospital sites based on the health requirements of the selected location.

Scientia Africana, Vol. 21 (No. 1), April, 2022. Pp 159-174 https://dx.doi.org/10.4314/sa.v21i1.14
© Faculty of Science, University of Port Harcourt, Printed in Nigeria *ISSN 1118 – 1931*

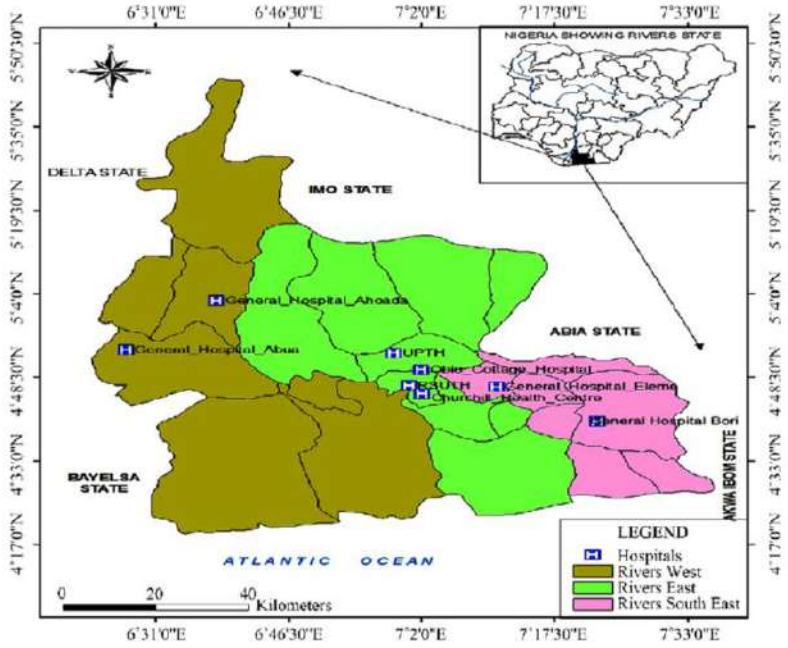

Fig. 1. Map of Rivers State showing existing hospitals.

METHODOLOGY AND ANALYSIS

The Rivers State Hospital dataset has fields without values and some values are more common than other values in the field, which makes the data distribution of the dataset unbalanced. In order to enhance the predictive performance of the model, a predictive machine learning method is proposed in this paper. The method consists of two phases: Data Preprocessing and Prediction. The whole process used in the methodology is shown in Fig 2.

Data Preprocessing

In the data preprocessing phase, data is cleaned and encoded for efficient performance of the predictive model. The data preprocessing approach used in this paper consist of three steps: Data cleaning, Value weighting and encoding.

i. *Data Cleaning:* This first step is performed to identify and correct errors in the dataset that may affect the prediction model. Columns that have a single value are probably useless for modelling and are considered as zero-variance predictors. Depending on the choice of modeling algorithm used, variables with a single value can also cause errors or unexpected results. Some columns referred to as near-zero variance predictors have few unique values (very small number close to zero) and occur infrequently in the data. Although near-zero variance predictors likely contain little valuable predictive information, they were still considered for prediction. To highlight these columns, we calculate the number of unique values for each variable as a percentage of the total number of rows in the dataset.

Visualization of Cleaned Data: The purpose of data cleaning process is to remove columns that don't contain much information and

duplicated rows to reduce the imbalance of dataset. Fig 3, 4, 5 and 6 shows the data visualization for the different parameters in the collected data indicating how they are distributed in some Local Governments Areas in Rivers State. Table 2 shows the Local Government Areas and the important variables for prediction.

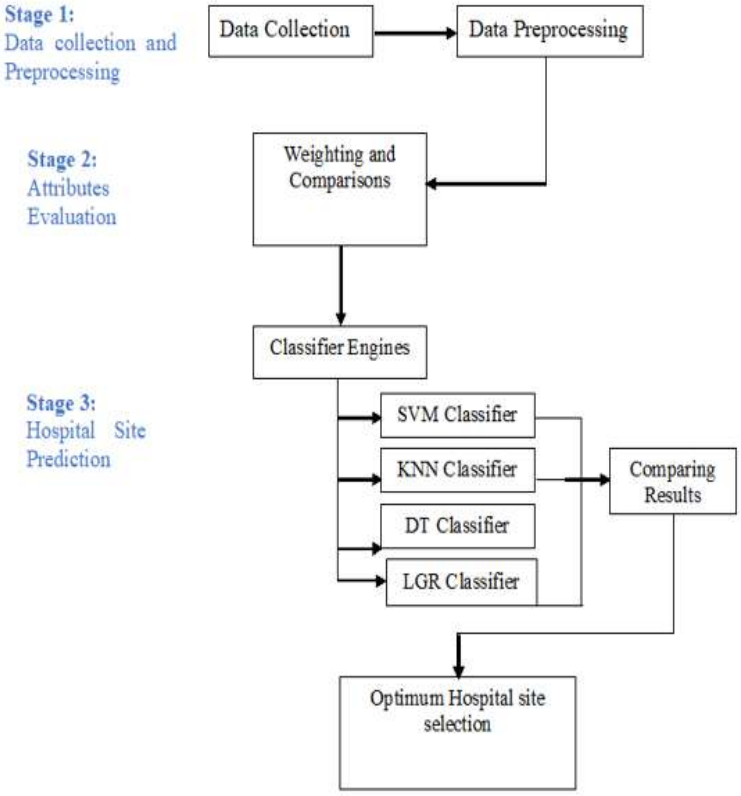

Fig. 2. System flowchart of the methodology used in this study.

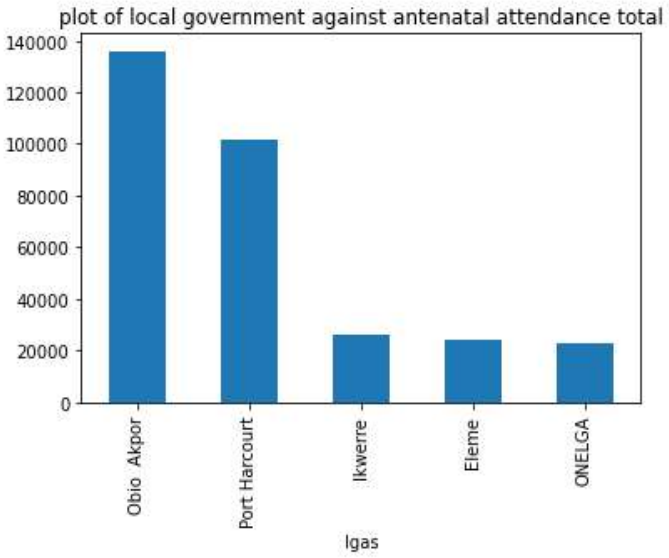

Fig. 3. Antenatal attendance across the Local Governments

Scientia Africana, Vol. 21 (No. 1), April, 2022. Pp 159-174 *https://dx.doi.org/10.4314/sa.v21i1.14*
© Faculty of Science, University of Port Harcourt, Printed in Nigeria *ISSN 1118 – 1931*

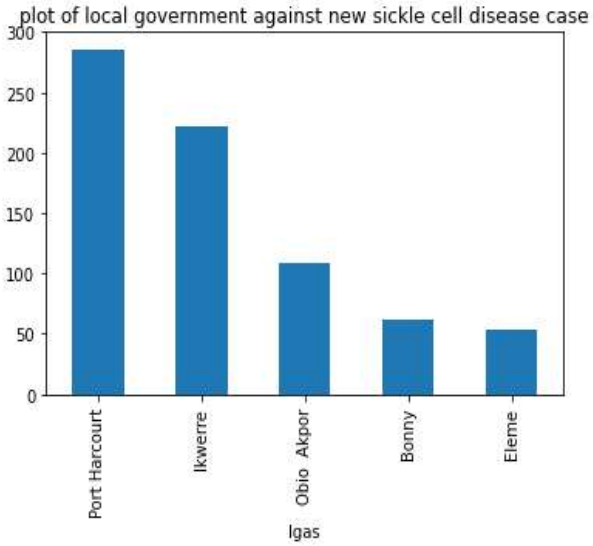

Fig. 4. HIV positive patients identified across the Local Governments

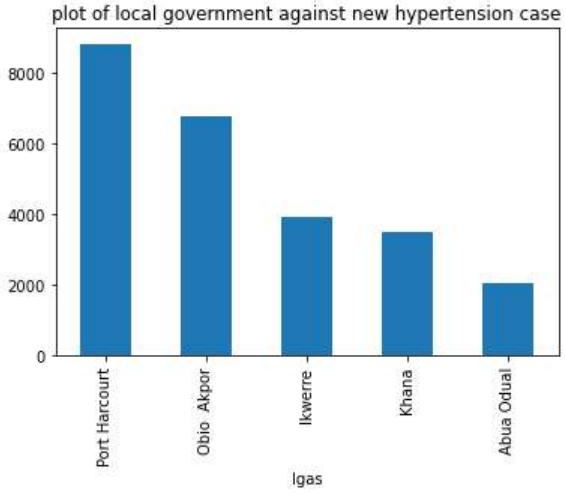

Fig. 5. Hypertension cases identified across the Local Governments

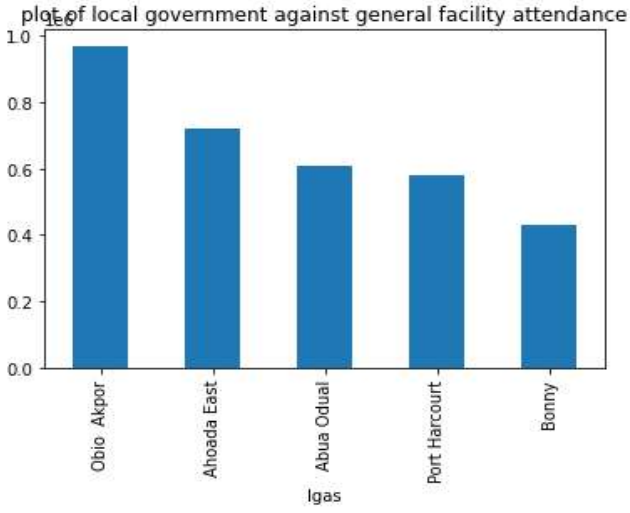

Fig. 6. The rate of attendance of patients to the hospitals in the Local Governments

Table 2: Important Variables for Prediction.

	Antenatal Care	HIV Positive	Hypertension	Hospital Access	Facility
ObioAkpor	136061	58470	6775	971100	
Port Harcourt	101533	33861	8832	579920	
Khana	170	29166	3500	94309	
Ikwerre	26019	364	3891	431265	
Eleme	24193	28252	554	85407	

Table 3: Feature importance score for the highest variables

UHC Category	Feature	Importance
Infectious diseases (ID)	HIV Positive	0.079
Reproductive, maternal, newborn and child health (RMNC)	Antenatal Care	0.056
Noncommunicable diseases (ND)	Hypertension	0.037
Service capacity and access (SCA)	Hospital Facility Access	0.037

ii. *Value Weighting:* Next, value weighing is performed as part of the data preprocessing phase. Value weighting deals with the fact that particular values in a field might be more common than other values in that field. The Machine Learning Algorithm used in this paper is supervised learning algorithm, so predicted output was derived based on the parameters or variables available by calculating percentage mean:

= [Sum of %n variables across each local government / Total number of variables]

The coincidence of rare values in a field adds more to the overall similarity than the coincidence of frequent values. A set average weight was given to be 0.75 based on the range of the values. A set average weight to each value according to its probability in the input data was given to be 0.75 corresponding to the range of the values. Rare values carry a large weight, while common values carry a small weight. This weight is used for both matching and non-matching records and determines where hospital can be located. Table 3 shows the feature importance score for highest values.

iii. *Encoding:* In this step, LGA variable is converted to numerical values by using label encoding in python as shown in Fig. 7, to enable the machine learning algorithms used in the predictive model to handle these variables. Most machine learning algorithms cannot handle non-numerical variables.

iv. *Feature Selection:* Most useful features which will be used to train the prediction model are selected in this step. Dimensionality reduction is used to remove features features that are not contributing enough to the overall variance. Important feature function was used to reduce the features to a shape of 5 rows and 124 columns as shown in Fig.7. There are different ranges of values for all variables and feature

Scientia Africana, Vol. 21 (No. 1), April, 2022. Pp 159-174 *https://dx.doi.org/10.4314/sa.v21i1.14*
© Faculty of Science, University of Port Harcourt, Printed in Nigeria *ISSN 1118 – 1931*

scaling was used to convert those values and have them under the same range of values.

The purpose of feature selection is to find the best feature subset that can maximize the performance of the prediction. Once the optimal training dataset and the optimal feature subset are selected, those will be taken into the Prediction phase.

Prediction Phase

In this phase, the goal is to predict the optimal site to build a new hospital with a suggestion of the type of hospital. Four machine learning algorithms Support Vector Machine (SVM), K-Nearest Neigbours (KNN), Decision Tree (DT) and Linear Logistic Regression (LGR). Fig. 8 shows the prediction hierarchical structure for the model decision-making with S1, S2, S3, and S4 selected as candidate sites for prediction. The attributes considered for the decision making are seen in Table 3. The classifiers were trained and tested using the dataset with the split ratio 75% for training data and 25% for the test data. Accuracy metrics were measured and confusion matrix of each model was calculated to validate the best model for implementation as shown in Fig. 9, 10, 11 and 12.

	general facility attendance	general outpatient attendance	antenatal attendance total	deliveries-assisted	caesarean section	deliveries complications	deliveries normal	preterm deliveries	pregnacy outcome-birth asphyxia	pregnacy outcome--neonatal-jaundice	...	individuals started on tb treatment ((hiv-ve)
0	114760.0	24053.0	4773.0	6.0	19.0	2.0	63.0	1.0	3.0	6.0	...	188.0
1	21936.0	4869.0	1626.0	6.0	19.0	2.0	63.0	1.0	3.0	6.0	...	23.0
2	21936.0	4869.0	1626.0	6.0	19.0	2.0	63.0	1.0	3.0	6.0	...	23.0
3	21936.0	4869.0	1626.0	6.0	19.0	2.0	63.0	1.0	3.0	6.0	...	23.0
4	21936.0	4869.0	1626.0	6.0	19.0	2.0	63.0	1.0	3.0	6.0	...	2.0

5 rows × 124 columns

Fig. 7. Label encoder and transformation

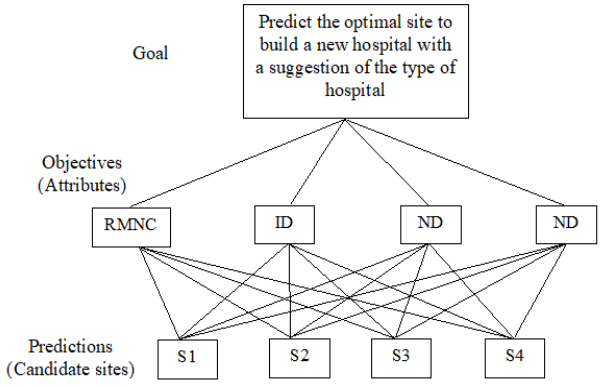

RMNC: *Reproductive, maternal, newborn and child health*
ID: *Infectious Diseases*
ND: *Noncommunicable diseases*
SCA: *Service Capacity and Access*
S: *Sites*

Fig. 8. Prediction hierarchical structure for decision-making

RESULTS

To test the model, an experiment was performed on a PC with Intel(R) Core (TM) i5-4460 at 3.6 GHz CPU and 8GB memory, running on Windows 10. Programs are coded in Python using PyCharm Professional Edition 2021.3.1 environment on the version of Anaconda 2020.11. Empirical values are used to obtain the parameters for the algorithm. The dataset used for the experiment was gotten from Rivers State Ministry of Health. Data was collected across all local government in Rivers State, Nigeria having a shape of 207 rows and 132 columns. Pairs of attributes are subjectively evaluated on a nine-point scale. The important healthcare attributes and sub-attributes considered for selecting optimal hospital sites as adopted from Universal Health Coverage are summarized in Table 1, these attributes and sub-attributes address the healthcare needs of different locations for siting hospitals. The dataset and codes for this study can be accessed on GitHub.

Four machine learning algorithms were used in the predictive model as seen in Fig. 2. To compare the performance of these algorithms and select the most efficient one for optimal hospital site selection, Fig. 9 shows the confusion matrix of the four algorithms used for prediction over the dataset. The results shows that Support Vector Machine (SVM) performed better compared to other algorithms for predicting the target variable. To verify the effectiveness of SVM for optimal hospital site selection model proposed in this paper, the precision, recall, and F1_score obtained as shown in Table 4.

Table 4: SVM performance on Precision, Recall, and F1-score

	Precision	Recall	F1-score	Support
0	0.98	1.00	0.99	47
1	1.00	0.80	0.89	5
Accuracy			0.98	52
Macro Avg	0.99	0.90	0.94	52
Weighted Avg	0.98	0.98	0.98	52

The results show the local governments where hospitals will not be built produced 0.98 and the local governments where hospitals will be built produced 1.00 in precision. Recall 1.00 for local governments where hospitals will not be built and 0.80 for local governments where hospitals should be built. For f1-score 0.99 for local governments where hospitals will not be built and 0.89 for local governments where hospitals will be built as classified by the proposed system model.

Scientia Africana, Vol. 21 (No. 1), April, 2022. Pp 159-174 *https://dx.doi.org/10.4314/sa.v21i1.14*

ISSN 1118 – 1931

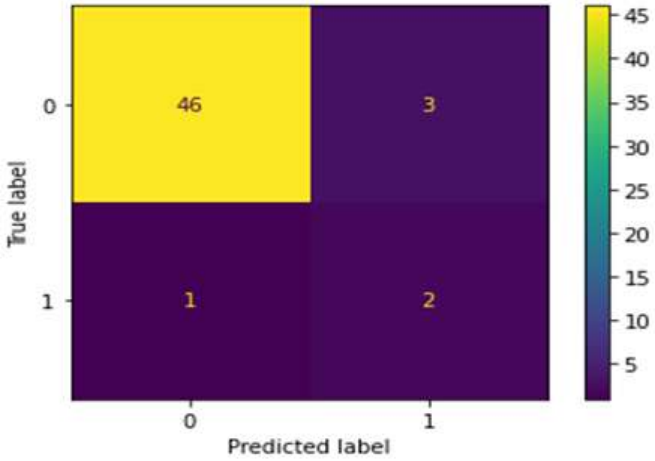

Fig. 9. Confusion matrix to show accuracy of SVM

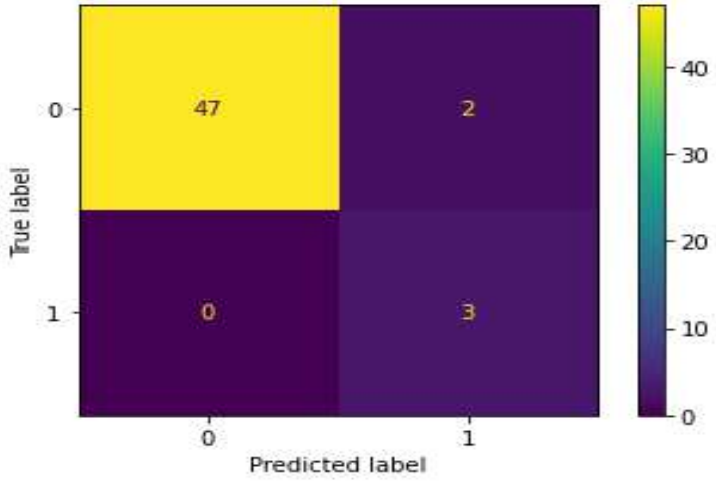

Fig. 10. Confusion matrix to show accuracy of KNN.

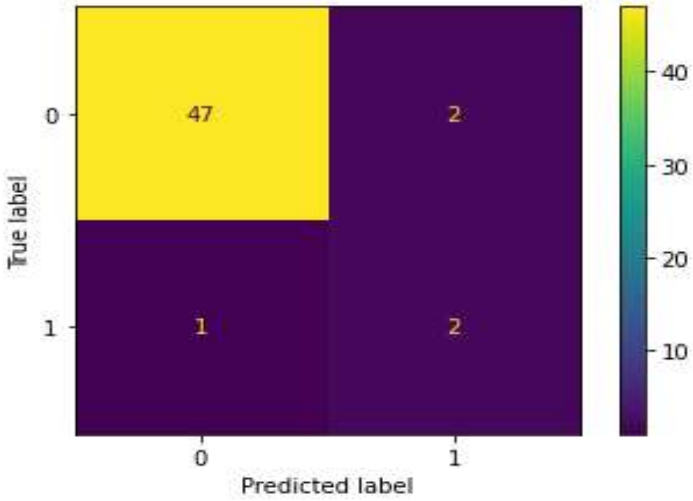

Fig. 11. Confusion matrix to show accuracy of LGR

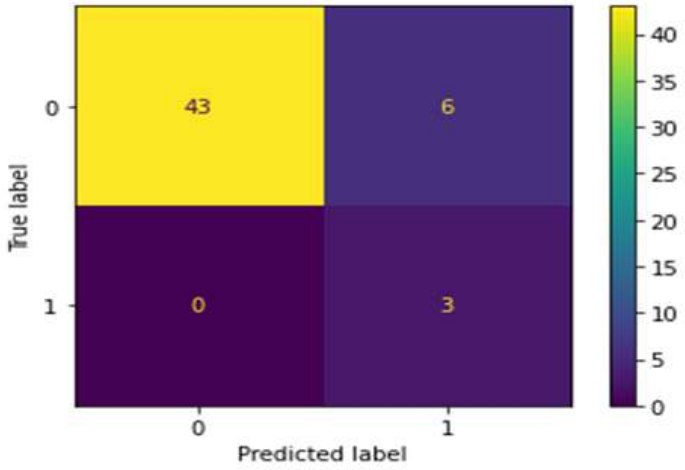

Fig. 12. Confusion matrix to show accuracy of DT

SVM showed accuracy rate of 96.15%, significantly higher compared to 94.23%, 92.31%, and 88.46% obtained by LGR, KNN, and DT classifiers respectively. It can be seen that SVM has achieved good performance on the prediction of optimal hospital site.

The Optimized Hospital Site Selection Predictive model is implemented with Support Vector Machine, due to high accuracy rate. The model is implemented with data trial and predicted that hospital can be built in Obi Akpor Local Government, while the model predicts that hospital should not be built in Emohua Local Government as shown in Figure 10.

CONCLUSION

Hospital site selection is a research problem common in developing countries with the goal to find the optimum location that satisfies some predefined criteria and give the populace of a particular locality have access to adequate healthcare services such as hospitals. Machine learning approach was applied using Support Vector Machine (SVM), K-Nearest Neighbours (KNN), Logistics Regression (LGR), and Decision Tree (DT) as classifier engines to predict hospital sites.

In this study, the model determined the optimum site for hospital site in Rivers State, Nigeria. The 23 local government areas in the state are used as possible location parameters. First, Percentage Mean of the features was determined for the screening and selection of appropriate options based on the World Health Organization (WHO) Universal Health Coverage (UHC) standard parameters to generate the possible local government to site a new hospital. Infectious Disease (ID) features were the predominant features selected as important features. In the second phase, important features are classified using different classifier engines. SVM performed better with accuracy rate of 96.15% compared to the results of KNN with accuracy rate of 92.31%, LGR with accuracy rate of 94.23%. Decision Tree with accuracy rate of 88.46%.

The proposed prediction method can be used as a reference for medical service administrators to select the optimal location for a new hospital to ensure that it

Scientia Africana, Vol. 21 (No. 1), April, 2022. Pp 159-174 https://dx.doi.org/10.4314/sa.v21i1.14
© Faculty of Science, University of Port Harcourt, Printed in Nigeria *ISSN 1118 – 1931*

meets the health care needs of people in a particular location using the Universal Health Coverage Standard. This can be considered as a valuable prototype and reference for hospital administrators and academics in establishing a standardized means of selecting location for medical care facilities. This study contributes healthcare intervention by suggesting a more robust decision-making tool for hospital site selection.

As a recommendation for further study on this research, more healthcare factors can be considered as criteria for alternatives. Some of potentially significant healthcare factors as suggested by World Health Organization (WHO) Universal Health Coverage (UHC) standard parameters and others like geographical, economical and socio-demographic factors affecting a hospital site selection were absent in the analysis. Also, a hybridized approach can be used combining the computing efficiencies of two or more machine learning techniques.

Acknowledgment

This study was sponsored by The World Academy of Science (TWAS) and German Research Foundation (DFG).

REFERENCES

Bloom, D. E., A. Khoury, and R. Subbaraman (2018). The promise and peril of universal health care. *Science*, 361(6404).

Bob H. (2012). 5 Challenges in Renovating or Building a Hospital, *retrieved online from http://www.beckershospitalreview.com /strategic-planning/5-challenges-in-renovating-or-building-a-hospital.html*, July 2017.

Boyacı, A. Ç., and A. Şişman (2021). Pandemic hospital site selection: a GIS-based MCDM approach employing Pythagorean fuzzy sets. *Environmental Science and Pollution Research*, 1-13.

Clarke, G. M., S. Conti, A. T. Wolters, and A. Steventon (2019). Evaluating the impact of healthcare interventions using routine data. *British Medical Journal*, 365.

Cynthia A. L., and Debra H. (2011). Design Details for Health: Making the Most of Design's Healing Potential. *2nd Edition John Wiley & Sons*, Inc.

Glasziou, P., I. Chalmers, D. G. Altman, H. Bastian, I. Boutron, and J. W. Williams (2010). Taking healthcare interventions from trial to practice. *British Medical Journal*, 341.

Marais D. L., I. Petersen (2015). Health system governance to support integrated mental health care in South Africa: challenges and opportunities. *International Journal Mental Health Systems*, 9(1), 14.

Mohammed, H., Z. Majid, Y. Yamusa, M. Ariff, K. Idris, and N. Darwin (2019). Sanitary landfill siting using GIS and AHP. *Engineering, Technology & Applied Science Research*, 9(3), 4100-4104.

Nsaif, Q. A., S. M. Khaleel, and A. H. Khateeb (2020). Integration of GIS And Remote Sensing Technique for Hospital Site Selection in Baquba District. *Journal of Engineering Science and Technology*, 15(3), 1492-1505.

Nygren-Krug, H. (2019). The right (s) road to universal health coverage. *Health and human rights*, 21(2), 215.

Okengwu, U. A., and E. N. Osuigbo (2021). Optimal Hospital Site Selection Software (Version 1.0) [Computer software]. https://github.com/ugodepaker/Riverss tate_Hospital_Model

Owen B. H., and P. Lawrence (1996). The Planning and Design Process, 2nd Edition by Rockvillie Md,

Petersen I., D. Marais, J. Abdulmalik (2017). Strengthening mental health system governance in six low-and middle-income countries in Africa and South Asia: challenges, needs and potential strategies. *Health Policy Plan*, 32(5), 699–709.

Roncarolo, F., A. Boivin, J.L. Denis, R. Hébert, P. Lehoux (2013). What do we know about the needs and challenges of health systems? A scoping review of the international literature. *BMC Health Serv Res*, 17(1), 636.

Schuurman, N., R. S. Fiedler, S. Grzybowski, and D. Grund (2006). Defining rational hospital catchments for non-urban areas based on travel-time. *International Journal of Health Geographics*, http://www.ijhealth geographics.com/content/5/1/43 (Accessed on 7th September 2021).

Senvar, O., I. Otay, and E. Bolturk (2016). Hospital site selection via hesitant fuzzy TOPSIS. *IFAC-Papers On Line*, *49*(12), 1140-1145.

Smit, L. C., J. Dikken, M. J. Schuurmans, N. J. de Wit, and N. Bleijenberg (2020). Value of social network analysis for developing and evaluating complex healthcare interventions: a scoping review. *British Medical Journal*, 10(11).

Soltani, A., E. Z. Marandi (2011). Hospital site selection using two stage fuzzy multi-criteria decision-making process. *Journal of Urban andenvironmental engineering*, 5(1), 32-43.

Vahidnia, M.H., A. Alesheikh, and A. Alimohammadi (2009). Hospital site selection using fuzzy AHP and its derivatives. *Journal of environmental management*, 90(10), 3048-3056.

Wu, C.R., C. Lin, and H. Chen (2007). Optimal selection of Taiwanese hospitals to ensure a competitive advantage by using analytical hierarchy process and sensitivity analysis. Building and environment, 42(3), 1431-1444.

Xu, Y., C. Huang, and U. Colón-Ramos (2015). Moving Toward Universal Health Coverage (UHC) to Achieve Inclusive and Sustainable Health Development: Three Essential Strategies Drawn from Asian Experience: Comment on" Improving the World's Health Through the Post-2015 Development Agenda: Perspectives from Rwanda". *International journal of health policy and management*, 4(12), 869.

Yang, J. and P. Shi (2002). Applying Analytic Hierarchy Process in Firm's Overall Performance Evaluation: A Case Study in China. *International Journal of Business.* 7(1), 30-46.

Scientia Africana, Vol. 21 (No. 1), April, 2022. Pp 175-182 https://dx.doi.org/10.4314/sa.v21i1.15
© Faculty of Science, University of Port Harcourt, Printed in Nigeria *ISSN 1118 – 1931*

NUTRITIONAL PROPERTY OF *MUCUNA PRURIENS* L. SEED POWDER AND EFFECT OF ITS GRADED DIETARY SUPPLEMENT ON SERUM CORTICOSTERONE IN MALE AND FEMALE ALBINO RATS

Ashidi, J. S.[1], Sonaya, O.E.[1]*, Feyisola, R.T.[1], Owagboriaye, F.O.[2], Sanusi A.S.[1] and Lawal, O.I.[1]
[1]Plant Science Department, Olabisi Onabanjo University, Ogun State, Nigeria
[2]Department of Zoology and Environmental Biology, Olabisi Onabanjo University, Ogun State, Nigeria
Corresponding Author Email: *dhammysho@gmail.com*

Received: 30-11-2021
Accepted: 20-03-2022

ABSTRACT

Mucuna pruriens(MP) is highly recognized for its diverse biology activities. Its seeds are not only utilized in Asian countries but also here in Nigeria. Hence, the need to evaluate Mucuna pruriens seed powder for its nutritional property and influence on the level of corticosterone hormone when supplemented with rat feed at varying doses. Rats were randomized into 4 groups and fed diets supplemented with graded inclusion levels of MP seed powder for 6 weeks; group 1 (control) was maintained on normal diet while group two, three and four were fed diets supplemented with the powder of MP seed at 0.5, 1 and 1.5 g corresponding to 3.33%, 6.67% and 10% inclusion level respectively. Phytochemical, proximate, L-Dopa, minerals and heavy metal compositions were analyzed using standard methods while serum level of corticosterone in rats was analyzed with Enzyme Linked Immuno-sorbent Assay after consecutive feeding. Saponins, steroids, alkaloids, flavonoids, phenolics, triterpenes, terpenoids, coumarins and glycosides were all present in MP seed powder. Proximate analysis revealed slightly-high carbohydrate (44.70), protein (28.80) and L-Dopa (3.11g/100g) contents. Mineral analysis revealed appreciable level of calcium (125.04 ppm), magnesium (3.31ppm) and iron (2.16 ppm). Level of serum corticosterone in both male and female rats fed diet supplemented with MP at 3.33%, 6.67% and 10% compared to their respective controls was not significantly different ($p>0.05$). It is thus concludedthat MP seed powder possess nutritional potentials and may not induce stress in animal at inclusion levels of 3.33%, 6.67% and 10%.

Keywords: Corticosterone, *Mucuna* seed, Stress hormones, Velvet bean

INTRODUCTION

Stress hormones are of utmost importance in assisting the body manage and respond to stressful situations. Corticosterone is a stress-related hormone exocytosed from the cortex of adrenal gland in response to environmental stressors (Neil, 2004). In humans onset of stress is often marked with increased secretion of cortisol or corticosterone (Jacobson, 2005; De Kloet and Rinne, 2007; Franklin *et al.*, 2012). Studies have revealed that high levels of these hormones in the body can negatively impact human and animal health, if left unchecked. However, there have been reports that the seed powder of *Mucuna pruriens* relieves stress.

Mucuna pruriens or Velvet bean is in the family Fabaceae. It is also referred to as Cow witch and Cow hage with a characteristically long hairy pod (Lampariello *et al.*, 2012). The Yorubas of

Nigeria call it 'werepe'. *M. pruriens* has wide range of recorded pharmacological uses such as anti-diabetic, aphrodisiac, anti-neoplastic, anti-epileptic and anti-microbial activities (Sathiyanarayanan and Arulmozhi, 2007).

Mucuna pruriens seeds are consumed as food by humans and added to animal feed in Nigeria (ThyagaRaju *et al.,* 2017). Besides compounds of pharmacological importance, some anti-nutritional agents such as lectins and protease inhibitors are also present in *M. pruriens* (ThyagaRaju *et al.,* 2017). Out of these compounds, L-Dopa is known to be the major active compound in the seed (Lorenzetti *et al*., 1998; Gurumoorthi *et al.,* 2008). Matured seeds of *M. pruriens* contain 3.1 to 6.1% of levodopa (ThyagaRaju *et al.,* 2017). Due to the high level of this active compound, a number of studies have been conducted on the possible effects of the seed on some ailments, organs and physiological functions of the body. For instance, the influence of the seed on the immune system has been demonstrated in mice (Vermal *et al.* 2014). Moreover, our previous study has reported the aphrodisiac property of *M. pruriens* seed powder in rats (Ashidi *et al.*, 2019). To the best of our knowledge, there is little or no information on the effect of different inclusion levels of *M. pruriens* seed powder on stress hormones of albino rats. Hence, the need for this study.

MATERIALS AND METHODS

Seed collection and preparation

The MP seeds (Figure 1) were collected from Ago-Iwoye, southwest Nigeria and identification was done at Elikaf Herbarium with voucher number EH/18/19/60011 in our institution. We powderdised the seed using mortar and pestle, and analysed the powder for its nutritional compositions.

Animals

A total of 64 adult albino rats comprising thirty-two (32) male and thirty-two (32) female rats of the Wistar strain, weighing 93.81 g - 155.1 g were used for this study. The rats were housed in a well ventilated and spacious room (27^{o}C±3^{o}C). Animals were acclimatized for 10 days with water and fed *ad libitum* with rat chow purchased from Animal Care Services Konsult (Nig.) Ltd before the commencement of the experiment.

Figure 1: *Mucuna pruriens* seeds

Scientia Africana, Vol. 21 (No. 1), April, 2022. Pp 175-182 *https://dx.doi.org/10.4314/sa.v21i1.15*
© Faculty of Science, University of Port Harcourt, Printed in Nigeria *ISSN 1118 – 1931*

Study design

We randomized the rats into four groups (groups one, two, three and four). Each group contained eight male and female albino rats. The control group (group 1) was fed 15 g of the rat chow every day for 6 weeks, group 2 was fed 14.5g standard rat chow mixed with 0.5 g *M. pruriens* seed powder corresponding to 3.33% inclusion level, group 3 was fed 14 g standard chow mixed with 1 g *M. pruriens* corresponding to6.67% inclusion level and rats in group 4 were fed 13.5 g standard rat chow mixed with 1.5 g with *M. pruriens* corresponding to10% inclusion level. The level of *Mucuna pruriens* seed powder inclusion was in accordance with our previous study (Ashidi *et al.,* 2019).

Sample collection

At exactly 24 hours following the last feeding regime, blood was sampled by cardiac puncture into plain sample tubes. We centrifuged the blood at 2500 rpm for 10 min and the sera obtained were stored at -20°C for corticosterone assay.

Phytochemical screening and proximate analysis

Seeds of *Mucuna pruriens*were screened to unravel the phytochemical constituents (Table 1) as previously described (Harborne 1973; Sofowora, 1993; Trease and Evans 1989). Determination of lipid, moisture content, ash, crude protein and fibre in the seed was in accordance with the Association of Official Analytical Chemists (AOAC, 2005). We used weight difference of crude protein, moisture, lipid and ash content to determine the seed carbohydrate content. Meanwhile, mineral and heavy metals compositions of the seed were analysed according to AOAC (2005).

L-dopa determination

Level of L-dopa in the seed was determined according to Myhrrman (2002) with little modifications. Briefly, 5 mL of distilled water was added to 2 g of the seed powder in a glass culture tube. The content of the tube was thoroughly mixed and allowed to stand in boiling water for 6 minutes. We later centrifuged the tube at 3000 rpm for 2 mins and the supernatants were diluted with deionized water to make 100 mL. The mixture was allowed to pass through 0.45 mm nylon membrane and cooled to 15°C. The level of L-dopa in the extract was determined using a high performance liquid chromatography connected to an ultraviolet detector with SB-C18 colunm. The mobile phase, which consists of buffer and methanol, was run at 1 mL/min and eluted at 10mL/min for up to 20 minutes with the injection volume of 40 µL. We quantified the L-dopa in the extract from the obtained standard L-dopa curve prepared by adding 1.00mM of standard L-dopa with water.

Corticosterone hormone determination

Corticosterone level in the sera of male and female rats was determined using the corticosterone Enzyme Linked Immunosorbent Assay (ELISA) kit. The assay sensitivity and range of detection were 0.029 ng/mL and 0.05-23 ng/mL respectively.

Data analysis

The obtained data were analysed with the IBM statistical package for Social Sciences (SPSS) version 20.0 (IBM Corp 2011). Analysis of variance (ANOVA) was used for the mean values comparison and the results were presented as mean ± standard error of mean. We used Students Newman

Keuls for the Post-hoc test and level of significance was set at $p < 0.05$.

RESULTS

Phytochemical composition of the *Mucuna pruriens* seeds

Result (Table 1) of the qualitative analysis of *Mucuna pruriens* seeds showed the presence of thirteen (13) phytochemicals which include saponins, tannin, phenolics, steroids, flavonoids, triterpenes, coumarin, glycoside, anthocayanin, terpenoids, phlobatanin, amino acid and alkaloids. Steroids (227.52±0.33 mg/100g) and triterpenes (165.77±0.42 mg/100g) respectively were the highest phytochemical components of *Mucuna pruriens* seeds (Table 2). These were followed by flavonoids, phenolics, alkaloids and terpenoids respectively. However, saponins had the least concentration.

Table 1: Phytochemical screening of *Mucuna* seeds

Phytochemical composition	Result
Saponins	+
Tannins	+
Phenolics	+
Steroids	+
Flavonoids	+
Triterpenes	+
Coumarins	+
Glycosides	+
Anthocyanins	-
Terpenoids	+
Phlobatanins	-
Alkaloids	+
Amino acids	-

Key: - Absent, + Present

Table 2: Quantitative phytochemical composition (mg/100g) of *Mucuna* seeds

Phytochemical composition	Mean±SD
Saponins	0.76±0.00
Steroids	227.52±0.33
Flavonoids	56.86±0.04
Phenolics	44.57±0.04
Alkaloids	42.31±0.00
Triterpenes	165.77±0.42
Terpenoids	22.92±0.02
Coumarins (µg/100g)	7.61±0.00
Glycosides	8.71±0.02

Scientia Africana, Vol. 21 (No. 1), April, 2022. Pp 175-182 *https://dx.doi.org/10.4314/sa.v21i1.15*
© Faculty of Science, University of Port Harcourt, Printed in Nigeria *ISSN 1118 – 1931*

Proximate composition and level of L-Dopa in *Mucuna pruriens* seeds

The seedscontain some levels of moisture content, ash, carbohydrate, calorie, crude protein, crude lipids, crude fibre and L-Dopa (Table 3). Moisture content of the seed was (10.81±0.06 %). It also contained calorific value, crude protein and carbohydrate contents of 1516.65±2.32kJ /100g, 28.80±0.55 % and 44.70±0.64 % respectively.

Mineral and heavy metal compositions of *Mucuna pruriens* seeds

Results (Table4) also showed the presence of some minerals in the *Mucuna pruriens* seeds. These include zinc, phosphorus, potassium, calcium, magnesium and iron. Trace levels of selenium and lead were also recorded. Of all the mineral compositions of *Mucuna* seeds, calcium is abundantly present and higher (125.04±2.00 ppm), followed by magnesium (3.31±0.20 ppm) and iron (2.16±0.10 ppm) respectively.

Table 3: Proximate composition and level of L-Dopa in *Mucuna pruriens* seeds

Proximate composition %	Mean±SD
Moisture	10.81±0.06
Ash	4.81±0.11
Carbohydrate	44.70±0.64
Calorific value kJ/100g	1516.65±2.32
Crude protein	28.80±0.55
Crude Lipids	7.63±0.02
Crude Fibre	3.24±0.06
L-Dopa (g/100g DM)	3.11±0.03

Table 4: Minerals and heavy metals composition(ppm) of *Mucuna pruriens* seeds

Mineral composition	Mean±SD
Se	0.39±0.01
Zn	1.06±0.04
Pb	0.36±0.00
P	1.93±0.02
Ca	125.04±2.00
Mg	3.31±0.20
Fe	2.16±0.10

Level of stress hormones in the blood

Serum corticosterone observed in in the control male and female rats as well male and female rats fed with 3.33%, 6.67% and 10% of *Mucuna pruriens* seed inclusion in diet was not significantly different ($p>0.05$) (Figure 2).

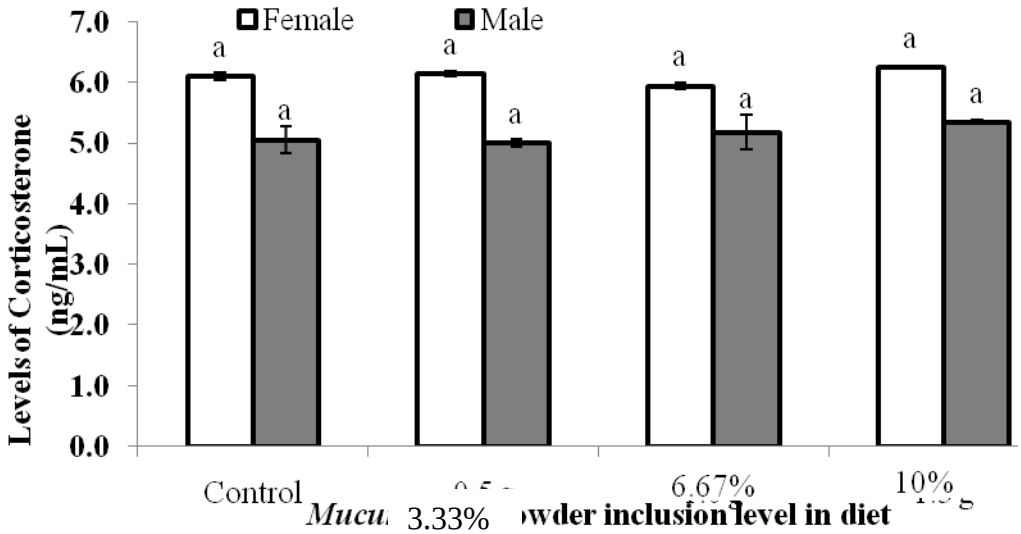

Figure 2: Serum corticosterone in male and female rats fed with varying concentrations of *Mucuna pruriens* seed.

DISCUSSION

Seeds of *Mucuna pruriens* have been globally proposed to be consumed as food by humans and supplemented with animal feed. Phytochemical analysis revealed that the seeds are rich in steroids (227.52±0.33 mg/100g), triterpenes (165.77±0.42 mg/100g) as well as phenolics, flavonoids, coumarin, glycoside, anthocyanin, terpenoids, phlobatannins, amino acids, alkaloids and saponins contributing to its notable medicinal potential. This finding is supported by Adebowale *et al.* (2005) who also noted a high level of these phytochemical constituents in *Mucuna pruriens* seeds.

From this study, seeds of *Mucuna pruriens* have high calorific value (1516.65 KJ/100g), appreciable amount of crude protein (28.80 %) and carbohydrate contents (44.70±0.64 %) including non-protein L-dopa (3.11 g/100g) of dry matter, indicating its nutritional value. This result was also confirmed by Adebowale *et al*. (2005), although, higher level of L-Dopa (4.99±0.03) was reported as against the value of 3.11±0.03 recorded for the seed used in this study.

Our results showed that calcium was the abundantly present mineral element above others. Moreover, the seeds also have high magnesium and iron contents as previously documented. For instance, Ravindran and Ravindran 1988 as well as Rajaram and Janardhanan 1991 had earlier documented the mineral content of *Mucuna utilis*: (calcium, 250.0 mg/100g) and *Mucuna gigantean*: (calcium, 518 mg/100 g). Surprisingly, lead was detected at low concentration (0.36 ppm) in *Mucuna pruriens* seeds. Although, the reason for the presence of lead in the seed is unknown, but we suspect metal pollution at the site where the seed was planted and harvested. On the contrary, Adebowale *et al.* (2005) reported lead below detection limit in the seed of *Mucuna pruriens*. Our findings therefore show that the site or location where *Mucuna pruriens* seeds were obtained should be taken into consideration in the determination and quantification of the nutritional properties of *Mucuna pruriens*.

Reports have shown an increased secretion of corticosterone as a physiological response to stress in animals (Franklin et

Scientia Africana, Vol. 21 (No. 1), April, 2022. Pp 175-182 *https://dx.doi.org/10.4314/sa.v21i1.15*
© Faculty of Science, University of Port Harcourt, Printed in Nigeria *ISSN 1118 – 1931*

al. 2012; Jacobson, 2005). It has been noted that a high serum corticosterone may induce a neurological disorder such as hippocampal dysfunction, which can result in memory function declarative deficits, reduction in neural survival, plasticity as well as cascades of promotion and inflammation (Franklin et al. 2012; Bremmer, 1999). A high level of corticosterone in the circulation may also destroy neurons by reducing glucose input and re-uptake glutamate (Sapolskey, 1995; Sapolskey, 1992). In addition, high blood pressure, muscle damage, reproductive and growth declines as well as immune suppression may also result from increased concentration of the hormone. Since the level of corticosterone was observed to be insignificantly different in male and female rats fed diet supplemented with *Mucuna pruriens* seed powder compared to their respective controls in this study, the seed at 3.33%, 6.67% and 10% inclusion level may not induce stress and the reported various physiopathological complications on the rats.

CONCLUSION

Seeds of *Mucuna pruriens* contain appreciable levels of minerals. No significant difference was observed in the serum level of corticosterone in both male and female rat's diet supplemented with *Mucuna pruriens* at 3.33%, 6.67% and 10% compared to their respective control. This study clearly shows that *M. pruriens* may possess medicinal and nutritional potential. Moreover, it may not induce stress in animal at inclusion level of 10% or less when added to diet.

REFERENCES

Adebowale, Y.A., Adeyemi, A. and Oshodi, A.A. (2005). Variability in the physicochemical, nutritional and anti-nutritional attributes of six *Mucuna* species. *Food Chemistry*, 89:37-48.

AOAC, (2005). Official Methods of Analysis, eighteenth ed. Association of Official Analytical, Chemists International, Maryland, USA.

Ashidi, J.S., Owagboriaye, F.O., Yaya, F.B., Payne, D.E., Lawal, O.I., Owa, S.O. (2019). Assessment of reproductive function in male albino rat fed dietary meal supplemented with Mucuna pruriens seed powder. Heliyon, 5: e02716. Netherlands.

De Kloet, E.R., Rinne, T. (2007). Neuroendocrine markers of early trauma: Implications for post-traumatic stress disorder. In E. Vermetten, M.J. Dorahy, & D. Spiegel (Eds.), Traumatic dissociation: Neurobiology and treatment. Washington, DC: American Psychiatric Press.

Franklin, T.B., Saab, B.J., Mansuy, I.M. (2012). Neural mechanisms of stress resilience and vulnerability. Neuron, 75(5):747-761.

Gurumoorthi, P., Janardhanan, K., Myhrman, R.V. (2008). Effects of differential processing methods on L-DOPA and protein quality in velvet bean, an underutilized pulse. *LWT-Food Science and Technology*, 41:588-596.

Harborne, J.B. (1973). Phytochemical methods. A guide to modern technique of plant analysis Chapman and Hall publishers, London 51-59.

Jacobson, L. (2005). Hypothalamic-pituitary-adrenocortical axis regulation. *Endocrinology and Metabolism Clinics of North America*, 34:271-292.

Lampariello, L.R., Cortelazzo, A., Guerranti, R., Sticozzi, C., Valacchi,

G. (2012). The magic Velvet bean of *Mucuna pruriens. Journal of Traditional and Complementary Medicine*, 2(4):331-339.

Lorenzetti, E., Mac Isaac, S., Arnason, J.T., Awang, D.V.C., Buckles, D. (1998). The phytochemistry, toxicology and food potential of velvet bean (*Mucuna* adans spp. Fabaceae) In: Buckles, D., Osiname, O., Galiba, M., Galiano, G., editors. Cover crops of West Africa; contributing to sustainable agriculture. Ottawa, Canada& IITA, Ibadan, Nigeria: IDRC;57.

Myhrrman, R. (2002). Detection and removal of LL -dopa in the legume Mucuna. In M. Florens, M. Eilitta, R. Myhrman, L. Carew, & R. Carsky (Eds.), Food and feed from Mucuna: Current use and the way forward. Proceedings of an International Workshop on Food and feed from Mucuna: Current uses and the way forward. Tegucigalpa, Honduras, April 26–29, 2000 (pp 142–162). Tegucigalpa, Honduras: CIDICCO, CIEPCA, and World Hunger Research centre.

Pugalenthi, M., Vadivel, V. and Siddhuraju, P. (2005). Alternative food/feed perspectives of an under-utilized legume *Mucuna pruriens* varutilis. *A review: Plant Foods for Human Nutrition*, 60:201-218.

Rajaram, N., Janardhanan, K. (1991). The biochemical composition and nutritional potential of the tribal pulse, Mucuna gigantea DC. Food and Human Nutrition, 41:45-51.

Ravindran, V., Ravindran, G. (1988). Nutritional and antinutritional characteristics of Mucuna (Mucuna utilis) bean seeds. *Journal of the Science of Food and Agriculture*, 46:71-74.

Sapolskey, R., 1992. Stress, the ageing brain and the mechanisms of neuron death. MIT Press; Cambridge

Sapolskey, R.M., 1995. Social subordinance as a marker of hypercortisolism: Some unexpected subtleties. *Annals of the New York Academy of Science*, 771:626-639.

Sathiyanarayanan, L. and Arulmozhi, S. (2007). Mucuna pruriens: A comprehensive review. *Pharmacognosy Review*, 1:157-162.

Sofowora, A., 1993. Medicinal and Traditional Medicine in Africa (6th edition). Chichester John Wiley and Sons, New York 285-286.

Taylor, D., 2002. Small Pet Handbook. Harper Collins Limited, London, Great Britain.

Trease, G., Evans, W. (1989). Pharmacognosy. Briallene Tindacallan (13th edition). Macmillian publishers.

ThyagaRaju, K., Suman, B., Venkataswamy, M., Divya, B.J. (2017). The traditional uses and pharmacological activities of *Mucuna pruriens* (L) DC: A comprehensive review. *Indo American Journal of Pharmaceutical Research*, 7(01).

Vanderlip, S.L. (2001). Mice: A Complete Pet Owner's Manual. Barron's Educational Series. Inc., New York, USA.

Vermal, S.C., Vashishth, E., Singh, R., Pant, P., Padhi, M.M. (2014). A Review on phytochemistry and pharmacological activity of parts of *Mucuna pruriens* used as an ayurvedic medicine. *World Journal of Pharmaceutical Research*, 3(5):138-58.

Scientia Africana, Vol. 21 (No. 1), April, 2022. Pp 183-194 https://dx.doi.org/10.4314/sa.v21i1.16
© Faculty of Science, University of Port Harcourt, Printed in Nigeria *ISSN 1118 – 1931*

MEASUREMENT OF ACTIVITY CONCENTRATIONS OF ROCK SAMPLES FROM ROCKS- SURROUNDED TOWN IN IGBETI, OYO STATE, NIGERIA

[*1]Ajetunmobi, A.E., [2]Biere, P., [1]Alausa, S.K., [1]Coker, J.O., [1]David, T.W., [1] Talabi, A.T.,[1] Oladujoye, H.T., and [1] Olojede, S.K.

[1]Department of Physics, Olabisi Onabanjo University, Ago-Iwoye, Ogun State, P.O. Box 16122,Nigeria.
[2]Niger Delta University, Wilberforce Island, Bayelsa State, Yenagoa , P.O. Box 1237, Nigeria.
Corresponding author E-mail address: abayomi.ajetunmobi@oouagoiwoye.edu.ng

Received: 15-03-2022
Accepted: 04-04-2022

ABSTRACT

Rocks are known to contain radionuclides that emit radiation continuously. The assessment of activity concentrations of rock samples from Igbeti, Oke-Ogun has been investigated. Twenty (20) rock samples were randomly collected from different rock sites. The rock samples were pulverized at the laboratory of the Department of Geology, University of Ibadan. 200g of each collected sample was allowed to attain secular equilibrium by enclosing it in a plastic container for twenty-eight (28) days. Radiometric analysis of the samples was carried out at the radiation laboratory of the Physics Department of the Federal University of Agriculture, Abeokuta using a thallium doped Sodium Iodide detector. Standard equations were used to estimate the radiological parameters associated with exposure to ionizing radiation from the natural radionuclides in the rock samples. The study revealed that the activity concentrations of ^{226}Ra, ^{232}Th, and ^{40}K lie between 14 − 487 (Bq/kg), 210 − 3680 (Bq/kg), and 242 − 1580 (Bq/kg) respectively. The absorbed dose rate (nGy/h), annual effective dose equivalent (μSv/y), (radium equivalent (Bq/kg), external and internal indices, activity utilization index and estimated excess lifetime cancer risks lie between from (180 − 2700) nGy/h, (0.10 − 14) , 400 − 6300 (Bq/kg), 1 − 17, 1 − 19, 2 − 41, and 0.6− 9.5 × 10^{-6} respectively. The values of the absorbed dose rates value are greater than the world average of 60 nGy/h while annual effective dose equivalent values are less than the world's average value of 1000 μSv/y respectively. The external and internal indices are greater than the permissible limit of (1) and likewise, the radium equivalent value is also greater than the acceptable limit of 370 Bq/kg. The estimated excess lifetime cancer risk for the study is below the permissible limit of 2.9 × 10^{-4} . Most of the estimated radiological parameters for the study are all greater than the permissible limit. This suggests that further exposure of dwellers to ionizing radiation may be possible and this calls for further investigation.

Keywords: measurement /activity concentrations / rocks-surrounded/rock samples

INTRODUCTION

Natural radioactivity in an environment is a result of the presence of natural radionuclides such as ^{238}U, ^{232}Th, and ^{40}K in the geological formation of the environment (Parakash *et al.*, 2017; Kaleel *et al.*, 2012). The levels of terrestrial environmental radiation is related to the geological composition of the region, and the concentrations of ^{238}U, ^{232}Th, and ^{40}K in rocks (Rangaswamy and Sannappa, 2016; UNSCEAR, 2000). The radioactivity due to natural radionuclides in rocks and soils generates a significant component to the background radiation exposure to the population (Kapanadze *et*

al., 2019). Rocks contain naturally occurring radionuclides that emit radiation continuously to their immediate environment (Adewoyin *et al.*, 2018). There are sixteen massive rocks surrounding Igbeti and one of the rocks called Iyamopo occupies over six kilometers of the landmass is as high as forty-seven meters and is known for shelter during attacks (Wikipedia(Igbeti), 2021). Residents are living very close to some of the rocks and this will result in continuous exposure of the villagers to ionizing radiation from the rocks and hence the need to measure the activity concentrations of the rocks surrounding Igbeti. The study aims to measure the activity concentrations of radionuclides in the rock samples and estimate appropriate radiological parameters associated with the exposure of Igbeti dwellers to ionizing radiation from naturally occurring radionuclides in the rock samples. There has been no study on the measurement of activity concentrations of rocks surrounding Igbeti, hence the result of the work will serve as the baseline for further study on the exposure to the ionizing radiation from rock samples in Igbeti. Lastly, the result of the study will contribute to the existing body of knowledge in the field.

Experimental procedure

Study area, sampling, and sample preparation

The study area is a rock-surrounded town located at Igbeti, Oyo State, with Lat.8.77' N and Long. 040 0' E. Igbeti, Oke-Ogun is a town located in the Northern part of Oyo State, Nigeria. It has a landmass area of 967km^2 and an estimated population of 81,000 (NPC, 2006). The study area is situated on the basement complex of granitic rock as shown in Figure 1. The basement complex rocks comprise older gneiss, schist, quartzite, older granite, and amphibolite (Alausa, 2014). This basement complex is rich in ^{226}Ra (^{238}U), ^{232}Th, and 4^0K radionuclide (Jibiri *et al.*, 2009) and there is a tendency that the rock from the study area may be high in radioactivity. The people in the area are farmers, miners, civil servants, and petty traders. The temperature typically varies from 63^{o}F to 94^{o}F. The rainy season span from June to October with an average daily of 85°F while the hot season lasts from January to April with an average daily temperature of 92°F (Climate and average weather year-round in Igbeti). The natural vegetation is guinea savanna noted with scanty forest with moderately thick forest along streams path.

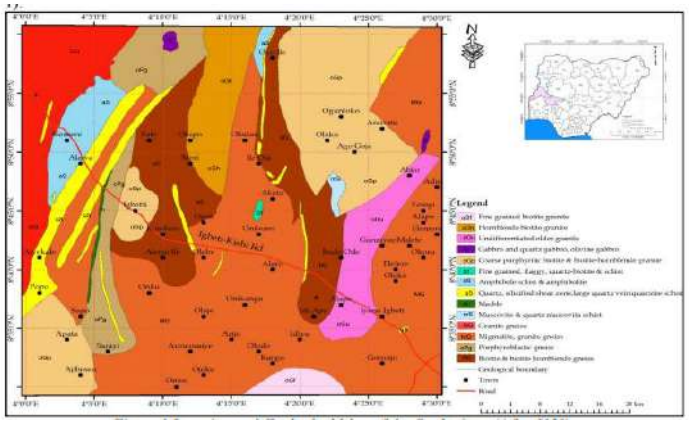

Figure 1: Geological and location map of the study area, (Olasunkanmi *et al.*, 2020)

Scientia Africana, Vol. 21 (No. 1), April, 2022. Pp 183-194 *https://dx.doi.org/10.4314/sa.v21i1.16*
© Faculty of Science, University of Port Harcourt, Printed in Nigeria *ISSN 1118 – 1931*

A total of twenty (20) rock samples 1.0kg each of twenty rock samples was randomly collected at the sites and packed in a polythene bag which was labeled for identification. The samples were taken to the Geology Department, University of Ibadan, where the rocks samples were crushed and pulverized into powdery form. 200g each of the pulverized samples were weighed and sealed in plastic containers and left for 28 days to attain secular equilibrium. Gamma spectrometry analysis of the samples was done at the radiation laboratory of the Physics department, of the Federal University of Agriculture, Abeokuta, Nigeria using Sodium Iodide spectrometer (NaI) (TI) spectrometer.

Spectrometry analysis of the rock samples in the study

20 rock samples were analyzed for activity concentrations of the radionuclides in the rock samples using thallium activated Canberra vertical high purity 2″×2″ Sodium iodide NaI (TI) detector connected to ORTEC 456 amplifier. The detector was connected to a computer program MAESTRO window that matched gamma energies to a library of possible isotopes. The cylindrical plastic containers for the samples were placed on the NaI (TI) detector with the dimension of 7.6 cm x 7.6 cm. The detector was shielded by 15cm thick lead on all sides and 10cm thick on top and bottom. The energy resolution of 2.0 Kev and relative efficiency of 33% at 1.33Mev was acquired in the system with the counting time of 10,800 seconds to lower the statistical uncertainty. The configuration and geometry were not changed for the period of the analysis, based on the established procedure of the radiation laboratory. The standard International Atomic Energy Agency (IAEA) sources were used for calibration (IAEA, 2003). From the counting spectra lines, the activity concentrations of the radionuclides, ^{238}U, ^{232}Th, and ^{40}K were determined using a computer program. The peak corresponding to 1460 KeV for ^{40}K, 1764.5 KeV (^{214}Bi) for ^{238}U, and 2614.5 keV (^{208}Ti) for ^{232}Th were considered in arriving at the activity levels (Bq kg^{-1}). The background counts were determined by counting an empty container of the same dimension as those containing the samples and subtracting from the gross count. The activity concentrations of the samples were determined using the net area under the photo peaks by the equation (1);

$$A_C = \frac{Cn}{P\gamma\, M\, \varepsilon} \qquad (1)$$

Where A_c is the activity concentrations of the radionuclides (^{238}U, ^{232}Th and ^{40}K) in the sample and unit is Bqkg^{-1}, C_n is the net count rate under the corresponding peak, P_γ is the absolute transition probability of the specific γ-ray, M is the mass of the sample (kg) and ε is the detector efficiency at the specific γ-ray energy. The containers were sealed and airtight to prevent the escape of gaseous ^{220}Rn and ^{222}Rn, incubated for about a month to bring the daughter radionuclide into secular radioactive equilibrium with their respective long-lived parents (Suresh Gandhi *et al*., 2013 and Shittu *et al.*, 2015).

Energy and Efficiency Calibration

An important criterion for the measurement of gamma emitters is the correct identity of photo peaks in a spectrum produced by the detector system. The energy calibration of the detector system is made by measuring mixed standard sources of a known radionuclide with well-defined energies provided by the IAEA Technology. The specific activity concentrations (equation 2) of the samples were determined using the net area under the photo peaks from the energy and efficiency calibration.

$$C\ (BqKg^{-1}) = K\, C_n \qquad (2)$$

Where C (BqKg^{-1}) is the specific activity concentrations of the radionuclide in the sample, C_n is the count rate enclosed by the corresponding peak, $K = 1/P^{\gamma}Ms$, ξ is the detector efficiency at the specific gamma-

ray energy, P^{γ} is the absolute transition probability of the specific gamma-ray and M_s is the mass of the sample (Jibiri and Okeyode, 2012).

Estimation of radiological parameters for the study

Annual Effective Dose rate

The annual effective dose *H*e was calculated using equation (3) where H_e is the annual effective dose rate in μSv/y and *D* is the value of absorbed dose rate calculated, T is the occupancy time (T= f × 24 × 365.25h y^{-1}) f is the occupancy factor and F_o is the conversion factor (0.7 $SvGy^{-1}$) UNSCEAR, 1993. Dose conversion factors are used to convert radioactivity taken into the body to radiation dose.

$$H_e = DTF_o \quad (3)$$

Radium Equivalent Activity

The significance of ^{40}K, ^{226}Ra, and ^{232}Th concentrations, to radiation exposure is expressed in terms of radium equivalent activity (Ra_{eq}), which was evaluated using Equation (4), (Beretka and Matthew, 1985). According to OECD, (1979), the maximum value must be less than 370 $Bq.kg^{-1}$ for the radiological effect to be considered negligible.

$$Ra_{eq} = A_{Ra} + 1.43A_{th} + 0.077A_K \quad (4)$$

External Hazard Index

External radiation hazard index (H_{int}) is a widely used hazard index that reflects the external exposure level due to gamma radiation. It is estimated from the relation in equation 5, (UNSCEAR, 2000):

$$H_{ex} = \frac{A_{Ra}}{370} + \frac{A_{th}}{259} + \frac{A_k}{4810} \quad (5)$$

Internal Hazard Index

In addition to the internal exposure to radiation is quantified by the internal hazard index (H_{ext}) as defined by UNSCEAR, (2000) in equation (6),

$$H_{in} = \frac{A_{Ra}}{185} + \frac{A_{Th}}{259} + \frac{A_k}{4810} \quad (6)$$

Activity Utilization Index (AUI)

The samples of rocks and soil samples from the mining sites were also examined to determine whether they satisfied the dose criteria for use as building materials. Activity utilization Index (U) was calculated using the model equation adopted by El-Gamal and El- Taher (2007), (equation 7).

$$AUI = \frac{A_U}{150} + \frac{A_{Th}}{100} + \frac{A_K}{1500} \quad (7)$$

Where A_U, A_{Th}, and A_K are as previously defined.

Excess Lifetime Cancer Risk (ELCR)

The probability of occurrence of cancer in any given population for a given lifetime exposure is measured by the excess lifetime cancer risk (ELCR). ELCR was calculated from the estimated AEDE using the equation (8),(Qureshi *et al.*, 2014):

$$ELCR = AEDE \times DL \times RF \quad (8)$$

Where DL is the life expectancy of 70 years, and RF is the risk factor given to be $0.05Sv^{-1}$ for stochastic effects (Taskin *et al.*, 2009).

RESULTS AND DISCUSSION

This section presents the results of pictorial representations and discussions. Statistical analysis of the parameters in the study is also presented. Table 1 shows the activity concentrations of ^{226}Ra, ^{232}Th, and ^{40}K in the rock samples and their ratio.

Scientia Africana, Vol. 21 (No. 1), April, 2022. Pp 183-194 *https://dx.doi.org/10.4314/sa.v21i1.16*
© Faculty of Science, University of Port Harcourt, Printed in Nigeria *ISSN 1118 – 1931*

Table 1: Activity concentrations of ^{226}Ra, ^{232}Th and ^{40}K in the rock samples and their ratios.

Rocks ID	226-Ra (Bq/kg)	232-Th (Bq/kg)	40-K (Bq/kg)	$\frac{232_{Th}}{226_{Ra}}$	$\frac{40_K}{226_{Ra}}$	$\frac{40_K}{232_{Th}}$
R1	16.56 ± 2.85	387.85 ± 13.22	1129.18 ± 34.04	23.42	68.20	2.91
R2	14.82 ± 1.38	232.85 ± 14.33	903.879 ± 12.27	15.71	60.98	3.88
R3	57.66 ± 2.07	358.56 ± 11.24	2046.78 ± 27.11	6.21	35.50	5.71
R4	32.19 ± 3.40	332.93 ± 13.44	1088.89 ± 12.06	10.34	33.83	3.27
R5	83.72 ± 1.18	220.65 ± 17.77	296.61 ± 27.17	2.64	3.54	1.34
R6	486.09 ± 1.24	3679.28 ± 14.64	5952.95 ± 47.27	7.57	12.25	1.62
R7	35.66 ± 1.34	395.17 ± 14.74	602.49 ± 22.86	11.08	16.89	1.52
R8	69.24 ± 0.79	210.89 ± 16.05	729.31 ± 25.49	3.05	10.53	3.45
R9	31.61 ± 1.00	464.73 ± 13.16	924.77 ± 27.57	14.70	29.26	1.99
R10	40.29 ± 2.33	509.89 ± 14.06	430.90 ± 15.16	12.65	10.69	0.85
R11	57.66 ± 2.53	574.57 ± 19.00	1579.77 ± 29.21	9.96	27.40	2.75
R12	47.24 ± 2.35	442.76 ± 21.60	1018.77 ± 12.82	9.37	21.56	2.30
R13	44.93 ± 2.50	335.37 ± 11.97	272.75 ± 23.74	7.46	6.07	0.81
R14	72.72 ± 11.25	354.89 ± 11.54	1341.05 ± 10.57	4.88	18.44	3.78
R15	31.98 ± 1.76	3422.9 ± 5.01	791.976 ± 36.66	107.04	24.77	0.23
R16	114.40 ±23.71	407.37 ± 11.34	242.91 ± 24.90	3.56	2.17	0.60
R17	38.56 ± 1.37	442.76 ± 12.06	602.49 ± 12.86	11.48	15.63	1,36
R18	47.24 ± 2.12	407.37 ± 16.91	729.31 ± 15.49	8.62	15.44	1.79
R19	33.35 ± 1.94	440.32 ± 14.06	924.77 ± 17.57	13.20	27.73	2.10
R20	54.77 ± 11.10	562.36 ± 12.75	430.90 ± 15.16	10.27	7.87	0.77
Mean	**355.95 ± 3.91**	**709.17 ± 13.94**	**1102.02 ± 22.50**	**10.05**	**15.62**	**1.55**

The values of the activity concentrations of the radionuclides found in the rock samples vary between 430 −2047 (Bq/kg) for ^{40}K, 1−115 (Bq/kg) for ^{226}Ra, and 273 −5960 (Bq/kg) for ^{232}Th. The values of the activity concentrations of the radionuclides (^{226}Ra, ^{232}Th, and ^{40}K) in the study were compared with similar studies in other countries and the world's average, (Table 2). The differences in the activity concentrations values of the radionuclides in the rock samples presented in Table 2, across the countries could be due to the different geological compositions across the countries. The ratios, $\frac{232_{Th}}{226_{Ra}}$, $\frac{40_K}{226_{Ra}}$ and $\frac{40_K}{232_{Th}}$ reveal the extent of depletion or enrichment of these radioisotopes. The ratio $\frac{40_K}{226_{Ra}}$ is greater in value than $\frac{232_{Th}}{226_{Ra}}$ and $\frac{232_{Th}}{226_{Ra}}$ and is greater in value than $\frac{40_K}{232_{Th}}$. This shows that ^{232}Th and ^{40}K are the dominant sources of gamma radiation in the area of study as also reported by Alnour *et al.,* 2012 in their study.

Table 2: Comparison of activity concentration values of ^{226}Ra, ^{232}Th and ^{40}K with other countries

Countries	Activity Concentrations Ranges (Bq/kg)			References
	^{226}Ra	^{232}Th	^{40}K	
Nigeria (Igbeti)	14 – 487	209 – 3680	429 – 5953	Present Study
Coorg	BDL –34.11	16.46–160.84	96.72–933.68	Prakash, *et al.*, 2017
Chika Manguluru	143.9–760.9	45.9–450.7	316.8–985	Manjunatha *et al.*, 1998
Kali river, India	41.0–322.6	BDL–26.1	147.2–2739	Narayana *et al.*, 2007
Cyprus	1–588	1–906	50–160.6	Michalis *et al*, 2003
Pakistan	33	32	57	Iqbal *et al.*, 2000
Sudetes Mountain, Poland	31—122	25–62	320–1200	Malczewski *et al.*, 2004
Wadi Karim area, Egypt.	14.0–227	10.5–183.0	2299–7356	El-Arabi., 2007
Piedmont, Italy	397	211	1265	Lucia *et al.*, 2006
Turkey	15.85	33.8	359	Osmanlioglu, 2006
World Average	35	30	400	UNSCEAR, 1993

Table 3: Estimated radiological parameters of rock samples in the study area

Rock ID	Ra_{eq} (Bq/kg)	Hazard Indices		Absorbed Dose rates (D) nGy/h	AEDE ($\mu Sv/y$)	AUI	ELCR (10^{-6})
		External	Internal				
R1	657.56	1.78	1.82	288.76	1.41	4.74	0.62
R2	417.39	1.13	1.17	185.18	0.91	3.03	3.97
R3	727.99	1.97	2.12	328.56	1.61	5.33	7.05
R4	592.12	1.59	1.69	261.37	1.28	4.27	5.61
R5	422.08	1.14	1.37	184.32	0.90	2.96	3.96
R6	6205.83	16.76	18.07	2695.09	13.22	44.00	5.78
R7	647.14	1.75	1.84	280.28	1.37	4.59	6.02
R8	426.97	1.15	1.34	189.78	0.93	3.06	4.08
R9	767.38	2.07	2.16	333.86	1.63	5.47	7.17
R10	1193.22	3.22	4.39	525.02	2.57	8.26	1.13
R11	1000.94	2.70	2.86	439.55	2.15	7.18	9.44
R12	758.84	2.05	2.18	331.74	1.63	5.42	7.12
R13	545.50	1.47	1.59	234.69	1.15	3.83	5.04
R14	683.48	1.85	2.04	303.87	1.49	4.93	6.63
R15	4987.84	13.47	13.55	2115.29	10.37	34.97	4.54
R16	715.64	1.93	2.24	309.03	1.51	4.99	6.64
R17	718.10	1.94	2.04	310.37	1.52	5.08	6.67
R18	885.93	1.85	1.97	298.28	1.46	4.87	6.41
R19	734.22	1.98	2.07	319.92	1.57	5.24	6.87
R20	892.13	2.41	2.56	382.94	1.88	6.28	8.22
Mean	**1199.02**	**4.22**	**3.45**	**515.89**	**2.53**	**8.43**	**5.65**
W.A	**370**	**1**	**1**	**60**	**1000**	**2**	**2.9×10^{-4}**

Again, Table 3 show that the range of the absorbed dose rates (nGy/h), annual effective dose equivalent (AEDE) (radium equivalent (Bq/kg), hazard indices (external and internal), the activity utilization index, and excess lifetime cancer risks ranged from (184.32–2695.09) nGy/h, with the mean of 515.89 nGy/h, (0.90 − 13.22) with the mean of 2.53 $\mu Sv/y$, 417.39 – 4987.84 (Bq/kg) with a mean of 1199.02 Bq/kg, 1.13 – 16.76 with a mean of 3.45 and 3.03 −

Scientia Africana, Vol. 21 (No. 1), April, 2022. Pp 183-194 https://dx.doi.org/10.4314/sa.v21i1.16
© Faculty of Science, University of Port Harcourt, Printed in Nigeria *ISSN 1118 – 1931*

44.00 with a mean of 8.43 and $(0.62 - 9.44) \times 10^{-6}$ with a mean of 5.65×10^{-6} respectively. The values of the absorbed dose rates are greater than the world average of 60 nGy/h while the values of the annual effective dose rates are less than the world average of 1000 μSv/y. The values of the external and internal hazard indices are greater than the permissible limit of one (1). The radium equivalent value is also greater than the acceptable limit of 370 Bq/kg and the activity utilization index is greater than the world's average. The values of these radiological parameters imply that there may be high gamma irradiation externally and internally if the dwellers of Igbeti are exposed to ionizing radiation from the radionuclides in the rocks during the annual festive period they observe at the rocks at Igbeti. However, the mean value of the excess lifetime cancer risk for the study is below the permissible limit of 2.9×10^{-4}, (UNSCEAR, 2000).

Table 4: Comparison of estimated radiological parameters for the study with other countries

Countries	Ra_{eq} (Bq/kg)	H_{ext}	H_{int}	Dose (D) nGy/h	AEDE ($\mu Sv/y$)	ELCR ($\times 10^{-6}$)	References
Present Study	1199.0	4.22	3.45	515.89	0.63	5.65	Present study
Egypt	56.00	0.15	0.18	28.60	40	-	El-Arabi, 2006
China	190.0	0.51	0.59	-	0.65	-	Xinwei *et al.*, 2006
Turkey	-	-	-	44	0.30	-	Wafaa, 2004
Turkey				43.2			Ahmet, 2006
Cyprus	-	-		1209	2970	-	Michalis *et al.*, 2003

Table 4 presents the comparison of the estimated radiological parameters associated with the exposure due to ionizing radiation from the radionuclides in rock samples for the study with similar studies from other countries.

Table 5: Statistical analysis of the Activity concentrations of ^{226}Ra, ^{232}Th and ^{40}K

Statistical Parameters	^{226}Ra	^{232}Th	^{40}K
Minimum	14.82	210.8	242.91
Maximum	5766.0	3679.28	5952.95
Mean	355.95	709.17	1102.02
Standard Deviation	1277.35	977.17	1228.34
Skewness	4.43	2.84	3.55
Kurtosis	19.71	6.97	14.12
Frequency	leptokurtic distribution	platykurtic distribution	leptokurtic distribution

The statistical analysis of the activity concentrations of ^{226}Ra, ^{232}Th, and ^{40}K are presented in Table 4. SPSS 17 software was used for the analysis. The curves showing the frequency distributions for ^{226}Ra, ^{232}Th, and ^{40}K (Figs. 2 – 4)

concentrations are normal. Skewness is a measure of the asymmetry of the probability distribution of a real-valued random variable around its mean. Knowledge of the Skewness of a data set indicates whether deviations from the mean are going to be positive or negative. The mean and the standard deviation of the activity concentrations of ^{40}K are close compared to that of ^{226}Ra and ^{232}Th. The measure of skewness of 4.43, 2.84, and 3.35 for ^{226}Ra, ^{232}Th, and ^{40}K concentrations show that the distributions of the three radionuclides are fairly symmetrical. Kurtosis is a measure of probability of data being peaked or flat relative to a normal distribution. Data sets with high kurtosis tend to have a distinct peak near the mean and decrease and forming heavy tails (leptokurtic distribution). Data sets with low kurtosis tend to have a flat top (Figure 3) and small tails (platykurtic distribution) (Figs. 2 and 3). Positive kurtosis indicates a peaked distribution and negative kurtosis indicates a flat distribution of the activity concentrations. The positive kurtosis values of 19.71, 6.97, and 14.12 for ^{226}Ra, ^{232}Th, and ^{40}K concentrations show that most of the samples have either very low values or very high values. The radionuclides in the rock samples for the study exhibit some degree of non-multi-modality. Multi-modal characteristics of the radioactive elements show the complexity of minerals in soil samples.

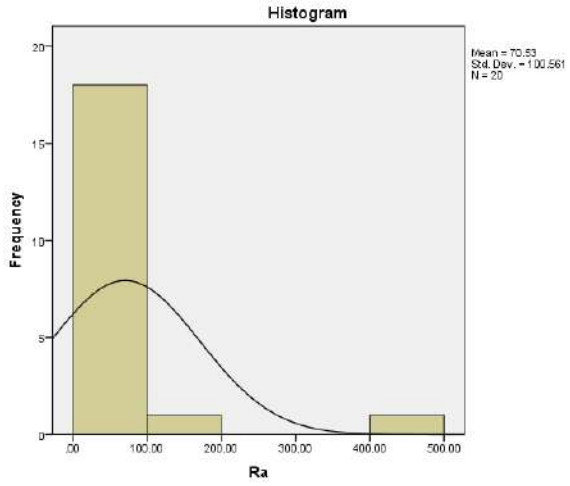

Figure 2: Frequency distribution curve for ^{226}Ra

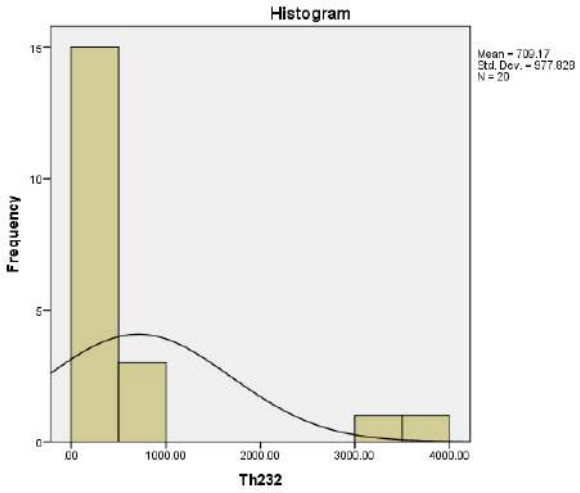

Figure 2: Frequency distribution curve for ^{232}Th

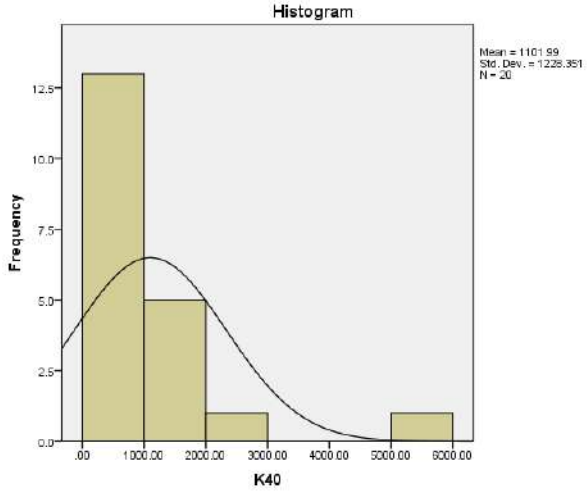

Figure 3: Frequency distribution curve for ^{40}K

Scientia Africana, Vol. 21 (No. 1), April, 2022. Pp 183-194 *https://dx.doi.org/10.4314/sa.v21i1.16*
© Faculty of Science, University of Port Harcourt, Printed in Nigeria *ISSN 1118 – 1931*

Table 6: Pearson correlation coefficient matrix for estimated radiological parameters of the study

Radiological Parameters	^{226}Ra	^{232}Th	^{40}K	Ext_{ind}	Int_{ind}	Ra_{eq}	Absorbed Dose rates(D) (nGy/h)	AEDE (μSv/y)	AUI	ELCR
^{226}Ra	1.00									
^{232}Th	0.67	1.00								
^{40}K	0.52	0.66	1.0							
Ext_{ind}	0.75	0.62	0.73	1.0						
Int_{ind}	0.73	0.99	0.72	0.62	1.0					
Ra_{equ}	0.73	0.99	0.73	0.63	0.99	1.0				
Dose(D) (nGy/h)	0.73	0.99	0.73	0.63	0.99	0.99	1.0			
AEDE(μSv/y)	0.73	0.99	0.73	0.62	0.99	1.00	1.0	1.0		
AUI	0.09	-0.02	0.16	-0.15	-0.05	-0.28	-0.03	-0.03	1.0	
ELCR	0.69	0.93	0.51	0.54	0.84	0.91	0.90	0.90	-0.23	1.0

Pearson correlation coefficient was used to establish the degree of relationship that exists between the radiological parameters in the study and the result is as presented in Table 6. There are strong correlations between all the radionuclides with the highest being 0.99. This implies that the levels of exposure of the dwellers of Igbeti to these natural radionuclides are close in range. This trend was also observed in the positive correlation that exists between the other estimated radiological parameters viz a viz; external and internal gamma indices, dose rates, annual dose rates, and excess lifetime cancer risks. This again explains the fact that quantifying the level of exposure of the dwellers of Igbeti to radionuclides in the rock surrounding the area concerning the estimated radiological parameters gives close-range values. Fusun *et al.*, 2020, Ajetunmobi, 2018, and Ghada and Arafat, 2018 reported the same trend of positive correlation between estimated radiological parameters in their study. However, there seems to be a negative and very low correlation between the activity utilization index and other radiological parameters for the study. This may be interpreted that the activity utilization index values (though greater than the world) do not hinder the use of the rocks as building materials. This is due to the low values of the activity concentrations of all the radionuclides in the rock samples. Unlike the work of Lasun *et al.*, 2019, which reported positive correlations between the activity utilization index and ^{226}Ra (0.99), ^{232}Th (0.57), external and internal indices (0.98, 0.99), and radium equivalent (0.99).

CONCLUSION

The activity concentrations of natural radionuclides in the rock samples from Igbeti and the associated radiological parameters have been investigated to estimate the number of exposures of the dwellers. The estimated radiological parameters for the study are all greater than the permissible limit with the exceptions of excess lifetime cancer risks and the annual effective dose rates. This shows that the rocks surrounding the dwellers of Igbeti town enhance natural radionuclides exposure. Further and regular radiological i nvestigations/measurements should be advised and encouraged in the areas studied and different pathways for

exposure to ionizing radiation should be considered.

REFERENCES

Adewoyin, O.O, Omeje, M., Joel, E.S., Akinwumi, S.A., Ehi-Eromoseled, C.O, Zaidi, E. (2018).Radionuclides proportion and radiological risk assessment of soil samples collected in Covenant University, Ota, Ogun State Nigeria. *Methods 5* :1419-1426

Ajetunmobi, A.E. (2018). Assessment of radiological and chemical effect of mining of tantalite in selected mining sites in Oke-Ogun, Nigeria. (Unpublished Ph.D. Thesis, Federal University of Agriculture, Abeokuta, Nigeria:289-290.

Alausa, S.K. (2014). Radiological Assessment of soils on the Waysides of the road under construction in Ijebu-Ode, Ogun State, Southwestern Nigeria Journal of Natural Science Research, 4, (15): 80-84.

Alnour, I. A., Wagiran, H., Ibrahim, N., Laili, Z., Omar, M., Hamzah, S. (2012). Natural radioactivity measurements in the granite rock of quarry sites, Johor, Malaysia. *Journal of Environmental Radioactivity*, 95 :98-106.

Beretka, J. and Matthew P.J. 1985.Natural Radioactivity of Australian Building Materials, Industrial wastes and By-Products *Health Phys. 48:87-95*

Climate and Average Weather Year Round in Igbeti. (https://weatherspark.com/y/50064/Average-Weather-in-Igbeti-Nigeria-Year-Round), date of access, 25th , March, 2022.

El-Arabi, A. M. (2006) . ^{226}Ra, ^{232}Th, and ^{40}K concentrations in igneous rocks from eastern desert, Egypt and its radiological implications. *Radiation Measurement*, 42(1), 94-100.

El-Gamal, A. Nasr, S. El-Tahe. (2007) A. study of the spatial distribution of Natural Radioactivity In The Upper Egypt Nile River Sediments. *Radiation Measurements*, 42, 457-465.

Fusun, Y., Nurdane., I, Mehet, D., Mustafa, G.Y., Alper, G. and Abdulla, K. (2020).Statistical Analysis of Natural Radioactivity Measurements for the Soil of Marsa Alam-Shalateen Red-Sea Coast Area, Egypt. International Journal of Advanced Scientific and Technical Research, 1(8), 71-85

Ghada, I. El-shanshoury and Arafat, A.A.(2018).Statistical analysis of natural radioactivity measurements for the soil of Marsa Alam-Shalateen Red-Sea Coast area, Egypt. International Journal of Advanced Scientific and Technical Research, 1(8), 71-85

IAEA, (2003). An annual report to the general conference concerning the affairs of the agency and any project approved by the Agency. A-1400, Vienna, Austria.

ICRP, (1990). Annals of the International Commission on Radiological Protection. Recommendations of the ICRP. ICRP Publication No. 60. Oxford Pergamon Press.

Iqbal, M. M. (2000). Measurement of natural radioactivity in marble found in Pakistan usin NaI(TI) gamma ray spectrometer. Journal of Environmental Radioactivity, *51*, 255-265.

Jibiri, N.N, Alausa S.K., and Farai, I.P (2009). Radiological hazard indices due to activity concentrations of natural radionuclides in farm soils from two background radiation areas in Nigeria. *International Journal of low Radiation, 6: 79–95.*

Jibiri, N.N and Biere, P.E. (2011). Activity concentrations of ^{232}Th, ^{226}Ra and ^{40}K and gamma radiation absorbed dose rate levels in farm soil for the production of different brands of

Scientia Africana, Vol. 21 (No. 1), April, 2022. Pp 183-194 *https://dx.doi.org/10.4314/sa.v21i1.16*
© Faculty of Science, University of Port Harcourt, Printed in Nigeria *ISSN 1118 – 1931*

cigarette tobacco smoked in Nigeria. *Iran J Radiat Res*, 8 (4), 201-206.

Kaleel, M., Thabayneh., M, Mohammed, J. (2012). Natural radioactivity Levels and estimation of radiation exposure in environmental soil Samples from Tulkarem province-Palestine. *Open Journal of Soil* Science, 2: 7-16

Kapanadze, K., Magalashvili A., Imnadze, P. (2019). Distribution of natural radionuclides in the soils and assessment of radiation hazards in the Khrami Late Variscan Crystal Massif (Georgia). 5:1-19

Kurnaz, A., Kucukomroglu, B., Keser, R., Olumusoglu, N. T., Korkmaz, F., Karahan, G, Cevik,. (2007) Determination of radioactivity levels and hazards of soil and Sediment Samples In Firtina Valley (Rize, Turkey). *Applied Radiation and Isotopes*, 65, 1281-1289.

Lasun, T. O, Patrick O., Ayeku , S. O. Inuyomi , O. M. Ogunsakin , O. F. Oladejo and Isiah, A.A. (2019). Assessment of naturally occurring ^{40}K, ^{232}Th and ^{238}U and their associated radiological hazard indices in soils used for building in Ondo West Local Government area, Southwestern, Nigeria

Lucia, S., Marco, F., Mauro, C., Giancarta, P., F. Ugo, F., Annita, C. (2006). Natural radionuclides in the rocks of the Valle del Carvo Pluto in Piedmon, *RadiationProtection Dosimetry*, 1-8.

Malczewski, M., Teper, L., and Dorda, J. (2004). Assessment of natural and anthropogenic radioactivity levels in rocks and soils in the environs of Swieradow Zdrojin Sudetes, Poland, by in situ gamma-ray spectrometry. Journal of Environmental Radioactivity, 73 (3),233-245

Mamant-Ciesla, K., Gwaiazdowski, B., Biernacka, M., and Zak, A. Radioactivity of building materials in Poland. NaturalRadiation Environment. New York: Halsted Press 1982: 551.

Manjunatha, S., Anandaram, B.N, Paramesh, L. and Venkataramaiah, P.(1998). Study of environmental radioactivity at the horizon of Uranium bearing quartz pebble conglomerates near Chickamangalur, India. Radiation Physics and Chemistry, 51(4-6): 619

Michalis, T. Haralabos, T., Stelios, C., and George, C. (2003) . Gamma radiation measurements and dose rates in commercially used natural tiling rocks (Granites). Journal of Environmental Radioactivity, 70(3): 223-235

Narayana, Y., Rajashekara, K.M, and Siddappa, K. (2007). Natural radioactivity in some major rivers of coastal Karnataka on the Southwest coast of India. Journal of Environmental Radioactivity, 95: 98-106.

National Population Commission, NPC. (2006). Nigerian population census report 2006

OECD, (1979). Exposure to Radiation from Natural Radioactivity in Building Materials. Report by NEA Group of Experts of the Nuclear Energy Agency, OECD, Paris, France.

Olasunkanmi, N. K., Sunmonu, L. A. and Adabanija, M. A. (2020).Geophysical investigation for mineral prospecting in Igbeti-Moro Area, Southwestern Nigeria, Kuwait J. Sci., 47(3): 2-14.

Osmanlioglu, A. E. (2006). Natural radioactivity and evaluation of effective dose equivalent of granites in Turkey,Radiation Protection Dosimetry, 121: 325-329.

Parakash, M.M., Kaliprasad C.S., Narayana, Y. (2017). Studies on natural radioactivity in rock of Coorg District, Karnataka State, India.Journal of Radiation Research and Applied Science, 10 (2):128-134.

Qureshi, A. A., Tariq, S., Ud Din K., Manzoor, S., Calligaris, C. and Waheed, A.(2014). Evaluation of excessive lifetime cancer risk due to natural radioactivity in the rivers sediments of Northern Pakistan. *Journal of Radiation Research and Applied Sciences*, (7): 438-447.

Rangaswamy, D. R., and Sannappa, J. (2016). Distribution of natural radionuclides and radiation level measurements in Karnataka State, India: An Overview, Journal of Radioanalytical Nuclear Chemistry, 1: 1-15

Rasha, S. A., Raghad, S. M. and Rana O. A. (2018). The activity concentrations and radium equivalent in samples collected from the Eastern Parts of Basrah Governorate in Southern Iraq. International Journal of Analytical Chemistry: 1-12.

Shittu, H. O., I.O. Olarinoye, A.N. Baba-Kutigi, S.F. Olukotun, OJO, E.O, and EGGA, E.O. (2015). Determination of the radiological risk associated with naturally occurring radioactive materials (NORM) at selected quarry sites in Abuja FCT, Nigeria: Using Gamma-Ray Spectroscopy. American Institute of Science Physics Journal, 2015, 1(2): 71-78.

Taskin, H., Karavus, M., Ay, P., Topuzoglu, A., Hindiroglu, S., and Karahan, G. 2009. Radionuclide Concentrations in Soil and Life time Cancer rRsk due to the Gamma Radioactivity in Kirklareli, Turkey. Journal of Environmental Radioactivity 100:49-53

UNSCEAR, (1988) United Nations Scientific Committee on the Effect of Atomic Radiation, Sources, Effects and Risk of Ionizing Radiation. United Nations, New York.

UNSCEAR, 1993: Exposure from natural sources of radiation, in United Nations Scientific Committee on the Effects of atomic Radiation, United Nations: New York.

UNSCEAR, 2000: Dose assessment methodologies UNSCEAR Report to the general assembly (New York: United State Environmental Protection Agency).

Wafaa, A. (2004). Specific activity and hazards of granite samples collected from the Eastern Desert of Egypt. Journal of Environmental Radioactivity, 75(3) : 315-32.

Wikipedia (Igbeti).(https://en.wikipedia.org/wiki/Igbeti), date of access, 29Th March, 2022.

Xinwei, L., Lingqing, W., Xiaodan, J. (2006). Radiometric analysis of Chinese commercial granites. Journal of Radioanalytical and Nuclear Chemistry 267(3):669-673

Scientia Africana, Vol. 21 (No. 1), April, 2022. Pp 195-206 https://dx.doi.org/10.4314/sa.v21i1.17
© Faculty of Science, University of Port Harcourt, Printed in Nigeria *ISSN 1118 – 1931*

EFFICIENCY OF MODIFIED CENTRAL COMPOSITE DESIGNS WITH FRACTIONAL FACTORIAL REPLICATES FOR FIVE-VARIABLE NON-STANDARD MODELS

Iwundu, M. P and Nwoshopo, D. E.
Department of Mathematics and Statistics, University of Port Harcourt, Nigeria.
mary.iwundu@uniport.edu.ng ; dennisejike3@gmail.com

Received: 22-11-2021
Accepted: 20-03-2022

ABSTRACT

The efficiencies of standard central composite designs are compared with modified central composite designs on non-standard models using D- and G-efficiency criteria. Diagonal elements of the Hat matrix are utilized in the construction of the modified central composite designs. Fractional factorial replicates are used to maintain manageable design sizes. Results show that D-efficiencies of the designs decline for standard CCDs as the number of missing quadratic terms increases but increase with modified CCDs for increased number of missing quadratic terms. Similarly, G-efficiencies of the designs decline for standard CCDs as the number of missing quadratic terms increases but increase with modified CCDs for increased number of missing quadratic terms.

Keywords: Standard CCDs, Modified CCDs, Non-Standard Model, Hat Matrix, Fractional Factorial Replicates, Design Efficiencies.

INTRODUCTION

Response Surface Methodology (RSM) strives to relate an output or a response variable to a number of input or predictors variables that affect it. Usually, the form of such a relationship is always not known, but low-order polynomial may be used as approximating models. Fractional factorial designs allow the study of a large number of factors with relatively few experimental trials. A well selected subset, or fraction, of the treatments can be employed with manageable loss of information about the main effects and key low-order interactions. At a later stage of experimentation, higher order design may be used to reflect the presence of curvature in the model.

3^kfull factorial designs have been useful in estimating all parameters in regression models. However, the number of treatment combinations required by 3^k design increase rapidly with increased number of factors.Central Composite Designs as well as other optimal response surface designs, serve purposely to truncate the challenges imposed by 3^k factorial designs. There are three basic components of Central Composite Designs, namely; the factorial portion, the axial portion and the centre portion. The factorial component of a CCD addresses estimation of linear main effects and all the factor interaction effects. The $2k$ axial (star) portion addresses the estimation of all quadratic effects. The center portions accounts for estimation of model's lack of fit.

Box and Hunter (1957) considered the subject of Rotatability. The rationale behind rotatability is that the scaled prediction variance at any two locations from the design center should be the same. As in Myers *et al.* (2009), Rotatability offers guidelines for the choice axial distance, α as well as the number of center runs, n_c.

Fundamental Model for the use of Second-order Response Surface Designs

The model that allows the use of second-order designs is

$$Y = \beta_0 + \sum_{i=1}^{k} \beta_i x_i + \sum_{j=i+1}^{k} \sum_{i=1}^{k-1} \beta_{ij} x_i x_j + \sum_{i=1}^{k} \beta_{ii} x_{ii}^2 + \varepsilon \quad (1)$$

having $p = \frac{(k+1)(k+2)}{2}$ model parameters.Y is the measured response;β's are model coefficients; x_i's are the input variables and ε is an error term associated with Y. The second-order model may be represented in matrix form as

$$Y = X\beta + \varepsilon \quad (2)$$

with solution

$$\hat{\beta} = (X^{'}X)^{-1}X^{'}Y \quad (3)$$

provided that $(X^{'}X)^{-1}$ is non-singular.

The unbiased estimate of the parameters, $\hat{\beta}$, is such that

$$\mathrm{E}(Y) = \hat{Y} = X\hat{\beta} = X(X'X)^{-1}X'Y = HY \quad (4)$$

where

$$H = X(X'X)^{-1}X' \quad (5)$$

is called the hat matrix.

The diagonal entries h_{ii} of the hat matrix are are such that $0 \leq h_{ii} \leq 1$ and $\sum_{i=1}^{n} h_{ii} = p$; where p is the number of model coefficients and n is the number of observations or runs in the design.

In modelling second-order response surface, test of significance of regression coefficients may reveal that some model components are not significant thus leading to such coefficients being removed from the full model. A second-order model with less than $p = \frac{(k+1)(k+2)}{2}$ model parameters is regarded as reduced or non-standard model. The ideal designs for second-order response surface models include the classical central composite designs, Box-Behnken designs, computer-aided designs and so many others that are contained in most literatures on Response Surface Methodology. Iwundu and Otaru (2019) constructed Hat-Matrix aided composite designs for Second-Order models. These designs were comparable with Standard Response Surface Methodology (RSM) designs and Computer-Generated designs. Their optimality and efficiency properties were further presented.

Scientia Africana, Vol. 21 (No. 1), April, 2022. Pp 195-206 https://dx.doi.org/10.4314/sa.v21i1.17
© Faculty of Science, University of Port Harcourt, Printed in Nigeria *ISSN 1118 – 1931*

A limitation in using classical response surface designs is that they naturally assume that all factors are equally easy to manipulate, by that giving way for complete randomization of experimental run order. In practice, the size of an experiment can become prohibitively large when a large number of factors is to be studied and cannot be completely randomized. However, these experiments are often conducted in a manner that restricts the randomization, which proceeds to split–plot structure. Some studies that investigate response surface experiments with split-plot structures include Letsinger *et al.* (1996), Vining *et al.* (2005) and Kowalsky *et al.* (2006).

In Iwundu (2018), steps are provided for constructing modified central composite designs for non-standard models. Unfortunately, the algorithm becomes difficult to use when $k \geq 5$. A way to handle this difficulty is to controllably reduce the number of experimental runs. For simplicity, it is logical to use fractional factorials instead of the full factorial. The aim of this research is to construct Modified Central Composite Design (MCCD) for non-standard models with fractional factorial replicates with the intents of comparing the performance of the modified central composite design with the standard central composite designs for non-standard models. For illustrative purpose, half fraction of full factorial designs in five variables is considered and three centre runs are employed in the design. An axial distance of $\alpha = F^{1/4}$ is used, where F is the number of fractional factorial points of Resolution V or higher. Thus, if N denotes the total number of experimental trials in the planned CCD, $N = 2^{k-q} + 2k + n_c$.

Fundamental Algorithm for Modified Central Composite Design

In constructing modified central composite designs with fractional factorial replicates, we rely on the procedure of Iwundu (2018) whose non-standard second-order model is formed using the Hierarchical method of Borkowski and Valeroso (1997). The standard central composite design is employed with fractional factorial replicates at the factorial portion. The diagonal elements of the hat matrix are $d_{v1}, d_{v2}, \ldots, d_{v2^k}$ for the factorial portion, $d_{\alpha 1}, d_{\alpha 2}, \ldots, d_{\alpha 2^k}$ for the axial portion and $d_{c1}, d_{c2}, \ldots, d_{cn_c}$ for the center portion. We search out for locations of the design points in each standard CCD portion where the uniqueness of diagonal elements has been lost. The design points in each portion of the standard CCD having the least diagonal elements are deleted from the CCD. Results show that the efficiency of the Modified Central Composite Design (MCCD) exceeds that of the classical or standard Central Composite Design (CCD).

The full second-order model in five design variables is given in expanded form as

$$y = \beta_0 + \beta_1 x_1 + \beta_2 x_2 + \beta_3 x_3 + \beta_4 x_4 + \beta_5 x_5 + \beta_{12} x_1 x_2 + \beta_{13} x_1 x_3 + \beta_{14} x_1 x_4 + \beta_{15} x_1 x_5 + \beta_{23} x_2 x_3 + \beta_{24} x_2 x_4 + \beta_{25} x_2 x_5 + \beta_{34} x_3 x_4 + \beta_{35} x_3 x_5 + \beta_{45} x_4 x_5 + \beta_{11} x_1^2 + \beta_{22} x_2^2 + \beta_{33} x_3^2 + \beta_{44} x_4^2 + \beta_{55} x_5^2 + \varepsilon \quad (6)$$

Following the hierarchical formation of non-standard models, the cases considered in this research involve the absence of one, two or three quadratic terms in the model.

The model when x_1^2 is absent is given as

$$y = \beta_0 + \beta_1 x_1 + \beta_2 x_2 + \beta_3 x_3 + \beta_4 x_4 + \beta_5 x_5 + \beta_{12} x_1 x_2 + \beta_{13} x_1 x_3 + \beta_{14} x_1 x_4 + \beta_{15} x_1 x_5 + \beta_{23} x_2 x_3 + \beta_{24} x_2 x_4 + \beta_{25} x_2 x_5 + \beta_{34} x_3 x_4 + \beta_{35} x_3 x_5 + \beta_{45} x_4 x_5 + \beta_{22} x_2^2 + \beta_{33} x_3^2 + \beta_{44} x_4^2 + \beta_{55} x_5^2 + \varepsilon \quad (7)$$

The model when x_1^2 and x_2^2 are absent is given as

$$y = \beta_0 + \beta_1 x_1 + \beta_2 x_2 + \beta_3 x_3 + \beta_4 x_4 + \beta_5 x_5 + \beta_{12} x_1 x_2 + \beta_{13} x_1 x_3 + \beta_{14} x_1 x_4 + \beta_{15} x_1 x_5 + \beta_{23} x_2 x_3 + \beta_{24} x_2 x_4 + \beta_{25} x_2 x_5 + \beta_{34} x_3 x_4 + \beta_{35} x_3 x_5 + \beta_{45} x_4 x_5 + \beta_{33} x_3^2 + \beta_{44} x_4^2 + \beta_{55} x_5^2 + \varepsilon \quad (8)$$

The model when x_1^2, x_2^2 and x_3^2 are absent is given as

$$y = \beta_0 + \beta_1 x_1 + \beta_2 x_2 + \beta_3 x_3 + \beta_4 x_4 + \beta_5 x_5 + \beta_{12} x_1 x_2 + \beta_{13} x_1 x_3 + \beta_{14} x_1 x_4 + \beta_{15} x_1 x_5 + \beta_{23} x_2 x_3 + \beta_{24} x_2 x_4 + \beta_{25} x_2 x_5 + \beta_{34} x_3 x_4 + \beta_{35} x_3 x_5 + \beta_{45} x_4 x_5 + \beta_{44} x_4^2 + \beta_{55} x_5^2 + \varepsilon \quad (9)$$

Two optimality criteria are employed in this research namely D-Optimality criterion and G-Optimality criterion. D-optimality criterion, which seeks to maximize the determinant of the moment matrix, has been so well studied as evident in prior and current researches such as in Kiefer and Wolfowitz (1959), Fedorov (1972), Atkinson and Donev (1992), Eze and Ngonadi (2018). Very recently, Nwanya *et al.* (2020) considered the performance of D-, G- and A-optimality criteria for reduced second-order models having no quadratic and no interaction terms for five variations of Central Composite Design. Wanyonyi *et al.* (2021) explored D-, A-, I-, and G- optimality criteria and their efficiency in determining an optimal split-plot design in mixture modelling. Jaja etal. (2021a) considered A-efficiency (a criterion closely related to D-efficiency) as a measure of the performance of CCDs and MCCDs constrained by missing observations for non-standard models. Jaja etal. (2021b) studied the robust properties of the designs in Jaja etal. (2021a). Iwundu and Oko (2021) utilized A-, D- and G-optimality criteria in studying the efficiency and optimal properties of four varieties of replicated Central Composite Design with full factorial portions. The efficiency of an experimental design can be quantified in interpretable form using one or more efficiency criteria. As in Goos and Jones (2011), D-efficiency of a design compares the determinant of the information matrix of that design to an "ideal" determinant associated with an orthogonal design.

D-efficiency of a design is mathematically given as

$$\text{D-efficiency} = \left(\frac{|X'X|}{N^p}\right)^{\frac{1}{p}} = \frac{|X'X|^{\frac{1}{p}}}{N} \quad (10)$$

where p is the number of parameters of the model.

G-Optimality criterion is concerned with designs whose scaled prediction variances have good prediction at a particular location in the design space. G-optimality criterion is symbolically written as

$$\text{minmax}\{Nf'(x)(X'X)^{-1} f(x)\} = \text{minmax}\{Nvar[\hat{y}(x)]\} \quad (11)$$

Scientia Africana, Vol. 21 (No. 1), April, 2022. Pp 195-206 *https://dx.doi.org/10.4314/sa.v21i1.17*
© Faculty of Science, University of Port Harcourt, Printed in Nigeria *ISSN 1118 – 1931*

G-efficiency, which has gained competitive usage with D-efficiency, is defined as

$$\text{G-efficiency} = \frac{p}{V(\underline{x})_{\max}} \tag{12}$$

where p is the number of parameters in the model and $V(\underline{x})_{\max}$ is the maximum scaled variance of prediction.

Construction of MCCD in five design variables

Consider the construction of modified central composite design for non-standard model having the absence of one quadratic term, x_1^2, of the full second-order model. The factorial portion of the CCD shall consist of 2^{5-1} half fractional factorial of Resolution V with the Defining Relation $I = +ABCDE$.

The 16 factorial points to include in the design are as follows;

-1	-1	-1	-1	1
1	-1	-1	-1	-1
-1	1	-1	-1	-1
1	1	-1	-1	1
-1	-1	1	-1	-1
1	-1	1	-1	1
-1	1	1	-1	1
1	1	1	-1	-1
-1	-1	-1	1	-1
1	-1	-1	1	1
-1	1	-1	1	1
1	1	-1	1	-1
-1	-1	1	1	1
1	-1	1	1	-1
-1	1	1	1	-1
1	1	1	1	1

The axial portion of the CCD comprises 10 axial points; $(\pm\alpha, 0, 0, 0, 0), (0, \pm\alpha, 0, 0, 0), (0, 0, \pm\alpha, 0, 0), (0, 0, 0, \pm\alpha, 0), (0, 0, 0, 0, \pm\alpha)$

where $\alpha = 2$. The center portion shall comprise n_c= 3 center runs defined by $(0, 0, 0, 0, 0), (0, 0, 0, 0, 0), (0, 0, 0, 0, 0)$

With $\alpha = 2$ and *N*=29 design points associated with the one-half fractional factorial runs, 10 axial runs and n_c= 3 center runs yields the design matrix

$X =$

1	-1	-1	-1	-1	1	1	1	1	-1	1	1	-1	1	-1	-1	1	1	1	1
1	1	-1	-1	-1	-1	-1	-1	-1	-1	1	1	1	1	1	1	1	1	1	1
1	-1	1	-1	-1	-1	-1	1	1	1	-1	-1	-1	1	1	1	1	1	1	1
1	1	1	-1	-1	1	1	-1	-1	1	-1	-1	1	1	-1	-1	1	1	1	1
1	-1	-1	1	-1	-1	1	-1	1	1	-1	1	1	-1	-1	1	1	1	1	1

1	1	-1	1	-1	1	-1	1	-1	1	-1	1	-1	-1	1	-1	1	1	1	1
1	-1	1	1	-1	1	-1	-1	1	-1	1	-1	1	-1	1	-1	1	1	1	1
1	1	1	1	-1	-1	1	1	-1	-1	1	-1	-1	-1	-1	1	1	1	1	1
1	-1	-1	-1	1	-1	1	1	-1	1	1	-1	1	-1	1	-1	1	1	1	1
1	1	-1	-1	1	1	-1	-1	1	1	1	-1	-1	-1	-1	1	1	1	1	1
1	-1	1	-1	1	1	-1	1	-1	-1	-1	1	1	-1	-1	1	1	1	1	1
1	1	1	-1	1	-1	1	-1	1	-1	-1	1	-1	-1	1	-1	1	1	1	1
1	-1	-1	1	1	1	1	-1	-1	-1	-1	-1	-1	1	1	1	1	1	1	1
1	1	-1	1	1	-1	-1	1	1	-1	-1	-1	1	1	-1	-1	1	1	1	1
1	-1	1	1	1	-1	-1	-1	-1	1	1	1	-1	1	-1	-1	1	1	1	1
1	1	1	1	1	1	1	1	1	1	1	1	1	1	1	1	1	1	1	1
1	-2	0	0	0	0	0	0	0	0	0	0	0	0	0	0	0	0	0	0
1	2	0	0	0	0	0	0	0	0	0	0	0	0	0	0	0	0	0	0
1	0	-2	0	0	0	0	0	0	0	0	0	0	0	0	0	4	0	0	0
1	0	2	0	0	0	0	0	0	0	0	0	0	0	0	0	4	0	0	0
1	0	0	-2	0	0	0	0	0	0	0	0	0	0	0	0	0	4	0	0
1	0	0	2	0	0	0	0	0	0	0	0	0	0	0	0	0	4	0	0
1	0	0	0	-2	0	0	0	0	0	0	0	0	0	0	0	0	0	4	0
1	0	0	0	2	0	0	0	0	0	0	0	0	0	0	0	0	0	4	0
1	0	0	0	0	-2	0	0	0	0	0	0	0	0	0	0	0	0	0	4
1	0	0	0	0	2	0	0	0	0	0	0	0	0	0	0	0	0	0	4
1	0	0	0	0	0	0	0	0	0	0	0	0	0	0	0	0	0	0	0
1	0	0	0	0	0	0	0	0	0	0	0	0	0	0	0	0	0	0	0
1	0	0	0	0	0	0	0	0	0	0	0	0	0	0	0	0	0	0	0

The design points and the associated diagonal elements of the hat matrix are presented in Table 1. The diagonal entries associated with the factorial portion are a constant $d_v = 0.8750$, the axial portion has a maximum diagonal value $d_{amax} = 0.5883$ at eight points and a minimum diagonal element $d_{amin} = 0.3667$ at two points. Associated with the 3 centre points is a unique diagonal element $d_c = 0.2000$. The points $(2,0,0,0,0)$ and $(-2,0,0,0,0)$ are dropped from the design and a modified design is formed.

The design points and the associated diagonal elements of the hat matrix for the Modified CCD are presented in Table 2. Table 3 gives the scaled prediction variances associated with standard CCD and modified CCD for five-variable non-standard model having one quadratic term of the model is removed. Table 4 gives the Summary Statistics on design efficiency when one quadratic term is removed from the full model. Table 5 gives the Summary Statistics on design efficiency when two quadratic terms are removed from the full model. Table 6 gives the Summary Statistics on design efficiency when three quadratic terms are removed from the full model.

Scientia Africana, Vol. 21 (No. 1), April, 2022. Pp 195-206 *https://dx.doi.org/10.4314/sa.v21i1.17*
© Faculty of Science, University of Port Harcourt, Printed in Nigeria *ISSN 1118 – 1931*

Table 1: Design points of 5-variable standard CCD and the h_{ii} values associated with the non-standard model having x_1^2 term absent.

Design point					h_{ii} value
-1	-1	-1	-1	1	0.8750
1	-1	-1	-1	-1	0.8750
-1	1	-1	-1	-1	0.8750
1	1	-1	-1	1	0.8750
-1	-1	1	-1	-1	0.8750
1	-1	1	-1	1	0.8750
-1	1	1	-1	1	0.8750
1	1	1	-1	-1	0.8750
-1	-1	-1	1	-1	0.8750
1	-1	-1	1	1	0.8750
-1	1	-1	1	1	0.8750
1	1	-1	1	-1	0.8750
-1	-1	1	1	1	0.8750
1	-1	1	1	-1	0.8750
-1	1	1	1	-1	0.8750
1	1	1	1	1	0.8750
-2	0	0	0	0	0.3667
2	0	0	0	0	0.3667
0	-2	0	0	0	0.5883
0	2	0	0	0	0.5883
0	0	-2	0	0	0.5883
0	0	2	0	0	0.5883
0	0	0	-2	0	0.5883
0	0	0	2	0	0.5883
0	0	0	0	-2	0.5883
0	0	0	0	2	0.5883
0	0	0	0	0	0.2000
0	0	0	0	0	0.2000
0	0	0	0	0	0.2000

Table 2: Design points of 5-variable MCCD and associated h_{ii} values in the absence of x_1^2 term

Design point					h_{ii} value
-1	-1	-1	-1	1	0.8958
1	-1	-1	-1	-1	0.8958
-1	1	-1	-1	-1	0.8958
1	1	-1	-1	1	0.8958
-1	-1	1	-1	-1	0.8958
1	-1	1	-1	1	0.8958
-1	1	1	-1	1	0.8958
1	1	1	-1	-1	0.8958

-1	-1	-1	1	-1	0.8958
1	-1	-1	1	1	0.8958
-1	1	-1	1	1	0.8958
1	1	-1	1	-1	0.8958
-1	-1	1	1	1	0.8958
1	-1	1	1	-1	0.8958
-1	1	1	1	-1	0.8958
1	1	1	1	1	0.8958
0	-2	0	0	0	0.5883
0	2	0	0	0	0.5883
0	0	-2	0	0	0.5883
0	0	2	0	0	0.5883
0	0	0	-2	0	0.5883
0	0	0	2	0	0.5883
0	0	0	0	-2	0.5883
0	0	0	0	2	0.5883
0	0	0	0	0	0.3333
0	0	0	0	0	0.3333
0	0	0	0	0	0.3333

Table 3: Scaled prediction variances for CCD and MCCD in absence of one quadratic model term

Design points					Scaled prediction variance for standard CCD	Scaled prediction variance for Modified CCD
-1	-1	-1	-1	1	25.3750	24.1875
1	-1	-1	-1	-1	25.3750	24.1875
-1	1	-1	-1	-1	25.3750	24.1875
1	1	-1	-1	1	25.3750	24.1875
-1	-1	1	-1	-1	25.3750	24.1875
1	-1	1	-1	1	25.3750	24.1875
-1	1	1	-1	1	25.3750	24.1875
1	1	1	-1	-1	25.3750	24.1875
-1	-1	-1	1	-1	25.3750	24.1875
1	-1	-1	1	1	25.3750	24.1875
-1	1	-1	1	1	25.3750	24.1875
1	1	-1	1	-1	25.3750	24.1875
-1	-1	1	1	1	25.3750	24.1875
1	-1	1	1	-1	25.3750	24.1875
-1	1	1	1	-1	25.3750	24.1875
1	1	1	1	1	25.3750	24.1875
-2	0	0	0	0	16.9167	-
2	0	0	0	0	16.9167	-
0	-2	0	0	0	16.9167	15.7500

Scientia Africana, Vol. 21 (No. 1), April, 2022. Pp 195-206 *https://dx.doi.org/10.4314/sa.v21i1.17*
© Faculty of Science, University of Port Harcourt, Printed in Nigeria *ISSN 1118 – 1931*

0	2	0	0	0	16.9167	15.7500
0	0	-2	0	0	16.9167	15.7500
0	0	2	0	0	16.9167	15.7500
0	0	0	-2	0	16.9167	15.7500
0	0	0	2	0	16.9167	15.7500
0	0	0	0	-2	16.9167	15.7500
0	0	0	0	2	16.9167	15.7500
0	0	0	0	0	5.8000	9.000
0	0	0	0	0	5.8000	9.000
0	0	0	0	0	5.8000	9.000

Table 4: Summary Statistics when one quadratic term is removed; $k = 5, n_c = 3, \alpha = 2$

Design Type	Missing Coefficients	$\det\left(\frac{1}{N}(X'X)\right)$	D-efficiency %	Max SPV	G-efficiency %
Standard CCD on Reduced Model N=29 and p=20	x_1^2	7.7801e – 004	69.91	25.3750	78.82
	x_2^2	7.7801e – 004	69.91	25.3750	78.82
	x_3^2	7.7801e – 004	69.91	25.3750	78.82
	x_4^2	7.7801e – 004	69.91	25.3750	78.82
	x_5^2	7.7801e – 004	69.91	25.3750	78.82
MCCD on reduced model when N=27 and p=20	x_1^2	0.0013	71.73	24.1875	82.69
	x_2^2	0.0013	71.73	24.1875	82.69
	x_3^2	0.0013	71.73	24.1875	82.69
	x_4^2	0.0013	71.73	24.1875	82.69
	x_5^2	0.0013	71.73	24.1875	82.69

Table 5: Summary Statistics when two quadratic terms are removed;$k = 5, n_c = 3, \alpha = 2$

Design Type	Missing Coefficients	$\det\left(\frac{1}{N}(X'X)\right)$	D-efficiency %	Max SPV	G-efficiency %
Full CCD on reduced model with $N = 29$ and $p = 19$	x_1^2, x_2^2	8.6959e – 004	69.01	25.2934	75.12
	x_1^2, x_3^2	8.6959e – 004	69.01	25.2934	75.12
	x_1^2, x_4^2	8.6959e – 004	69.01	25.2934	75.12
	x_1^2, x_5^2	8.6959e – 004	69.01	25.2934	75.12
	x_2^2, x_3^2	8.6959e – 004	69.01	25.2934	75.12
	x_2^2, x_4^2	8.6959e – 004	69.01	25.2934	75.12
	x_2^2, x_5^2	8.6959e – 004	69.01	25.2934	75.12
	x_3^2, x_4^2	8.6959e – 004	69.01	25.2934	75.12
	x_3^2, x_5^2	8.6959e – 004	69.01	25.2934	75.12
	x_4^2, x_5^2	8.6959e – 004	69.01	25.2934	75.12
Modified CCD	x_1^2, x_2^2	0.0030	73.66	22.8860	83.02
	x_1^2, x_3^2	0.0030	73.66	22.8860	83.02

on reduced model when $N = 25$ and $p = 19$	x_1^2, x_4^2	0.0030	73.66	22.8860	83.02
	x_1^2, x_5^2	0.0030	73.66	22.8860	83.02
	x_2^2, x_3^2	0.0030	73.66	22.8860	83.02
	x_2^2, x_4^2	0.0030	73.66	22.8860	83.02
	x_2^2, x_5^2	0.0030	73.66	22.8860	83.02
	x_3^2, x_4^2	0.0030	73.66	22.8860	83.02
	x_3^2, x_5^2	0.0030	73.66	22.8860	83.02
	x_4^2, x_5^2	0.0030	73.66	22.8860	83.02

Table 6: Summary Statistics when three quadratic terms are removed; $k = 5,\ n_c 3, \alpha = 2$

Design Type	Missing Coefficients	$\det\left(\frac{1}{N}(X'X)\right)$	D – Efficiency %	Max SPV	G- efficiency %
Full CCD On Reduced Model with N = 29 and p = 18	x_1^2, x_2^2, x_3^2	9.3716e – 004	67.88	25.2377	71.32
	x_1^2, x_2^2, x_4^2	9.3716e – 004	67.88	25.2377	71.32
	x_1^2, x_2^2, x_5^2	9.3716e – 004	67.88	25.2377	71.32
	x_1^2, x_3^2, x_4^2	9.3716e – 004	67.88	25.2377	71.32
	x_1^2, x_3^2, x_5^2	9.3716e – 004	67.88	25.2377	71.32
	x_1^2, x_4^2, x_5^2	9.3716e – 004	67.88	25.2377	71.32
	x_2^2, x_3^2, x_4^2	9.3716e – 004	67.88	25.2377	71.32
	x_2^2, x_3^2, x_5^2	9.3716e – 004	67.88	25.2377	71.32
	x_2^2, x_4^2, x_5^2	9.3716e – 004	67.88	25.2377	71.32
	x_3^2, x_4^2, x_5^2	9.3716e – 004	67.88	25.2377	71.32
MCCD On Reduced Model when N = 23 and p = 18	x_1^2, x_2^2, x_3^2	0.0082	76.58	21.6104	83.29
	x_1^2, x_2^2, x_4^2	0.0082	76.58	21.6104	83.29
	x_1^2, x_2^2, x_5^2	0.0082	76.58	21.6104	83.29
	x_1^2, x_3^2, x_4^2	0.0082	76.58	21.6104	83.29
	x_1^2, x_3^2, x_5^2	0.0082	76.58	21.6104	83.29
	x_1^2, x_4^2, x_5^2	0.0082	76.58	21.6104	83.29
	x_2^2, x_3^2, x_4^2	0.0082	76.58	21.6104	83.29
	x_2^2, x_3^2, x_5^2	0.0082	76.58	21.6104	83.29
	x_2^2, x_4^2, x_5^2	0.0082	76.58	21.6104	83.29
	x_3^2, x_4^2, x_5^2	0.0082	76.58	21.6104	83.29

DISCUSSION OF RESULTS

In comparing design's efficiencies for standard CCD and modified CCD on non-standard model having one missing quadratic term, the determinant value of the normalized information matrix associated with the modified central composite designs are larger than those associated with the standard central composite design. Consequently, D-efficiency values associated with the modified central composite designs are higher than those associated with the standard central composite designs. Specifically, the D-efficiency value associated with the standard CCD is 69.91% and the D-efficiency value associated with the Modified CCD is

Scientia Africana, Vol. 21 (No. 1), April, 2022. Pp 195-206 *https://dx.doi.org/10.4314/sa.v21i1.17*
© Faculty of Science, University of Port Harcourt, Printed in Nigeria *ISSN 1118 – 1931*

71.73%. The modified CCD also performs better than the standard CCD in term of G-optimality and efficiency. Specifically, G-efficiency associated with the standard CCD is 78.82% and that associated with the modified CCD is 82.69%.

For two missing quadratic terms, the D-efficiency values associated with the modified central composite designs are higher than those associated with the standard central composite designs. Specifically, the D-efficiency value associated with the standard CCD is 69.01% and the D-efficiency value associated with the Modified CCD is 73.66%. The maximum scaled prediction variance for standard CCD gives G-efficiency value of 75.12% and that associated with the Modified CCD gives G-efficiency value of 83.02%. Similarly, for three missing quadratic terms, the D-efficiency values associated with the modified central composite designs are higher than those associated with the standard central composite designs. In each case of absence of three quadratic terms, the D-efficiency value associated with the standard CCD is 67.88% and the D-efficiency value associated with the Modified CCD is 76.58%. As in one and two missing quadratic model terms, G-efficiency is higher for the Modified CCD. Specifically, G-efficiency for standard CCD is 71.32% while G-efficiency for modified CCD is 83.29%.

REFERENCES

Atkinson, A. C. and Donev, A. N. (1992). Optimum Experimental Designs, Oxford: Oxford University Press.

Borkowski, and Valeroso (1997). Robustness of central composite and Box-Belinken designsover classes of posterior models. Conference paper: 1996 Joint Statistical Meetings. Section on Physical and Engineering Sciences, 198-203.

Box, G.E.P. and Hunter, J.S. (1957) Multi-Factor Experimental Designs for Exploring Response Surfaces. Annals of Mathematical Statistics, 28, 195-241

Eze, F. C. and Ngonadi, L. O. (2018). Alphabetic Optimality Criteria for 2k Central Composite Design. Academic Journal of Applied Mathematical Sciences, 4(9), 107-118.

Fedorov, V. V. (1972), Theory of Optimal Experiments, New York. Academic Press.

Goos, P. and Jones, B. (2011). Optimal Designs of Experiments: A Case Study Approach, *1st Edition, Wiley, New York.*

Iwundu, M. P. (2018). Construction of Modified Central Composite Designs for Non-standard Models. International Journal of Statistics and Probability. 7(5), 95 -119.

Iwundu, M. P. and Oko, E. T. (2021), Design Efficiency and Optimal Values of Replicated Central Composite Designs with Full Factorial Portions. African Journal of Mathematics and Statistics Studies 4(3), 89-117. DOI: 10.52589/AJMSSAJWDYP0V.

Iwundu and Otaru (2019). Construction of Hat-Matrix Aided Composite Designs for Second- Order Models. American Journal of Computational and Applied Mathematics. 9(3): 62-84, DOI:10.5923/j.ajcam.20190903.03

Jaja E.I., Iwundu M.P., Etuk, E.H. (2021a). The Comparative Study of CCD and MCCD in the

Presence of a Missing Design Point. African Journal of Mathematics and StatisticsStudies 4(2), 10-24. DOI: 10.52589/AJMSSJF1A1DZA.

Jaja E.I., Etuk E.H., Iwundu M.P., Amos E. (2021b), Robustness of Central Composite Design and Modified Central Composite Design to a Missing Observation for Non-Standard Models. African Journal of Mathematics and Statistics Studies 4(2), 25-40. DOI: 10.52589/AJMSSC5NKOI81.

Kiefer, J. and Wolfowitz, J. (1959). Optimum Designs in Regression Problems. The Annals of Mathematical Statistics. 30(2), 271 – 294.

Kowalski, S. M., Parker, A. P., and Vining, G. G. (2006). Tutorial: Industrial Split-plotExperiments. Quality Engineering, 19:1-15.

Letsinger, J. D., Myers, R. H. and Lentner, M. (1996). Response Surface Methods for Bi-Randomization Structures. Journal of Quality Technology, 28:381-397.

Myers, R.H, Montgomery, D.C. and Anderson-Cook, C.M.(2009) Response Surface Methodology: Process and product Optimization using designed experiments 3rd Edition. John Wiley & Sons, Inc. New Jersey.

Nwanya, C. J., Mbachu, H. I. and Dozie, K. C. N. (2020). Design Optimality Criteria of Reduced Models for Variations of Central Composite Design. *Archives of Current Research International*, *19*(4), 1-7. https://doi.org/10.9734/acri/2019/v19i430164

Vining, G. G., Kowalski, S. M. and Montgomery, D. C. (2005). Response Surface Designs Within a Split-Plot Structure. Journal of Quality Technology, 37:115- 129.

Wanyonyi, S. W., Okango, A. A., & Koech, J. K. (2021). Exploration of D, A-, I- and G- Optimality Criteria in Mixture Modeling. *Asian Journal of Probability and Statistics*, *12*(4), 15-28. https://doi.org/10.9734/ajpas/2021/v12i430292

Scientia Africana, Vol. 21 (No. 1), April, 2022. Pp 207-222 *https://dx.doi.org/10.4314/sa.v21i1.18*
© Faculty of Science, University of Port Harcourt, Printed in Nigeria *ISSN 1118 – 1931*

STOCHASTIC MODEL FOR THE PREDICTION OF SHORT TIME NUMBER OF FIRE ACCIDENT OCCURRENCE IN NIGER STATE USING VITERBI ALGORITHM

Lateef, I.[1*], Adamu[1], L., Didigwu, N. E.[2], Abubaka, A.[3], and Yakubu, D. S.[4]
[1] Department of Mathematics, Federal University of Technology, Minna, Nigeria
[2]Department of Industrial Mathematics/Applied Statistics, Enugu State University of Science and Technology, Agbani, Enugu, Nigeria
[3]Department of Mathematics, Faculty of Science, Air Force Institute of Technology, Kaduna, Nigeria
[4]Department of Mathematical Science, Ibrahim Badamasi Babagida University, Lapai, Nigeria
lawal.adamu@futminna.edu.ng

Received: 19-02-2022
Accepted: 20-03-2022

ABSTRACT

In this paper, we look into ways by which fire outbreak (accident) can be suppressed. A stochastic model that predicts the number of fire accident occurrence in Niger State using Viterbi Algorithm is presented. A three-State stochastic model was formulated using the principle of Markov and each state of the model has four possible observations. The parameters of the model were estimated using the fire accident data collected from the archive of Niger State Fire Service, after which the model was trained using Baum-welch Algorithm to attend maximum likelihood. The Validity test for the model recorded 75% accuracy for short time prediction and shows 50% accuracy for long time prediction. This indicates that the model is more reliable and dependable for short time prediction.Information for this study could serve as a guide to the government in policy formulation that might assist in curbing the number of fire accident occurrences in Niger State.

Keyword: Hidden Markov Model, Transition Probability, Observation Probability, Fire accident Occurrence, Viterbi Algorithm

INTRODUCTION

Fire is the rapid oxidation of a material in the exothermic chemical process of combustion, releasing heat, light, and various reaction products (Charles, 2000). Fires start when a flammable and/or a combustible material, in combination with a sufficient quantity of an oxidizer such as oxygen gas or another oxygen-rich compound is exposed to a source of heat or ambient temperature above the flash point for the fuel and is able to sustain a rate of rapid oxidation that produces a chain reaction (Yusuf, 2012). Fires are both natural and social phenomena that cause extensive harm to societies in terms of human lives, economic losses, and operational costs (Corcoran *et al*., 2011; Corcoran and Higgs, 2013; Jennings, 2013; spatenkova and Virrantaus, 2013). Fires also affect communities, their livelihoods and productivity, and can create serious damage and havoc to urban infrastructure, reserved or unreserved (Jennings, 2013 and Corcoran, 2007). All types of fire that is residential fires pose the greatest risk to human lives and the surrounding environment because of their higher likelihood to lead to fatal consequences

(Ceyhan *et al*., 2013).The complexity of people's behaviour at an individual and collective level in cities has made fire risk extremely complicated to model and theorize (Corcoran *et al*., 2011; Jennings, 2013; Spatenkova and Virrantaus, 2013). While the number of studies have been increasing in recent years, the current knowledge about the spatial aspects of fire risk is still limited to a few studies mostly from developed countries, such as the United Kingdom (UK), Australia, Canada, Sweden and Finland (Corcoran *et al.* 2007; Chhetri*et al.*, 2010; Asgary*et al.*, 2010; Corcoran *et al.*, 2011; Spatenkova and Virrantaus 2013; Wuschke*et al.* 2013; Guldaker*et al.* 2018; Ardianto and Chhetri 2019).

Dry weather has been identified as the major cause of the recent spate of incidents while storing of petrol in living houses and markets, careless disposal of cigarette stubs, adulterated fuel, power surge, electric sparks and illegal connection of electricity are all sources of fire outbreaks. Many people have faulted the responsiveness of fire services and emergency first responders in the country, who have been reputed to always arrive late and without sufficient equipment to the scene of fire incidents. There have also been renewed calls for the federal and state governments to adequately fund the fire department and emergency agencies, and the culture of insuring properties is not imbibed by Lagos residents to mitigate the damage and misery of the misfortune (Yusuf, 2012). Many countries have introduced, or are planning to introduce in the near future, performance-based codes by the use of engineering analysis of fire development and occupant evacuation. The performance-based codes were considered and the level of safety provided to the occupants in a building by a particular fire safety design were assessed Central to this performance, based on the approach that was used for a suitable design fires that can characterize typical fire growth in a fire compartment. Pantousa*et al*. (2017), developed a Fire-Structure Interface (FSI) simplified dual-layer model. The model calculates the temporal evolution of the gas-temperature in the fire compartment in every virtual zone which is divided in two layers (hot and cold layer). Sakurahara *et al*. (2018), developed an integrated probabilistic risk assessment methodological framework for Fire PRA. The Fire Simulation Module (FSM), includes state-of-the-art models of fire initiation, fire progression, post-fire failure damage propagation, fire brigade response, and scenario-based damage is used in simulation using a computational fluid dynamics (CFD) code, fire dynamics simulator.

The outbreak of fire in Niger State and some other parts of the country is one of the challenging situation faced by inhabitants of this geographical location as in most cases lives and properties worth millions of naira are lost. Fire accident could be very difficult to combat/fight as it can emanate from diverse sources. Prediction of fire accident has been a task to researchers for several decades, because its occurrence is stochastic in nature.

Hence the need to use a stochastic model with pattern recognition capability based on the empirical data to conceivably capture the behavior of the system become paramount. It is on this note, that Hidden Markov Model is selected for this purpose.

Scientia Africana, Vol. 21 (No. 1), April, 2022. Pp 207-222 https://dx.doi.org/10.4314/sa.v21i1.18
© Faculty of Science, University of Port Harcourt, Printed in Nigeria *ISSN 1118 – 1931*

Hidden Markov models are extensions of Markov models where each observation is the result of a stochastic process in one of several unobserved states. Hidden Markov model is very influential in stochastic because of its track record of unraveling hidden parts of a complex system and make prediction with high level of accuracy. Hidden Markov Models have been successfully applied in the following areas; automatic speech recognition and speech synthesis (Rabiner, 1989), identification and inverse filtering (Robert Mattila, 2020), molecular biology for DNA and protein sequencing (Durbin *et al*., 1998), pattern recognition (Fink, 1989) and in rainfall pattern prediction (Lawal, 2018), Rice yield forecast (Yahaya and Lawal, 2020).

METHODOLOGY

a. Hidden Markov Model

A Hidden Markov Model (HMM) is a double stochastic process in which one of the stochastic processes is an underlying Markov chain which is called the hidden part of the model, the other stochastic process is an observable one. Also a HMM can be considered as a stochastic process whose evolution is governed by an underlying discrete (Markov chain) with a finite number of states which are hidden, i.e. not directly observable (Enza and Daniele, 2007)

b. Characteristics of Hidden Markov Model

Hidden Markov Model is characterized by the following

N = number of states in the model
M = number of distinct observation symbols per state
Q = state sequence

$$Q = q_{1,} q_2, q_3, \ldots\ldots\ldots\ldots q_T$$

O = observation sequence

$$O = o_{1,} o_{2,} o_3 \ldots\ldots\ldots\ldots o_T$$

Transition probability matrix $A = \{a_{ij}\}$

Observation probability matrix $B = \{b_j(o_t)\}$

where $b_j(o_t) = p(o_t \mid q_t = s_j)$

If the observation is continuous a probability density function is used as follows:

$$\int_{-\infty}^{+\infty} b_j(x)dx = 1$$

$\pi = \{\pi_j\}$ Initial state probabilities

$\lambda = (A, B, \pi)$ The overall HMM

c. Model Formulation

Fire accidents are influence by many complex factors such as environment, climate, Fire investment, public fire safety consciousness and so on, the statistical data of fire accidents always take on the characteristic of both randomicity and fluctuations (Sun and Mao 2011). Since the fire accident occurrence depends on these factors and these factors are not static both varies along the quarters of the year this means that, the number of occurrence of fire accident also varies along the quarters of the year. This situation is stochastic in nature and of the double type. This means that the number of occurrence of fire accident in each quarter of the years varies and the factor influencing the occurrence of the fire accident also varies along the quarters of the year. In general, fire accident occurrence among quarters of the year is a double stochastic process. It is based on this that HMM is being adapted to model number of fire accident occurrence in Niger State.

Now, Let the number of fire accident occurrence within the quarters of the year be taken as the state of the model and the factors influencing fire accident occurrence within the quarters be taken as emission of the Hidden Markov Model, hence we have the following model assumptions

(i) The transition between the states is governed by first order Markov dependency as represented in equation (1)

$$P\{X_{n+1} = j \mid X_0 = i_0, ..., X_{n-2} = i_{n-2}, X_{n-1} = i_{n-1}, X_n = i\} = P_{ij} \quad (1)$$

(ii) The probability of generating current observation symbol depends on current state, as represented by equation (2)

$$P(O \mid Q, \lambda) = \prod_{t=1}^{T} P(o_t \mid q_t, \lambda) \quad (2)$$

(iii) The number of fire accident occurrence in a year is considered be low, if it is less than 83

(iv) The number of fire accident occurrence in a year is considered to be moderate, if it is within the range (83 - 159)

(v) The number of fire accident occurrence in a year is considered to be high, if it is above 159

Hence, we have the following states and observations for the Hidden Markov Model of fire accident occurrence prediction in Niger state

State 1: Low Fire accident occurrence
State 2: Moderate Fire accident occurrence
State 3: High Fire accident occurrence

Observations:

$Q_1 = O_1$ = Quarterly (January to March)
$Q_2 = O_2$ = Quarterly (April to June)
$Q_3 = O_3$ = Quarterly (July to September)

Scientia Africana, Vol. 21 (No. 1), April, 2022. Pp 207-222 *https://dx.doi.org/10.4314/sa.v21i1.18*
© Faculty of Science, University of Port Harcourt, Printed in Nigeria *ISSN 1118 – 1931*

Q_4= O_4 = Quarterly (October to December)

The classification of states and the observations, and the assumption made in this work are based on the study area and the data obtained

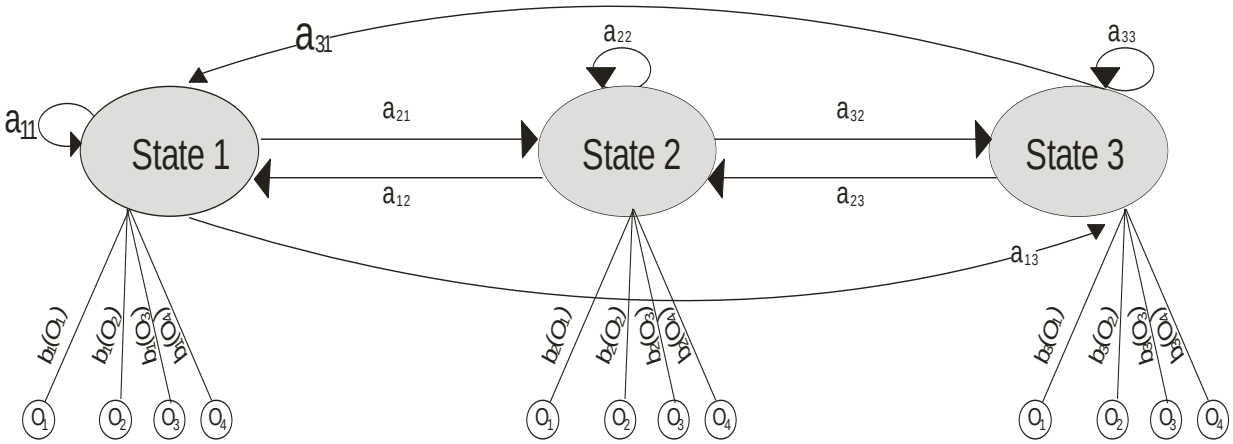

Figure 1: Transition Diagram of the Fire Accident Occurrence Model

Transition Probability Matrix

The transition between the states are represented by equation (3)

$$A = \begin{bmatrix} a_{11} & a_{12} & a_{13} \\ a_{21} & a_{22} & a_{23} \\ a_{31} & a_{32} & a_{33} \end{bmatrix} \quad (3)$$

Observation probability matrix

The matrix below represents observation emitted from the model

$$B = \begin{bmatrix} b_1(O_1) & b_1(O_2) & b_1(O_3) & b_1(O_4) \\ b_2(O_1) & b_2(O_2) & b_2(O_3) & b_2(O_4) \\ b_3(O_1) & b_3(O_2) & b_3(O_3) & b_3(O_4) \end{bmatrix} \quad (4)$$

Initial probability distribution

The initial probability distribution for the model is given below

$$\pi = [\pi_1, \pi_2, \pi_3] \quad (5)$$

The Hidden Markov Model for Fire Accident Occurrence

The general Hidden Markov Model for the number of fire accident occurrence prediction is given by the compact notation in equation (6)

$$\lambda = (\mathrm{A}, \mathrm{B}, \pi) \quad (6)$$

RESULTS

Application of the Hidden Markov Model for Prediction of Fire accident Occurrence

The data used in this research work were collected from the Niger State Fire service for the period of 8 years (20013 – 2020). Niger state with a population of 5,556,247 million people (National population commission, 2020) is located in the North central zone along the Middle Belt region of Nigeria. It is classified as one of the largest states in the country (in terms of landmarks), spanning over 86,000 km^2 in land area. The summary is presented in Table1below

Table 1: Summary of State and Observation of Fire Occurrence for a Period of Eight Years

Years	States	Observations
2013	1 (L)	(Q_1)
	1(L)	(Q_2)
	1(L)	(Q_3)
	1(L)	(Q_4)
2014	1(L)	(Q_1)
	1(L)	(Q_2)
	1(L)	(Q_3)
	1(L)	(Q_4)
2015	1(L)	(Q_1)
	1(L)	(Q_2)
	1(L)	(Q_3)
	1(L)	(Q_4)
20016	1(L)	(Q_1)
	1(L)	(Q_2)
	1(L)	(Q_3)
	1(L)	(O_4)
2017	2(M)	(Q_1)
	1 (L)	(Q_2)
	1(L)	(Q_3)
	1(L)	(Q_4)
2018	2(M)	(Q_1)
	1(L)	(Q_2)
	1(L)	(Q_3)
	1(L)	(Q_4)
2019	2(M)	(O_1)
	2(M)	(Q_2)
	1(L)	(Q_3)
	2(M)	(Q_4)

Scientia Africana, Vol. 21 (No. 1), April, 2022. Pp 207-222 *https://dx.doi.org/10.4314/sa.v21i1.18*
© Faculty of Science, University of Port Harcourt, Printed in Nigeria *ISSN 1118 – 1931*

2020	3(H)	(Q_1)
	2(M)	(Q_2)
	1(L)	(Q_3)
	2(M)	(Q_4)

Validity Test for the Model

To test for the validity of the model, the parameters of the HMM were estimated using the fireaccident occurrence data from 2013 to 2017, then make forecast for 2018, 2019 and 2020.

The Transition Count Matrix (C), Pseudo count Transition Matrix (S) and Transition Probability Matrix (A) are given in Equations (7), (8) and (9) respectively.

$$C = \begin{bmatrix} 17 & 1 & 0 \\ 1 & 0 & 0 \\ 0 & 0 & 0 \end{bmatrix} \quad (7)$$

$$S = \begin{bmatrix} 18 & 2 & 1 \\ 2 & 1 & 1 \\ 1 & 1 & 1 \end{bmatrix} \quad (8)$$

$$A = \begin{bmatrix} 0.8571 & 0.0952 & 0.0476 \\ 0.5000 & 0.2500 & 0.2500 \\ 0.3333 & 0.3333 & 0.3333 \end{bmatrix} \quad (9)$$

While Observation count matrix (E), Pseudo count Observation matrix (D) and Observation probability matrix (B) are given in equations (10), (11) and (12), respectively.

$$E = \begin{bmatrix} 4 & 5 & 5 & 5 \\ 1 & 0 & 0 & 0 \\ 0 & 0 & 0 & 0 \end{bmatrix} \quad (10)$$

$$D = \begin{bmatrix} 5 & 6 & 6 & 6 \\ 2 & 1 & 1 & 1 \\ 1 & 1 & 1 & 1 \end{bmatrix} \quad (11)$$

$$B = \begin{bmatrix} 0.625 & 0.750 & 0.750 & 0.750 \\ 0.250 & 0.125 & 0.125 & 0.125 \\ 0.125 & 0.125 & 0.125 & 0.125 \end{bmatrix} \quad (12)$$

The initial state probability is given below

$$\pi = [0.95, 0.05, 0] \quad (13)$$

The general HMM1 is represented by equation (14)

$$\lambda_1 = (A, B, \pi) \tag{14}$$

After 1000 iteration of the Baum Welch Algorithm, Theequation stabilised to equation(15) we trained equation *(*14) using a built-in Baum algorithm function in the Matlab 2015.

$$\lambda_1^* = \left(\hat{A}, \hat{B}, \hat{\pi}\right) \tag{15}$$

where

$$\hat{A} = \begin{bmatrix} 0.5556 & 0.4444 & 0.0000 \\ 0.0000 & 0.0000 & 1.0000 \\ 1.0000 & 0.0000 & 0.0000 \end{bmatrix} \tag{16}$$

$$\hat{B} = \begin{bmatrix} 0.000 & 0.000 & 0.500 & 0.500 \\ 1.000 & 0.000 & 0.000 & 0.000 \\ 0.000 & 1.000 & 0.000 & 0.000 \end{bmatrix} \tag{17}$$

And $\pi =$ [0.95, 0.05, 0] (18)

Making Prediction with the Model

From the summary of the fire accident data presented in table 1, the process is in State 1at the last Quarter of 2017 (that is with Observation Q_4). Now, to obtain the likely state sequence of the process in 2018 given the observation sequence of the year 2018 that is Q_1, Q_2, Q_3 and Q_4, we use Viterbi algorithm as shown in figure 1

To avoid underflow of the Viterbi algorithm, we normalised each of the obtained node in the computation process using the following equations:

$$c_t = \frac{1}{\sum_{t=1}^{N} \alpha_t(i)} \tag{19}$$

$$\hat{\alpha}_t(i) = c_t \times \alpha_t(i) = \frac{\alpha_t(i)}{\sum_{t=1}^{N} \alpha_t(i)} \tag{20}$$

Scientia Africana, Vol. 21 (No. 1), April, 2022. Pp 207-222 https://dx.doi.org/10.4314/sa.v21i1.18
© Faculty of Science, University of Port Harcourt, Printed in Nigeria *ISSN 1118 – 1931*

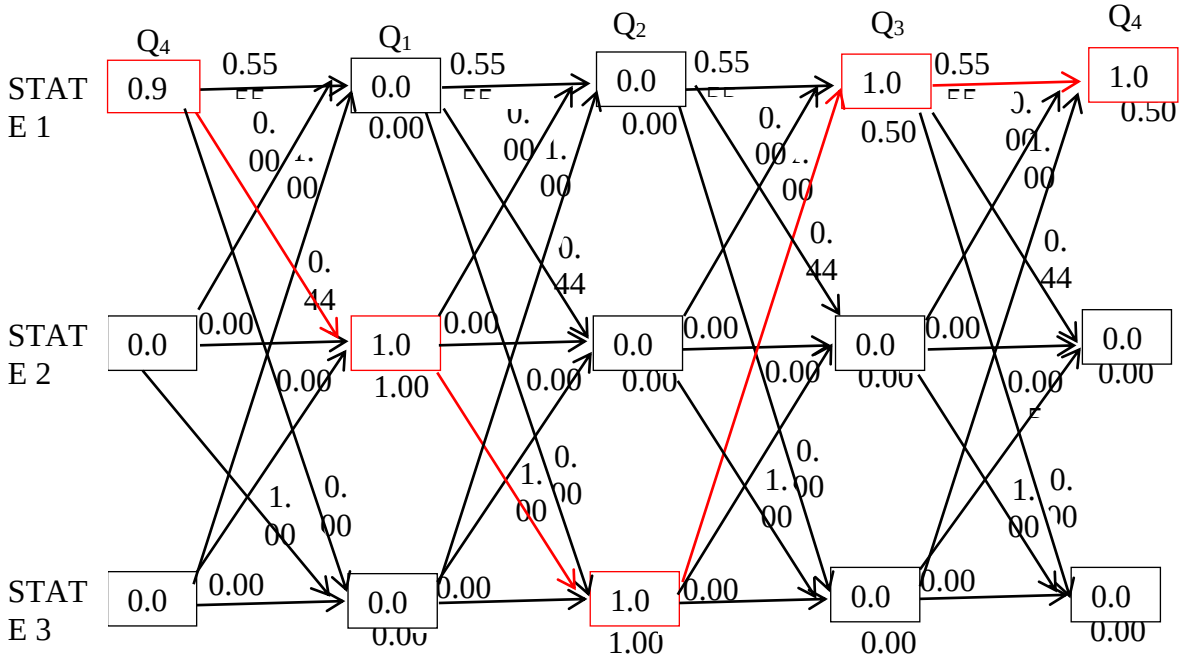

Figure 2: Viterbi algorithm for Observation Sequence $Q_4,Q_1,Q_2,Q_3Q_4$of 2018

State 1 to state 2, has the highest probability value under Q_1 that is, (0.95 x 0.44)1.00=0.4222, normalising this value using equation (19) and (20) we obtain the value 1, then we move to the next path of computation.

State 2 to state 3, has the highest probability value under Q_2 that is (0.05 x 1.00)1.00=0.0500, normalising this value using equation (19) and (20) we obtain the value 1, then we move to the next path of the computation.

State 3 to state 1, has the highest probability value under Q_3 that is (0.95 x 0.55)0.50=0.2639, normalising this value using equation (19) and (20) we obtain the value 1, then we move to the next path of the computation.

State 1 to state 1, has the highest probability value under Q_4 that is, (0.95 x 0.55)0.50=0.2636, normalising this value using equation (19) and (20)we obtain the value 1, The results of the computation of figure 2 are represented in Table 2 below.

Table 2: The Result for 2018 Number of FireAccident Occurrence Based on Viterbi Algorithm Prediction

Year/Months	2017		2018		
States:	1	2	3	1	1
Observation:	Q_4	Q_1	Q_2	Q_3	Q_4

Similarly, from the calculation of Table 2, the process is in State 1 at the last Quarter of 2018 (that is with Observation Q_4). Now, to obtain the likely state sequence of the process in 2019 given the observation sequence of the year 2019 that is Q_1, Q_2, Q_3 and Q_4, we use Viterbi algorithm as shown in figure 3.To avoid underflow of the Viterbi algorithm we normalised

each of the obtained node in the computation process using the following equations (19) and (20)

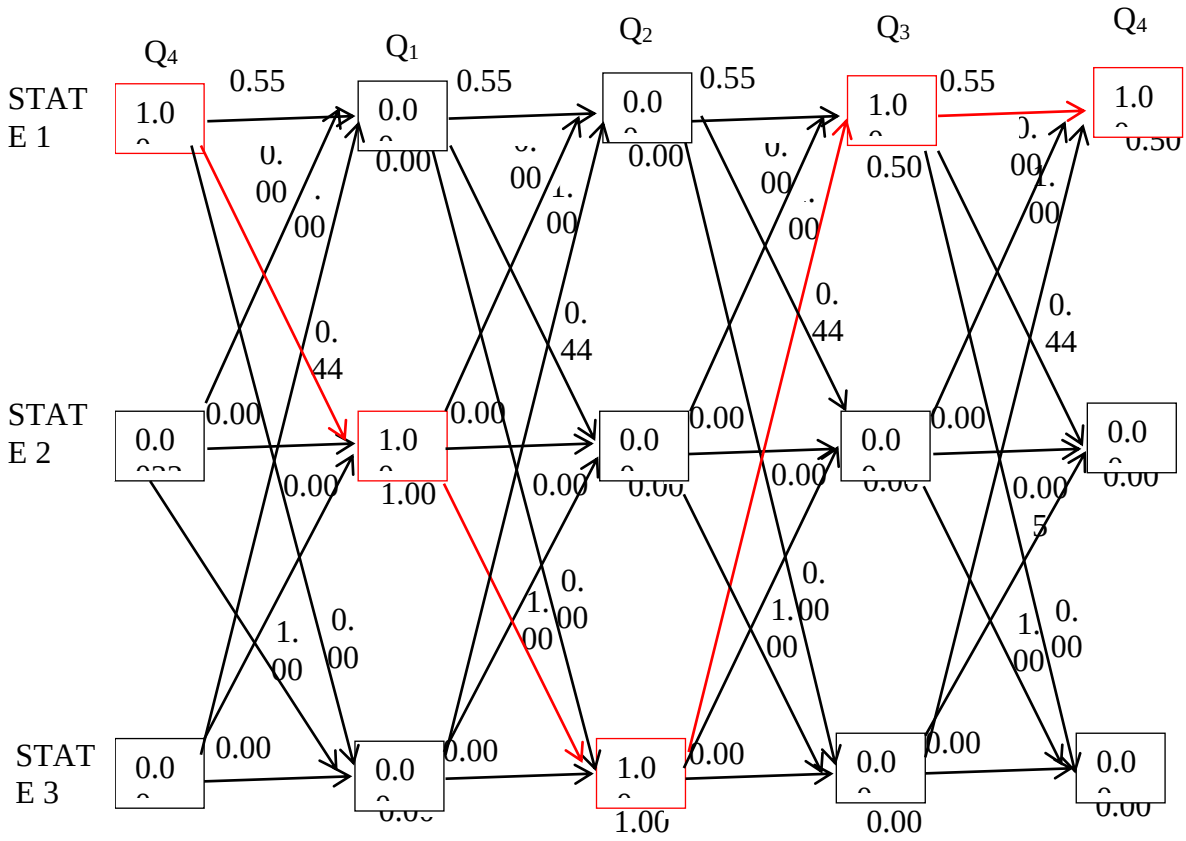

Figure 3: Viterbi algorithm for Observation Sequence $Q_4,Q_1,Q_2,Q_3Q_4$of 2019

State 1 to State 2, has the highest probability value under Q_1 that is (0.444 x 1.00)1.00=0.444, normalising this value using equation (19) and (20)we obtain the value 1,

State 2 to State 3, has the highest probability value under Q_2 that is, (1.000x1.000)1.00=1.000, normalising this value using equation (19) and (20) we obtain the value 1.

State 3 to state 1, has the highest probability value under Q_3 that is, (1.000x1.000)0.50= 0.50, normalising this value using equation (19) and (20) we obtain the value 1.

State 1 to state 1, has the highest probability value under Q_4 that is, (1.000x0.55)0.50 = 0.2775, normalising this value using equation (19) and (20) we obtain the value 1.

The results of the computation of figure 3 are represented in Table 3.

Table 3: The Result for 2019 Number of FireAccident Occurrence Based On Viterbi Algorithm Prediction

Years		2019		
States	2	3	1	1
Observation	Q_1	Q_2	Q_3	Q_4

Scientia Africana, Vol. 21 (No. 1), April, 2022. Pp 207-222 https://dx.doi.org/10.4314/sa.v21i1.18
© Faculty of Science, University of Port Harcourt, Printed in Nigeria *ISSN 1118 – 1931*

Similarly, the process is in State 1at second Quarter of 2019 (that is with Observation Q_4). Now, to obtain the next likely state sequence of the process in 2020 given the observation sequence of the year 2020 that is Q_1, Q_2, Q_3 and Q_4, we use Viterbi algorithm as shown in figure 4.

To avoid underflow of the Viterbi algorithm we normalised each of the obtained node in the computation process using the following equations (19) and (20).

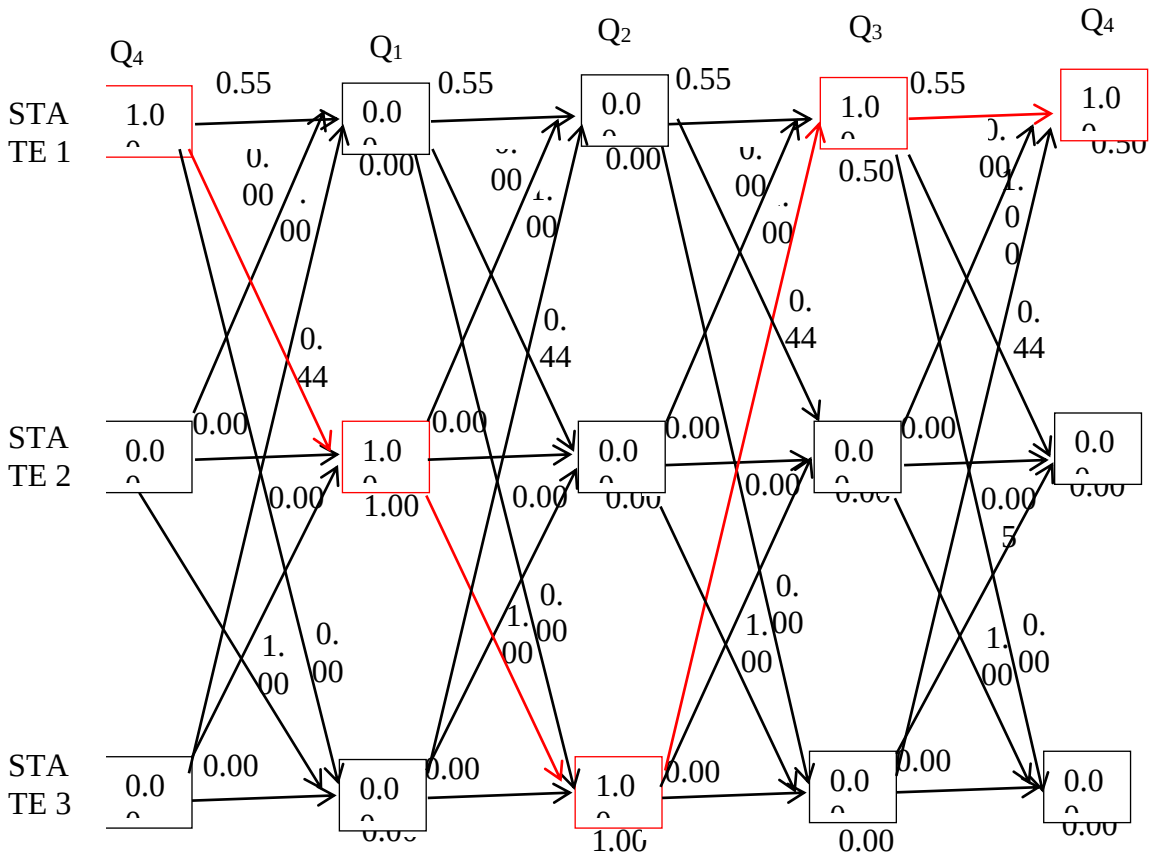

Figure 4: Viterbi algorithmfor Observation Sequence $Q_4,Q_1,Q_2,Q_3Q_4$of 2020

state 1 to state 2, has the highest probability value under Q_1 that is(0.444 x 1.00)1.00=0.444, normalising this value using equation (19) and (20) we obtain the value 1,

State 2 to state 3, has the highest probability value under Q_2 that is, (1.000x1.000)1.00=1.000, normalising this value using equation (19) and (20) we obtain the value 1,

State 3 to state 1, has the highest probability value under Q_3 that is, (1.000x1.000)0.50= 0.50, normalising this value using equation (19) and (20) we obtain the value 1,

State 1 to state 1, has the highest probability value under Q_4 that is, (1.000x0.55)0.50 = 0.2775, normalising this value using equation (19) and (20)we obtain the value 1,

The results of the computation of figure 4 are represented in Table 4 below.

Table 4: The Result for 2020 Number of FireAccident Occurrence Based On Viterbi Algorithm Prediction

Year			2020	
States	2	3	1	1
Observation	Q_1	Q_2	Q_3	Q_4

In general, the summary of the fire accident occurrence which shown below in table 5

Table 5: Summary of the Fire Accident Occurrence

Year	2018				2019				2020			
States	2	3	1	1	2	3	1	1	2	3	1	1
Observation	Q_1	Q_2	Q_3	Q_4	Q_1	Q_2	Q_3	Q_4	Q_1	Q_2	Q_3	Q_4

Table 6: Comparison of the Predicted States and Observations, and the Actual States and Observations from Table 1.

Year	2018				2019				2020			
Actual States	2	1	1	1	2	2	1	2	3	2	1	2
Predicted States	2	3	1	1	2	3	1	1	2	3	1	1
Observation	Q_1	Q_2	Q_3	Q_4	Q_1	Q_2	Q_3	Q_4	Q_1	Q_2	Q_3	Q_4

From the table 6, it can be observed that the prediction for 2018 Quarters has 75% accuracy, then 2018 to 2019 Quarters has 62.5% accuracy and lastly for 2018 to 2020 has 50% accuracy. The result of the model clearly shows that, the model perform better for only short time prediction and perform fairly for long time prediction.

Hidden Markov Model for future prediction

Hidden Markov model for future prediction is developed to predict number of Fire Accident Occurrence for future years, the parameters of the model were determined using Fire Accident Occurrence data from 2013 to 2020 (the whole data set) after which, we predict for 2021 and 2022.

Transition Count Matrix

$$C = \begin{bmatrix} 19 & 5 & 0 \\ 4 & 1 & 1 \\ 0 & 1 & 0 \end{bmatrix} \tag{21}$$

Pseudo count Transition Matrix

Scientia Africana, Vol. 21 (No. 1), April, 2022. Pp 207-222 https://dx.doi.org/10.4314/sa.v21i1.18
© Faculty of Science, University of Port Harcourt, Printed in Nigeria *ISSN 1118 – 1931*

$$S = \begin{bmatrix} 20 & 6 & 1 \\ 5 & 2 & 2 \\ 1 & 2 & 1 \end{bmatrix} \tag{22}$$

Transition Probability Matrix

$$A = \begin{bmatrix} 0.7407 & 0.2222 & 0.0370 \\ 0.5555 & 0.2222 & 0.2222 \\ 0.2500 & 0.5000 & 0.2500 \end{bmatrix} \tag{23}$$

Observation Count Matrix

$$C = \begin{bmatrix} 4 & 6 & 8 & 6 \\ 3 & 2 & 0 & 2 \\ 1 & 0 & 0 & 0 \end{bmatrix} \tag{24}$$

Pseudo count Observation Matrix

$$S = \begin{bmatrix} 5 & 7 & 9 & 7 \\ 4 & 3 & 1 & 3 \\ 2 & 1 & 1 & 1 \end{bmatrix} \tag{25}$$

Observation Probability Matrix

$$\mathrm{B} = \begin{bmatrix} 0.4545 & 0.6363 & 0.8181 & 0.6363 \\ 0.3636 & 0.2727 & 0.0909 & 0.2727 \\ 0.1818 & 0.0909 & 0.0909 & 0.0909 \end{bmatrix} \tag{26}$$

Initial State Probability

$$\pi = \begin{bmatrix} 0.75 & 0.2187 & 0.0312 \end{bmatrix} \tag{27}$$

$$\lambda_2 = (A, \quad B, \quad \pi) \tag{28}$$

After 900 iteration of Baum Welch Algorithm, equation (28) stabilized to (29)

$$\lambda^* = \begin{pmatrix} \hat{A}, & \hat{B}, & \hat{\pi} \end{pmatrix} \tag{29}$$

Where

$$\hat{A} = \begin{bmatrix} 0.5333 & 0.4667 & 0.0000 \\ 0.0000 & 0.0000 & 1.0000 \\ 1.0000 & 0.0000 & 0.000 \end{bmatrix} \tag{30}$$

$$\hat{B} = \begin{bmatrix} 0.0000 & 0.0000 & 0.6000 & 0.4000 \\ 1.0000 & 0.0000 & 0.0000 & 0.0000 \\ 0.0000 & 1.0000 & 0.0000 & 0.0000 \end{bmatrix} \quad (31)$$

$$\hat{\pi} = \begin{bmatrix} 0.75 & 0.2187 & 0.0312 \end{bmatrix} \quad (32)$$

Prediction for 2021 and 2022

Following similar method of predictionprocedures andusing equation(30) to (32)the results for 2021 and 2022 predictions are presented in the table 7 below

Table 7:The Result for 2021 and 2022Number OfFireAccident OccurrenceBased on Viterbi Algorithm Prediction

Year	2020	2021				2022			
States:	1	2	3	1	1	2	3	1	1
Observation:	Q_4	Q_1	Q_2	Q_3	Q_4	Q_1	Q_2	Q_3	Q_4

DISCUSSION OF RESULTS

The parameter of the validity test model was determined usingfire Accident Occurrencedata from 2013 to 2017. After 1000 iterations of the Baum Welch Algorithm, λ_1 stabilised to a new model $\lambda_1^{\bullet}$, Viterbi Algorithm was then used to make a prediction for Fire Accident Occurrence for 2018, 2019, and 2020. From the table 1, the HMM1 was in state 1 at 2017last Quarter(Q_4), It make transition to state 2 in 2018emitting observation(Q_1),then it make move to state 3 emitting observation(Q_2),at that point, it also make move to state 1emitting observation(Q_3),it then make move to state 1emitting observation(Q_4). The Validity test for the Quarters of 2018 shows 75% Accuracy.

Similarly in 2019 the process is in state 2first Quarter (Q_1), then make move to state 3 emitting observation(Q_2), at that point, it also make move to state1emitting observation (Q_3),it also make move to state 1emitting observation(Q_4).The validity test for 2018 and 2019 Quarters showed 62.5% Accuracy.

Similar interpretation is given in 2020, the process is in state 2at first Quarter of 2020 (Q_1). then it make move to state 3 emitting observation(Q_2),at that point, it also make move to state 1emitting observation(Q_3),it also make move to state 1emitting observation at (Q_4),The validity test for 2018, 2019 and 2020 shows 50% Accuracy.

Generally, the result for the validity test showed that the model perform better for short time prediction and performed fairly for long time prediction.

For the Future predictionthe parameter of the HMM were estimated usingFire Accident Occurrencedata from 2013 to 2020. After 900 iteration of the Baum Welch algorithm λ_2, stabilised to another model $\lambda_2^{\bullet}$, the Viterbi Algorithmwas then used to make a prediction for future Quarters. From the table1, the HMM wasin

Scientia Africana, Vol. 21 (No. 1), April, 2022. Pp 207-222 *https://dx.doi.org/10.4314/sa.v21i1.18*
© Faculty of Science, University of Port Harcourt, Printed in Nigeria *ISSN 1118 – 1931*

state 2last Quarter of 2020, then it make move to state 2 emitting observation(Q_1)in 2021, at that point, it also make move to state 3emitting observation(Q_2),it also make move to state 1emitting observation(Q_3)it also make move to state 1emitting observation(Q_4) at 2021.

Similar interpretation is given to the movement instate 2 emitting observation(Q_1), at 2022at that point, it also make move to state 3emitting observation(Q_2),it also make move to state 1emitting observation(Q_3), it also make move to state 1emitting observation(Q_4)at year 2022.

CONCLUSION

The study has developHidden Markov Model that predicts the number of fire accident occurrence in Niger State using Viterbi Algorithm. The Validity test for the model showed 75% accuracy for short time prediction and shows 50% accuracy for long time prediction. The result indicates that the model is more reliable and dependable for only short time prediction. Information for this study could serve as a guide to the government in policy formulation that might assist in curbing the number of fire accident occurrences in Niger State.

REFERENCES

Ardianto, R. &Chhetri, P. (2019).Modeling Spatial–Temporal dynamics of urban residential fire risk using a Markov Chain technique.*International Journal of Disaster Risk Science*, 4(3), 45 - 98.

Asgary, A., Ghaffari, A. & Levy, J. (2010). Spatial and temporal analyses of structural fire incidents and their causes: A case of Toronto, Canada. *Fire Safety Journal*, 45(1), 44-57.

Ceyhan, E., Ertuğay, K. &Düzgün, Ş. (2013). Exploratory and inferential methods for spatio-temporal analysis of residential fire clustering in urban areas.*Fire Safety Journal*, 58,226-239.

Charles, J. (2000). Fire Technology. Malaysia International Conference, 35, 13- 89.

Chhetri, P., Corcoran, J., Stimson, R. &Inbakaran, R. (2010).Modelling potential socio-economic determinants of building fires in South East Queensland.*Geographical Research*, 48(1), 75-85.

Corcoran, J. & Higgs, G. (2013).Special issue on spatial analytical approaches in urban fire management.*Fire Safety Journal*, 6(2), 1-2.

Corcoran, J., Higgs, G., Brunsdon, C., Ware, A. & Norman, P. (2007). The use of spatial analytical techniques to explore patterns of fire incidence: A South Wales case study. Computers, Environment and Urban Systems, 31(6), 623-647.

Corcoran, J., Higgs, G., Rohde D. & Chhetri, P. (2011b).Investigating the association between weather conditions, calendar events and socio-economic patterns with trends in fire incidence: an Australian case study. *Journal of Geographical Systems*, 13(2), 193-226.

Durbin, R., Eddy, S.Y., Krogh. A., & Mitchison,.G. (1998). Biological Sequence Analysis: Probabilistic Models of Proteins and Nucleic Acids. Cambridge, UK: Cambridge University Press.

Enza, M., & Daniele, T.(2007). Hidden Markov models for scenario generation. *Journal of Management Mathematics*, 19, 379-401.

Fink,G.A.(1989). Markov Models for Pattern Recognition. From Theory to Applications Second Edition. London, UK: Springer.

Guldåker, N. &Hallin, P-O., Nilsson, J. &Tykesson, M. (2018).Spatio-temporal patterns of intentional fires, social stress and socio-economic determinants: A case study of Malmö, Sweden. *Fire Safety Journal,* 7(3), *71-80.*

Jennings, C. (2013). Social and economic characteristics as determinants of residential fire risk in urban neighbourhoods: a review of the literature and commentary. *Fire Safety Journal*, 6(2), 13-19.

Lawal Adamu (2018). "Hidden Markov Model and its Application in Rainfall Pattern Prediction" (A Monograph in Mathematics) LAP Lambert Academic Publishing: ISBN: 978-613-4-98532-1

Pantousa,D. E. M. (2017). Interface modelling between CFD and FEM analysis: the dual-layer post-processing model. *Engineering Computations Journal Impact,* 3(1), 45 -133.

Rabiner, L.R. (1989). A tutorial on hidden Markov models and selected applications in speech recognition. Proc. IEEE, 77, 257-286.

Robert Mattila (2020). Hidden Markov Models: Identification, Inverse Filtering and Applications Doctoral Thesis in Electrical Engineering KTH Royal Institute of Technology Stockholm, Sweden

Sakurahara, T., Mohaghegh, Z. &Reihani, S. (2018). An integrated methodology for spatio-temporal incorporation of underlying failure mechanisms into fire probabilistic risk assessment of nuclear power plants. *Journal of Statistical Scholar.* 3(2), 121 – 145.

Špatenková, O. & Virrantaus, K. (2013). Discovering spatio-temporal relationships in the distribution of building fires. *Fire Safety Journal, 62, pp. 49-63.*

Sun, T. M., & Mao S. W. (2011). Optimal Simultaneous Delivery of siRNA and Paclitaxel via a "Two-in-One" Micelleplex Promotes Synergistic Tumor Suppression. *Engineering Computations Journal Impact,* 3(1), 65 -73.

Wuschke, K., Clare, J. & Garis, L. (2013). Temporal and geographic clustering of residential structure fires: A theoretical platform for targeted fire prevention. *Fire Safety Journal, 62, pp. 3-12.*

Yahaya, M and **Lawal**. A (2020) "A Stochastic Model for Rice Yields Forecast"*Lapai Journal of Applied and Natural Sciences,*5(1): 16-25.

Yusuf, O. (2012). A literature review of fire incidence with an emphasis on urban residentialfires. 8, 116-130.

Scientia Africana, Vol. 21 (No. 1), April, 2022. Pp 223-232 *https://dx.doi.org/10.4314/sa.v21i1.19*
© Faculty of Science, University of Port Harcourt, Printed in Nigeria *ISSN 1118 – 1931*

THE EFFECT OF CRUDE OIL POLLUTION ON MACROPHYTE ASSEMBLAGE IN KPORGHOR RIVER, SOUTHERN NIGERIA

[1]Eke-John, H., [2]Owoleke, V. A., and *[1]Komi, G. W.
[1]Department of Animal and Environmental Biology, Faculty of Science, University of Port Harcourt, East-West Road, Choba, P.M.B. 5323 Port Harcourt
[2] Department of Plant Science and Biotechnology, Kogi State University, Anyigba, Kogi State, Nigeria
*Corresponding author: gentle.komi@uniport.edu.ng

Received: 29-11-2021
Accepted: 20-02-2022

ABSTRACT

A study of the effects of crude oil pollution on macrophyte assemblage was carried out in Kporghor River, Rivers State. Standard procedures were used in data collection. Temperature, total dissolved solutes, dissolved oxygen, pH and electrical conductivity were taken in-situ using Extech multi-parameter equipment while biological oxygen demand was incubated in a BOD bottle and determined using standard methods. Aquatic macrophytes were sampled with 0.5m × 0.5m quadrant and estimates of the percentage cover of each species inside the 0.5 × 0.5 m quadrant was transformed onto a scale based on Braun-Blanquet. The diversity and abundance of the different species were higher in Station (2), followed by station (3) and Station (1) respectively. Bambus vulgaris having a percentage of (29.7%) being the most abundant with percentage abundance, Cyrtospermum senegalense (8.72%), Nymphaea lotus (5.81), Acanthophoenix crinite (4.65%), Pistia stratiotes and Eichornia grassippes (2.91%) respectively. Unidentified species of macrophyte collected from the sampling area accounted for 11.62% species abundance. The result of physico-chemical parameters: temperature (29±0.63^{o}C to 29.15±0.72^{o}C), pH (6.03±0.12 to 6.9±0.15), TDS (36.23±6.82mg/ to 40.05±5.30mg/L), conductivity (4430±792.42µS/cm to 4914.75±569.42µS/cm), DO (5.20±1.20mg/L to 5.50±0.49mg/L) and BOD (3.08±0.94mg/L to 3.40±0.61mg/L). Copper (0.015mg/L) level was below WHO, SON and DPR standards for Cu in water bodies. Cadmium (0.10mg/L), Lead (0.18mg/L) and Nickel (0.28mg/L) concentrations were above WHO permissible limits. The abundance of Bambusa vulgaris (an alien species) suggests its adaptation to the study area. However, mitigation actions are recommended to restore this polluted ecosystem.

Keywords: Oil spill, aquatic plants, Kporghor Tai, exotic species

INTRODUCTION

Environmental challenges in Nigeria especially in the Niger Delta have become worrisome. The Niger Delta region is known for its rich biodiversity which has served as a source of sustenance of traditional livelihoods of its local people for centuries (Vidal, 2010). However, the biodiversity is under severe threat as a result of oil and gas exploration activities (Baird, 2010). There is hardly any year without recorded incidences of oil pollution in the Niger Delta; as such crude oil spill is a common occurrence in the Niger delta region. Crude Oil Spill as used in this context can be defined as the introduction of crude oil or its derivatives with its associated gases into the environment (land, air and water) in quantities that is capable of causing

immediate physical, chemical and biological damage to the affected ecosystem (Tanee and Anyanwu, 2008).

The behaviour of metals in natural waters is a function of the substrate sediment composition, suspended sediment composition and the water chemistry (Barakat *et al.,* 2012). Sedimentation is important in removing metals because these metals are adsorbed to organic and inorganic materials or forms chemical bonds with components of the sediment. Sediments act as the ultimate reservoir for the numerous potential chemical and biological contaminants that may be contained in effluents originating from these activities (Adeleye *et al.,* 2012).

However, in water, there is continuous exchange between sediments and the water column, which may cause the release of large proportion of dissolved metals adsorbed to particulate matter (Harikumar*et al.,* 2009). Ogoni-land has faced several incidences of Crude oil spill. This has caused huge negative impacts on the land and waters of the impacted community; little or no literature has report the impact of these oil spills on the macrophytes assemblage. Thus, this study was designed to examine the macrophyte composition of the study area.

Map of the Study Area

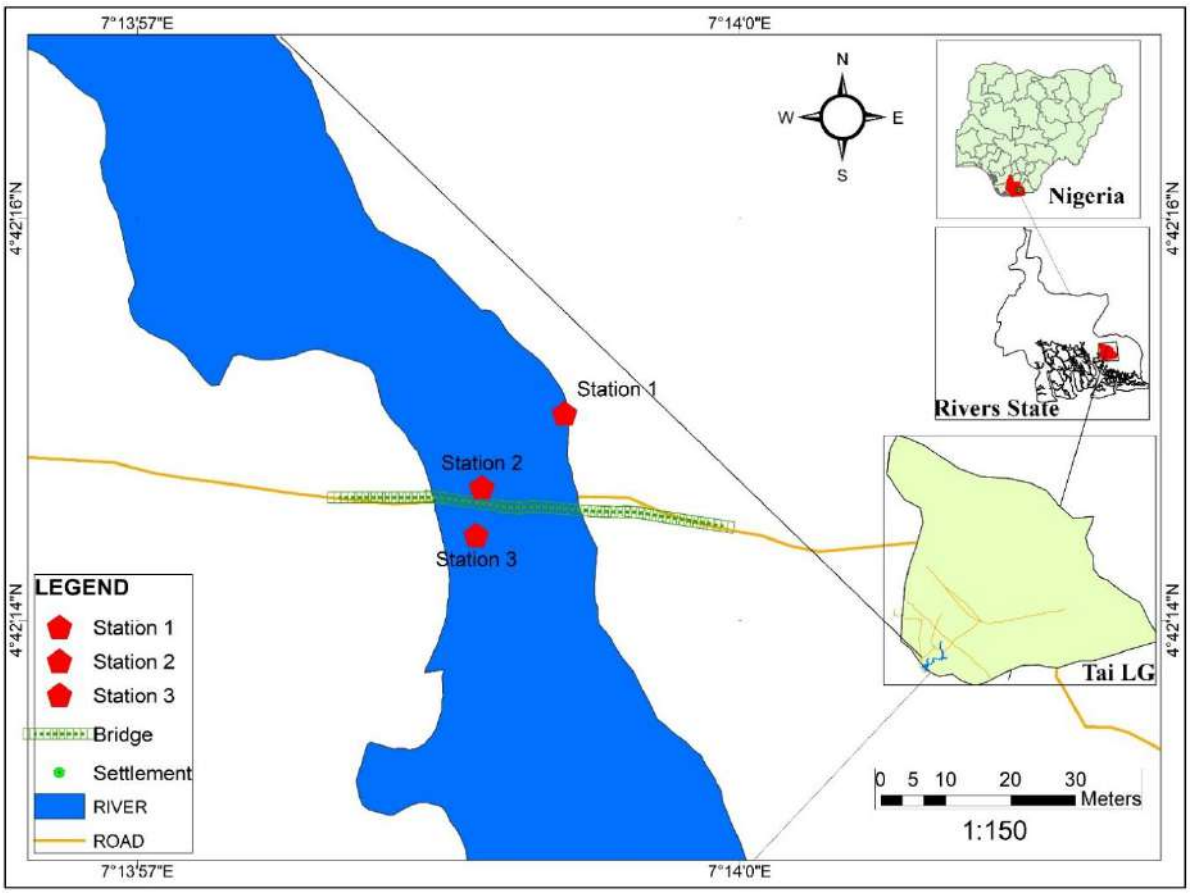

Figure 1.0: Map of the Study Area

Scientia Africana, Vol. 21 (No. 1), April, 2022. Pp 223-232 *https://dx.doi.org/10.4314/sa.v21i1.19*
© Faculty of Science, University of Port Harcourt, Printed in Nigeria *ISSN 1118 – 1931*

MATERIALS AND METHOD

The study was carried out at Kporghor Creek, Tai Local Government Area, Rivers State. Kporghor lies between N4° 42'.3257" and E7° 13'.7397". The Creek is a tidal brackish water ecosystem. The community and the Creek are surrounded by Gio, Wakama, Borobara and Gbam communities. Traditionally, Kporghor Creek serves as a strong livelihood support base for the people of the area and their neighborhoods. The Creek provides ready incentives for capture fisheries, transportation, cassava fermentation, fuel wood production and small-scale domestic waste disposal. The anthropogenic activities carried out around the Creek include illegal refining of crude oil (bunkering) and fishing. Its vegetation is dominated by red mangrove (*Rhizophora racemose*) with the presence of white mangrove (*Avicennia africana*), black mangrove (*Lagunculari racemosa*), mangrove sedge (*Paspalum vaginatum*), and Nypa palm (*Nypa fructicans*). The upper part of the Creek is vegetated by coconut (*Cocus nucifera*) and mango (*Mangifera indica*).

Sampling of Macrophytes

Sampling of macrophyte was carried out using a 0.5m x 0.5m quadrat. Macrophyte assemblages' abundance was assessed by visual estimates of the percentage cover of each species inside the 0.5 × 0.5 m quadrat which was transformed onto a scale based on Braun-Blanquet (1: < 5%; 2: 6-25%; 3: 26-50%; 4: 51-75; 5: 76-100%) (Roger *et al.*, 2013). In addition to the quadrats, macrophytes in the littoral region were also visually inspected from a boat. All macrophytes collected were identified at the Plant and Biotechnology Herbarium, University of Port Harcourt.

Water Sample Collection and analyses

Surface water samples for physical and chemical analysis were collected at 15-30 cm (0.49-0.98ft) depth (The depth of the sample location was determined using tape measurement procedure, as it was calibrated in feet of 1-100ft.), and it was determined by lowering the tape into the River and the measurement taken. The water samples were collected using niskin bottles. Samples collected were transferred into 70ml amber coloured reagent bottles for dissolved oxygen (DO) and biochemical oxygen demand (BOD) determination. Whereas, water collected for physical and chemical analysis was transferred into one-litre Plastic containers while, 120ml vial bottles were utilized for collection of water samples for trace heavy metals analysis. All sampling containers were properly washed with double distilled water, dried, corked with covers, well labelled and stored in cool box under laboratory condition 24 hours prior to samples collection.

All sample containers and niskin bottles were rinsed three times with the river water at each sampling point before samples collected collected with niskin bottles was transferred into them. Each sample was treated following standard APHA, 1998 procedure. Thereafter, all the samples were stored in the cool box and subsequently transported to the laboratory for treatment and analysis.

The physico chemical parameters of Kpoghor River determined are; temperature, hydrogen ion concentration (pH), electrical conductivity (EC), Total

Dissolved Solids (TDS), Dissolved Oxygen (DO) and Biochemical Oxygen Demand (BOD).

The pH, temperature, conductivity, total dissolved solids (TDS) and dissolved oxygen (DO) were determined in-situ in the field using Extech, a multiple parameter digital meter (DO:700 model), after calibrating the instrument with the necessary standard solutions The units of measurement were temperature (^oC), conductivity (μS/cm), TDS (mg/l) and DO (mg/l), TDS (mg/l).

Determination of Heavy Metals

Water samples for heavy metals analysis was collected from each station with sterilized, well labelled amber coloured bottles and transported to the laboratory for analysis. Prior to analysis, water Samples were digested using a mixture of concentrated HNO_3: HCl (1:3). Thereafter, the sample was analysed for heavy metal using Atomic Absorption Spectrophotometry (Nwajei *et al.,* 2014).

RESULTS AND DISCUSSION

Physicochemical parameter

The mean values recorded are shown on table 1. The lowest (29±0.63^{o}C) mean temperature was reported in Station 2 while highest (29.15±0.72^{o}C) was reported in Station 1. The pH values recorded in this study, which ranged from 6.50±0.44 to 6.65±0.44, are within the range previously reported for freshwater bodies in the Niger Delta (Asonye *et al.,* 2008) and DPR (2002) limits of 6.0 to 9.0. TDS ranged between 36.83±6.82mg/L and 40.05±5.30mg/L in the study. Electrical conductance in this study, minimum, (4430.50±0796.42µS/cm) at Station 2 and maximum (4914.75±569.42µS/cm) at Station 1. This study at Kporghor River showed the range of dissolves oxygen from 5.20±1.20mg/L to 5.50±0.49mg/L which is around the tolerance range for fish. Detail is shown in table 1.

Macrophytes

The details about the abundance of macrophytes across study locations are shown in table 2. The study identified 11 taxa and 11 species of macrophytes in Kporghor River. The diversity and abundance of the different species were higher in Station (2), followed by station (3) and Station (1) respectively. *Bambus vulgaris* having a percentage of (29.7%) being the most abundant with percentage abundance, *Cyrtospermum senegalense (8.72%),Nymphaea lotus (5.81), Acanthophoenix crinite (4.65%), Pistia stratiotes* and *Eichornia grassippes (2.91%)* respectively. Unidentified species of macrophyte collected from the sampling area accounted for 11.62% species abundance

Heavy metals

Heavy metals associated with crude oil identified in the study are Copper, Nickel, Lead and Cadmium. Lead had the overall highest concentrations across sampling stations ranging from 0.1290±0.1219 to 0.2393±0. Nickel and Cadmium has same values of 0.001mg/l across sampling stations. This is within the safe limit for drinking water of 0.02mg/l and 0.005mg/l respectively.

Scientia Africana, Vol. 21 (No. 1), April, 2022. Pp 223-232 *https://dx.doi.org/10.4314/sa.v21i1.19*
© Faculty of Science, University of Port Harcourt, Printed in Nigeria *ISSN 1118 – 1931*

Table 1: Spatial variation of the physico-chemical parameters of Kporghor River

Stations	Temperature (°C)	pH	TDS (mg/L)	EC (μS/cm)	DO (mg/L)	BOD (mg/L)
STN1	29.15±0.72	6.5±0.44	36.83±6.82	4914.75±569.42	5.38±0.84	3.08±0.94
STN 2	29±0.63	6.65±0.44	39.53±5.18	4430.5±796.42	5.2±1.20	3.4±0.61
STN 3	29.08±0.60	6.5±0.45	40.05±5.30	4432±828.42	5.5±0.49	3.35±0.66
MEAN	29.08	6.55	38.80	4592.42	5.36	3.28
DPR 2002	25-30	6.5-8.5	2,000-5,000	na	4.0-5.0	30-45

Key: DPR= Department of Petroleum Resources for regulation and compliance to petroleum laws. pH = Hydrogen ion concentration; TDS = Total Dissolved Oxygen; EC = Electric Conductivity; DO = Dissolved Oxygen; BOD = Biological Oxygen Demand, STN = Station; mg/L = milligram per liter, °C= degree Celsius; μS/cm = microSiemens per centimetre; na = not available.

Table 2: Macrophytes Abundance across the three stations of Kpoghor River

S/N	Common Name	Scientific Name	STN 1	STN 2	STN 3	Total Number of species	Percentage Abundance (%)
1.	Water lily	*Nymphaea lotus*	2	6	4	10	5.81
2.	Water lettuce	*Pistia stratiotes*	-	3	2	5	2.91
3.	Water hyacinth	*Eichhornia crassipes*	1	2	2	5	2.91
4.	Arrow head weed	*Cyrtospermum senegalense*	4	8	3	15	8.72
5.	Bamboo	*Bambusa vulgaris*	13	29	8	50	29.07
6.	Palm tree	*Acanthophoenixcrinite*	1	2	5	8	4.65
7.	Sunflower	*Helianthus annuus*	2	3	3	8	4.65
8.	Cassava	*Manihot esculentum*	4	3	3	10	5.81
9.	Nypa palm	*Nypa fruticans*	6	5	1	12	6.98
10.	White mangrove	*Rhizophora racemosa*	2	6	2	10	5.81
11.	Red mangrove	*Avicenia africana*	11	5	3	19	11.05
12.	Unidentified species	-	4	12	4	20	11.62
		Total				**172**	

Table 3: Spatial variation of Heavy Metals In Kpoghor River

STATION	Cu (mg/L)	Ni (mg/L)	Pb (mg/L)	Cd (mg/L)
STATION 1	0.0013±0.0005	0.0010±0	0.1708±0.1999	0.0010±0
STATION 2	0.0015±0.0010	0.0010±0	0.1290±0.1219	0.0010±0.0005
STATION 3	0.0013±0.0005	0.0010±0	0.2393±0.1981	0.0010±0
MEAN	0.0014	0.0010	0.141	0.0010
WHO 2011	0.015	0.07	0.01	0.003
SON 2007	1.00	0.02	0.01	0.003
DPR 2002	1.5	Na	0.05	0.03

Key: Cu = Copper; NI = Nickel; Pb = Lead; Cd = Cadmium; mg/L = milligram per liter; na = not available; WHO = World Health Organization; SON = Standard Organization of Nigeria; DPR = Department of Petroleum Resources

The physico-chemistry of the River showed variations across study location. The lowest (29±0.63ºC) mean temperature in Station 2 and the highest mean temperature (29.15±0.72ºC) in Station 1 reflected an optimal condition for the survival of aquatic life, and are consistent with temperatures recorded in surface water bodies in the tropics and freshwater in the Niger Delta region (Ezekiel *et al.*, 2011, Agedah*et al.*, 2015).According to Talling (2010). The pH ranging from 6.50±0.44 to 6.65±0.44 in the study location , are within the range previously reported for freshwater bodies in the Niger Delta (Asonye *et al.*, 2008) and DPR (2002) limits of 6.0 to 9.0. The pH value reported in this present study may be attributed to the decomposition of substances with high organic content due to the effect of the pollution (Vincent-Apku *et al.*, 2019). Consequently, drastic changes in pH will affect all other physico-chemical parameters of the water, including the aquatic organisms (Zhang *et al.*, 1995).

TDS which ranged between 36.83±6.82mg/L and 40.05±5.30mg/L in the study agrees with Vincent-Apku *et al*., (2019), who attributed it to the total dissolved solutes of a natural water body to salt intrusion of organic sources such as leaves, silt and planktons from the sea, as well as industrial wastes and sewages, while Essien-Ibok *et al.*, (2010) in a similar study at Mbo River posited attributed to evapo-crystallization process and low precipitation in the Rivers.

The minimum Electrical Conductance in this study was (4430.50±0796.42µS/cm) at Station 2 and maximum (4914.75±569.42µS/cm) at Station 1. This was quite higher than (195 ± 74[b] 2870 ± 234[a]) that was reported by Vincent-Akpu *et al.*, (2015) at Bodo Creek. They postulated that conductivity is strongly influenced by the concentrations of dissolved constituents, temperature, BOD, pH and DO, as these parameters are negatively correlated with EC.

According to Jingxi *et al.*, (2020), dissolved oxygen is a measure of the degree of pollution by organic matter and the destruction of organic substances, as well as the self-purification capacity of the water body. They also indicated that the maximum tolerance for fish is 5mg/L. This study at Kporghor River showed the range of dissolves oxygen from 5.20±1.20mg/L to 5.50±0.49mg/L which is around the tolerance range for fish.

Biological oxygen demand is a measure of the quantity of oxygen consumed by microorganisms during the decomposition of organic matter. Values for biological oxygen demand ranged between 3.08±0.94mg/L and 3.35±0.66mg/L.

Macrophytes

The research identified 11 taxa and 11 species of macrophytes in Kporghor River, the depletion in macrophytes availability in the Kporghor River is an indication that pollution has occurred in the river which has led to only 11 species of macrophytes. Oil spill pollution in Kporghor River has negative impacts on the first (station 1) and

Scientia Africana, Vol. 21 (No. 1), April, 2022. Pp 223-232 *https://dx.doi.org/10.4314/sa.v21i1.19*
© Faculty of Science, University of Port Harcourt, Printed in Nigeria *ISSN 1118 – 1931*

last sampling station (station 3 - located at the extreme of the river, hence making station (2) more abundant in macrophytes assemblage than stations (1) and (3) respectively. This is attributed to the impact of the crude oil spillage on the surrounding land and Kporghor River which affects the macrophytes vegetation negatively.

Macrophytes grow in different water bodies and in different forms either as emergent, submerged, or free floating. Most of these macrophytes need the services of sediments to grow effectively (John and Michael, 1986) but are been hampered by oil spill pollution which affect their productivity and relative abundance. Macrophytes provide food, shelter and cover against predators as well as generating oxygen as by-product of photosynthesis (Lesiv, Polishchuk and Antonyak, 2020). These essential services are lost through oil spill pollution in rivers and lakes where macrophytes are destroyed. This in turn, negatively affects the productivity of the river. Hence, Kporghor River is in jeopardy.

Heavy metals

The high concentrations of lead in the study area could be the attributed to hydrocarbons pollution in the river. Lead, which is carcinogenic, interferes with vitamin D metabolism, and affects mental development in infants, due to its toxicity to the central and peripheral nervous systems (SON, 2007). The overall concentration (0.1290±0.1219 to 0.2393±0) of lead across sampling stations falls within the permissible limit in WHO (2011) and SON (2007).The metal concentration trend recorded in this study was such that metal concentrations decreased as distance from the source of spill increased. This is similar to the trend reported by Zhang *et al.*(2015), where the concentration of heavy metal of a lake in Louisiana gradually declined with distance from the source of oil pollution.

Nickel and Cadmium has same values of 0.001mg/l across sampling stations. This is within the safe limit for drinking water of 0.02mg/l and 0.005mg/l respectively, as approved by the United Nations Environmental Protection Agency (EPA, 2013) but are in contrast to the findings of Ifelebuegu *et al*., (2017) at an oil polluted freshwater site in Nun River where heavy metal values, including Nickel and Cadmium exceeded the regulatory limits of the Department of Petroleum Resources (DPR, 2002). Copper ranged between 0.0013±0.0005 at Stations 1 and 3 and 0.0015±0.0010 at Station 2. This range does not compromise the quality of drinking water (EPA, 2013) and as such does not pose threats to health (Government of Western Australia, Department of Health, 2016).

CONCLUSION

Kporghor River is one of the rivers that have suffered from the impact of oil spill and pollution of several kinds. The elements which are present in these spills affect the productivity of water bodies and as such, the plants and animal species found in them suffer the same effects. Macrophytes grow and have high productivity when the water bodies are healthy and functioning at optimal levels, but are impacted negatively when oil spills and pollutions occur. The Macrophytes assemblage of the Kporghor River has been greatly affected with the heavy metals which also in turn affect the physico-

chemical parameters of the water hence reducing the abundance and percentage composition of the different species that are present in the water. The impacts of oil spill on the water bodies and on macrophytes assemblage led to the spatial and less distribution of macrophytes in the water. The lesser and relative abundance of macrophytes as seen in the different stations is an indication that oil spills affect macrophytes assemblage drastically and hence subsequent spills should be stopped to allow for macrophytes abundance and more distribution in Kporghor River.

REFERENCES

Adeleye A. O., Shelle, R. O. D., and Akinnigbagbe A. E. (2012). Pollutant Dynamics and Distribution In Sediments North Of Lagos Lagoon Ecosystem. *Nature and Science*, **9(5),** 13-16.

Agedah, E.C., Ineyougha, E.R., Izah, S.C. and Orutugu, L.A. (2015). Enumeration of total heterotrophic bacteria and some physico-chemical characteristics of surface water used for drinking sources in Wilberforce Island, Nigeria. *Journal of Environmental Treatment Techniques*, 3(1), 28-34.

Aloulou, F., Kallell, M. and Belayouni, H. (2011). Impact of oil field-produced water discharges on sediments: a case study of SabkhatBoujemal, Sfax, Tunisia. *Environmental Forensics*, *12(3)*, 290-299.

APHA (1998). Standard methods for the examination of water and waste waters. American Public Health Association. 874pp.

Asonye, C.C., Okolie, N.P., Okenwa, E.E. and Iwuanyanwu, U.G. (2007). Some physico-chemical characteristics and heavy metal profiles of Nigerian rivers, streams and waterways. *African Journal of Biotechnology*, 6(5), 617.

ASTM (1999) standard test methods for analysis of cast iron by Spark Atomic Emission Spectrometry.

Baird, J. (2010). 'Oil's Shame in Africa.' Newsweek, 27.

Barakat, A. Baghdadi, M. El Rais J. &Nadem S., (2012). Assessment of Heavy Metal in Surface Sediments of Day River at Beni-Mellal Region, *Morocco Research Journal of Environmental and Earth Sciences* **4(8),** 797-806, 2012.

DPR (2002). Environmental Guidelines and Standards. Department of Petroleum Resources. Revised Edition. https://ngfcp.dpr.gov.ng/media/1066/dprs-egaspin-2002-revised-edition.pdf.

EPA (2013). Summary of the Safe Drinking Water Act. United Nations Environmental Protection Authority. https://www.epa.gov/laws-regulations/summary-safe-drinking-water-act. Retrieved 2021-04-07.

Essien-Ibok, M. A.,Akpan, A. W., Udo, M. T.,Chude, L. A., Umoh, A. I., and Asuquo, I. E. (2010). Seasonality in the physical and Chemical Characteristics of Mbo River, Akwa Ibom State, Nigeria. Nigerian Journal of Agriculture, Food and Environment. 6(1&2):60-72.

Ezekiel, E. N., Hart, A. I., Abowei, F. F. N. (2011). The sediment physical and chemical characteristics in Sombreiro River, Niger Delta, Nigeria. *Research*

Scientia Africana, Vol. 21 (No. 1), April, 2022. Pp 223-232 *https://dx.doi.org/10.4314/sa.v21i1.19*
© Faculty of Science, University of Port Harcourt, Printed in Nigeria *ISSN 1118 – 1931*

Journal of Environmental and Earth Science, 3(4), 341-349.

Government of Western Australia, Department of Health (2016). Copper in drinking water. https://ww2.health.wa.gov.au/Articles/A_E/copper-in-drinking-water. Last reviewed: 2016-06-24. Retrieved: 2021-04-07.

Harikumar, P. S., Nasir, U. P., Mujeebu and Rahman, M. P., (2009). Distribution of heavy metals in the core sediments of a tropical wetland system. *Int. J. Environ. Sci. Tech.*, **6 (2)**, 225-230.

Ifelebuegu, A, Ukpebor, J, Ahukannah, AU, Theophilus, S &Nnadi, E (2017), 'Environmental effects of crude oil spill on the physicochemical and hydrobiological characteristics of the Nun River, Niger Delta' *Environmental Monitoring and Assessment*, vol 189, 173.

Jingxi Ma, Shuqing Wu, N. V. Ravi Shekhar, Supriya Biswas, and Anoop Kumar Sahu (2020). Determination of Physicochemical Parameters and Levels of Heavy Metals in Food Waste Water with Environmental Effects. Bioinorganic Chemistry and Applications. Bioinorg Chem Appl.2020;2020:8886093. doi:10.1155/2020/8886093. htpps://www.ncbi.nlm.nih.gov/pmc/articles/PMC7455830. Published online: 2020-08-20. Retrieved 2021-05-17.

John, W. B., & Michael, R..S., (1986). Sediments-Related Mechanisms of Growth Limitation in Submersed Macrophytes. *Ecology:* 67 (5), 1328-1340.

Lesiv M.S., Polishchuk A.I., Antonyak H.L. (2020). Aquatic macrophytes: ecological features and functions. *Studia Biologica, 14*(2); 79–94 • DOI:https://doi.org/10.30970/sbi.1402.619

Nwajei, G. E.1; Dibofori-Orji A. N.2, Iwegbue, C. M. A.3 &Ojuh, B. O.4 *(2014).* Distribution of Trace Elements in Surface Water and Sediments from Crayford Creek in Warri, Delta State of Nigeria *Academic Research International Vol. 5(4).*

Ordinioha, B. and Brisibe, S. (2013). The human health implications of crude oil spills in the Niger Delta, Nigeria: An interpretation of published studies. *Nigerian Medical Journal,* 54(1), 10.

Roger Paulo Mormu, SidineiMagela Thomaz1 and Lisandro Juno Soares Vieira (2013).Richness and composition of macrophyte assemblages in four Amazonian lakes. Maringá, v. 35 (3,) p. 343-350.

SON (2007). Nigerian Standard for Drinking Water Quality. Standard Organization of Nigeria. https://health.gov.ng/doc/StandardWaterQuality.pdf. Retrieved 2021-04-28.

Talling, J.F. (2010). pH, the CO2 system and freshwater science. *Freshwater Reviews, 3(2*), 133-146.

Tanee, F.B.G. and D.I. Anyanwu, 2008. Comparative studies of the growth and yield of two cassava lines (TMS 30572 and TMS 30555) in a crude oil polluted habitat. Scientia Afr., 6: 81-84.

Vincent-Akpu, I. F. And Offiong, U. S. (2019). Assessment of physico-chemical parameters of Qua Iboe Estuary, Nigeria. Nigerian Journal of Fisheries, 16(1), 1677-1683.

WHO (2011). Guidelines for drinking water quality. Fourth edition.

Zhang, J., Yan, J. and Zhang, Z. F. (1995). Nationwide river chemistry trends in China: Huanghe and Changjiang. Ambio, 275-279.

Zhang, Z., Wang, J. J., Tang, C. and DeLaune, R. D. (2015). Heavy metals and metalloids content and enrichment in Gulf Coast sediments in the vicinity of an oil refinery. *Journal of Geochemical Exploration, 159*, 93-100.

Scientia Africana, Vol. 21 (No. 1), April, 2022. Pp 233-244 *https://dx.doi.org/10.4314/sa.v21i1.20*
© Faculty of Science, University of Port Harcourt, Printed in Nigeria *ISSN 1118 – 1931*

QUANTILE CROSSING AS IT PERTAINS TO SAMPLE SIZE AND GOODNESS OF FIT: A SIMULATION STUDY

[1]Nwakuya, M. T. and [2]Masha, M. I.
[1&2]Department of Mathematics and Statistics, University of Port Harcourt.
Email: [1]maureen.nwakuya@uniport.edu.ng and [2]mashamify@gmail.com

Received: 05-02-2022
Accepted: 30-03-2022

ABSTRACT

Estimation of quantile regression curves individually causes quantile crossing, which eventually leads to an invalid estimation of the predictor effect. This work implemented quantile regression coefficient modeling (QRCM) where the regression coefficients are modeled as parametric functions of the order of the quantile in other to eliminate crossing. Four different samples of sizes 30, 50, 100 and 500 were simulated in other to investigate the effect of sample size on crossing and also to investigate the effect of crossing on model fit. The results show that as the sample sizes were increased crossing was reduced, but with a very large sample size crossing was not observed at all. The results also revealed that the presence of crossing caused the models not to be well specified but with the elimination of crossing the models were seen to be well specified.

Keywrods: Quantile Crossing, Quantile Regression, Goodness of Fit, Cross Index and Quantile Function.

INTRODUCTION

Quantiles are said to be points in a distribution that pertains to the rank order of values in that distribution. Quantiles seem inseparably linked to the operations of ordering and sorting the sample observations that are usually used to define them. So it comes as a mild surprise to observe that we can define the quantiles through a simple alternative expedient as an optimization problem. Just as we can define the sample mean as the solution to the problem of minimizing a sum of squared residuals, we can define the median as the solution to the problem of minimizing a sum of absolute residuals, (Koenkerand Hallock,2001). Given a set of covariates, the linear-regression model (LRM) specifies the conditional mean function whereas the Quantile Regression model (QRM) specifies the conditional-quantile function. The LRM is a standard statistical method that focuses on modeling the conditional mean of a response variable without accounting for the full conditional distributional properties of the response variable. In contrast, the QRM facilitates analysis of the full conditional distributional properties of the response variable. The QRM and LRM are similar in certain respects, as both models deal with a continuous response variable that is linear in unknown parameters, but the QRM and LRM model deal with different quantities and rely on different assumptions about error terms. The issue of crossing arises during multiple percentiles estimation, the quantile curves can cross, leading to an invalid distribution for the response, such as wrong coefficient effects Nwakuya and

Onyegbuchulam (2021) investigated the effects of crossing on regression coefficients and they found out that crossing has a significant effect on regression coefficients. It's paramount that crossing should be eliminated in quantile regression analysis. Some authors like Lui and Wu(2011), proposed a new kernel-based multiple QR estimate technique called simultaneous non-crossing quantile regression, the method applies constraints on the kernel coefficients to avoid crossing. Chernozhukov et al. (2010) proposed estimating noncrossing quantile curves via a monotonic rearrangement of the original nonmonotonic function. Most recently Santos and Kneib (2020) considered a flexible Bayesian quantile regression model with Gaussian process adjustment to achieve a noncrossing property. Jiang and Yu(2022) considered single-index models and developed methods for QR that guarantees non-crossing quantile curves which they extended to composite quantile regression. Patto and Matteo (2016) described an approach for modeling the regression coefficients as parametric functions of the order of the quantile. The method proved to be advantageous in terms of parsimony, efficiency and removal of crossing. Patto et al. (2021) applied this approach to longitudinal data were they described how the QRCM paradigm can be applied to longitudinal data. This work aims at investigating crossing as it relates to sample size and goodness of fit while modeling the regression coefficients as parametric functions of the order of the quantile, following the work of Patto and Matteo (2016).

The quantile regression model is given by;

$$Q_\tau(y_i) = \beta_0(\tau) + \beta_1(\tau)x_{i1} + \cdots + \beta_p(\tau)x_{ip} + e_i \quad (1)$$

Where p is the number of predictor variables, $\beta(\tau)$is the τth effect on the response variable while e and x are the error term and predictor variable respectively. The best median Quantile regression line is found by minimizing median absolute deviation.

$$MAD = \frac{1}{n}\sum_{i=1}^{n} \rho_\tau \left(y_i - \left(\beta_0(\tau) + \beta_1(\tau)x_{i1} + \cdots + \beta_p(\tau)x_{ip}\right)\right) \quad (2)$$

Here the function ρ is the check function which gives asymmetric weights to the error depending on the quantile and the overall sign of the error.

$$\rho_\tau(e) = e(\tau - 1(e < 0)) = \begin{cases} \tau|e|, & e \geq 0 \\ (1-\tau)|e|, & e \leq 0 \end{cases}$$

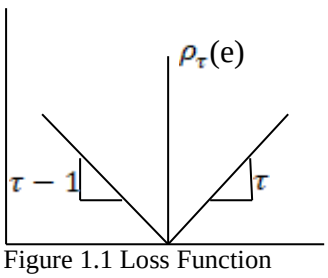

Figure 1.1 Loss Function

Scientia Africana, Vol. 21 (No. 1), April, 2022. Pp 233-244 *https://dx.doi.org/10.4314/sa.v21i1.20*
© Faculty of Science, University of Port Harcourt, Printed in Nigeria *ISSN 1118 – 1931*

In figure 1.1, $\rho_\tau(0) = 0$ increases linearly with slope τ as e moves away from zero to the right and it increases linearly with slope $1 - \tau$ as e moves away from zero on the left. Nwakuya (2020) opined that the traditional frequentist quantile regression makes minimum assumptions that tolerate errors that are not normal given that the response variable (y) is continuous even in Bayesian framework. John & Nduka (2009) concluded that quantile regression offers a comprehensive strategy for completing the regression picture as it goes beyond this primary goal of determining only the conditional mean, and enables one to pose the question of relationship between the response variable and explanatory variables at any quantile of the conditional distribution function. Studying For better understanding of the intuition of quantile regression, let's begin with the intuition of ordinary least squares. Given the model

$$y_i = \beta' X_i + \varepsilon_i \tag{3}$$

the least squares estimate minimizes the sum of the squared error terms

$$\sum_i^N \sum (y_i - \hat{y}_i)^2 \tag{4}$$

Comparatively, quantile regression minimizes a weighted sum of the positive and negative error terms:

$$\tau \sum_{y_i > \hat{\beta}_\tau' X_i} |y_i - \hat{\beta}_\tau' X_i| + (1 - \tau) \sum_{y_i < \hat{\beta}_\tau' X_i} |y_i - \hat{\beta}_\tau' X_i| \tag{5}$$

where τ is the quantile level.

The τ^{th} conditional quantile $\tau \in 0{,}1$ of a real valued random variable Y given a vector of *k* predictors is given by;

$$Q_\tau(Y|X) = \inf (\Pr (Y \leq y|X)) \geq \tau. \tag{6}$$

The earliest research by Koenker and Bassset (1978) recognized that the solutions were determined by fitting certain observations exactly. When the quantile regression were introduced, it was found out that fitting certain observations exactly forced the regression quantile fits to cross, thus causing the conditional quantile function to be non-monotonic in its statement, τ at some values of the predictor variables, Koenker (2005). Crossing in quantile regression happens when regression predictions for different quantile probabilities do not increase as probability increases.

QUANTILE CROSSING

In view of the fact that quantile regression curves are estimated individually, these curves may cross, leading to an invalid distribution for the response. Reviewing the conditional distribution of the response given the predictor, one of the processes is to estimate multiple conditional quantile functions. Theoretically, the various conditional quantile functions ought not to cross each other as claimed by the basic principle of conditional distribution functions. However, this naive individual estimation can lead to estimated conditional quantile functions that may cross each other. Authors that worked on non-crossing include, He (1997) that suggested a technique to estimate the quantile curves while ensuring that it does not cross. Nevertheless, the approach presumes a heteroscedastic regression model for the response, which permits the predictors to have effect on the distribution of the response via a location

and scale change of an underlying base distribution. Wu and Liu (2009) suggested a technique to ensure non-crossing, by fitting the quantiles sequentially and constraining the current curve to not cross the previous curve. Dette and Volgushev (2008) and Chernozhukov et al. (2009), all secured non-crossing by the approach of modifying the estimation of the conditional distribution function. The indirect technique is considered if focus is purely in estimation of the conditional quantile. However, when our focus is on quantifying the effects of the predictors, the quantile curves are typically modeled via a parametric form, such as linear predictor effects, and a direct estimation approach is required.

METHODOLOGY

Let y denote the outcome of interest conditional on a p dimensional vector x, where y is a continuous random variable with cumulative distribution function $F_{y_i}(.)$ and let $Q_{y_i}(\tau|x)$ be the quantile function· The Quantile regression model with the τth quantile for response (y|x) is of the form; $Q_\tau(y|x) = \inf(\Pr(Y \leq (y|x) \geq \tau$, it is assumed that for $\tau \in 0{,}1$ and that there is a p dimensional vector $\beta(\tau)$ such that;

$$Q(\tau/x) = X^T\beta(\tau) \quad (7)$$

$\beta(\tau)$, describes the effect of predictors on the τ^{th} quantile of the response variable and we assume that the quantile regression coefficient function $\beta(.)$ can be modeled parametrically as $\beta(\tau) = \beta(\tau/\theta)$, where θ is an unknown parameter. We can define $\beta(\tau)$ as a function of τ that depends on a finite-dimensional parameter θ, so that;

$$\beta(\tau/\theta) = \theta b(\tau) \quad (8)$$

Where $b(\tau) = [b_1(\tau), \ldots, b_k(\tau)]^T$ is a set of k known functions of τ. θ is a matrix with entries θ_{ij}. Hence the conditional quantile function is;

$$Q(\tau/x,\theta) = x^T\theta b(\tau)\,, \quad (9)$$

this can be written as; $y = x^T\theta b(\tau)$ (10)

Considering a simple model given as $y_i = \beta_o(\tau/\theta) + \beta_1(\tau/\theta)x$ (11)

If we denote the quantile function of distribution of a standard normal distribution as $z(\tau)$then;

$\beta_o(\tau/\theta) = \theta_{00} + \theta_{01}\xi(\tau)and\beta_1(\tau/\theta) = \theta_{10}$, where $\beta_1$is linear in τ and β_0 depends on $\xi(\tau)$.

In this model θ_{00} is the intercept of $\beta_o(\tau/\theta)$, θ_{10} is the slope associated with $\xi(\tau)$ and the regression coefficient $\beta_1(\tau/\theta)$ is assumed to be constant across quantiles enforcing homoscedasticity. In other to estimate the τ^{th}quantile regression coefficients under equation (7) we minimize the objective function;

$$L(\beta(\tau)) = \sum_i^n (\tau - w_{\tau,i})(y_i - X^T\beta(\tau_t)) \quad (12)$$

Subject to $X_i^T\beta_{\tau t} \geq X_i^T\beta_{\tau t-1}$, t=2,…,q

Scientia Africana, Vol. 21 (No. 1), April, 2022. Pp 233-244 https://dx.doi.org/10.4314/sa.v21i1.20
© Faculty of Science, University of Port Harcourt, Printed in Nigeria *ISSN 1118 – 1931*

Given that; $w_{\tau,i} = I\left(y_i \leq X_i^T \beta(\tau)\right)$ where I(.) is an indicator function. $\theta$is estimated by minimizing the integrated objective function given in equation (13)below with respect to the order of the quantile.

$$L(\theta) = \int_0^1 L(\beta(\tau/\theta))d\tau \quad (13)$$

This approach allows the estimation of the entire quantile process without allowing crossing. This work applied simulated datasets with sample sizes 30, 50, 100 and 500 in other to investigate effect of sample size on crossing and to check the fitness of the model without crossing and with crossing.The simulated dataset with crossing was generated for binomial and uniform distribution, while the response was generated as a function of both the predictors from both distributions, for sample size n = 30, 50, 100 and 500. The work was analyzed using Quantreg package and qrcm package in R.

Goodness of fit test:

Let $F_n(X)$ denote the empirical distribution function of the data defined by $F_n(X) = \frac{1}{n}\sum_{i-1}^{n} I(x_i \leq x), -\infty < x < \infty,$ where the indicator function $I(a,b)$ is defined as 1 for a ≤ b and as 0 otherwise. Since $F_n(X)$ is the proportion of observations less than or equal to x if $F(X)$ is the true distribution of X, we expect $F_n(X)$ to be close$F(X)$. The closeness of $F_n(X)$ to $F(X)$ is assessed by the Cramer-von Mises statistics defined by Richard A. L. (2019) as;

$$w_n^2 = n\int_{-\infty}^{\infty}[F_n(X) - F(X)]^2 dF(X)$$

The hypothesis is given as;

$H_0: \tau_1, \ldots, \tau_q \sim u(0,1)$ (model is correctly specified)

$H_1: \tau_1, \ldots, \tau_q \nsim u(0,1)$ (model is not correctly specified)

Cross index: Cross index is the average length, across observations, of the sub-intervals of τ. Cross index lies from 0 to 1, with 0 indicating no crossing and 1 indicating that observations cross at all quantiles. Cross index close to 0 indicates minimal crossing while cross index close to 1 indicates high crossing.

RESULTS

Sample size = 30. The dataset had crossing with a cross index of 0.3105, which is minimal crossing.

Table 4.1: Quantile regression coefficient results at different quantiles with crossing:

Quantiles	Coefficients	Estimate	std.err	z value	p(>|z|))
25%	Intercept	0.6659	5.2904	0.126	0.900
	β_1	2.3316	2.6715	0.873	0.383
	β_2	5.3758	4.9869	1.078	0.281
50%	Intercept	0.5452	5.7178	0.095	0.924
	β_1	2.9888	5.0242	0.595	0.552
	β_2	6.3411	7.0616	0.898	0.369
75%	Intercept	5.708	17.947	0.318	0.750
	β_1	2.239	6.435	0.348	0.728
	β_2	1.607	16.995	0.095	0.925
95%	Intercept	33.74	18.92	1.784	0.0745
	β_1	-7.32	11.11	-0.659	0.5099
	β_2	-17.76	15.51	-1.145	0.2522

*Significant at 0.05 level of significance

Table 4.1 presents the quantile regression coefficients with crossing and it shows that all the predictors are insignificant.

AFTER REMOVING CROSSING: Number of observations that crossed is 0 (0%), with cross index of 0.0005462.

Table 4.2 Quantile regression coefficient results at different quantiles after removal of crossing:

Quantiles	Coefficients	Estimate	std.err	z value	p(>|z|))
25%	Intercept	-0.9878	6.8540	-0.144	0.885410
	β_1	2.8530	0.8106	3.519	0.000433*
	β_2	7.0496	7.0053	1.006	0.3143
50%	Intercept	0.8662	0.5311	1.631	0.103
	β_1	2.5729	0.2969	8.667	<2e-16*
	β_2	6.0500	0.6023	10.044	<2e-16*
75%	Intercept	3.131	6.440	0.486	0.627
	β_1	2.805	1.444	1.943	0.050*
	β_2	4.076	6.336	0.643	0.520
95%	Intercept	23.5386	17.3947	1.353	0.176
	β_1	0.2412	10.3794	0.023	0.981
	β_2	-10.3701	14.8580	-0.698	0.485

*Significant at 5% level of significance.

The table 4.2 above shows that the removal of crossing affected the effects of the predictors. We can see that β_1 is now significant at the 25th, 50th and 75th quantiles but it showed no effect at the 95th quantile.

Scientia Africana, Vol. 21 (No. 1), April, 2022. Pp 233-244 https://dx.doi.org/10.4314/sa.v21i1.20
© Faculty of Science, University of Port Harcourt, Printed in Nigeria *ISSN 1118 – 1931*

Table 4.3: Goodness of fit test result

Test Statistics	statistic	p-value
Cramer-Von Mises (With Crossing)	0.036759	0.03061224
Cramer-Von Mises (Without Crossing)	0.065670	0.68141414

With crossing the model was seen not to be well specified but it can be seen that the removal of the crossing resulted to a well specified model. Table 4.3 shows that the model without crossing is well specified.

SAMPLE SIZE = 50

Number of observations that crossed were 28, the analysis shows that 56% of the observations has crossing somewhere in the domain with a cross index of 0.167.

Table 4.4: Quantile regression coefficient results at different quantiles with crossing:

Quantiles	Coefficients	Estimate	std.err	z value	p(>|z|))
25%	Intercept	-0.3813	29.6825	-0.013	0.990
	β_1	2.4084	0.4750	5.070	3.97e-07*
	β_2	6.8926	29.6886	0.232	0.816
50%	Intercept	-0.1664	18.7418	-0.009	0.992916
	β_1	2.8370	0.8352	3.397	0.000682*
	β_2	7.0754	18.7010	0.378	0.7052
75%	Intercept	0.7110	1.1470	0.620	0.535
	β_1	3.0647	0.7577	4.045	5.23e-05*
	β_2	6.7818	0.8928	7.596	3.05e-14*
95%	Intercept	3.314	5.162	0.642	0.5210
	β_1	3.183	4.682	0.680	0.4967
	β_2	6.168	2.902	2.125	0.0335*

*Significant at 5% level of significance

Table 4.4 above shows that at all quantiles at least one predictor is significant. The effects in this result are similar to the effects in 25th quantile without crossing. We can say that even with crossing a little increase in the sample reveals some effects that were not visible with a smaller sample size.

After Removing Crossing

Number of observations that crossed: 0 (0%) with cross index of 0.00.

Table 4.5: Quantile regression coefficient results at different quantiles after removing crossing:

Quantiles	Coefficients	Estimate	std.err	z value	p(>|z|))
25%	Intercept	-0.006231	0.956783	-0.007	0.995
	β_1	2.490053	0.223359	11.148	< 2e-16*
	β_2	6.4684	0.9532	6.786	1.15e-11*
50%	Intercept	0.2236	1.5700	0.142	0.886766
	β_1	2.7864	0.8063	3.456	0.000549*

	β_2	6.6696	1.2180	5.476	4.36e-08*
75%	Intercept	1.100	2.016	0.546	0.58525
	β_1	3.202	0.464	6.900	5.19e-12*
	β_2	6.217	2.100	2.960	0.0031*
95%	Intercept	3.390	10.245	0.331	0.741
	β_1	3.621	4.319	0.838	0.402
	β_2	5.477	8.133	0.673	0.501

*Significant at 5% level of significance

The Table 4.5 above reveals that after the removal of crossing all the predictors were seen to have a significant effect except for the 95th quantile. This also reveals an improvement in the significance of the predictors when crossing was removed.

Table 4.6: Goodness of fit test result

Test Statistics	statistic	p-value
Cramer-Von Mises (With Crossing)	0.0269145	0.04061224
Cramer-Von Mises (Without Crossing)	0.0556175	0.9895233

We can see that the removal of the crossing resulted in a well specified model. But with crossing the model is seen not to be well specified.

SAMPLE SIZE = 100

Number of observations that crossed: 4 (4%), the analysis shows that 4% of the observations has crossing somewhere in the domain with a cross index of 0.2018, which is minimal crossing.

Table 4.7: Quantile regression coefficient results at different quantiles with crossing:

Quantiles	Coefficients	Estimate	std.err	z value	p(>|z|))
25%	Intercept	0.8173	2.1689	0.377	0.706
	β_1	2.2319	2.3523	0.949	0.343
	β_2	5.5892	4.8617	1.150	0.250
50%	Intercept	0.7969	0.4585	1.738	0.0822
	β_1	3.1353	0.3558	8.813	<2e-16*
	β_2	5.4893	0.4666	11.765	<2e-16*
75%	Intercept	1.105	2.830	0.390	0.696
	β_1	3.570	3.004	1.188	0.235
	β_2	5.824	1.435	4.059	4.93e-05*
95%	Intercept	1.763	13.935	0.127	0.899
	β_1	4.108	7.459	0.551	0.582
	β_2	6.047	5.236	1.1556	0.248

*Significant at 5% level of significance

Scientia Africana, Vol. 21 (No. 1), April, 2022. Pp 233-244 https://dx.doi.org/10.4314/sa.v21i1.20
© Faculty of Science, University of Port Harcourt, Printed in Nigeria *ISSN 1118 – 1931*

The Table 4.7 above shows that only at 50th and 75th quantile were the predictors significant.

After Removing Crossing

Number of observations that crossed: 0 (0%) with cross index: 0.0005462.

Table 4.8: Quantile regression coefficient results at different quantiles after removing crossing:

Quantiles	Coefficients	Estimate	std.err	z value	p(>|z|))
25%	Intercept	0.4839	0.1712	2.827	0.00469*
	β_1	2.7247	0.2083	13.080	< 2e-16*
	β_2	5.7347	0.2707	21.182	< 2e-16*
50%	Intercept	0.7592	0.5305	1.431	0.152
	β_1	3.0785	0.3651	8.432	<2e-16*
	β_2	5.6786	0.3911	14.520	<2e-16*
75%	Intercept	1.2280	0.5583	2.199	0.0279*
	β_1	3.3802	0.6632	5.097	3.46e-07*
	β_2	5.8394	0.3644	16.024	<2e-16*
95%	Intercept	2.0509	0.8777	2.337	0.01946*
	β_1	4.1482	1.3904	2.984	0.00285*
	β_2	5.3353	0.8545	6.244	4.27e-10*

*Significant at 5% level of significance

The Table 4.8 above shows that after removing crossing all the predictors at all the quantiles were seen to be significant. Showing that the increase in the sample size has a role to play in reducing crossing.

Table 4.9: Goodness of fit test result

Test Statistics	statistic	p-value
Cramer-Von Mises (With Crossing)	0.0465311	0.00
Cramer-Von Mises (Without Crossing)	0.098252	0.72433

We can see that the removal of the crossing resulted to a well specified model.

SAMPLE SIZE = 500

Number of observations that crossed: 0 (0%), the analysis shows that 0% of the observations has crossing somewhere in the domain with a cross index of 0.000713. This shows us that when the sample size is very large crossing is eliminated.

Table 4.10: Quantile regression coefficient results at different quantiles after removing crossing:

Quantiles	Coefficients	Estimate	std.err	z value	p(>|z|))
25%	Intercept	0.22442	0.06062	3.702	0.000214*
	β_1	2.51083	0.08875	28.291	< 2e-16*
	β_2	6.89674	0.15379	44.844	<2e-16*
50%	Intercept	0.6673	0.1685	3.96	7.5e-05*
	β_1	3.0750	0.1279	24.05	< 2e-16*
	β_2	6.6703	0.1870	35.67	< 2e-16*

75%	Intercept	1.3039	0.2549	5.116	3.12e-07*
	β_1	3.5608	0.1693	21.035	< 2e-16*
	β_2	6.7486	0.2995	22.534	< 2e-16*
95%	Intercept	2.5857	0.5098	5.072	3.94e-07*
	β_1	4.1522	0.2778	14.944	< 2e-16*
	β_2	7.4926	0.4412	16.984	<2e-16*

*Significant at 5% level of significance

From table 4.10, we can see that all of the covariates were significant at the P-value 0.05.

We also noticed that as the sample size increase the number of observations that crossed reduces significantly. With a sample size of 500, no crossing was observed at any point.

CONCLUSION

This paper investigated the effect of sample on crossing and also looked at how crossing affects model fitness. The analysis modeled the regression coefficients as parametric functions of the order of the quantile. This process removes crossing as was shown by Patto and Matteo (2016). In the analysis four different datasets were simulated with sample sizes 30, 50, 100 and 500. Using sample size of 30 with crossing all the predictors was seen to be insignificant and after crossing removal some of the predictors showed significant effects. There was an improvement when the sample size was increased to 50, even with crossing some predictors were seen to be significant and after removing crossing all the predictors were seen to be significant except the 95^{th} quantile. For sample size 100, after the removal of crossing all the predictors were seen to significant and also at sample size of 500, there was no crossing at all. We also looked at the goodness of fit of the models and we discovered that without crossing the models were well specified while the presence of crossing produced models that were not well specified Based on the findings we can conclude that this work has been able to show that increase in sample size reduces crossing but with very large samples sizes crossing is totally eliminated. Also the work has been able to show that crossing affects the fit of a model by producing unspecified models while removal of crossing produces well specified model.

REFERENCES

Chernozhukov, V., Fernandez-Val, I., and Galichon, A. (2009). Improving point and interval estimators of monotone functions by rearrangement. Biometrikavol 96: 559-575.

Chernozhukov, V., Fernandez-Val, I., and Galichon, A. (2010), "Quantile and Probability Curves Without Crossing," Econometrica, 78, 1093–1125

Dette, H. and Volgushev, S. (2008). Non-crossing non-parametric estimates of quantile curves. Journal of the Royal Statistical Society B 70: 609-627.

He, X. (1997). Quantile curves without crossing. American Statistician. 51: 186-192.

John O.O., and E.C. Nduka (2009). Quantile Regression Analysis As A Robust Alternative To Ordinary Least Squares, Scientia Africana, 8 (No.2): 61-65.

Scientia Africana, Vol. 21 (No. 1), April, 2022. Pp 233-244 *https://dx.doi.org/10.4314/sa.v21i1.20*
© Faculty of Science, University of Port Harcourt, Printed in Nigeria *ISSN 1118 – 1931*

Heagerty P.J. and M.S. Pepe, (1999). Semiparametric estimation of regression quantiles with application to standardizing weight for height and age in US children. Applied Statistics. 48: 533-551.

Koenker, R. and Hallock K. (2001). Quantile Regression. Journal of Economic Perspectives, 15(4): 143–156

Koenker, R. and G. Bassett, 1978. Regression quantiles. Econometrica, 46: 33-50.

KonkerR. (2005).Quantile regression; Econometric Society Monograph Series, Cambridge. Cambridge University Press.

Lui Y. and Wu Y. (2011). SimultaneousMultiple Non-Crossing Quantile Regression Estimation Using Kernel Constraints. Journal of Non-Parametric Statistics, 23(2): 415-437, doi: 10.1080/10485252.2010.537336

Nwakuya M. T. (2020). Assessment of Mental Health of Undergraduate Student based on Age: A Bayesian Ordinal Quantile Regression Approach. Quarterly Journal of Econometrics Research, June 2020, 6(1): 12-17.

Paolo F. and B. Matteo (2016). Parametric modeling of quantile regression coefficient functions, Biometrics, 72 (1): 74-84.

Paolo F., B. Matteo and I. Fern´andez-Val (2021). Parametric modeling of quantile regression coefficient functions with longitudinal data. Statistical Methods & Applications

Lockhart, R.A., & Navaratna, C.W. (2019). A goodness of fit test for two component two parameter Weibull mixtures. *arXiv: Methodology.*

Rong J. and Keming Y. (2022). No-Crossing Single-Index Quantile Regression Curve Estimation. Journal of Business & Economic Statistics, Doi: 10.1080/07350015.2021.2013245

Santos, B.,
and Kneib, T. (2020), "Noncrossing Structured Additive Multiple-Output Bayesian Quantile Regression Models," Statistics and Computing, 30, 855–869.
DOI: https://doi.org/10.1007/s11222-020-09925-x.

Wu, Y. and Y. Liu, (2009). Stepwise multiple quantile regression estimation using non-crossing constraints. Statistics and It's Interface, 2: 299-310.

Scientia Africana, Vol. 21 (No. 1), April, 2022. Pp 245-252 *https://dx.doi.org/10.4314/sa.v21i1.21*
© Faculty of Science, University of Port Harcourt, Printed in Nigeria *ISSN 1118 – 1931*

INVESTIGATION OF *HIBISCUS SABDARIFFA* AS A NEW ECO-FRIENDLY PHOTO-LARVICIDAL NATURAL PRODUCT FOR THE CONTROL OF MOSQUITOES

T. A. Ugboaja; G. I. Ndukwe*; G. K. Fekerurhobo
Department of Chemistry, Rivers State University, Port Harcourt, Nigeria
*Corresponding author's email: gloria.ndukwe@ust.edu.ng

Received: 11-01-2022
Accepted: 30-02-2022

ABSTRACT

The Culex spp. is a vector of several disease-causing organisms including filarial parasites, encephalitis virus and the West Nile Virus; the control of these diseases is hinged on controlling the vector. Synthetic insecticides have previously been applied in the control of Culex spp. which poses a danger to the environment. In the present research, the use of light and a naturally occurring product, methanol extract of Hibiscus sabdariffa calyces (HSME), in controlling the breeding and spread of Culex tritaeniorhynochus was investigated. Third instar larvae of C. tritaeniorhynochus were fed with HSME and exposed to light for 18 hours. Results indicate over 80% mortality of the test sample with LC_{50} of 528.44 ppm; also increase in percentage mortality with corresponding increase in HSME concentration and longer irradiation time was established. The trend observed in light reactions was not seen in the control and dark reactions, implying that the presence of light and the photosensitizer (HSME) is required to induce mortality in Culex tritaeniorhynochus larvae population.

Keywords: *Culex*, Larvicide, Mosquito, Photosensitizer, Photo-larvicidal, *Hibiscus Sabdariffa*, Insecticide

INTRODUCTION

The quest for environmentally friendly larvicides and insecticides to combat the threat of mosquito-borne diseases, especially in the tropics, has accelerated in recent years. A lot of synthetic insecticides have been in use as they are very efficient in insect control. Many of them, however, have been shown to be detrimental to the environment and human health. They cause ecosystem disruptions, are harmful to a wide variety of non-target species and have a high proclivity for accumulating in the environment (Szymon *et al*., 2014). Insecticides can be classified by their mechanisms of operation as they interact with different target and non-target sites, including receptors, enzymes, and many other known and unknown molecules. Photo-insecticides can therefore be defined as those chemicals (dyes) that can exert toxicity on insects through the absorption of light of an appropriate wavelength.

When visible light encounters photosensitizers, it produces substances called photo toxins that are damaging to living cells. According to Tardivo *et al*. (2005), a photosensitizer is a substance that absorbs energy directly from a light source and then transfers it to molecular oxygen to create an activated form of oxygen called singlet oxygen ($^1O_2$). John & Jason (2000) evaluated the toxic effect of photoactive dyes, rose Bengal and phloxine B, on American and migratory grasshoppers at various concentrations. Both were found to

be effective at inducing mortality of grasshoppers when applied at 2 and 5% to bran bait. Lima *et al*. (2018) used eosin-methylene blue (EMB) as a photosensitizer for photodynamic control of *Aedes aegypti* larval populations. They subjected third instar *A. aegypti* larvae to different EMB concentrations in different light doses and found EMB as an effective photoactive compound to control larval populations.

Ulva lactuca seaweed extract was used as a reducing and capping agent in the synthesis of zinc nanoparticles (NPs) by Ishwarya *et al*. (2018) and the larvicidal activity of the *U. lactuca* fabricated ZnO NPs was tested on fourth instar *A. aegypti* larvae at 50 µg/ml within 24 h. Thandapani *et al*. (2018) fabricated TiO_2 nanoparticles by treating *P. hysterophorus* leaf extracts with TiO_4 solution and the larvicidal activity of TiO_2 NPs was studied against fourth instar larvae of *A. aegypti* and *C. quinquefasciatus.* These studies reported over 80% mortality in the populations.

Patil *et al.* (2015) used dyes from *Beta vulgaris* subsp. *Vulgaris* (beetroot) to activate the *Bacillus thuringiensis* (Bt) toxin to improve its efficiency as an insecticide. This preparation was evaluated on fourth instar *Anopheles stephensi* and *Aedes aegypti* and found to improve the larvicidal activity of the Bt toxin more than 60%. Other dyes that have been studied for their photo-insecticidal activity as enumerated by Robinson (1983) are eosin, erythrosine, and rose bengal, among others. These have been found to be effective larvicides.

The *Culex* spp. has been found to be one of the vectors for filarial parasites (Sabatinelli *et al.*, 1994), *encephalitis virus* and the West Nile Virus (Paul *et al.*, 2014). *Lymphatic filariasis* commonly called elephantiasis is a tropical, parasitic disease that affects the lymph nodes and lymph vessels, causing swelling in the legs, arms and the genitalia. In Nigeria, it is estimated that 80 to 120 million people are at risk of the disease (Hotez *et al*., 2012). Viral encephalitis is an inflammation of the brain parenchyma that is indicated by fever, headache and in extreme cases, seizures (fits), confusion, drowsiness, and loss of consciousness, and even coma (Saema & Michael, 2020). The West Nile Fever is a flavivirus (a group of single stranded RNA viruses that cause severe endemic infections and epidemics on a global scale) that has similarities with the viruses that cause St. Louis encephalitis, Japanese encephalitis, and yellow fever and infects humans, horses, and a variety of bird species. Most infected people show no symptoms, but a small percentage of them develop severe neurological disease that can be deadly.

The Illinois Department of Public Health (2017) describes the *Culex* as medium-sized mosquitoes that are brown with whitish markings on the abdomen. These are the house mosquitoes (*C. pipiens* and *C. quinquefasciatus*) that develop in urban areas, and the western encephalitis mosquito (*C. tarsalis*) that is frequently seen in rural communities. Typically active in the evenings, they bite at dusk and after dark and rest by day in and around structures and vegetation. They have a life cycle of between 10 and 4 days, or longer in chilly weather with four stages in their life cycle. These include the egg which hatches mostly within 48 hours, the larva that lives in water and develops into pupa

Scientia Africana, Vol. 21 (No. 1), April, 2022. Pp 245-252 *https://dx.doi.org/10.4314/sa.v21i1.21*
© Faculty of Science, University of Port Harcourt, Printed in Nigeria *ISSN 1118 – 1931*

within 5 days. In 2 to 3 days, the pupa develops into an adult.

Substances introduced directly to the body of water in which *Culex* mosquito larvae develop can be used to suppress them. These substances may be organisms that consume them such as larvivorous fish (Chandra *et al.,* 2013) poisonous biological substances that can cause illnesses peculiar to them and can kill them (Ramírez-Lepe & Ramírez-Suero, 2012), compounds that interfere with their development or physiology, such as methoprene -an insect growth regulator (Lawler & Lanzaro, 2005); or suffocating oils and films (Bukhari *et al*., 2011). However, oils and films also suffocate non-target aquatic life. While the insects can develop resistance to chemicals applied for their control, biological methods can be expensive to sustain.

Hibiscus sabdariffa commonly called Roselle (also known as 'zobo' in Nigeria) belonging to the family *Malvaceae,* and is widely grown in Central and West Africa, Southeast Asia and elsewhere (Cahlíkováa *et al*., 2015), was evaluated as a viable photo-larvicide to control the spread of *Culex* spp. in this study. The red calyces of the flower are consumed for their health benefits; the juice or concoction prepared from the plant is taken as a preventive and curative measure against diabetes and hypertension (Owoade *et al*., 2019).

MATERIALS AND METHODS

Reagents

Methanol and ethyl acetate used for extraction were products of Guangdong Guanghua Sci-Tech Co. Ltd, China. Distilled water was used to dissolve the extract.

Plant Material

Dried calyces of *Hibiscus sabdariffa* was purchased from the Fruit Garden Market in Port Harcourt, Nigeria. The plant was identified by Dr. J. O. Elemchukwu (Taxonomist), Department of Plant Science and Biotechnology, Rivers State University, Nigeria. It was prepared by careful separation of unwanted particles from the plant material and drying to a constant weight of 90.9 g.

Organism Used

Photo-larvicidal tests were conducted with third instar larvae of *Culex tritaeniorhynochus* harvested from natural environment by Mr. I. D. Ekerette of Malaria Vector Surveillance and Insecticide Resistance Monitoring Laboratory, Department of Animal and Environmental Biology, Rivers State University, Nigeria.

Extraction

Dried calyces of *H. sabdariffa* (90.9 g) were pulverized and sequentially extracted with ethyl acetate (300 ml) and methanol (300 ml) at room temperature (Ndukwe *et al*., 2020). The methanol extract was filtered through cotton wool and concentration to dryness using a rotary evaporator at 45 ℃ afforded 9.6 g of HSME. HSME (8 g) was dissolved in 4 L of distilled water and was considered as stock solution (2000 ppm). From the stock solution, different concentrations were prepared.

Photo-Larvicidal Test

The test was conducted (using third instar larvae of *Culex tritaeniorhynochus)* according to WHO (2005) test guidelines. The test comprises of the light and dark

reactions, each done in duplicates containing 30 third instar larvae in each test jar containing 300 ml of test photosensitizer (HSME) dissolved in distilled water and 3 ml of dissolved cabin biscuit as food. From the stock solution, different concentrations (25, 50, 100, 250 and 500 ppm) of the HSME were made for both reaction conditions as well as the control (0 ppm). Irradiation was done using a sodium-tungsten lamp (500 W) for 18 hours with temperature maintained between 28 ℃ and 30 ℃. The experiment was repeated to determine the LC_{50} with expanded concentrations of 200, 400, 600, 800 and 1000 ppm for the light set up and 200, 400, 600, 700, 800, 900 and 1000 ppm for the dark set up. The number of dead larvae was counted after 18 hours for the first test and hourly for 18 hours of exposure for the second test and expressed as percent mortality (equation 1). Larvae were considered dead when motionless and showed no response to any form of mechanical stimulus.

$$\text{Mortality}(\%) = \frac{\text{Number of dead larvae}}{\text{Number of larvae tested}} \times 100 \quad (1)$$

Data Analyses

All experiments were performed in duplicates and the percentage mortalities were calculated as an average of the duplicates. Data obtained were analyzed by one-way analysis of the variance (ANOVA) on Microsoft excel. Probit analysis was used to determine the LC_{50} value.

RESULTS AND DISCUSSION

Results as presented in Figures I, II and III show that exposure of third instar larvae of *Culex tritaeniorhynochus* to HSME and light induces mortality in the larvae. Percentage mortality of the test sample increased with increase in concentration of the photosensitizer, HSME (Figures I and II) and time of exposure to light (Figure III), which agrees with previously reported works by Souza *et al*. (2017) and Mezzacappo *et al*. (2021). This trend is absent in the control as well as in the dark reactions. The implication is that even with the presence of a photosensitizer, light is required to induce mortality in the population. It also implies that even when light is present, a photosensitizer is also required for mortality to be induced in the population. The lethal concentration at which 50 % of the test samples die (LC_{50}) was determined using probit analysis to be 528.44 ppm. The number of deaths recorded in the dark reaction can be attributed to handling and preparation as Tielong Xu *et al*. (2014) reported that mosquito sample collection and preparation methods significantly affected mortality rates in the standard WHO tube resistance bioassay. Because sunlight is one of the most crucial factors in its effectiveness, employing photosensitive materials like HSME to eliminate *Culex* spp. larvae can be regarded as safe and low-cost alternative, especially given the abundance of *Hibiscus sabdariffa* calyces within the environment at photo-chemically active doses. According to Fabris *et al*. (2012), photogenerated cytotoxic intermediates often act through a multi-target method, causing damage to a wide variety of cell constituents (such as proteins, unsaturated lipids, and steroids) at the same time. As a result, unlike most chemical insecticides, HSME and visible light work together to limit the chances of the larvae developing resistance.

Scientia Africana, Vol. 21 (No. 1), April, 2022. Pp 245-252 *https://dx.doi.org/10.4314/sa.v21i1.21*
© Faculty of Science, University of Port Harcourt, Printed in Nigeria *ISSN 1118 – 1931*

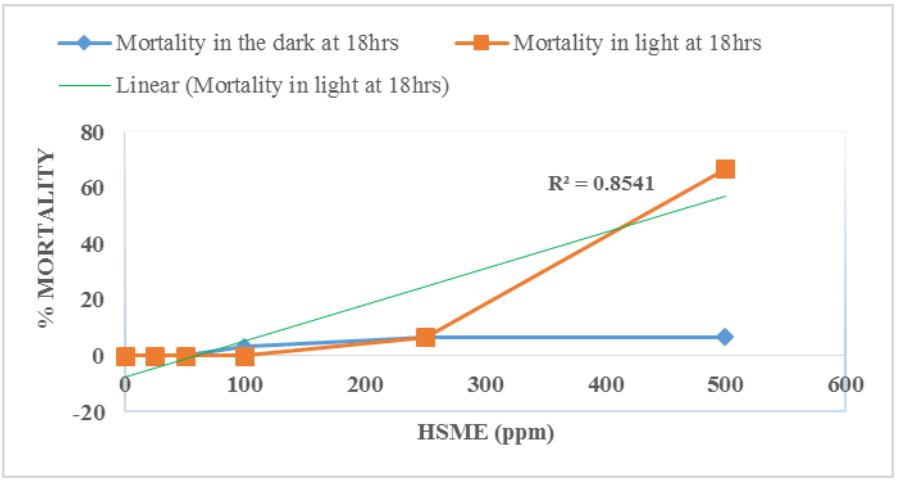

Figure I: Photo-larvicidal Activity of HSME

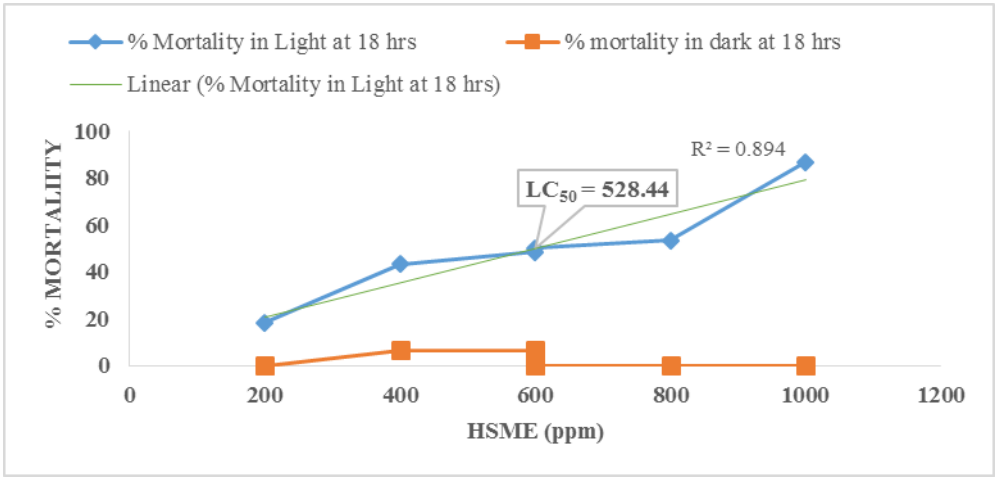

Figure II: Dependence of Mortality on Concentration of HSME

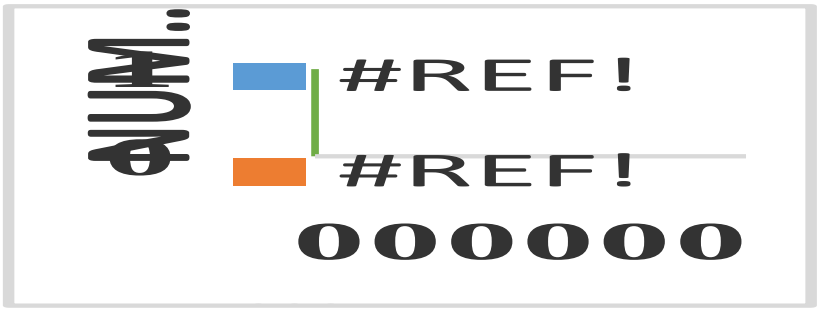

Figure III: Mortality Dependency on Irradiation Time and HSME Concentration

CONCLUSION

The findings of this study have shown the effectiveness of *Hibiscus sabdariffa* calyces as a good photo-larvicide. Using plant extract such as *Hibiscus sabdariffa* to control mosquito population at the larval stage in the environment can have a wide range of benefits for vector control and management.

Acknowledgement

The authors acknowledge the Malaria Vector Surveillance and Insecticide Resistance Monitoring Laboratory of the Department of Animal and Environmental Biology, Rivers State University, Nigeria for harvesting and selecting the *Culex tritaeniorhynchus* larvae used in this work.

REFERENCES

Bukhari, T., Takken, W., Githeko, A. & Koenraadt, C. (2011). Efficacy of Aquatain, a monomolecular film, for the control of malaria vectors in rice paddies. PloS One 6. *PLoS ONE*, *6*(6), e21713. doi: https://doi.org/10.1371/journal.pone.0021713

Cahlíkováa, L., Alib, B., Havlíkovác, L., Ločáreka, M., Siatkad, T., Opletala, L. & Blunden, G. (2015). Anthocyanins of *Hibiscus sabdiffera* Calyces from Sudan. *Natural Products Communications*, *10*(1), 77-79.

Chandra, G., Ghosh, A., B. I. & Ghosh, S. (2013). *Use of larvivorous fish in biological and environmental control of disease vectors.* (M. Cameron, & L. Lorenz, Eds.) UK: CABI.

Fabris, C., Ouédraogo, R., Coppellotti, O., Dabiré, R., Diabaté, A., Di Martin, P. & Habluetzel, A. (2012). Efficacy of sunlight-activatable porphyrin formulates on larvae of *Anopheles gambiae* M and S molecular forms and *An. arabiensis*: A potential novel biolarvicide for integrated malaria vector control . *Acta Tropica , 123*, 239-243.

Hotez, P., Asojo, O. & Adesina, A. (2012). Nigeria: "Ground Zero" for the High Prevalence Neglected Tropical Diseases. *PLoS Negl Trop Dis, 6*, e1600.

Illinios Department of Public Health. (2017, March 29). *Prevention and Control - Mosquitoes and Diseases*. Retrieved from Envronmental Health: http://www.idph.state.il.us/envhealth/pcmosquitoes.htm

Ishwarya, R., Vaseeharan, B., Kalyani, S., Banumathi, B. G., Alharbi, N. K., N.Al-anbr, M. & Benelli, G. (2018). Facile green synthesis of zinc oxide nanoparticles using *Ulva lactuca* seaweed extract and evaluation of their photocatalytic, antibiofilm and insecticidal activity. *Journal of Photochemistry and Photobiology B: Biology*, *178*, 249-258. doi: https://doi.org/10.1016/j.jphotobiol.2017.11.006

John, L. C. & Jason, M. S. (2000). Insecticidal Activity of Photoactive Dyes to American and Migratory Grasshoppers (*Orthoptera: Acrididae*). *Journal of Economic Entomology , 93*(3), 662-666.

Lawler, S. & Lanzaro, G. (2005). Managing Mosquitoes on the Farm. *ANR Publication*, 8158. Retrieved July 29, 2021, from http://anrcatalog.ucdavis.edu/pdf/8158.pdf

Lima, A. R., Cicera, M. S., Caires, C. S., Esmael, D. P., Luciana, R. P., Isaias,

Scientia Africana, Vol. 21 (No. 1), April, 2022. Pp 245-252 *https://dx.doi.org/10.4314/sa.v21i1.21*
© Faculty of Science, University of Port Harcourt, Printed in Nigeria *ISSN 1118 – 1931*

C. & Anderson, R. L. (2018). Evaluation of eosin-methylene blue as a photosensitizer for larval control of *Aedes aegypti* by a photodynamic process. *Insects*, *9*(3), 109. doi: https://doi.org/10.3390/insects9030109

Mezzacappo, N. F., Souza, L. M., Inada, N. M., Dias, L. D., Garbuio, M., Venturini, F. P. & Bagnato, V. (2021). Curcumin/d-mannitol as photolarvicide: induced delay in larval development time, changes in sex ratio and reduced longevity of *Aedes aegypti*. *Pest Management Science*, *77*(5), 2530-2538. doi: https://doi.org/10.1002/ps.6286

Ndukwe G. I., Clark P. D. & Jack I. R. (2020). In vitro antioxidant and antimicrobial potentials of three extracts of *Amaranthus hybridus* L. leaf and their phytochemicals. *European Chemical Bulletin*, 9(7):164-173. doi: http://dx.doi.org/10.17628/ecb.2020.9.164-173

Owoade, A., Adetutu, A. & Olorunnisola, O. (2019). A review of chemical constituents and pharmacological properties of *Hibiscus sabdariffa L*. *International Journal of Current Research in Biosciences and Plant Biology*, *6*(4), 42-51.

Patil, C., Rahul, S., Hemant, B., Chandrankant, N., Bipinchandra, S., & Satish, P. (2015). Maintenance of residual activity of Bt toxin by using natural and synthetic dyes: a novel approach for sustainable mosquito vector control. *Natural Products Research*, *29*(24), 2350-2354. doi: https://doi.org/10.1080/14786419.2015.1013956

Paul, R., NgRoy, F., HallDavid, A., SmithCheryl, W. & A, J. (2014). Arbovirus Infections. In R. Y. Paul, F. NgRoy, A. HallDavid, W. SmithCheryl, J. A, F. Jeremy, J. H. Peter, J. Thomas, K. Gadandeep, L. David, & J. W. Nocholas (Eds.), *Manson's Tropical Infectious Diseases* (23 ed., pp. 129 -161). Amsterdam: Elsevier Ltd.

Ramírez-Lepe, M., & Ramírez-Suero, M. (2012). Biological control of mosquito larvae by *Bacillus thuringiensis subsp. Israelensis*. In F. Parveen, *Insecticides- Pest Engineering* (pp. 239-244). Mexico: IntechOpen. doi: DOI:10.5772/29139

Robinson, J. (1983). Photodynamic insecticides: A review of studies on photosensitizing dyes as insect control agents, their practical application, hazards, and residues. In F. Gunther, & G. F.A (Ed.), *Residue Reviews* (Vol. 88, pp. 66-100). New York: Springer. doi: https://doi.org/10.1007/978-1-4612-5569-7

Sabatinelli, G., Ranieri, E., Gianzi, F., Papakay, M. & Cancrini, G. (1994). Role of *Culex quinquefasciatus* in the transmission of *bancroftian filariasis* in the Federal Islamic Republic of Comoros (Indian Ocean). *Parasite, 1*(1), 71-76.

Saema, S. & Michael, K. (2020, August 10). *Viral Encephalitis.* Retrieved from National Center for Biotechnology Information, U.S. National Library of Medicine: https://www.ncbi.nlm.nih.gov/books/NBK470162/

Souza, L., Inada, N., Pratavieira, S., Corbi, J., Kurachi, C. & Bagnato, V. (2017). Efficacy of Photogem®

(Hematoporphyrin Derivative) as a Photoactivatable Larvicide against *Aedes aegypti* (*Diptera: Culicidae*) Larvae. *Journal of Life Sciences, 11*, 74-81. doi: doi:10.17265/1934-7391/2017.02.003

Szymon, C., Milena, K., Paweł, M. & Grzegorz, R. (2014). Synthetic Insecticides – is There an Alternative? *Polish Journal of Environmental Studies, 23*(2), 291 - 302.

Tardivo, J., Oliveira, C., Giglio, A., Gabrielli, A., Junquira, H., Tada, D. & Turchiello, R. (2005). Methylene blue in Photodynamic therapy: from basic mechanisms to clinical applications. *Photodiagnosis and Photodynamic therapy, 2*, 175-191.

Thandapani, K., Kathiravan, M., Namasivayam, E., Padiksan, I., Natesan, G., Tiwari, M. & Perumal, V. (2018). Enhanced larvicidal, antibacterial, and photocatalytic efficacy of TiO2 nanohybrids green synthesized using the aqueous leaf extract of *Parthenium hysterophorus* . *Environmental Science and Pollution Research, 25,* 10328-10339. doi: https://doi.org/10.1007/s11356-017-9177-0

Tielong Xu, 1. D., Xuelian, C., Fengyang, F., Guiyun, Y. & Bin, Z. (2014). *Anopheles sinensis* mosquito insecticide resistance: comparison of three mosquito sample collection and preparation methods and mosquito age in resistance measurements. *Parasites and Vectors, 7*(54), 54. doi: https://dx.doi.org/10.1186%2F1756-3305-7-54

WHO. (2005). Guidelines For Laboratory and Field Testing of Mosquito Larvicides. *World Health Organization Communicable Disease Control, Prevention and Eradication WHO Pesticide Evaluation Scheme* . Geneva: WHO.

Scientia Africana, Vol. 21 (No. 1), April, 2022. Pp 253-266 *https://dx.doi.org/10.4314/sa.v21i1.22*
© Faculty of Science, University of Port Harcourt, Printed in Nigeria *ISSN 1118 – 1931*

INVESTIGATION OF SOIL CONTAMINATION IN A LUBRICANT RETAIL MARKET IN IKOKU, PORT HARCOURT, NIGERIA.

Obioma, E. Dike O.[1], *Duru, U. Remy[2]
[1]Department of Industrial Chemistry, Madonna University, Elele, Nigeria
[2]Department of Pure and Industrial Chemistry, University of Port Harcourt, Nigeria
remy.duru@uniport.edu.ng

Received: 12-11-2021
Accepted: 20-02-2022

ABSTRACT

The physicochemical properties, total polycyclic aromatic hydrocarbons (PAH) concentration as well as that of lead, zinc, chromium, cadmium and arsenic in soil obtained from a lubricant retail market were determined. The PAHs, lead, chromium and zinc concentrations were found to be higher in comparison to the soil samples obtained from a typical residential area 2 km away. The average values for total PAH concentration in the sample soil were 3.76 /4.70 mg kg^{-1} (topsoil/subsoil). The values for the control (topsoil/subsoil) were 0.189/ 0.286 mg kg^{-1}. The average concentrations of lead, zinc, chromium and cadmium in the sample (top-soil/ sub-soil) were 3.70/ 3.85, 9.7/9.69, 197.29/82.18 and 7.42/3.35 mg kg^{-1} respectively while in the same order, their values in the control gave 0.75/0.94, 8.86/9.40, 103.66/59.50 and 4.08/0.87 mg kg^{-1}. The sample soil also showed an increase in some physicochemical parameters such as Total Organic Carbon (TOC), sulphate and nitrate contents as well conductivity both in the topsoil and the subsoil.

Keywords: Soil contamination; Lubricant retailing market; Polycyclic aromatic hydrocarbons; Heavy metals.

INTRODUCTION

Lubricants are substances placed between the contact surfaces of solid moving parts, for the primary purpose of reducing friction and wear. They also carry out other functions such as removal of heat, corrosion prevention, transfer of power, providing a liquid seal at moving contacts and suspension and removal of wear particles (Dorinson and Ludema, 1985; Boyde, 2002; Nowak *et al*. 2019). Most lubricants are 95% oil-based which may be natural, mineral or synthetic depending on their applications, (Lu and Kaplan, 2008; Stachowiak and Batchelor, 1993); However, a lubricant may be graphite, or any substance- gas, liquid, semisolid, or solid that permits free action of mechanical devices and prevents damage by abrasion and seizing of metal or other components through unequal expansion caused by heat.

The increased use of machinery in various areas of human activities has led to an increase in the demand and production of lubricants and consequently, an increased contribution to environmental pollution. Due to its low cost and a wider range of applications, mineral oil-based lubricants are readily available. Contaminants resulting from the use of lubricants are either inherited from the crude oil feedstock or were components of the lubricant formulations. Lead naphthenates, for example, is employed as an extreme pressure additive while mild corrosion of components of certain machinery

components can be the source of metal contaminants such as copper, cadmium etc. (Stachowiak and Batchelor, 1993). Lubricants, therefore, pose similar environmental problems similar to hydrocarbons when substantial quantities are deposited in the biota (Vazquez-Duhalt, 1989; Wang *et al*., 2000; Syahir *et al*., 2017).

Like most products of crude oil, the mineral oil used for the production of lubricating oils contains compounds such as aromatic and polycyclic aromatic hydrocarbons (PAHs), heteroatomic compounds, paraffins, naphthenes and heavy metals which could act as pollutants once their permissible range in an ecosystem is exceeded. Their sources of entry into the environment have been identified as spills, deliberate disposal, leakages at the retail outlets and mishandling of fresh and used products (Nespeca *et al*., 2018). It can also be from the operation of devices and machinery that use lubricants, such as two-stroke engines, open chain saws and agricultural equipment (Betton 2010; Nowak *et al*., 2019). Betton (2010) specifically stated that only 32% of total lubricants produced in Europe is 'successfully disposed of' by burning and recycling. He concluded that the greater percentage enters the environment in one way or the other in the course of 'consumption'.

Fresh and used lubricating oils contain a variety of aliphatic, aromatic and polycyclic aromatic hydrocarbons (PAHs). PAHs are classes of persistent organic pollutants made up of multiple carbon ring structures. These compounds have become a global concern owing to their persistence in the environment and have been listed as priority pollutants by both the US Environmental Protection Agency (EPA) and European Union (EU) due to their carcinogenic and mutagenic properties (Tang, et al, 2005; Aichner *et al*., 2007). Polycyclic aromatic hydrocarbons are perhaps the most common contaminant that has been associated with both used and unused lubricating oils which has been investigated by several researchers (Wang et al 2000; Obini *et al*., 2013; Rengarajan et al., 2015; Ekanem and Ogunjobi 2017; Wu et al., 2017; Mao et al., 2020).

Several studies have profiled the negative impact of lubricating oil in both plants (soil) (Vwioko *et al*., 2006; Agbogidi, 2009; Stephen *et al*., 2013; Ekanem and Ogunjobi, 2017; Hazim and Al-Ani, 2018; Nyarko *et al.*, 2019; Nwachukwu *et al*., 2020) and aquatic ecosystems.

Although different strains of bacteria have been identified to appreciably degrade contaminants associated with lubricating oils or the source crude oil (Lopes *et al*., 2010; Ramadan, 2012; Ron and Rosenberg 2014; Raju et al 2017), none is 100% efficient as they only reduce the contaminants without guaranteeing a reduction in toxicity (Saterbak *et al*., 2000). More so, some of the products of biodegradation may yield harmful secondary contaminants that are more eco-toxic than their precursors (Plaza *et al*., 2005; Aruyor and Ori-jesu, 2009). Soroldoni and his co-workers (2019) in particular, reported the extent of toxicity of spent lubricant oil-contaminated soil to *Eisenia andrei* after 22 months of bioremediation.

From the foregoing, it is evident that the most adequate method of protecting the environment from the harmful effects of

Scientia Africana, Vol. 21 (No. 1), April, 2022. Pp 253-266 *https://dx.doi.org/10.4314/sa.v21i1.22*
© Faculty of Science, University of Port Harcourt, Printed in Nigeria *ISSN 1118 – 1931*

lubricants is by avoiding or minimising spills, disposals and leakages.

This study aims at investigating the soil contents of a local lubricant retailing market; Ikoku, Port Harcourt, Nigeria, for pollutants and comparing same with a typical residential area. It is believed that the activities in this market have impacted negatively on the surrounding soils and may eventually sip to underground water or nearby farmlands.

MATERIALS AND METHODS

The Study Area: Ikoku lubricant retail market is one of the commercial establishments in Port Harcourt, Nigeria, and has been in operation for more than 30 years. Although with lock-up shops, several drums of lubricating oils both filled and empty are always stacked in the available open spaces. The marketers make transfer of the liquid contents in the open with attendant spills. Some auto spare parts (both new and fairly used) shops are also located within this vicinity.

The study area lies within longitude 6^0 58' 30" E through longitude 7^0 1' 30" E and Latitude 40 43' 30" N through latitude 40 54' 30" N (Figure 1).

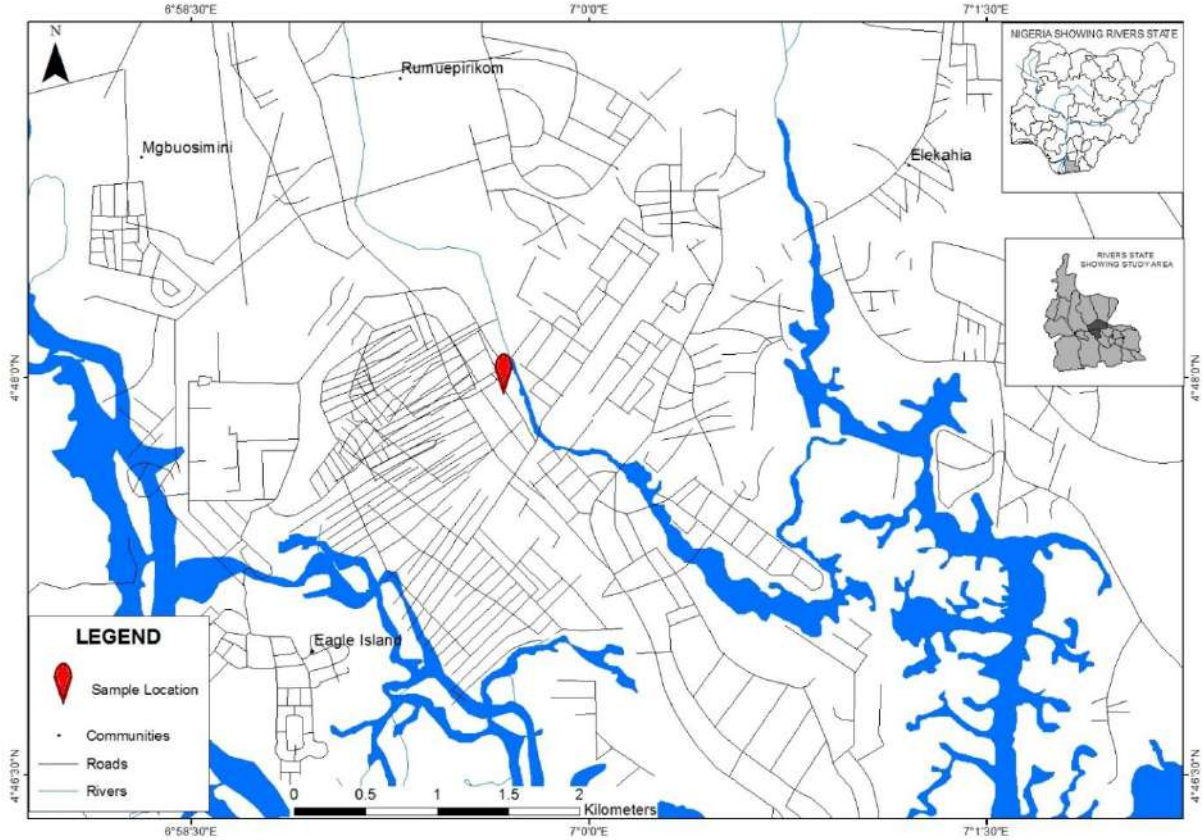

Figure 1: Sample location map

Soil Sampling and Pretreatment

Twelve samples were collected using an improvised auger from the three corners of a virtual triangular mapping of the two

sites (six samples from each); the lubricant market and a residential area that is 2 km away. Each corner was analyzed and random points picked. Two composite samples from each site were prepared; one, by mixing the three samples from the surface or topsoil of the three corners and the other by mixing the subsoil (7-15cm depth) of the three corners. The composite samples were collected in polyethylene bags and labelled S_T and S_S representing the topsoil and the subsoil respectively from the lubricant market site and C_T and C_S representing that from the control site. Samples were air-dried by spreading in an open airy space for 3 days with occasional stirring to expose fresh surfaces for proper drying. Before analysis, samples were further demagnetized, ground and sieved.

Instrumentation

Jenniary Digital pH, Hama Instruments Hi 83200 multiparameter bench photometer, GBC sensAA Atomic Absorption Spectrophotometer (AAS) and Agilent Technologies 7890A Gas chromatograph.

Physicochemical Parameters of Soil

The pH, conductivity, moisture, nitrate, sulphate and phosphate contents were determined at the Chemistry Department of the University of Port Harcourt using standard laboratory procedures (reference). TOC, the concentration of heavy metals and PAHs were conducted at International Energy Services Limited, Port Harcourt.

The samples were prepared for AAS by weighing the dried (2 g) into a digestion flask and adding an acid mixture (20 ml) containing concentrated nitric acid (HNO_3) (650 ml), Perchloric acid ($HClO_4$) (80 ml) and concentrated sulphuric acid (H_2SO_4) (20ml). The flask was then heated until a clear digest is obtained. Distilled water (50ml) was added to dilute the digested sample and then filtered using No. 42 Whatman filter paper into a 250 ml flask and made up to the mark with distilled water. Afterwards, appropriate dilutions were made for each element. The sample is thoroughly mixed by shaking and 100 ml was transferred into a glass beaker of 250 ml volume. The sample is aspirated into the oxidizing air-acetylene flame. When the aqueous sample is aspirated, the sensitivity for 1% absorption is observed in a GBC sensAA Atomic Absorption Spectrophotometer (AAS)

For the PAHs determination, each sample (5 g) was extracted with 100 ml of solvent (Hexane & dichloromethane 1:1 v/v) in a Soxhlet apparatus. After 16 hours of extraction, the contents of the flask were filtered and evaporated by a rotatory vacuum evaporator. The dried residue was resuspended into 2.5 ml of methanol and passed through a 5 cm anhydrous sodium sulphate column to remove moisture. The PAH contents in each soil sample were measured by reverse phase HPLC analysis.

Briefly, the 20 µl of the methanol soil extracts were injected into an HPLC system fitted with a 5 µm particle diameter C18 column. The elution gradient was programmed as follows [shown as percent (by volume) of methanol in water, acidified with 0.76 ml of H_3PO_4 per liter]: 50% for 2min, linear gradient to 80% at 5% per min, holding at 80^oC for 16 min. The flow rate was kept at 1 ml/min. Peaks were measured at 254 nm. Concentrations of PAHs were calculated by comparing peak areas of sample chromatogram with that of peak area of standard chromatogram.

Scientia Africana, Vol. 21 (No. 1), April, 2022. Pp 253-266 *https://dx.doi.org/10.4314/sa.v21i1.22*
© Faculty of Science, University of Port Harcourt, Printed in Nigeria *ISSN 1118 – 1931*

RESULTS AND DISCUSSION

Physicochemical Analysis

The physicochemical parameters of the samples are summarized in Table 1. The mean pH values for the site under study are 6.3 for the topsoil (S_T) and 5.6 for the subsoil (S_S). While that for the control soils are 6.6 for the topsoil (C_T) and 6.2 for the subsoil (C_S), indicating a slight increase in acidity of the soil from the lubricating oil market. The lower pH of 5.6 in the Ss sample is an indication of a mildly acidic soil. In their separate works, Njoku *et al*., (2008) and Johan *et al*., (2020) had linked decrease in soil pH to oil pollution.

Table 1: Physicochemical parameters of soil samples

S/N	PARAMETERS	C_T	C_S	S_T	S_S
1	PH	6.6	6.2	6.3	5.6
2	CONDUCTIVITY (µs/cm)	71	89	152	209
3	NITRATE (mg/kg)	18.5	19.4	32.5	47.6
4	PHOSPHATE(PO_4^{3-}) (mg/kg)	43.5	22.5	14.7	19.5
5	PHOSPHORUS(P) (mg/kg)	14	7.5	4.8	6.4
6	PHOSPHATE(P_2O_5) (mg/kg)	32.5	17	11	14.6
7	SULPHATE (mg/kg)	0	0	40	20
8	MOISTURE CONTENT (%)	3.2	4.4	3.6	8.6
9	ORGANIC CARBON (%)	8.9	7.93	10.52	10.16

C_T = Control TopSoil; C_S = Control SubSoil; S_T = Sample TopSoil; S_S = Sample SubSoil

Increased mean conductivities for the samples from the site under study was observed (152µs/cm and 209µs/cm respectively for the topsoil and the subsoil) when compared to their respective values of 71µs/cm and 89us/cm for the control soil samples. The trend is the same for TOC, 10.52% and 10.16% for the soil under investigation, against 8.9% and 7.93% for the control samples. However, according to Arshi and Khan (2018), both the conductivity and TOC values in the control and site samples are higher than the standard values (2.0 µs/cm and 1.0% respectively) required for normal plant activities.

The mean nitrate contents of the soil samples from the lubricating oil market are 32.5 mg/kg for the topsoil and 47.6mg/kg for the subsoil. These are high values compared to the mean values for the control soil samples which are 18.5mg/kg for the topsoil and 19.4mg/kg for the subsoil. This is contrary to an expected increase in nitrate concentration due to the hydrocarbon-degrading activities of indigenous micro-organisms as observed in a work with crude oil (Devatha *et al*., 2019). However, it was established in another investigation, that the percentage of biodegradation of hydrocarbons is less in lubricating oils (used or unused) when compared with kerosene and diesel. Also, the higher nitrate level in the contaminated soil could be due to a high concentration of the contaminants which can be inhibitory to microorganisms by toxic effects (Ijah and Antai, 2003; Abioye *et al*., 2012)

The mean moisture contents for the samples from the site under study are 3.6% for the topsoil and 8.6% for the subsoil, which is high compared to that of the

control soil samples (3.2% and 4.4% for the topsoil and the subsoil respectively). These values are shown pictorially in Appendix A. Some related earlier investigations that have to do with crude oil contamination reported decreases in moisture content with increasing crude oil contamination (Ghouse *et al*., 1980; Devatha *et al*., 2019). The variation could be attributed to not only the other additives in lubricating oils but to the fact that the site of investigation is full of human activities, enough to thoroughly homogenize the oil and water content of the soil unlike in those reported cases. As such, the oil films will form barriers that would rather reduce the natural evaporation and sipping-down of the soil water.

The mean phosphate (PO_4 3^-)/Phosphorus (P)/ Phosphate (P_2O_5) for the soil samples from the Ikoku market are 14.7/4.8/11mg/kg respectively for the topsoil, 19.5/6.4/14.6mg/kg for the subsoil. These are much lower than the control samples collected from a location that is 2 Km away which are 43.5/14/32.5mg/kg for the topsoil and 22.5/7.5/17mg/kg for the subsoil. The decrease may be attributed to microbial metabolism as posited by Margesin and Schinner (2001).

The mean sulphate values for the site under study are 40mg/kg for the topsoil and 20mg/kg for the sample subsoil compared to the controls soils which null values for both the top and subsoils. This could be attributed to the high level of contamination of the soil with lubricating oil. Mangas *et al*., 2014) had posited that lubricating oils deteriorate as they become contaminated and undergo chemical changes by oxidation, with acidic materials as the major products.

Heavy Metals

Table 4.2 shows the values for the concentration of heavy metals for the sampling locations. The mean concentrations for Lead (Pb) are 3.70ppm and 3.85ppm for the sample topsoil and subsoils respectively. While the mean concentration of Lead (Pb) for the control samples were lower at 0.75ppm and 0.94ppm for the control topsoil and subsoils respectively.

Table 2: Heavy Metal Content of Soil Samples

S/N	Metals	Concentrations (mg kg^{-1})			
		C_T	C_S	S_T	S_S
1	Lead	0.75	0.94	3.70	3.85
2	Zinc	8.86	9.41	9.71	9.69
3	Arsenic	0.00	0.00	0.00	0.00
4	Chromium	103.66	59.5	197.29	82.18
5	Cadmium	4.08	0.87	7.42	3.35

Chromium and cadmium also exhibited higher levels of concentration in the site sample 197.29/82.18 mg kg^{-1} and 7.42/ 3.35 mg kg^{-1} respectively for the topsoil/subsoil. Their respective values in the control are 103.66/ 59.5 for chromium and 4.08/ 0.87 mg kg^{-1} for cadmium. Zinc also exhibited higher levels, with 9.71 mg

Scientia Africana, Vol. 21 (No. 1), April, 2022. Pp 253-266 *https://dx.doi.org/10.4314/sa.v21i1.22*
© Faculty of Science, University of Port Harcourt, Printed in Nigeria *ISSN 1118 – 1931*

kg^{-1} and 9.69 mg kg^{-1} for the sample top soil and subsoil respectively, while the control showed lower levels of 8.86 mg kg^{-1} and 9.41 mg kg^{-1} for the control topsoil and subsoils respectively. Arsenic showed zero concentration for all the samples. The respective World Health Organization target value concentrations in soil for lead, cadmium, zinc and chromium is 85, 0.8, 50 and 100 mg/Kg (W.H.O., 1996). The lubricant retail market can therefore be said to be contaminated with respect to cadmium and chromium.

Appendix B is an illustration of the concentration values of the metal with a histogram.

PAH

The total PAH levels for the soil samples collected at the lubricant retailing market was 3.757mg/kg for the topsoil and 4.696mg/kg for the subsoil which in turn is higher than those of the control samples which are 0.189mg/kg for the topsoil and 0.286mg/kg for the subsoil (Figure 1). This indicates an increase in the level of poly aromatic hydrocarbons, which in turn is due to the improper handling and disposal of lubricants in the market. The European classification system of soil contamination graded total PAHs concentration of 0.6–1 mg/kg as moderately polluted and over 1 mg/kg as heavily polluted (Maliszewska-Kordybach, 1996).

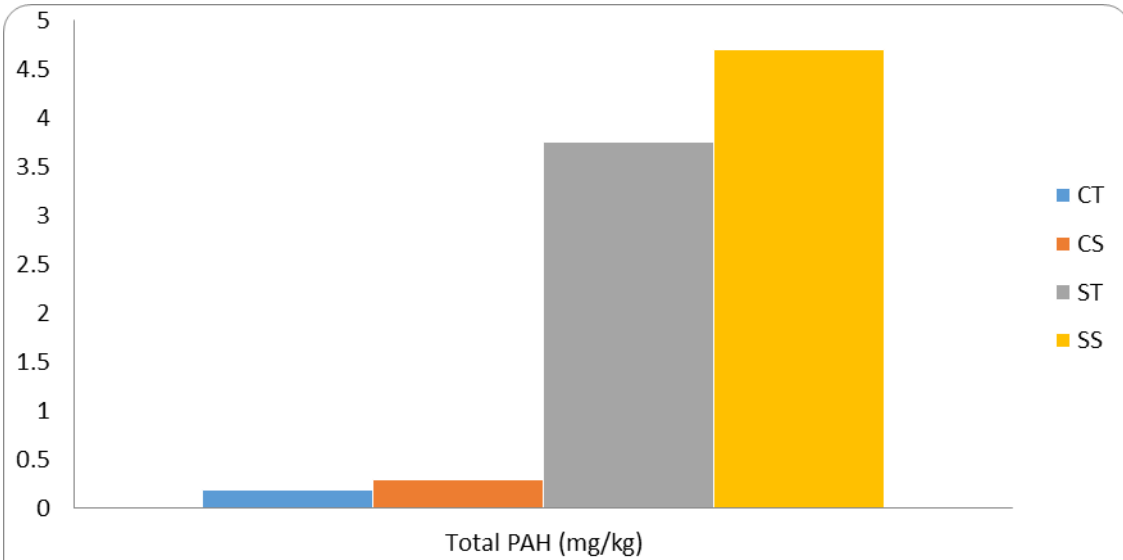

Fig 1: A histogram illustrating the total levels of PAH in the sample and control soils

The various PAHs and their concentrations are shown in Figure 2. Flouranthene showed the highest concentration of PAHs in all the soil samples. Flourene, Anthracene Benzo (a) Pyrene and Acenaphthene also showed high presence while Benzo (g,h,i) Perylene, Indeno (1,2,3-cd) Pyrene and Dibenzo (a,h) Anthracene made negligible contributions to the total PAH concentration.

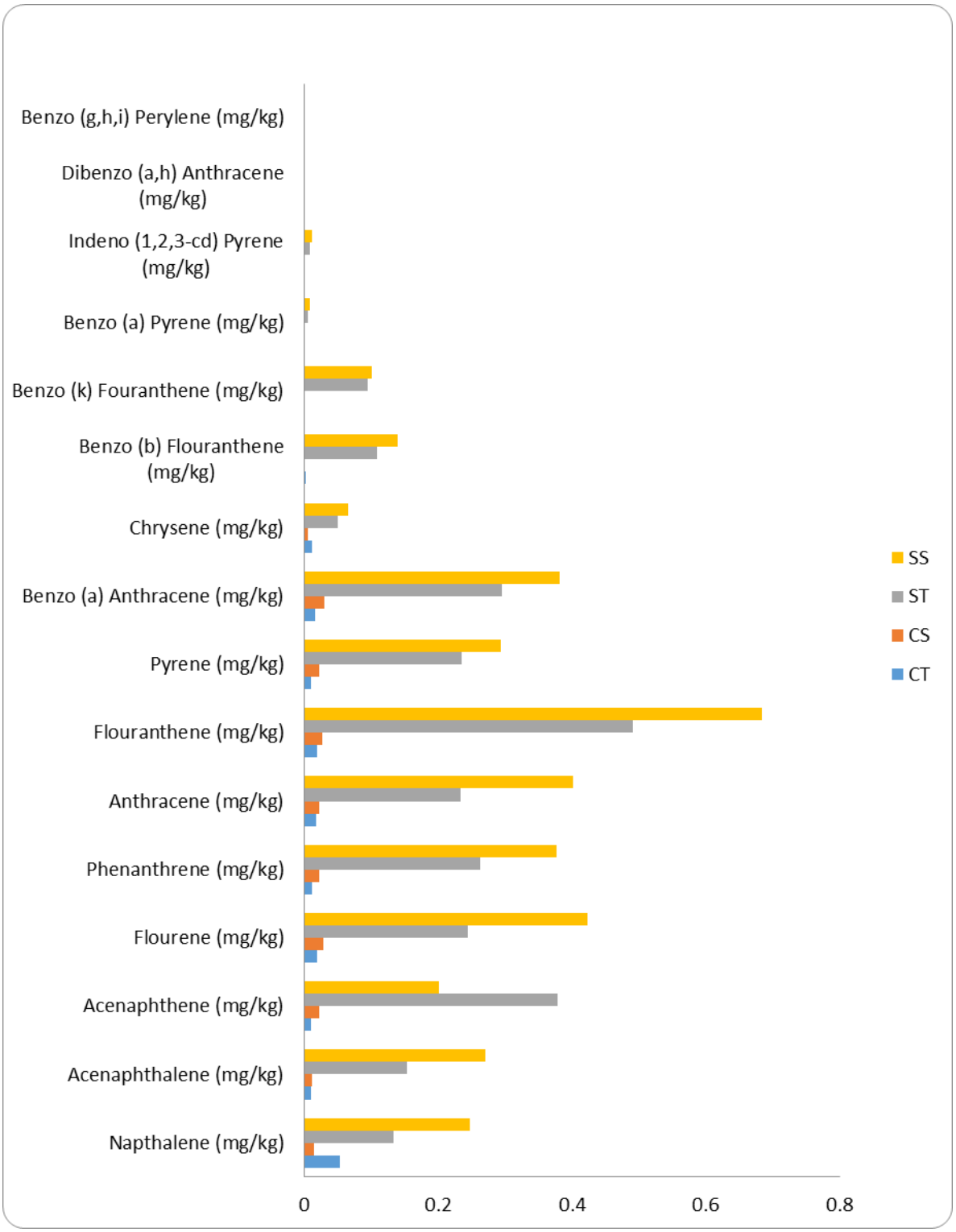

Figure 2: Various PAH Contents of the Soil Samples

Scientia Africana, Vol. 21 (No. 1), April, 2022. Pp 253-266 *https://dx.doi.org/10.4314/sa.v21i1.22*
© Faculty of Science, University of Port Harcourt, Printed in Nigeria *ISSN 1118 – 1931*

APPENDIX A: A Histogram illustrating the physicochemical properties and their level in both the sample and control soils

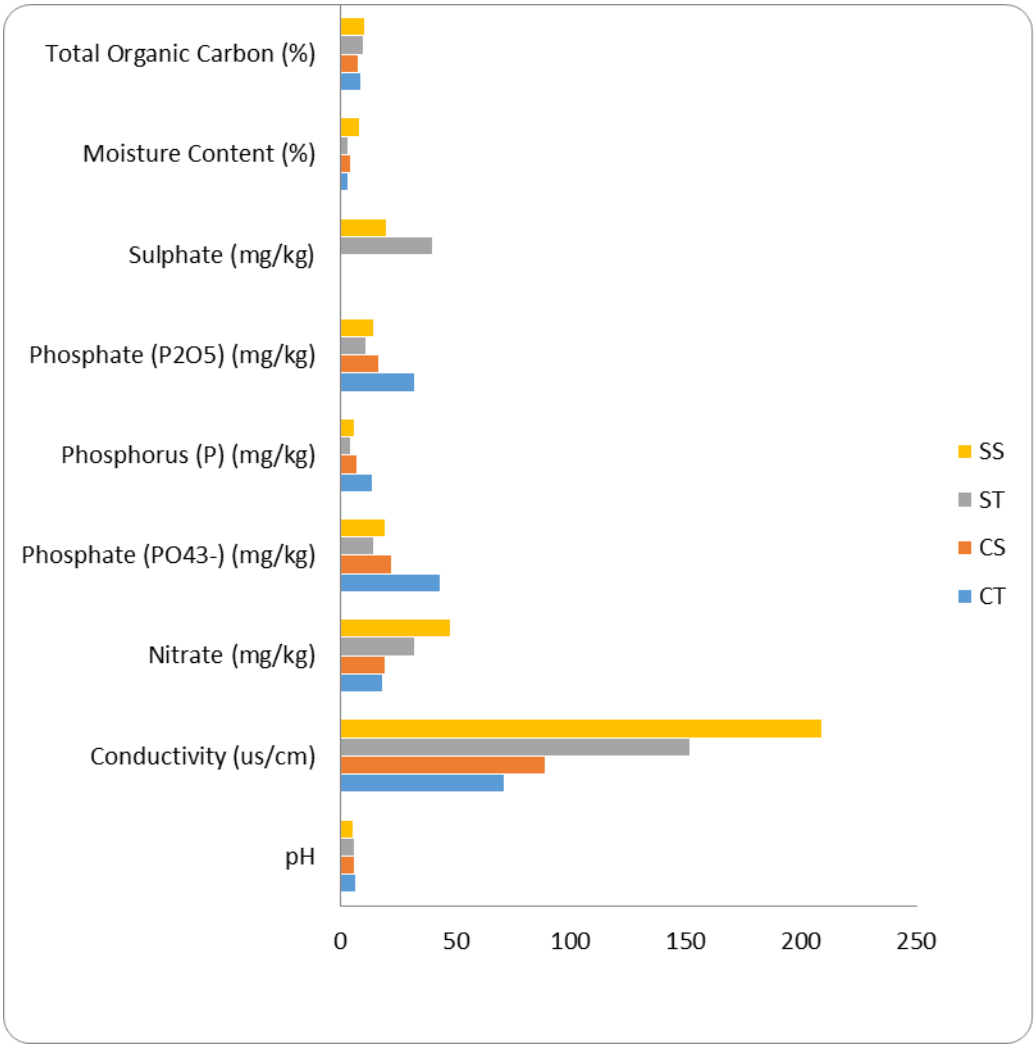

APPENDIX B: A Histogram illustrating levels of heavy metals in the sample and control

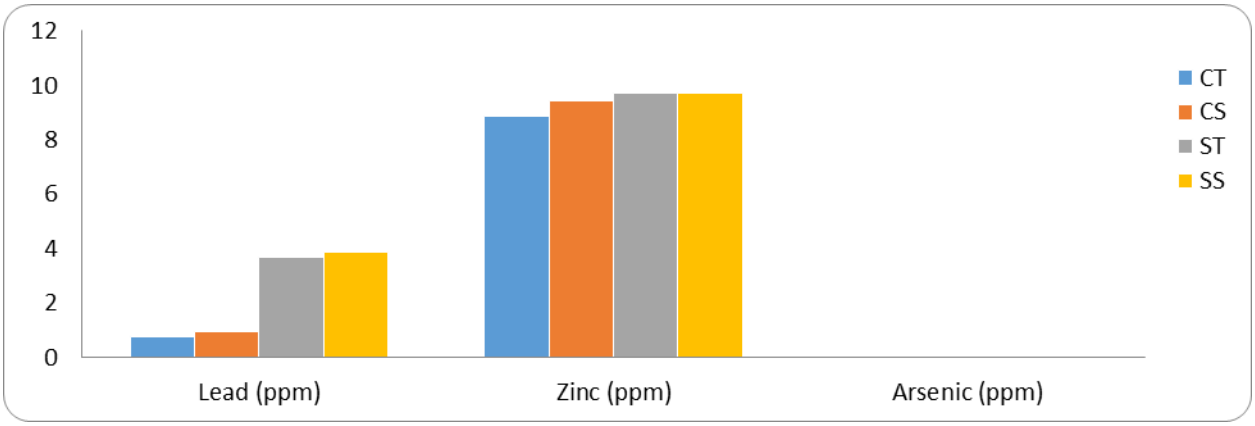

CONCLUSIONS

The physicochemical properties of soil sampled from Ikoku lubricant market indicate some alterations. Increased levels are seen in the conductivities, TOC nitrates and sulphate contents which are typical of hydrocarbon contamination. Also, the recorded decreases were seen in the pH and phosphate contents when compared with the control sample. Neither the increased nor the decreased properties seemed desirable for normal plant life. The total PAH concentration, the values cadmium and chromium are all indicators of polluted soil. The activities in the lubricant retailing market are the most likely source of the differences in the values of these parameters in the site and control soil samples. The implication is that these toxic compounds and elements could be washed off to nearby farmlands or sipped down to underground water with the attendant consequences.

REFERENCES

Abioye, O., Agamuthu, P.1., AbdulAziz, A. (2012). Biodegradation of used motor oil in soil using organic waste Amendments. *Biotechnology Research International*. 2012, 1-8

Agbogidi, O. M. (2015). Effects of soil contaminated with spent lubricating oil on the germination of Gmelina arborea (Roxb.) seeds. *African journal of natural sciences (ajns)* issn 1119-1104, 12.

Aichner, B., Glaser, B. and Zech, W. (2007). Polycyclic aromatic hydrocarbons and polychlorinated biphenyls in urban soils from Kathmandu, Nepal. *Organic Geochemistry,* 38:200-715.

Iram, A. and Khan, T. (2018). Analysis of Soil Quality Using Physico-Chemical Parameters with Special Emphasis on Fluoride from Selected Sites of Sawai Madhopur Tehsil, Rajasthan. *International Journal of Environmental Science & Natural Resources* 12(5): 555847. DOI: 10.19080/IJESNR.2018.12.555847.

Betton, C. I. (2010). Lubricants and their environmental impact. In *Chemistry and technology of lubricants* (pp. 435-457). Springer, Dordrecht. https://doi.org/10.1023/b105569_15

Boyde, S. (2002). Green lubricants. Environmental benefits and impacts of lubrication. *Green Chemistry* 4:293-307

Devatha, C. P., Vishal, A. V., & Rao, J. P. C. (2019). Investigation of physical and chemical characteristics on soil due to crude oil contamination and its remediation. *Applied Water Science*, *9*(4), 1-10.

Dorinson, A. and Ludema, K.C., 1985. Mechanics and chemistry in lubrication (Vol. 9). Elsevier

Ekanem, J. O. and Ogunjobi, A. A. (2017). Hydrocarbon Degradation Potentials of Bacteria Isolated from Spent Lubricating Oil Contaminated Soil. *Journal of Applied Sciences & Environmental Management*, 21(5). doi: 10.4314/jasem.v21i5.26

Ghouse, A. K. M., Zaidi, S. H. and Atique, A. (1980). Effect of pollution on the Folier Organs of *Calistemon citrinus Stapf*. *Journal of Scientific Research*, 2: 207-209

Hazim, R. N. and Al-Ani, M. A. (2019). Effect of petroleum hydrocarbons contamination on soil microorganisms and biodegradation. *Rafidain Journal*

Scientia Africana, Vol. 21 (No. 1), April, 2022. Pp 253-266 *https://dx.doi.org/10.4314/sa.v21i1.22*
© Faculty of Science, University of Port Harcourt, Printed in Nigeria *ISSN 1118 – 1931*

of Science, *28*:13-22. doi: 10.33899/rjs.2019.159391

Ijah, J., Antai, S. (2003). The potential use of chicken-drop micro-organisms for oil spill remediation. Environmentalist. 23(1), 89–95.

Jahan, R., Bodratti, A. M., Tsianou, M. and Alexandridis, P. (2020). Biosurfactants, natural alternatives to synthetic surfactants: physicochemical properties and applications. *Advances in colloid and interface science*, 275:102061.

Lopes, P. R. M., Montagnolli, R. N., de Fátima Domingues, R. and Bidoia, E. D. (2010). Toxicity and biodegradation in sandy soil contaminated by lubricant oils. *Bulletin of environmental contamination and toxicology* 84:454-458. doi 10.1007/s00128-010-9945-8

Lu, S. T. and Kaplan, I. R. (2008). Characterization of motor lubricating oils and their oil–water partition. *Environmental Forensics 9*: 295-309. https://doi.org/10.1080/15275920802119441

Mao, Y., Zhang, L., Wang, Y., Yang, L., Yin, Y., Su, X., Liu, Y., Pang, H., Xu, J., Hu, Y. and Shen, X. (2020). Effects of polycyclic aromatic hydrocarbons (PAHs) from different sources on soil enzymes and microorganisms of Malus prunifolia var. Ringo. *Archives of Agronomy and Soil Science*, 1-15 https://doi.org/10.1080/03650340.2020.18204

Maliszewska-Kordybach B. (1996). Polycyclic aromatic hydrocarbons in agricultural soils in Poland: Preliminary proposals for criteria to evaluate the level of soil contamination. *Applied Geochemistry*, 11:121–127. https://doi.org/10.1016/0883-2927(95)00076-3.

Mangas, I, Sogorb, M. A. and Vilanova, E. (2014). (lubricating oils) in Philip Wexler (Editors), Encyclopedia of Toxicology, Elsevier Inc. pg. 670-676

Margesin, R., and Schinner, F. (2001). Bioremediation (natural attenuation and biostimulation) of diesel-oil-contaminated soil in an alpine glacier skiing area. *Applied and environmental microbiology*, *67*(7), 3127-3133.

Nespeca, M. G., Piassalonga, G. B., and de Oliveira, J. E. (2018). Infrared spectroscopy and multivariate methods as a tool for identification and quantification of fuels and lubricant oils in soil. *Environmental monitoring and assessment*, 190:1-12. https://doi.org/10.1007/s10661-017-6454-9

Nowak, P., Kucharska, K., and Kamiński, M. (2019). Ecological and Health Effects of Lubricant Oils Emitted into the Environment. *International journal of environmental research and public health* 16:3002.

Nwachukwu, M. O., Azorji, J. N., Adjero, L. A., Green, M. C., Igwe, C. E., and Nnadozie, R. I. A. (2020). Influence of Spent Engine Oil Pollution and Organic Amendment on Soil Physicochemical Properties, Microbial Population and Growth of Capsicum annuum (L.). *Asian Soil Research Journal*, 17-25. DOI: 10.9734/asrj/2020/v3i130064

Nyarko, H. D., Okpokwasili, G. C., Joel, O. F., and Galyuon, I. A. K. (2019). Effect of petroleum fuels and lubricants on soil properties of auto-mechanic workshops and garages in

Cape Coast metropolis, Ghana. *Journal of Applied Sciences and Environmental Management* 23:1287-1296. doi: 10.4314/jasem.v23i7.15

Obini, U., Okafor, C. O. and Afiukwa, J. N. (2013). Determination of levels of polycyclic aromatic hydrocarbons in soil contaminated with spent motor Engine oil in Abakaliki Auto-Mechanic Village. *Journal of Applied Sciences and Environmental Management* 17:169-175. doi: 10.4314/jasem.v17i2.1

Obiukwu, S.C and Kadafa A.A (2016). An Assessment on the Level of Compliance in Handling and Disposal of Spent Oils from Retail Fuel Service Stations in Gwarinpa District of Abuja, Nigeria. *Universal Journal of Environmental Research & Technology* 6(4).

Plaza, G., Ulfig, K., Worsztynowicz, A., Malina, G., Krzeminska, B. and Brigmon, R. L. (2005). Respirometry for assessing the biodegradation of petroleum hydrocarbons. *Environmental technology* 26:161-170.

Raju, M. N., Leo, R., Herminia, S. S., Morán, R. E. B., Venkateswarlu, K. and Laura, S. (2017). Biodegradation of Diesel, Crude Oil and Spent Lubricating Oil by Soil Isolates of Bacillus spp. *Bulletin of environmental contamination and toxicology* 98:698-705. DOI 10.1007/s00128-017-2039-0

Ramadan, K. M., Azeiz, A. A., Hassanien, S. E. and Eissa, H. F. (2012). Biodegradation of used lubricating and diesel oils by a new yeast strain Candida viswanathii KA-2011. *African Journal of Biotechnology* 11:14166-14174.

Rengarajan, T., Rajendran, P., Nandakumar, N., Lokeshkumar, B., Rajendran, P. and Nishigaki, I. (2015). Exposure to polycyclic aromatic hydrocarbons with special focus on cancer. *Asian Pacific Journal of Tropical Biomedicine* 5:182-189. https://doi.org/10.1016/S2221-1691(15)30003-4

Ron, E. Z. and Rosenberg, E. (2014). Enhanced bioremediation of oil spills in the sea. *Current Opinion in biotechnology* 27:191-194.

Saterbak, A., Toy, R. J., McMain, B. J., Williams, M. P. and Dorn, P. B. (2000). Ecotoxicological and analytical assessment of effects of bioremediation on hydrocarbon-containing soils. *Environmental Toxicology and Chemistry: An International Journal* 19:2643-2652.

Soroldoni, S., Silva, G., Correia, F. V. and Marques, M. (2019). Spent lubricant oil-contaminated soil toxicity to Eisenia andrei before and after bioremediation. *Ecotoxicology* 28:212-221.

Stachowiak G.W and Batchelor A.W (1993) Lubricants and their Composition. *Tribology Series* 24: 59–119. https://doi.org/10.1016/S0167-8922(08)70577-7

Stephen, E., Usman, A. S., Okolo, M. O., Akogu, E. A. and Abioye, O. P. (2013). Microbiological and physicochemical properties of diesel simulated soil. *Futa J. Res. Science* 9:82-86.

Syahir, A. Z., Zulkifli, N. W. M., Masjuki, H. H., Kalam, M. A., Alabdulkarem, A., Gulzar, M., Khuong, L.S. and

Scientia Africana, Vol. 21 (No. 1), April, 2022. Pp 253-266 https://dx.doi.org/10.4314/sa.v21i1.22
© Faculty of Science, University of Port Harcourt, Printed in Nigeria *ISSN 1118 – 1931*

Harith, M. H. (2017). A review on bio-based lubricants and their applications. *Journal of Cleaner Production* 168:997-1016. https://doi.org/10.1016/j.jclepro.2017.09.106

Tang, L., Tang, X., Zhu, Y., Zheng, M.H. and Miao, Q. (2005). Contamination of polycyclic aromatic hydrocarbons (PAHs) in urban soils in Beijing, China. *Environment international* 31:822 – 828.

Vazquez-Duhalt, R. (1989). Environmental impact of used motor oil. *Science of the total environment* 79:1-23. https://doi.org/10.1016/0048-9697(89)90049-1

Vwioko D.E., Anoliefo G.O. and Fashemi S.D. (2006). Metal concentration in plant tissues of Ricinus communis L. (Castor oil) grown in soil contaminated with spent lubricating oil. *Journal of Applied Science and Environmental Management* 10: 127-134

Wang, J., Jia, C. R., Wong, C. K. and Wong, P. K. (2000). Characterization of polycyclic aro12matic hydrocarbons created in lubricating oils. *Water, Air, and Soil Pollution*, 120:381-396

W.H.O (1996). Permissible limits of heavy metals in soil and plants (Geneva: World Health Organization), Switzerland.

Wu, H., Zhao, J., Xia, W., Cheng, X., He, A., Yun, J. H.,Wang, L., Huang, H., Jiao, S., Huang, L. and Jiang, Z. (2017). A study of the tribological behaviour of TiO2 nano-additive water-based lubricants. *Tribology International*, 109:398-408. https://doi.org/10.1016/j.triboint.2017.01.013